Iowa Research Online
The University of Iowa's Institutional Repository

University of Iowa
Iowa Research Online

Theses and Dissertations

Fall 2011

Chemical investigations of secondary metabolites from selected fungi and from peanut seeds challenged by Aspergillus caelatus

Scott Andrew Neff
University of Iowa

Copyright 2011 Scott Andrew Neff

This dissertation is available at Iowa Research Online: http://ir.uiowa.edu/etd/2750

Recommended Citation
Neff, Scott Andrew. "Chemical investigations of secondary metabolites from selected fungi and from peanut seeds challenged by Aspergillus caelatus." PhD (Doctor of Philosophy) thesis, University of Iowa, 2011.
http://ir.uiowa.edu/etd/2750.

Follow this and additional works at: http://ir.uiowa.edu/etd

Part of the Chemistry Commons

CHEMICAL INVESTIGATIONS OF SECONDARY METABOLITES FROM SELECTED FUNGI AND FROM PEANUT SEEDS CHALLENGED BY *ASPERGILLUS CAELATUS*

by

Scott Andrew Neff

An Abstract

Of a thesis submitted in partial fulfillment
of the requirements for the Doctor of
Philosophy degree in Chemistry
in the Graduate College of
The University of Iowa

December 2011

Thesis Supervisor: Professor James B. Gloer

ABSTRACT

Many years of study have revealed that fungi are excellent sources of novel bioactive secondary metabolites. Some of these secondary metabolites possess therapeutic qualities that improve the quality of life for millions of people. Such metabolites include well known classes such as the penicillins, cephalosporins, and statins, yet many fungi remain underexplored as sources of biologically active metabolites. The research described in this thesis employs an ecology-based approach to targeting fungi for chemical investigation, and describes studies of fungi from two niche groups, fungicolous/mycoparasitic and endophytic fungi, as possible sources of new secondary metabolites with biological activities. In a parallel project, the structures of bioactive compounds isolated from peanut seeds that had been subjected to fungal attack were elucidated in the pursuit of compounds with beneficial bioactivities.

Mycoparasitic fungi are those that colonize other fungi by parasitizing the host, often leading to damage to the host fungus. Fungicolous fungi are those that colonize other fungi, but have not been proven to be true mycoparasites. The damage often caused by colonization of host fungi indicates that mycoparasitic and fungicolous fungi can produce antifungal compounds. Chemical investigations of such fungi described in this thesis afforded 37 compounds representing various biosynthetic types, seven of which were new. Many of these compounds show antifungal, antimicrobial, and/or cytotoxic effects. Endophytic fungi live asymptomatically within plant tissues and in some cases may provide benefits to the host plant through the production of secondary metabolites. Chemical investigations of corn, wheat, and sorghum endophytes described in this thesis led to the isolation and characterization of 20 compounds, seven of which were identified as being new. Many of the fungal metabolites encountered in this work showed antifungal, antimicrobial, and/or cytotoxic effects.

Seven new secondary metabolites, isolated from peanut seeds, were produced in response to fungal attack by an *Aspergillus caelatus* strain. All of these compounds were stilbene-derived phytoalexins, which are considered to be inducible chemical defenses whose production is elicited or enhanced upon microbial attack. Further studies of these newly identified compounds and their production could lead a better understanding of how the plant defends itself. Such knowledge could enable researchers to manipulate this mechanism to obtain greater peanut resistance to invasion by pests. Additionally, the health benefits from related stilbene-derived compounds (e.g., resveratrol) from peanuts and other plants have been widely established. Knowledge about the presence of compounds of this type could add to the importance of peanut crop production.

The compounds identified in this work were isolated using multiple chromatographic techniques, and the structures were established based on analysis of 1D and 2D NMR data combined with MS, chemical derivatization, and/or optical measurement data. Absolute configuration assignments were achieved by application of Mosher's method, CD spectral analysis, computational investigation, and/or chemical derivatization. Details of the isolation, structure elucidation, and biological activity of these compounds are presented in this thesis.

Abstract Approved: _____
Thesis Supervisor

_____
Title and Department

_____
Date

CHEMICAL INVESTIGATIONS OF SECONDARY METABOLITES FROM SELECTED FUNGI AND FROM PEANUT SEEDS CHALLENGED BY *ASPERGILLUS CAELATUS*

by

Scott Andrew Neff

A thesis submitted in partial fulfillment
of the requirements for the Doctor of
Philosophy degree in Chemistry
in the Graduate College of
The University of Iowa

December 2011

Thesis Supervisor: Professor James B. Gloer

Graduate College
The University of Iowa
Iowa City, Iowa

CERTIFICATE OF APPROVAL

_____

PH.D. THESIS

_____

This is to certify that the Ph.D. thesis of

Scott Andrew Neff

has been approved by the Examining Committee
for the thesis requirement for the Doctor of Philosophy
degree in Chemistry at the December 2011 graduation.

Thesis Committee: _____
James B. Gloer, Thesis Supervisor

_____
Ned B. Bowden

_____
Christopher M. Cheatum

_____
Gregory K. Friestad

_____
Horacio F. Olivo

To All of My Coaches
and Teachers who Laid
the Foundation for Me to
Reach as High as I Desired

ACKNOWLEDGEMENTS

The idea of attending graduate school was a distant thought, even as my undergraduate career at St. Ambrose University was coming to a close. It was Dr. Art Serianz, an individual who also received his Ph.D. from the University of Iowa and the first person who believed that I would do well in graduate school, who helped me pursue a graduate school education. Without his guidance, and the guidance of the chemistry department at St. Ambrose University, including Dr. Marge Legg, Dr. Andy Axup, and Dr. George Bailey, I certainly would not be in the position I am today. I am grateful to all of them for their support and belief in me.

I would like to thank my research advisor, Dr. James B. Gloer, for his guidance and advice during the course of my graduate studies. His knowledge of natural products chemistry in certainly unparalleled, and without his patience, my understanding of natural product chemistry would not be what it is today.

I would like to acknowledge the current and former Gloer group members. Without their willingness to answer questions and give advice on a daily basis, I would have been lost on many different occasions. I offer them many thanks for all they have done and the time they have sacrificed.

I would also like to thank the multiple professors that I had the pleasure of getting to know through being a TA, as well as those who I the pleasure of learning from as a student. The guidance I was given from them during my time in graduate school is greatly appreciated.

A special thanks goes out to Dr. Donald T. Wicklow, our research group's mycological collaborator from the USDA in Peoria, IL, whose hard work and dedication allows the Gloer group to continue working with samples that are of the highest quality. Dr. Wicklow and his team collected, identified, and cultured fungal material that was crucial to my research, as well as many others who preceded me. He also supervised

crucial bioassays on the collected material, which was the driving force for the majority of this research.

I would like to thank Dr. Victor S. Sobolev of the USDA's National Peanut Research Laboratory in Dawson, GA for affording me the opportunity to collaborate with him for a good portion of my research. He has graciously allowed me to include much of this collaboration material within the pages of this thesis.

Having grown up in Iowa, I certainly felt the need to expand my horizons by attending college outside of the state or even the Midwest. However, with opportunities to do just that, I ended up choosing my undergraduate institutions within the borders of the state that I knew so well. It was no different when I chose to attend graduate school at the University of Iowa. The first-hand experience that I had of the city and campus when making my decision was only enhanced with the warm welcome that I received from various individuals in the chemistry department when I first arrived. I realized quickly that individuals like Janet and Sharon were willing to go the extra mile to assist me during my education and growth as a professional. This was not only demonstrated by the administrative staff, but also by the professors and fellow graduate students that I have had the pleasure of knowing. For going above and beyond, thank you to all of the people who were "behind the scenes" during my education at the University of Iowa.

I would also like to thank the individuals in the NMR and MS facilities for all of their hard work. They were able to assist me whenever I needed them to, and more importantly; they were able to do so in a timely manner that allowed my research to move forward smoothly. Financial support from the National Science Foundation and the National Institutes of Health are also appreciated.

Finally, this thesis is dedicated to my family who, in all ways possible, supported me in my journey to achieve this goal. To my mother, Dorothy; you not only helped to support me financially throughout all my years of college, but you were also the one who pushed me to achieve more academically than anyone else. To my dad, Mike; you were

the one who taught me what hard work and dedication means and what it can yield. Both of you were proud of me every step of the way and I cannot thank you both enough for that. To my brother, Ryan; you kept me grounded and focused not only in my education but also in life in general, my deepest thanks goes to you.

Para Amber: hemos pasado por dificultades, y a veces los dos hemos andado como perdidos, pero al final, encontramos el amor que tenemos. Tu apoyo y amor fueron monumentales para mi empeño en lograr esta meta final. Del fondo de mi corazón, gracias.

TABLE OF CONTENTS

LIST OF TABLES ix

LIST OF FIGURES x

LIST OF SCHEMES xiv

LIST OF ABBREVIATIONS xv

CHAPTER

1. INTRODUCTION 1

2. SCREENING OF FUNGI 24

3. ISOLATION AND CHARACTERIZATION OF AFLAQUINOLONES A-G: SECONDARY METABOLITES FROM FUNGICOLOUS AND MARINE ISOLATES OF *ASPERGILLUS* SPP. 38

   Structure Elucidation of Aflaquinolones A (**43**) and B (**44**) 40
   Structure Elucidation of Aflaquinolones C-G (**47**-**51**) 49

4. CHEMICAL INVESTIGATIONS OF A CRYPTIC FUNGICOLOUS ISOLATE OF *ASPERGILLUS* SP. (SECTION *FLAVIPEDES*; MYC-1580 = NRRL 58569) 60

   Structure Elucidation of Asperlarin A (**52**) and Flavipeptide A (**53**) 63
   Structure Elucidation of PF1233B (**54**) 69

5. CHEMICAL INVESTIGATIONS OF AN ENDOPHYTIC ISOLATE OF *EMERICELLA NIDULANS* (ENDO-3111 = NRRL 58893) 75

   Structure Elucidation of Emeridin A (**65**) 80
   Structure Elucidation of O-Methylsecoemestrin C_1 (**66**) 87
   Structure Elucidation of Compounds **67** and **68** 90

6. ADDITIONAL NEW SECONDARY METABOLITES OBTAINED FROM OTHER FUNGICOLOUS FUNGI 93

   Chemical Investigation of a Fungicolous Isolate of *Trichoderma longibrachiatum* (MYC-1515 = NRRL 54514) 93
      Structure Elucidation of Tetrahydrosorbicillinol (**71**) 95
   Chemical Investigations of a Fungicolous Isolate of *Stachybotrys parvispora* (MYC-2013 = NRRL 54531) 98
      Structure Elucidation of Agistatine F (**77**) 100
   Chemical Investigations of an Unidentified Fungicolous Fungus (MYC-1991) 103
      Structure Elucidation of Dihydrosporothriolide (**82**) 104

7. NEW STILBENE-DERIVED PHYTOALEXINS FROM PEANUT (*ARACHIS HYPOGAEA*) SEEDS CHALLENGED BY *ASPERGILLUS CAELATUS* 108

Structure Elucidation of Chiricanine A (**84**) and Arahypins 1-7 (**85-91**) 110

8. NEW PTEROCARPENES ELICITED FROM PEANUT (*ARACHIS HYPOGAEA*) SEEDS UPON COLONIZATION BY *ASPERGILLUS CAELATUS* 126

Structure Elucidation of Aracarpenes 1 (**92**) and 2 (**93**) 129

9. SUMMARY AND CONCLUSIONS 135

10. EXPERIMENTAL 138

General Experimental Procedures 138
Solvents and Reagents 138
Mass Measurements 138
Evaporation 138
General Chromatography Information 139
Chromatography of Plant Metabolites – Chiricanine A (**84**) and Arahypins 1-5 (**85-89**) 140
Chromatography of Plant Metabolites – Arahypins 6-7 (**90** and **91**) 141
Chromatography of Plant Metabolites – Aracarpenes 1-2 (**92** and **93**) 141
General Spectroscopic Information 142
GCMS Conditions for Amino Acid Derivative Analysis 144
Electronic Circular Dichroism (ECD) Analysis 144
Additional Details of Spectroscopic Measurments in Studies of Marine *Aspergillus* sp. Isolate (Chapter 3) 144
Additional Details of Spectroscopic Measurments in Studies of Plant Metabolites – Chiricanine A (**84**), Arahypins 1-7 (**85-91**), and Aracarpenes (**92** and **93**) 145
General Procedures for Individual NMR Experiments 146
DEPT Experiment 146
Homonuclear Decoupling Experiment 146
NOESY Experiment 147
HMQC Experiment 147
HMBC Experiment 149
General Procedures for Solid-Substrate Fermentaions 149
General Procedures for Antifungal Assays 150
General Procedures for Antiinsectan Assays 151
General Procedures for Antibacterial Assays 152
Bacillus subtilis 152
Staphlococcus aureus 153
Escherichia coli 153
General Procedures for Cell Proliferation Assay 154
Procedures for the Isolation and Characterization of Metabolites from Fungicolous and Marine Isolates of *Aspergillus* spp. (MYC-2048 = NRRL 58570 and *Aspergillus* sp. SF-5044) 154
Sodium Borohydride Reduction of Aflaquinolone A (**43**) 159
Preparation of Aflaquinolone B (**44**) Mosher Esters 160

Energy Minimizations and ECD Calculations 160
Procedures for the Isolation and Characterization of Metabolites from a Cryptic Fungicolous Isolate of *Aspergillus* sp (secion *Flavipedes*; MYC-1580 = NRRL 58569).....161
Amino Acid Analysis of Asperlarin A (**52**) and Flavipeptide (**53**) 164
Procedures for the Isolation and Characterization of Metabolites from an Endophytic Isolate of *Emericella nidulans* (ENDO-3111 = NRRL 58893) 165
Attempted Chemical Degradations of Emeridin A (**65**) using OsO_4 and $KMnO_4$ 167
Ozonolysis of Emeridin A (**65**) 168
Procedures for the Isolation and Characterization of Metabolites from Various Fungicolous Fungi (MYC-1515 = NRRL 54514, MYC-2013 = NRRL 54531, and MYC-1991) 169
MYC-1515 (= NRRL 54514) Fungal Material 169
MYC-2013 (= NRRL 54531) Fungal Material 170
MYC-1991 Fungal Material 171
Procedures for the Isolation and Characterization of Pseudocitreoindole (**23**) from MYC-1805 (*Penicillim* sp.).....172
Procedures for the Isolation and Characterization of Stilbene-Derived Phytoalexins Chiricanine A (**84**) and Arahypins 1-5 (**85**-**89**).....174
Procedures for the Isolation and Characterization of Stilbenoid Dimers **90** and **91**.....177
Procedures for the Isolation and Characterization of Pterocarpenes **92** and **93**.....179

APPENDIX SELECTED NMR SPECTRA 182

REFERENCES 231

LIST OF TABLES

Table

1. Antifungal and Antiinsectan Bioassay Results for the EtOAc Extracts of Selected Fungicolous/Mycoparasitic (MYC) and Endophytic (ENDO) Fungal Cultures. 27

2. ^{1}H and ^{13}C NMR Data for Aflaquinolones A (**43**) and B (**44**) in $CDCl_3$ 41

3. NMR Spectroscopic Data for Aflaquinolones C (**47**) and D (**48**) in Acetone-d_6 50

4. ^{1}H and ^{13}C NMR Data for Aflaquinolones E-G (**49-51**) in CD_3OD. 54

5. Growth Inhibitory Activity of Compounds **43**, **44**, **47**, and **49-51** on Tumor Cell Lines. 59

6. ^{1}H and ^{13}C NMR Data for Asperlarin A (**52**) in CD_3OD. 64

7. ^{1}H and ^{13}C NMR Data for Flavipeptide A (**53**) in Actone-d_6....67

8. NMR Spectroscopic Data for PF1233B (**54**) in Acetone-d_6. 70

9. NMR Spectroscopic Data for Emeridin A (**65**) in $CDCl_3$. 82

10. NMR Spectroscopic Data for O-Methylsecoemestrin C_1 (**66**) in $CDCl_3$. 89

11. ^{1}H and ^{13}C NMR Data for Compounds **67** and **68** in CD_3OD....91

12. NMR Spectroscopic Data for Tetrahydrosorbicillinol (**71**) in CD_3OD. 96

13. NMR Spectroscopic Data for Agistatine F (**77**) in $CDCl_3$. 101

14. ^{1}H and ^{13}C NMR Data for Dihydrosporothriolide (**82**) in $CDCl_3$. 105

15. ^{1}H NMR Data (400 MHz) for Compounds **86-89**. 112

16. ^{13}C NMR Data (100 MHz) for Compounds **86-89**. 113

17. NMR Spectroscopic Data for Arahypin-6 (**90**) in $CDCl_3$. 119

18. NMR Spectroscopic Data for Aracarpene-1 (**92**) and Aracarpene-2 (**93**). 131

LIST OF FIGURES

Figure

1. Depiction of Right-Handed Circularly Polarized Light (Perpendicular Waves are of Equal Amplitude).....6

2. Depiction of Right-handed Elliptically Polarized Light (Perpendicular Waves are of Unequal Amplitude) 8

3. Experimental and Calculated CD Spectra of (+)-Diversonol (**6**).....9

4. Experimentally Measured CD Spectrum of *S*-Parazoanthine A (**7**) (Top) and TDDFT-Calculated CD Spectra of the *S* (**7**) and *R* (**8**) Enantiomers (Bottom).....13

5. Solution and Solid-State CD Spectra of Tetrahydropyrenophorol (**9**), and TDB3LYP/TZVP-Calculated CD of the Conformation Reflected in its X-ray Structure.....15

6. Isolation Scheme for Aflaquinolones A (**43**) and B (**44**).....39

7. Key NOESY Correlations of the Cyclohexanone Unit of Aflaquinolone A (**43**).....43

8. Experimental ECD Curve (Top) and TDDFT-Calculated ECD Curve (Bottom) for Aflaquinolone A (**43**).....45

9. Key NOESY Correlations for the Cyclohexane Unit of Aflaquinolone B (**44**).....47

10. Experimental ECD Spectrum of Aflaquinolone B (**44**).....48

11. Observed Chemical Shift Differences ($\Delta\delta = \delta_S - \delta_R$, ppm; 400 MHz) for the *S*- (**44a**) and *R*-MTPA (**44b**) Esters of Aflaquinolone B (**44**). 48

12. Combined Experimental ECD Curves for Aflaquionolone A (**43**) and C (**47**).....51

13. Combined Experimental ECD Curves for Aflaquinolones A-E (**43**, **44**, and **47**-**49**).....55

14. Experimental ECD Spectrum (Top) and TDDFT-Calculated ECD Spectrum (Bottom) for Aflaquinolone G (**51**).....57

15. Isolation Scheme for Metabolites **52**-**54** from MYC-1580.....61

16. HMBC Correlations for Asperlarin A (**52**).....65

17. Isolation Scheme for Metabolites **65**-**68** from ENDO-3111.....79

18. Key NOESY Correlations of the Bicyclic Ring System (A) and Cyclopentanone Ring (B) of Emeridin A (**65**).....83

19. Key HMBC Correlations for Compounds **67** and **68**.....91

20. Isolation Scheme for Metabolites **71**-**73** from MYC-1515.....94

21. Isolation Scheme for Metabolites **77**-**79** from MYC-2013.....99

22. Isolation Scheme for Dihydrosporothriolide (**82**) from MYC-1991.....104

23. Isolation Scheme for the MeOH Extract of Peanut Seeds Challenged by *Aspergillus caelatus* that Yielded Stilbenoids **84**-**89**.....110

24. Isolation Scheme for the MeOH Extract of Peanut Seeds Challenged by *Aspergillus caelatus* that Yielded Dimeric Stilbenoids **90** and **91**.....117

25. Experimental ECD Curves of **90**, **91**, and a MeOH Blank.....122

26. Antifungal Properties of Compounds **84**-**89** against *P. viticola* and *P. obscurans*. Captan is Used as the Standard. Antifungal Assays were Performed (and Chart Produced) by D. E. Wedge and Co-Workers.....125

27. Formation of a Pterocarpan Skeleton.....127

28. Isolation Scheme for the MeOH Extract of Peanut Seeds Challenged by *Aspergillus caelatus* that Yielded Compounds **92** and **93**.....129

29. Antimicrobial Properties of Aracarpenes 1 (**92**) and 2 (**93**) against *Bacillus subtilis*, *Escherichia coli*, *Staphylococcus aureus*, and *Aspergillus flavus*. *Data were not Collected at 20 μM. Antifungal Tests were Performed (and Charts Produced) by A. J. De Lucca and Co-Workers.....133

A1. ^{1}H NMR Spectrum of Aflaquinolone A (**43**, 600 MHz, $CDCl_3$).....183

A2. ^{13}C NMR Spectrum of Aflaquinolone A (**43**, 100 MHz, $CDCl_3$).....184

A3. ^{1}H NMR Spectrum of Aflaquinolone B (**44**, 400 MHz, $CDCl_3$).....185

A4. ^{1}H NMR Spectrum of Aflaquinolone B (**44**, 400 MHz, Acetone-d_6).....185

A5. ^{13}C NMR Spectrum of Aflaquinolone B (**44**, 100 MHz, $CDCl_3$).....186

A6. ^{1}H NMR Spectrum of Aflaquinolone C (**47**, 400 MHz, Acetone-d_6).....187

A7. ^{13}C NMR Spectrum of Aflaquinolone C (**47**, 100 MHz, Acetone-d_6).....188

A8. ^{1}H NMR Spectrum of Aflaquinolone D (**48**, 400 MHz, Acetone-d_6).....189

A9. ^{1}H NMR Spectrum of Aflaquinolone E (**49**, 400 MHz, CD_3OD).....190

A10. ^{13}C NMR Spectrum of Aflaquinolone E (**49**, 100 MHz, CD_3OD).....191

A11. ^{1}H NMR Spectrum of Aflaquinolone F (**50**, 400 MHz, CD_3OD).....192

A12. ^{13}C NMR Spectrum of Aflaquinolone F (**50**, 100 MHz, CD_3OD) 193

A13. ^{1}H NMR Spectrum of Aflaquinolone G (**51**, 400 MHz, CD_3OD).....194

A14. ^{13}C NMR Spectrum of Aflaquinolone G (**51**, 100 MHz, CD_3OD) 195

A15. ^{1}H NMR Spectrum of Asperlarin A (**52**, 400 MHz, CD_3OD).....196

A16. ^{13}C NMR Spectrum of Asperlarin A (**52**, 100 MHz, CD_3OD).....197

A17. ^{1}H NMR Spectrum of Flavipeptide A (**53**, 400 MHz, Acetone-d_6) 198

A18. HMBC Spectrum of Flavipeptide A (**53**, 600 MHz, Acetone-d_6).....199

A19. ^{1}H NMR Spectrum of PF1233B (**54**, 400 MHz, Acetone-d_6) 200

A20. ^{13}C NMR Spectrum of PF1233B (**54**, 100 MHz, $CDCl_3$) 201

A21. ^{1}H NMR Spectrum of Emeridin A (**65**, 400 MHz, $CDCl_3$).....202

A22. ^{13}C NMR Spectrum of Emeridin A (**65**, 100 MHz, $CDCl_3$).....203

A23. ^{1}H NMR Spectrum of O-Methylsecoemestrin C_1 (**66**, 400 MHz, $CDCl_3$) 204

A24. HMBC Spectrum of O-Methylsecoemestrin C_1 (**66**, 600 MHz, $CDCl_3$) 205

A25. ^{1}H NMR Spectrum of 5-(Hydroxymethyl)-2,4-dimethylbenzene-1,3-diol (**67**, 400 MHz, CD_3OD).....206

A26. HMBC Spectrum of 5-(Hydroxymethyl)-2,4-dimethylbenzene-1,3-diol (**67**, 600 MHz, CD_3OD).....207

A27. ^{1}H NMR Spectrum of 5-(Hydroxymethyl)-3-methoxy-2,4-dimethylphenol (**68**, 400 MHz, CD_3OD).....208

A28. ^{13}C NMR Spectrum of 5-(Hydroxymethyl)-3-methoxy-2,4-dimethylphenol (**68**, 100 MHz, CD_3OD).....209

A29. ^{1}H NMR Spectrum of Tetrahydrosorbicillinol (**71**, 400 MHz, CD_3OD).....210

A30. HMBC Spectrum of Tetrahydrosorbicillinol (**71**, 600 MHz, CD_3OD) 211

A31. ^{1}H NMR Spectrum of Agistatine F (**77**, 600 MHz, $CDCl_3$).....212

A32. ^{13}C NMR Spectrum of Agistatine F (**77**, 100 MHz, $CDCl_3$).....213

A33. ^{1}H NMR Spectrum of Dihydrosporothriolide (**82**, 400 MHz, $CDCl_3$).....214

A34. ^{13}C NMR Spectrum of Dihydrosporothriolide (**82**, 100 MHz, $CDCl_3$).....215

A35. ^{1}H NMR Spectrum of Arahypin-1 (**86**, 400 MHz, $CDCl_3$) 216

A36. ^{13}C NMR Spectrum of Arahypin-1 (**86**, 100 MHz, $CDCl_3$).....217

A37. ^{1}H NMR Spectrum of Arahypin-3 (**87**, 400 MHz, CD_3OD) 218
A38. ^{13}C NMR Spectrum of Arahypin-3 (**87**, 100 MHz, CD_3OD) 219
A39. ^{1}H NMR Spectrum of Arahypin-4 (**88**, 400 MHz, CD_3OD) 220
A40. ^{13}C NMR Spectrum of Arahypin-4 (**88**, 100 MHz, CD_3OD) 221
A41. ^{1}H NMR Spectrum of Arahypin-5 (**89**, 400 MHz, $CDCl_3$) 222
A42. ^{13}C NMR Spectrum of Arahypin-5 (**89**, 100 MHz, $CDCl_3$) 223
A43. ^{1}H NMR Spectrum of Arahypin-6 (**90**, 400 MHz, $CDCl_3$) 224
A44. HMBC Spectrum of Arahypin-6 (**90**, 600 MHz, $CDCl_3$).....225
A45. ^{1}H NMR Spectrum of Arahypin-7 (**91**, 400, Acetone-d_6) 226
A46. ^{1}H NMR Spectrum of Aracarpene-1 (**92**, 400 MHz, $CDCl_3$).....227
A47. ^{13}C NMR Spectrum of Aracarpene-1 (**92**, 100 MHz, Acetone-d_6) 228
A48. ^{1}H NMR Spectrum of Aracarpene-2 (**93**, 400 MHz, Acetone-d_6) 229
A49. HMBC Spectrum of Aracarpene-2 (**93**, 600 MHz, Acetone-d_6) 230

LIST OF SCHEMES

Scheme

1. Equations that Relate Ellipticity and Molar Ellipticity to the Beer-Lambert Law and the Interactions Chiroptical Molecules with Circularly Polarized Light in a CD Experiment. 8

2. Proposed $OsO_4/NaIO_4$ and $KMnO_4$ Oxidative Cleavage Reactions of Emeridin A (**65**) and the Potential Products. 85

3. Ozonolysis of Emeridin A (**65**) with Reductive Work-Up Using Me_2S. 86

LIST OF ABBREVIATIONS

~	approximately
$[\alpha]_D$	specific rotation
Ac	acetyl
Ar	Argon
ATCC	American Type Culture Collection
ax	axial
BBI	broadband inverse
BBO	broadband observe
br	broad
°C	degrees Celsius
C_{18}	octadecylsilyl
calcd	calculated
CD	circular dichroism
CE	Cotton effect
cm	centimeter
COSY	correlation spectroscopy
cz	clear zone
d	doublet
δ	chemical shift
DEPT	distortionless enhancement by polarization transfer
DMSO	dimethyl sulfoxide
DS	dummy scans
DW	dwell time
ε	extinction coefficient

ECD	electronic circular dichroism
EIMS	electron impact mass spectrometry
eq	equatorial
ESIMS	electrospray ionization mass spectrometry
EtOAc	ethyl acetate
eV	electron volt
EXPO	experiment number
FID	free induction decay
g	gram(s)
GCMS	gas chromatography – mass spectrometry
hr	hour(s)
HMBC	heteronuclear multiple bond correlation
HMQC	heteronuclear multiple quantum correlation
HPLC	high performance/pressure liquid chromatography
HREIMS	high-resolution electron impact mass spectrometry
HRESIMS	high-resolution electrospray ionization mass spectrometry
HRESITOFMS	high-resolution electrospray ionization time-of-flight mass spectrometry
HRESITOFMSMS	high-resolution electrospray ionization time-of-flight tandem mass spectrometry
Hz	hertz
IR	infrared
IUPAC	International Union of Pure and Applied Chemistry
J	coupling constant
kcal	kilocalories

L	liter(s)
µ	micro
m	multiplet
M^+	molecular ion
mg	milligram
MHz	megahertz
min	minute(s)
mL	milliliter(s)
mm	millimeter
mol	mole(s)
mp	melting point
MS	mass spectrometry
m/z	mass-to-charge ratio
mz	mottled zone
NCI	National Cancer Institute
NCAUR	National Center for Agricultural Utilization Research
nm	nanometer
NMR	nuclear magnetic resonance
NOE	nuclear Overhauser effect (1D)
NOESY	nuclear Overhauser effect spectroscopy (2D)
NRRL	Northern Regional Research Laboratory
NS	number of scans
obsd	observed
OR	optical rotation
PDA	potato dextrose agar

ppm	parts per million
PW	pulse width
q	quartet
RD	relaxation delay
rel int	relative intensity
rg	reduced growth
RP	reversed phase
rpm	revolutions per minute
rt	room temperature
s	singlet
sec	second(s)
SF	spectral frequency
sh	shoulder
SI	size of real spectrum
SW	spectral width
t	triplet
TD	number of data points to acquire
TDDFT	time-dependent density functional theory
TLC	thin-layer chromatography
TMS	tetramethylsilane
t_R	retention time
USDA	United States Department of Agriculture
UV	ultraviolet
VLC	vacuum liquid chromatography
wk	weak

CHAPTER 1

INTRODUCTION

In terms of the estimated number of species, Kingdom Fungi is second only to that of Kingdom Animalia. Conservative estimates suggest that there are more than 1.5 million fungal species, of which only approximately 5% have been identified by taxonomists (~72, 000 known species).[1,2] Fungi are abundant, biologically diverse, and play many different roles. For example, they play crucial roles in both the health and maintenance of ecosystems through their ability to degrade organic waste such as forest leaf litter. Fungi can also act as pathogens, predators, parasites, hosts, and/or symbionts of animals, plants, and other microorganisms.[3] Fungi have garnered a widespread negative connotation since they were first reported to cause disease in 1839.[4] In particular, fungi are known to produce mycotoxins, which have been linked to numerous types of human and animal diseases.[4] Mycotoxins are especially problematic in agriculture because fungi (and the metabolites they produce) can contaminate both cereal crops and stored grains. On the other hand, fungi can also be used in a beneficial manner. For example, some fungi (e.g., yeasts) are used in fermentation processes in the preparation of certain foods/drinks, while others are important to the industrial production of beneficial enzymes.[5]

Perhaps more importantly, fungi have long been recognized as possessing the ability to produce novel bioactive secondary metabolites, some of which have enabled significant advances in human health and agriculture, with vast impacts on societal and economic growth.[6] Although fungi have proven to be prolific producers of diverse bioactive secondary metabolites, a great many fungi remain to be chemically explored. These observations argue strongly for continued exploration of fungal chemistry in order to help meet the increasing demand for new medicinally and agriculturally beneficial agents.

Fungi are often categorized into various ecological groups. Some of these groups include freshwater fungi (fungi isolated from both flowing and still freshwater habitats), fungicolous/mycoparasitic fungi (fungi isolated from tissues of other fungi), endophytic fungi (fungi living symbiotically with plants), and plant pathogenic fungi (fungi that cause disease/damage to host plants).

Some of the most well-known classes of fungal metabolites are the penicillins and the cephalosporins. The penicillins were discovered and named by Fleming in 1928. Penicillins were originally isolated from the fungus *Penicillium notatum* and are still considered to be extremely important antibiotics. Penicillin G (**1**) was first used on a large scale during World War II to treat soldiers wounded on battlefields to stave off infections.[7] Cephalosporin C (**2**) was first isolated from *Cephalosporium acremonium* by Brotzu in 1948,[8] and displayed activity against the cause of typhoid fever. The so-called 4th generation cephalosporins are currently used to treat patients that are allergic to penicillins, and their broad spectrum of activity and excellent safety profiles make them one of the most widely prescribed class of antimicrobials in the world.[9] Fungal secondary metabolites continue to serve as an important source of lead structures for new drug compounds.[10-15]

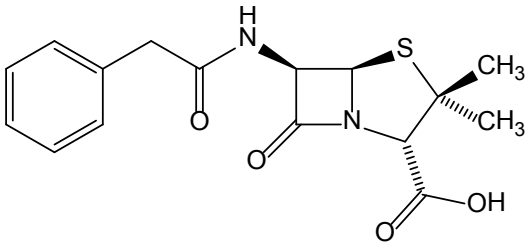

1

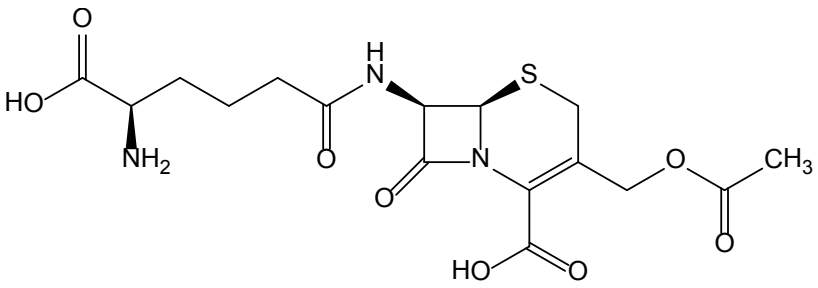

2

In order for a secondary metabolite produced by a fungus, or any other organism, to have a useful impact on human health, or provide agricultural benefits, the active component must be produced on a large scale. Typically, the initial source of the metabolite is unable to produce the active component in sufficient amounts, or not enough of the initial source is readily accessible in nature. In some cases (e.g., with fungal sources), fermentation methods can be developed that provide spectacular improvement in yields of target compounds, thereby making fermentation a viable source for such compounds. In other instances, synthetic methods are often used for mass production of the active target component. In either case, full characterization of the natural product is crucial to the process of developing a useful therapeutic drug. Even a single stereocenter difference can drastically affect the activity of a compound. For example, *S*-isomer of Ibuprofen (**3**) is a potent analgesic, but the *R*-isomer (**4**) is biologically inactive when used in the same manner.[16]

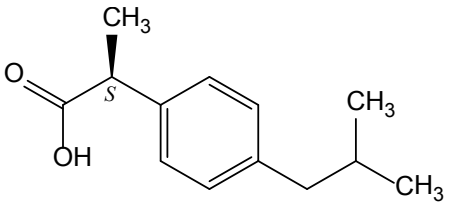

3

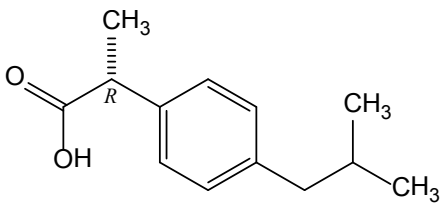

4

In the past, and to a certain extent, today, material was typically lost to chemical degradation, derivatization, or other destructive methods in order to determine the configuration and/or constitution of a molecule. An example of this is the antifungal agent griseofulvin (**5**), the first fungal metabolite that was shown to inhibit the growth of other fungi.[17] Its structure was elucidated by chemical degradation methods performed by multiple research groups, but it was not until later that the absolute configuration of **5** was assigned[18] and confirmed by X-ray crystallographic analysis of bromogriseofulvin,[19] a method that required derivatization of the natural product.

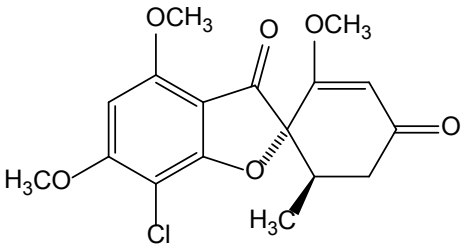

5

When the amount of an isolated metabolite is limited, e.g., due to the availability of the source material that produced it, it is especially imperative that non-destructive methods be utilized as extensively as possible to characterize the component. Non-destructive characterization methods include NMR, UV-vis, IR, CD, and, more recently, computational methods, among others. These methods have grown in complexity over the years to a point where gross structures can usually be established non-destructively. However, determination of absolute configuration is often particularly difficult, and many methods still commonly require compound degradation or derivatization. Encouragingly, recent advancements in computational methods have shown an increasing ability to help determine the absolute configuration of complex compounds when used in parallel with electronic circular dichroism (ECD) and/or optical rotation ($[\alpha]_D$) data.

As described above, a change in configuration of a single stereocenter in a molecule can have drastic effects on a compound's pharmacological activity. All receptors in the human body are inherently chiral and thus tend to interact differently with each stereocenter of any chiral drug.[15,20] Pharmaceutical regulatory agencies have begun to more fully recognize the essential role that stereochemistry plays. Any chemist currently developing new drug leads is required to identify the absolute configuration of the compound in question.[15,21-23] If a compound can be crystallized, such information can often be obtained by X-ray crystallographic analysis, but complex organic compounds often do not readily crystallize.

Because of differences in bond angles and interatomic distances within diastereomers, determination of the relative configuration of chirality elements can often be achieved through analysis of NMR data such as coupling constants and NOE effects (see below). However, this approach is not always effective, and can be especially difficult if the chirality elements are insulated from one another in a molecule. Determination of absolute stereochemistry tends to be more difficult because the differences between enantiomers are much more subtle.

The major role in the determination of the constitution of a natural product is typically played by standard NMR techniques such as ^{1}H, ^{13}C, DEPT, HMQC, and possibly HMBC. Diastereomeric structures can often be distinguished by measuring NOE or NOESY spectra, which are sensitive to three-dimensional structural features. In addition, *J*-couplings of vicinal nuclei are correlated to some degree to their reciprocal dihedral angle, and can be approximated through Karplus type equations.[24] These types of measurements often lead to the determination of relative configuration. However, NMR is intrinsically unable to discriminate between enantiomers unless material is sacrificed to a chiral derivatizing agent (e.g., Mosher's method).[15,25] Unfortunately, such derivatization methods tend to be useful only for very specific types of molecules.

Moreover, non-destructive methods would be preferable for the assignment of absolute configuration of molecules that are in limited supply.

An overwhelming majority of biologically important molecules, including secondary metabolites from fungi, are chiral.[26-28] Chirality of molecules is manifested in chiroptical effects such as specific rotation ($[\alpha]_D$) and ECD data, both of which can be measured without the loss of material. Optical rotation is observed when plane-polarized light is passed through a chiral environment, which causes the light plane to rotate in a particular direction.[29-31] Optical rotatory dispersion (ORD) – variations seen in the rotation of plane-polarized light when the wavelength of light is changed – can be of use if additional information is required. Circular dichroism (CD) is based on the differential interaction of a chiral sample with left-helical and right-helical circularly polarized light.[32,33] Circularly polarized light and the more familiar plane-polarized light are readily interconvertible through the implementation of a quarter-wave retarder. Plane-polarized light consists of right-and left-circularly polarized beams of equal intensity, while circularly polarized light consists of two orthogonal plane-polarized beams of equal intensity that are 90° out of phase (Figure 1).[33]

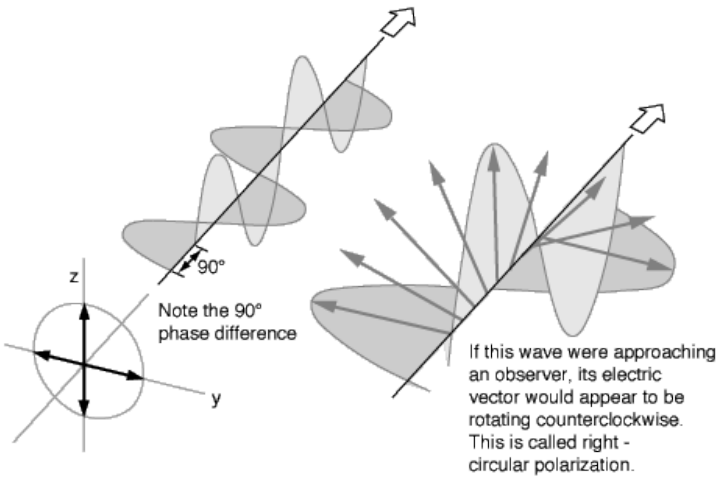

Figure 1. Depiction of Right-Handed Circularly Polarized Light (Perpendicular Waves are of Equal Amplitude).[33]

A CD spectrum has a general appearance that bears resemblance to a UV spectrum, except that a CD spectrum incorporates both positive and negative values. When a material absorbs left-handed and right-handed circularly polarized light unequally, due to molecular asymmetry involving a chromophore, a differential absorption manifests itself in the form of elliptically polarized light (Figure 2). As modeled in the equations in Scheme 1, the shape of the CD curve is the result of this unequal absorption at varying wavelengths.[34] For example, if a material absorbs right-handed circularly polarized light more than left-handed circularly polarized light, at a particular wavelength, a negative value in the CD spectrum will result and is reported as molar ellipticity (θ) on the *y*-axis. When analyzing a CD-active compound, a particular configuration of the molecule will result in a unique CD spectrum, and if one were to analyze the enantiomer of the compound, one would observe a CD curve that is the inverse of the original. This is due to the fact that if a molecule absorbs right-handed circularly polarized light more at a particular wavelength, its enantiomer (opposite configuration) will absorb left-handed circularly polarized light more at the same wavelength, resulting in a θ that is exactly opposite. This difference is one of the reasons why CD can distinguish between enantomeric forms of chiroptical compounds. A series of simple mathematical equations (Scheme 1) that relates CD to the Beer-Lambert law, where ε_l is the molar extinction coefficient of the solute measured using the ellipticity value reported in CD data, is shown below.[34] In these equations, ΔA is the difference in absorbance, *c* is the concentration, and *l* is the path length.

$$\Delta A = \Delta\varepsilon cl, \text{ where } \Delta\varepsilon = \varepsilon_l - \varepsilon_r$$

$$\theta = 33\ \Delta\text{A},$$
(θ = ellipticity, approximated in radians)
(enables direct correlation of CD to ellipticity)

$$[\theta] = 100\theta/cl,$$
([θ] = the molar ellipticity)

$$\therefore, [\theta] = 3300\Delta\varepsilon$$

Scheme 1. Equations that Relate Ellipticity and Molar Ellipticity to the Beer-Lambert Law and the Interactions Chiroptical Molecules with Circularly Polarized Light in a CD Experiment.[34]

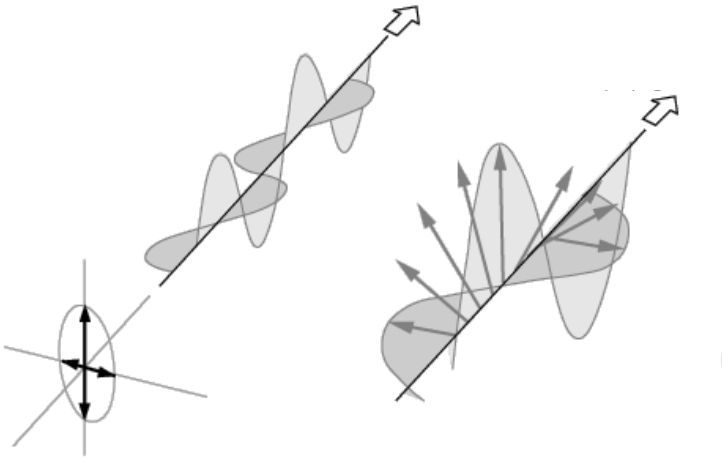

Figure 2. Depiction of Right-handed Elliptically Polarized Light (Perpendicular Waves are of Unequal Amplitude).[33]

Djerassi pioneered the application of ORD and CD to the determination of absolute configuration in which he related ORD to CD, and vice versa.[35,36] CD is generally simpler to interpret than ORD and is by far more commonly used. As

previously mentioned, because CD arises through electronic transitions, the spectra bear similarities to UV-vis data, but the mathematical sign of a CD peak at a given wavelength depends on absolute configuration of the molecule causing it.[37] A representative CD spectrum of a chiral molecule, diversonol (**6**), isolated from the endophytic fungus *Microdiplodia* sp., can be seen in Figure 3.[12] Both experimental and calculated spectra are shown. Methods for calculating CD spectra will be discussed later in this Chapter.

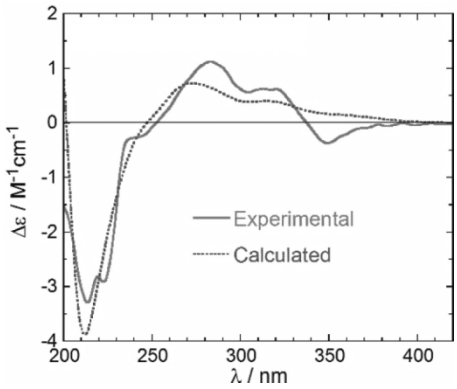

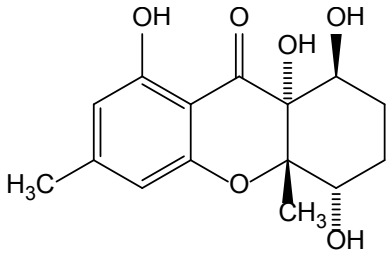

6

Figure 3. Experimental and Calculated CD Spectra of (+)-Diversonol (**6**).[12]

Interpreting a CD spectrum and relating the data to absolute configuration is sometimes straightforward but is also sometimes difficult, if not impossible. CD data alone do not provide a direct measurement of absolute configuration.[38] Comparison of CD curves to those of analogous compounds in which the absolute configuration has already been established, or combining CD data with additional analytical data of other types is typically employed in order to assign absolute configuration. Because CD data is related to molecular shape, it is often difficult to separate configurational from conformational factors, so rigid molecules tend to be somewhat more amendable to CD approaches.[15]

Traditionally, analysis of CD data involved application of various empirical and semi-empirical rules for individual molecule classes enable proposal of the stereochemistry of a molecule. Empirical and semi-empirical approaches are, in some cases, the simplest way of interpreting CD spectra, although their application has diminished in recent years as complimentary computational methods have emerged.[15] Evaluation of the Cotton effect (CE)[43-45] observed in the CD spectrum lead to the development of these well-established empirical "rules", which include the octant rules, first described by Djerassi *et al.* in 1960,[36,42] and the exciton chirality method, pioneered by Nakanishi, et al.,[42-45] which sometimes requires chemical derivatization of the compound in order to incorporate additional chromophores. Each of these methods are reviewed in detail in other publications,[36,42-45] so they are not addressed here, and neither is applicable to all cases.

In principle, any chiral compound that contains even a weak chromophore, such as a ketone, that absorbs in the UV-vis region of the spectrum (190-700 nm) is liable to show some features in its CD spectrum that are likely to be related in some way to absolute configuration. However, many such compounds do not have the structural features required to enable straightforward application of the above empirical "rules".

Over the past couple of decades, computational chemistry based on *ab initio* (first-principles) theory has gone from being a highly specialized endeavor to mainstream practice.[26] These first-principle methods can be used to predict, confirm, and even assign experimental data. Chiroptical data (i.e., CD and $[\alpha]_D$) can now be predicted using semi-empirical quantum mechanical methods such as density functional theory (DFT) or time-dependent DFT (TDDFT) for moderately complex molecules.[46-49] Thus, comparison of experimental CD spectra with spectra calculated using such methods offers an emerging method for non-destructive assignment of absolute stereochemistry, even for molecules that do not lend themselves well to analysis by empirical methods.

The calculations associated with determining energy minimized structures and then computing chiroptical properties are somewhat daunting for non-specialists. A wide variety of mathematical equations are used in the calculation of chiroptical properties, but detailed discussion of these protocols are beyond the scope of this thesis. Reviews and additional examples that contain in-depth mathematical descriptions of these methods can be found in the literature.[26,32,50-55]

The mathematical equations that are employed for these calculations include a wide variety of functionals, the most popular of which is B3LYP (Becke, 3-parameter, Lee-Yang-Parr implicit density functional).[53] Functionals comprise a map from a vector space (three-dimensional space) to the field underlying the vector space, (i.e., a functional takes a vector as the input and returns a scalar – a "projection"). In the quantum mechanics of chemical structures, this means that functionals search for a state of the system that minimizes the energy functional (i.e., they seek to determine a structure's global energy minimum). Other typically used functionals include PBE0,[56] BH&HLYP,[57,58] and BP86,[58,59] as well as basis sets such as TZYP,[60] aug-TZYP,[61] ADZP,[62] and aug-cc-pVDZ.[63] Basis sets are sets of linearly independent vectors that, in combination, represent all vectors for a given space or coordinate system. This allows the computational process to uniquely express every element ("atom in a molecule") within that space, thus allowing for structural identification of a molecule within the defined space.

Input parameters and various aspects of the state, conformation, stereochemistry, and flexibility of a given compound dictates how complex and computationally intensive these calculations will be. Even with the vast computer capabilities available today, calculations for energy minimization and subsequent CD spectra calculations at a suitable level of theory can take days. In addition, such calculations often prove reliable only on molecules of moderate size (~30 non-hydrogen atoms).[45,64,65] However, due to continued improvements in both hardware and software, and the availability of clusters, the time

spent on calculations can be substantially decreased. When taking into consideration the costs and benefits of being able to make absolute configuration assignments with the aid of calculations, this method is rapidly becoming a premier, and increasingly reliable, way in which to acquire such information.

A recent paper by Cachet, N., *et al.*,[66] exemplifies the benefits of TDDFT calculations. Parazoanthine A was isolated as a major constituent of the Mediterranean sea anemone *Parazoanthus axinellae*, and its structure was elucidated through the use of NMR spectroscopic and mass spectrometric analyses.[66] In order to assign the absolute configuration of parazoanthine A as either *S* (**7**) or *R* (**8**), a comparison was made between the experimental and TDDFT-calculated CD spectra. Both of the enantiomers were subjected to energy minimization and subsequent CD spectral calculations using the B3LYP/6-31++G functional approach (Figure 4).[66] The experimental CD curve of parazoanthine A exhibited a negative Cotton effect (CE) at 281 nm, and was therefore in agreement with the calculated CD spectrum of the *S*-enantiomer, enabling assignment of the structure of parazoanthine A as **7** (Figure 4).

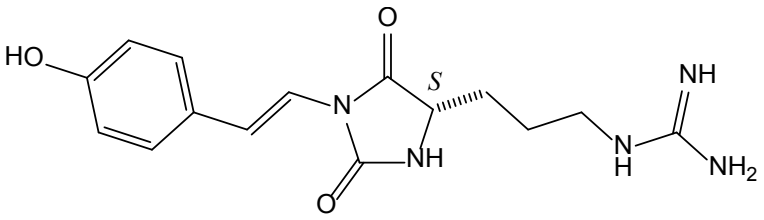

7

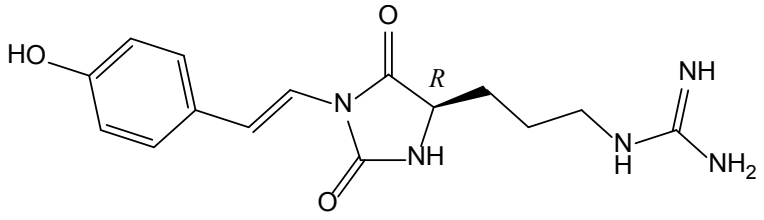

8

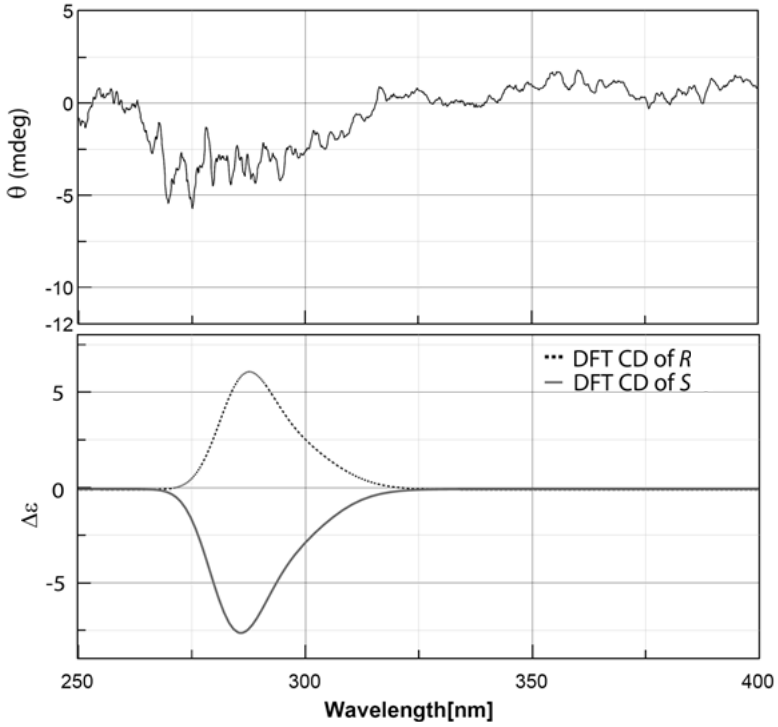

Figure 4. Experimentally Measured CD Spectrum of *S*-Parazoanthine A (**7**) (Top) and TDDFT-Calculated CD Spectra of the *S* (**7**) and *R* (**8**) Enantiomers (Bottom).[66]

CD spectra can be collected for samples in various physical phases, including gas, solid, and solution.[10,67,68] Each have their virtues and drawbacks when attempting to characterize natural products, but when it comes to utilizing calculations to assign the absolute configuration, a CD measurement in the solid state is far superior. The reasons for this are tied largely to the fact that a CD spectrum collected for a solution will be a weighted average of the contributions from all populated conformations, whereas in the solid state, especially in a crystalline lattice, configurations present tend to be much more homogeneous.[15] However, most of the time, natural products are available in only small quantities (and seldom tend to be crystalline), making solution spectra the only kind that can readily be obtained. Because of this, a large set of input structures must be considered in the calculations, and the results must be representative of the entire group. An obvious pitfall to this approach is the heavy reliance on calculations to determine

which conformers contribute to the overall spectrum and to what degree, before the CD spectra themselves can even be calculated. Once all conformers of interest are determined, CD calculations must then be run on each structure at the same level of theory, resulting in significant additional calculation time when the molecule being analyzed is flexible. Moreover, in order to deal with solute-solvent interactions, CD calculations require a solvent model to be considered,[64] adding further computation time and sophistication.

Compounds that are able to be crystallized and undergo X-ray analysis have inherent advantages to solute-solvent CD experiments. In the solid state, the overall structure is determined with a high amount of accuracy by X-ray single-crystal diffraction, and the molecular conformation is fixed (except for polymorphs).[15] Both of these advantages allow the prediction of the solid-state CD spectrum to be relatively straightforward because the conformation has already been determined, thereby avoiding the need for energy minimization calculations.[69,70] Thus, it is typical that one sees excellent agreement between experiment and theory in CD calculations for crystalline solids, allowing the absolute configuration to be assigned with higher confidence.

The absolute configuration assignment of tetrahydropyrenophorol (**9**), a bioactive secondary metabolite from an endophytic *Phoma* sp., using the solid-state/TDDFT methodology is a prime example of the difference in results obtained for solid state vs. solution state data. (Figure 5).[71] In this example, the experimental CD data collected in the solution state is more or less inverted from that of the experimental CD data collected in the solid state. This is caused by the extreme flexibility of the macrocycle in **9**, leading to a very different situation in the solution state. Through structure optimization using AM1 energy calculations, it was discovered that there were at least 60 conformers in solution that were within 3 kcal/mol of one another for **9**.[71] If one were to try and produce a calculated CD spectrum for all of the identified conformers in the solution state, and generate a relevant weighted average spectrum, it would be overwhelming

time-consuming. Because of this, TDDFT calculated ECD in the solution state was not included in the data given in Figure 5.[71] Clearly, having a molecule that can be analyzed in the solid, crystalline state can have tremendous advantages over analyzing a flexible compound in solution. In the case of **9**, such calculation enabled assignment of the absolute configuration shown. Even in the solid state, however, problems can arise that can hinder CD analysis and calculations.[72-75]

It is important to note that all of these approaches are still considered to provide an assignment, and such assignments are not always necessarily going to be correct, but in most cases that have been independently investigated by other methods, they generally turn out to be so.

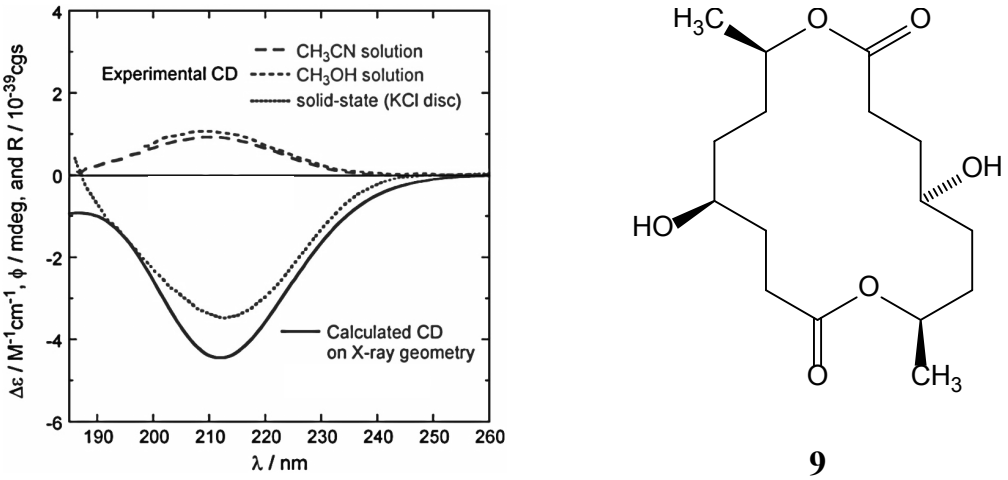

Figure 5. Solution and Solid-State CD Spectra of Tetrahydropyrenophorol (**9**), and TDB3LYP/TZVP-Calculated CD of the Conformation Reflected in its X-ray Structure.[71]

In the research described in this thesis, TDDFT calculation of ECD data, using functionals and basis sets described here, were employed in the assignment of the absolute configuration of the aflaquinolones (Chapter 3). A full description of that

process and results will be presented in Chapter 3. Such an approach may also ultimately be useful in assign the absolute configuration of emeridin A (Chapter 5) although further complexities are present in that case.

As was stated above, other chiroptical properties, such as $[\alpha]_D$, can also be calculated based on similar quantum mechanics functionals and mathematical equations used for CD calculations. Even calculation of theoretical CD spectra is a relatively new capability in the field, the ability of increasingly advanced calculations to predict stereochemistry directly from $[\alpha]_D$ would be beneficial, as $[\alpha]_D$ is a simpler measurement than CD and does not require the molecule have a particular chromophore. It has long been understood that one can relate $[\alpha]_D$ and its dispersion (ORD) to CD, and vice versa, through Kramers-Kronig (KK) transformations.[76-79] The KK transformations provide the foundation for determining absolute configuration of a compound directly from $[\alpha]_D$.

Through the application of simple mathematical equations, in tandem with *ab initio* TDDFT and gauge-invariant atomic orbitals (GIAOs),[50,80] Stephens, *et al.* have developed a methodology for calculating $[\alpha]_D$.[55] In doing so, they also used the hybrid functionals, mentioned above, as well as additional base functions. Using the sodium D line for measurements, they were able to establish an average deviation between calculated and experimental specific rotation of 20–25 degrees.[55] One obvious problem given these results is that molecules that have specific rotations less than 25 degrees, or values of similar magnitude would not be amenable to reliable analysis by this method. For example, an attempt was made to calculate the $[\alpha]_D$ of endo-isocamphane (**10**),[81] and a value of -11 was determined. When compared to the experimental value of +6.3 for **10**, the unreliability of this method is obvious.[81] However, when an attempt was made to calculate the $[\alpha]_D$ of prezizaene (**11**), originally isolated by Anderson and co-workers,[82] a value of +54 was determined, and when compared to the experimental value of +55 clearly demonstrating the promise this method could have in assigning the absolute configuration directly from $[\alpha]_D$ for small, rigid molecules. Overall, Stevens and co-

workers have been able to analyze 65 small, rigid compounds with varying degrees of accuracy, but a promising sign for the development of this method is that the majority of their calculated optical rotations for these molecules are at least the same sign as those reported for the corresponding compounds.[55]

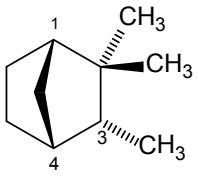

1*S*,3*R*,4*R*

10

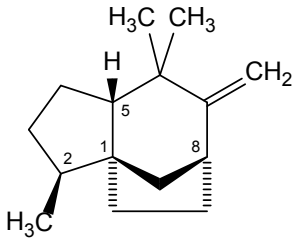

1*S*,2*S*,5*S*,8*R*

11

A review of different methods used to assign the absolute configuration directly from $[\alpha]_D$, including the implementation of coupled cluster (CC) theory, has been presented by Crawford, *et al*.[50] Beratan, *et al*.,[83-86] have applied such methods to natural products, including hennoxazole (**12**),[83] a marine natural product, plakortolide G (**13**),[85] a peroxylactone from the sponge *Plankinastrella onkodes* that exhibited potent activity against *Toxoplasma gondii*, and pitiamide A (**14**),[86] a metabolite isolated from an assemblage of *Lyngbya majuscula* and *Microcoleus* sp. cyanobacteria growing on hard coral.[87]

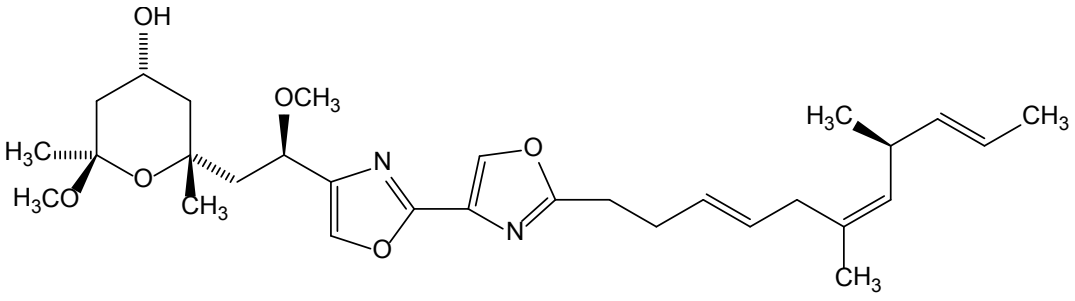

12

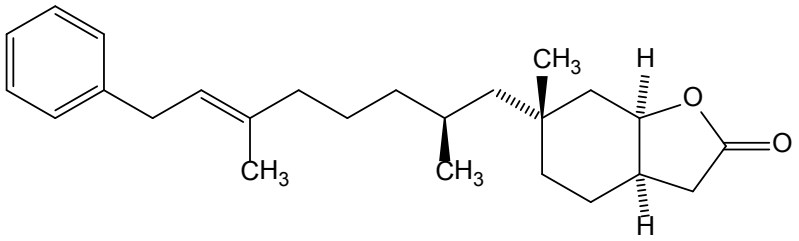

13

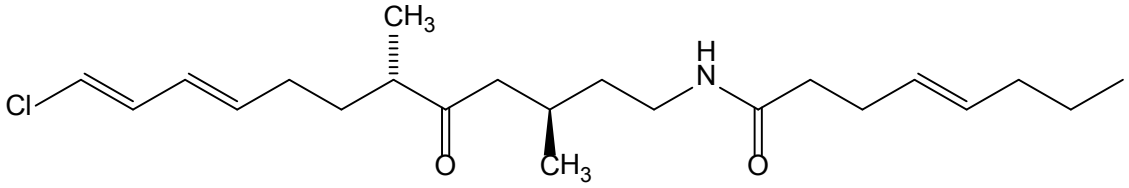

14

It is important to note that the protocols for determination of absolute configuration directly from $[\alpha]_D$ are in their infancy, even more so than the employed for CD calculations. The molecules in which these approaches have been tested upon are quite small, and the majority of the compounds tested are rigid. Even so, new ideas have already begun to emerge as improvements to the "old" methods. For example, recent studies have shown that using the Kohn-Sham density matrix method with London atomic orbital theory, rather than the relatively well-established Hartree-Frock method,[88,89] has shown promise when used with the B3LYP functional.[53]

As will be discussed in Chapter 3, we employed the use of calculations to estimate rotations of individual aflaquinolones, but the limitations mentioned above came into play in this effort. Most natural products are significantly larger than the test compounds typically used in developing these calculations, and they are far from rigid. Ultimately, CD calculations have advantages over $[\alpha]_D$ calculations in the inherent

measurement of values at many wavelengths, rather than a single wavelength data point. Thus, conclusions are based how an overall shape of a curve rather than how a single data point compares with a measured value.

This section has focused on providing a background summary of how chiroptical data, in combination with calculations based on quantum mechanics, can assist researchers in assigning absolute configuration of chiral natural products. These techniques are becoming invaluable to the characterization process for bioactive natural products because they provide new avenues for elucidating stereochemistry, which is traditionally one of the most difficult features of a structure to determine. The methods described provide non-destructive, and increasingly more accurate and less time-consuming methods to fully characterize stereochemical features of a wide variety of metabolites. The use of these techniques provided us with the ability to assign the absolute configuration of the aflaquinolones (Chapter 3) without having to destroy a significant portion of the limited amount of sample that was available.

Up to this point, this introduction has focused on the application of modern chiroptical methods in combination with computational methods to assign absolute configuration. Another substantial portion of this thesis (Chapters 7 and 8) discusses the details of the characterization of secondary metabolites from *Arachis hypogaea* (peanut) seeds that were challenged by the fungal species *Aspergillus caelatus*.[90-93] The remainder of this introduction provides a brief background on secondary metabolites previously isolated from *A. hypogaea*. Similarities between our chemical investigations of fungi and peanut seeds are evident, as both projects involve efforts to discover new bioactive natural products. However, the peanut research did not require detailed stereochemical investigations, and was facilitated to some degree by the background information available on previously described peanut metabolites summarized here.

Peanut crops are a significant source of income for local and state economies in the Southeastern United States. In 2010, the nation-wide peanut harvest brought in

nearly $1 billion.[94] Continued yields that are this high, or higher ($1.2 billion in 2008),[94] depend heavily on the crop's ability to resist invasion by fungi or other pests, especially during reproductive stages. Peanut plants naturally produce secondary metabolites that help to protect from outside invasion (phytoalexins). These antibiotic phytoalexins include both flavonoids and stilbenes.[95] One of the major functions of flavonoids in the peanut plant is to kill or inhibit the growth or reproduction of prospective pathogenic bacterial, fungal, and viral invaders, as well as protozoans.[95,96] Examples of flavonoids isolated from peanut plants include eriodicyol (**15**),[97] medicapin (**16**),[98] and quercetin-3-glucoside (**17**).[96]

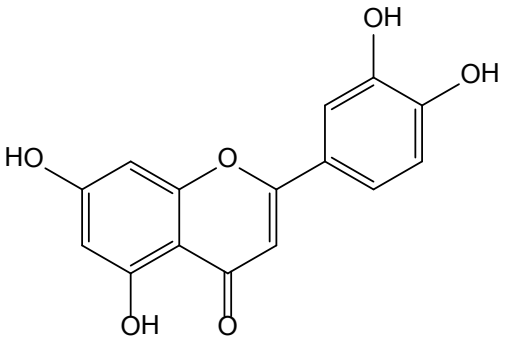

15

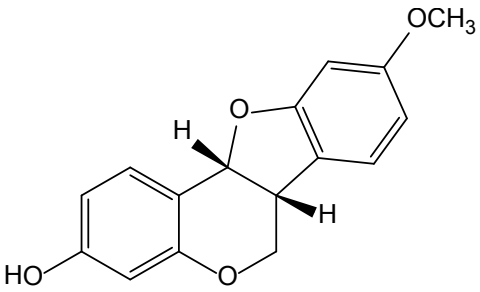

16

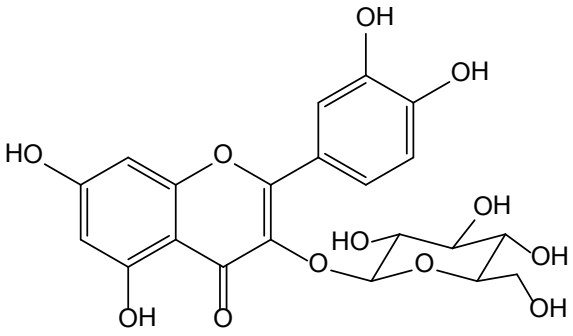

17

Peanut stilbenoids (stilbenoid phytoalexins) are similar to flavonoids in that they display varying levels of antifungal activity against *A. flavus*, *A. parasiticus*, and other fungi.[99-103] The biosynthetic pathway leading to the formation of these stilbene phytoalexins has been extensively studied.[95,104] In brief, the stilbenoid skeleton is biosynthesized from malonyl-CoA and *p*-coumaroyl-CoA and catalyzed by stilbene synthase (SS or STS), a well-known enzyme that carries out relevant condensation reactions.[95,104] Examples of stilbenoids isolated from *A. hypogaea* include mucilagin (**18**)[99] and piceatannol (**19**),[105] an anticancer compound. Other examples will be discussed in Chapters 7 and 8.

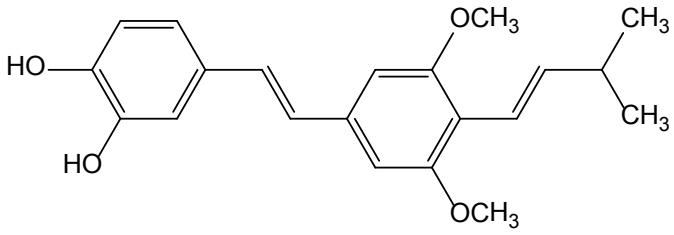

18

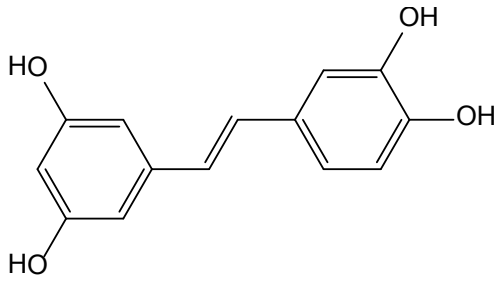

19

Other crucial components to the survival of the peanut plant are phenolic acids and various alkaloids. Phenolic acids have been linked to various functions, including nutrient uptake, protein synthesis, enzyme activity, photosynthesis, dormancy, and

allelopathy.[100] Examples of phenolic acids isolated from peanut seeds include chlorogenic acid (**20**) and chicoric acid (**21**).

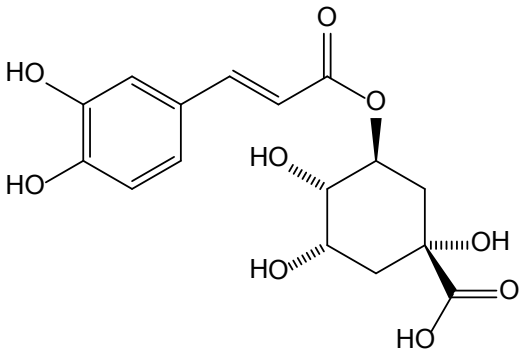

20

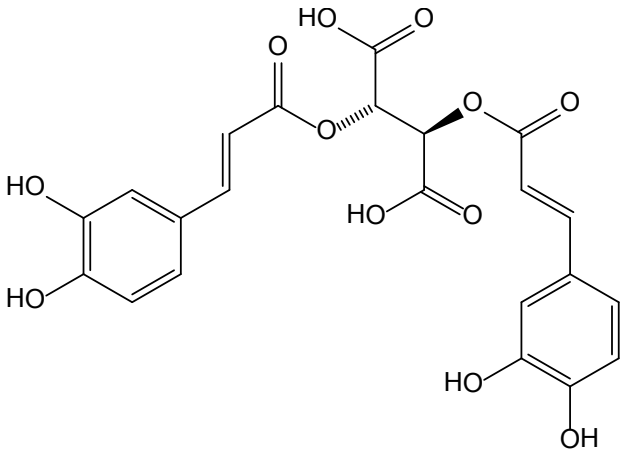

21

The most widely-recognized secondary metabolite isolated from peanuts is resveratrol (**22**).[106] Resveratrol (**22**), a stilbenoid, is one of the most well-known "heart-healthy", anti-oxidant, and (purportedly) cancer chemopreventative compounds in the human diet. It is perhaps most widely publicized as a constituent of red wine and grapes, but is present in similar abundance in peanuts.[107]

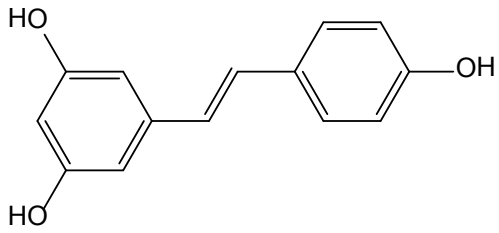

22

In peanuts (*A. hypogaea*) and other higher order plants, the accumulation of these stilbene phytoalexins are used for defense, protection, cell-to-cell signaling, and possibly other stress adaptations by the plant.[95] These compounds not only benefit the plant itself, but some of them have also demonstrated high antioxidant properties, as well as other benefits noted above, which could benefit human health. Production of some of these metabolites in peanuts, as well as other plants such as grapes and berries, can be upregulated through stress, such as wounding or temperature manipulations, on the plant.[95] In the research presented here, challenging peanut seeds with *A. caelatus* led to enhanced production of stilbenoid phytoalexins in the plant, thereby allowing isolation and characterization of novel stilbenes which could potentially be more effective as phytoalexins and/or beneficial to humans than the peanut stilbenoids currently known.

In summary, studies of five different fungicolous/mycoparasitic fungal isolates (Chapters 3, 4, and 6) and one endophytic fungal isolate (Chapter 5) will be described in this thesis. Some of the known bioactive compounds encountered in these studies will be summarized in Chapter 2. Additionally, a culture of the fungus *Aspergillus caelatus* was used to elicit the production of multiple new bioactive secondary metabolites from peanut seeds, studies of which are discussed in Chapters 7 and 8.

CHAPTER 2

SCREENING OF FUNGI

Most programs that seek to discover new bioactive fungal metabolites usually screen large numbers of uncharacterized fungal isolates that are collected at random. Individual isolates are then selected for chemical investigation on the basis of ensuing bioassay results. However, this approach often leads to frequent encounters with known compounds because different extracts may show similar activities due to the same common component. In any such work, efficient dereplication processes are needed in order to identify known compounds quickly and efficiently, leaving more time for the analysis of novel compounds.

Most of our ongoing research projects employ an ecology-based approach to explore the chemistry of fungi that compete with other fungi within specific ecological niches.[6,108] In certain types of fungal interactions, one or both of the competing fungi display antagonism towards the other. This can be caused by the production of chemical agents by one or both of the species that inhibit the growth of the other.[6] Mycoparasitic fungi are a group of fungal species that act as parasites of others, and the invaded fungi often suffer damage from this colonization, suggesting the possible production of antifungal metabolites by the mycoparasite.[6] A true parasitic relationship is difficult to prove in most cases,[109] and therefore the term "fungicolous" is used to describe a fungus found colonizing another, but for which a true parasitic relationship has not been unambiguously established.

Our group has shown that studies of fungicolous fungi can lead to the isolation of a variety of new bioactive fungal metabolites, including antifungal agents.[110-115] In the course of our ongoing studies of fungicolous/mycoparasitic fungi, several additional bioactive isolates were selected for chemical investigation in the work described here. Some of these produced known compounds, while others yielded new metabolites.

In order to obtain fungicolous isolates for investigation, field collections are performed primarily by a team lead by Dr. Donald T. Wicklow of the USDA, NCAUR in Peoria, Illinois. Collections are most often made from the surfaces of long-lasting fungal physiological structures such as stromata and basidiomata. The long-lived nature of these kinds of nutrient-rich fungal bodies makes them especially prone to colonization by fungicolous fungi. Fungicolous fungi are harvested from the surface of these structures and cultured on potato dextrose agar (PDA) slants. Individual colonies are subsequently isolated and cultured again until spores form. A spore suspension is then prepared and added to autoclaved rice for solid-substrate fermentation lasting approximately 30 days. The cultures are then extracted with EtOAc, and the resulting extracts are screened for activity in standard disk assays against the fungi *Aspergillus flavus* (NRRL 6541) and *Fusarium verticillioides* (NRRL 25457), as well as against *Spodoptera frugiperda* (the fall armyworm), an economically important crop pest. *A. flavus* is not only an opportunistic pathogen in humans,[116] but it is also known to produce crop-contaminating aflatoxins (carcinogenic metabolites),[117] while *F. verticillioides* is a plant pathogen that can damage cereal crops and produces fumonisins, which are also considered carcinogenic.[118]

In addition to screening fungicolous and mycoparasitic fungi, our research group also actively explores the chemistry of certain types of endophytic fungi.[119,120] Endophytes are fungi that occur within the tissues of plants, often without causing damage to the host. Our initial interest in fungal endophytes related to those found in corn plants because of the prominence of corn in the economy of the Midwest, and because endophytes of corn are underexplored. Corn (maize; *Zea mays* L.) is one of the most important grains grown in the United States, valued at over $66 billion for the 2010 harvest alone.[121] Iowa is the producer of approximately one fifth of the U.S. corn crop, making it especially important to our state's economy. Fungal endophytes have a widespread presence across plant taxa and frequently produce structurally and

biologically intriguing compounds. The presence of any such types of compounds in corn would take on added significance due to the likely exposure of livestock and humans, either directly or indirectly, to their various effects. Therefore, metabolites produced by these fungi in corn could be important to economics and public health.

Investigations of EtOAc extracts of both fungicolous/mycoparasitic and endophytic fungi that were selected for study, due to their initial bioactivity, typically begins by partitioning between acetonitrile and hexanes to partially de-fat the sample. A ^{1}H NMR spectrum of the acetonitrile-soluble portion is evaluated and if it is deemed to be potentially interesting, e.g., to consists of metabolites other than simple aromatics, lipids, or other well-known metabolites, it is further separated by NMR- and/or bioassay-guided fractionation to assist in isolation of the compounds of interest and the identification of known compounds that might be present. Dereplication of known compounds is accomplished through comparisons of collected NMR and MS data and evident partial structures to data available in-house and in commercial databases.[122,123] Ideally, this can be accomplished at an early stage before extensive efforts are undertaken. If no matches are encountered, the structures of the novel compounds are determined using various spectroscopic techniques, including 2D NMR and HRMS. Novel compounds that are isolated in sufficient amounts are tested for bioactivity.

Fifteen fungal extracts, including both endophytic and fungicolous isolates, were selected for chemical investigation based on initial bioassay results (Table 1). Of those fifteen, six of the isolates yielded various new secondary metabolites and the studies of these isolates are described in this thesis.

Table 1. Antifungal and Antiinsectan Bioassay Results for the EtOAc Extracts of Selected Fungicolous/Mycoparasitic (MYC) and Endophytic (ENDO) Fungal Cultures

Organism (Culture Number)	*Aspergillus flavus*[a]	*Fusarium verticillioides*[a]	*Spodoptera frugiperda*[b]
Chaetomium sp. (ENDO-3063)	mg/rg=21	cz/mz=8	na
Emericella nidulans (ENDO-3111)	mz=17 + rg=29	mz=17 + rg=23	90% rgr
Unidentified (ENDO-3191)	cz/mz=33	cz=33	50% rgr
Trichoderma longibrachiatum (MYC-1515)	mz=17	rg=57	25% rgr
Aspergillus sp. (section *Flavipedes*) (MYC-1580)	na	rg=33	>75% rgr
Unidentified (MYC-1645)	na	rg=21	na
Penicillium sp. (MYC-1729)	rg/mz=19	mz=23 + rg=27	na
Penicillium sp. (MYC-1805)	rg=33	rg/mz=25	75% rgr
Aspergillus puniaceus (MYC-1817)	cz=23	mz=17 + rg=31	75% rgr
Unidentified (MYC-1991)	na	mz/rg=23	na
Stachybotrys parvispora (MYC-2013)	na	mz=23	na
Penicillium sp. (MYC-2032)	cz=23 + mz=19	rg=21	na
Aspergillus sp. (section *Flavipedes*) (MYC-2048)	mz/rg=25wk	mz=17 + rg=37	75% rgr
Unidentified (MYC-2109)	cz=37	mz/rg=27	na
Aspergillus sp. (section *Flavipedes*) (MYC-2144)	na	mz=17 + rg=35	58%M; >75% rgr

[a]Antifungal assays were performed at test levels of 500 µg/disk (disk diameter = 12.5 mm; the diameters of the resulting inhibition zones are measured after 48 hr and given in mm). cz = clear zone (no growth throughout the zone from agar surface to the petri dish bottom); mz = mottled zone (mosaic of clear zone areas and appearance of patchy colony growth as a result of retarded development of small individual colonies); rg = reduced growth (fungus covers entire agar surface, but colony development is suppressed when contrasted with colony development outside the zone of inhibition); wk = weak; na = not active.

[b]Antiinsectan assays of crude extracts were usually performed at an approximate dietary level of 2000 ppm. Results are expressed as % rgr (reduced growth rate) relative to controls, and when appropriate, % M (mortality).

Studies of the remaining nine extracts, listed in Table 1, yielded only known metabolites from various classes. Twelve other extracts (not listed in the table) were not investigated after partitioning and preliminary ^{1}H NMR analysis due to the appearance of the spectrum. For example, if the data suggested the presence of only simple metabolites or fat (*Aspergillus clavatus* ENDO-3047, *Spegazzina tessarthra* ENDO-3107, *Paecilomyces variotii* ENDO-3135, *Fusarium chlamydosporum* ENDO-3172, and unidentified isolates MYC-1738, MYC-1750, and MYC-2148) the extract was abandoned. Results arising from studies of the extracts that yielded known fungal metabolites, but did not afford novel compounds, are discussed briefly below.

Chemical investigation of a *Penicillium* sp. (MYC-1805) that showed modest antifungal activity against *A. flavus*, *F. verticillioides*, and significant antiinsectan activity against the fall armyworm, afforded the known compounds pseudocitreoindole (**23**)[124] and cycloaspeptide A (**24**),[125] the latter being a major metabolite of the culture. Although diketopiperazines are commonly encountered as secondary metabolites, the occurrence of β-Phe is relatively rare.[124] Compound **23** was reported to show no activity against *A. flavus* (NRRL 6541) at 200 µg/disk or in various disk assays against *B. subtilis* (ATCC 6051), *S. aureus* (ATCC 29213), and *C. albicans* (ATCC 90029).[124] Cycloaspeptide A (**24**) is not considered to be antifungal or antibacterial,[125] but it does show modest antiplasmodial activity against the malarial parasite *Plasmodium falciparum.*[126]

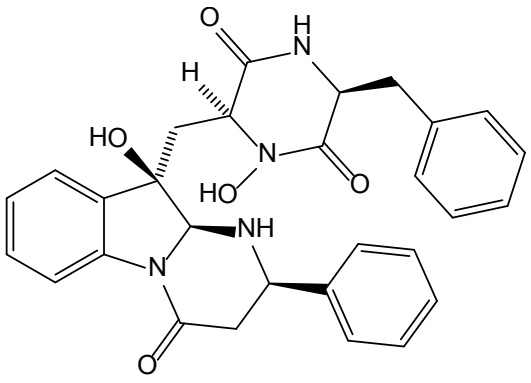

23

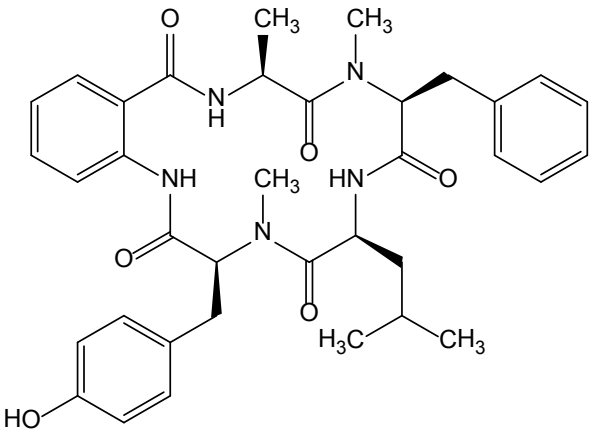

24

Studies of a cryptic *Aspergillus* sp. (section *Flavipedes*; MYC-2144) extract afforded the known compound *trans*-dehydrocurvularin (**25**)[127] as well as multiple compounds from the aspochalasin family, including aspochalasins C (**26**),[128] E (**27**),[129] I (**28**),[130] and J (**29**),[130] and TMC-169 (**30**).[131] The extract showed moderate antifungal activity against *F. verticillioides* but showed potent antiinsectan activity against the fall armyworm, killing 58% of the test insects while reducing the growth of the survivors by more than 75%. Compound **25** is known to display a wide variety of activities including antifungal,[132] and anti-tumor effects,[133] inhibition of plant pathogens,[127] and antibacterial activity against *Pseudomonas syringae.*[133] Members of the aspochalasin family are known to exhibit cytotoxicity against tumor cell lines[130,131] and antimicrobial activity against bacteria, fungi, and yeasts.[128,134] However, literature does not describe any antiinsectan activity for any of these compounds. Compound **25**, **28**, and **29** were also isolated from the organic extracts of MYC-2048 (Chapter 3) and MYC-1580 (Chapter 4), both of which were also cryptic *Aspergillus* sp. (section *Flavipedes*) extracts. The cause of the antiinsectan activity of this extract has yet to be accounted for, as these known bioactive compounds were not tested for antifungal activity against the fall armyworm at the time of this report.

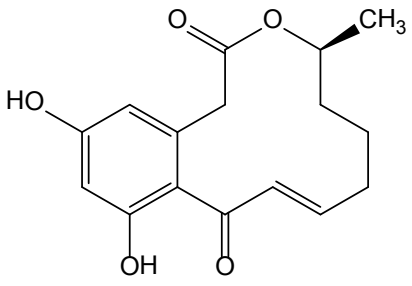

25

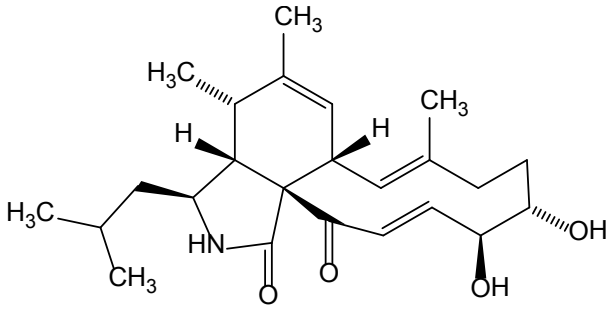

26

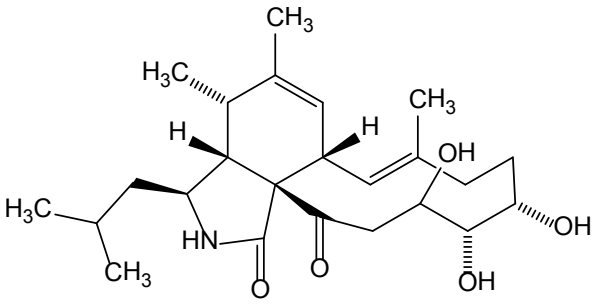

27

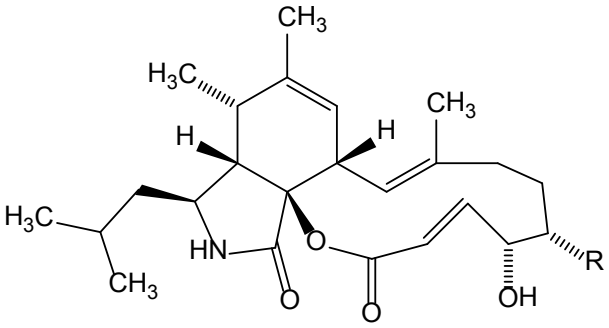

28 R = OH
29 R = H

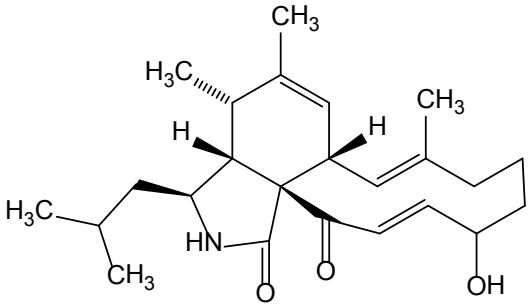

30

The extract from MYC-1729, a *Penicillium* sp., showed moderate antifungal activity against both *A. flavus* and *F. verticillioides*. Chemical investigations afforded the known compound citrinin (**31**)[135,136] as the major component of the extract. Citrinin (**31**) was originally isolated from the fungus *Penicillium citrinum* and has subsequently been isolated from other fungi. The compound is known to show phytotoxic activity.[137] Compound **31** showed activity in our assay against *F. verticillioides*, exhibiting an mottled inhibition zone of 22 mm after 48 hr when tested at 200 µg/disk. It also caused a limited reduction (16%) in growth rate relative to controls in assays against the fall armyworm when tested at a dietary level of 320 ppm.[138]

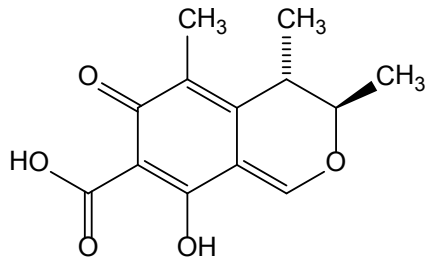

31

Chemical investigation of the extract of an unidentified fungal culture (MYC-2109) that showed antifungal activity against both *A. flavus* and *F. verticillioides*, afforded the well-known compound cyclosporin A (**32**)[139] as the major component. Compound **32** is an immunosuppressive agent that is used clinically after transplant surgery,[139-141] and it also possesses antifungal and antiinsectan activity.[140-142]

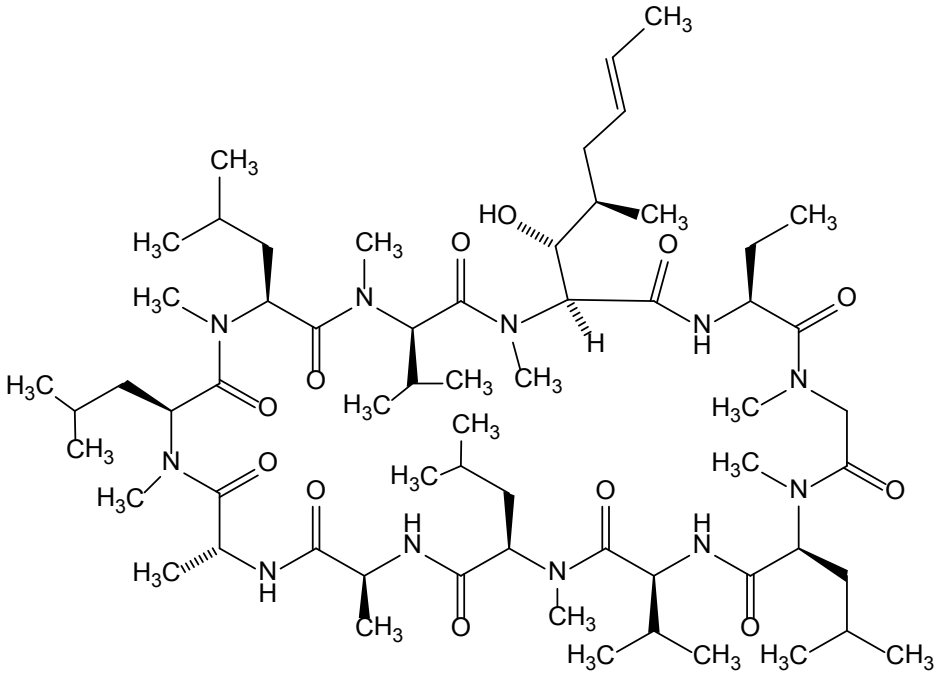

32

An *Apsergillus puniaceus* (MYC-1817) extract showed significant antifungal activity against *A. flavus*, as well as moderate antifungal activity against *F. verticillioides*. The extract also reduced the growth rate of the fall armyworm by 75%, when compared to controls in a dietary assay. Chemical investigation yielded the known compounds cinereain (**33**)[143] and dihydropergillin (**34**).[144] Compound **33** reportedly does not possess any antimicrobial activity,[145] but compounds **33** and **34** both show significant inhibition of the growth of wheat coleoptiles.[143,144] Although not a direct antifungal test, wheat coleoptile bioassays have been used to detect mycotoxins, immunosuppressants, and antifungal agents.[143] Literature for compounds **33** and **34** do not mention antiinsectan activity, so the component(s) responsible for the observed activity against the fall armyworm in the crude extract were not explicitly identified.

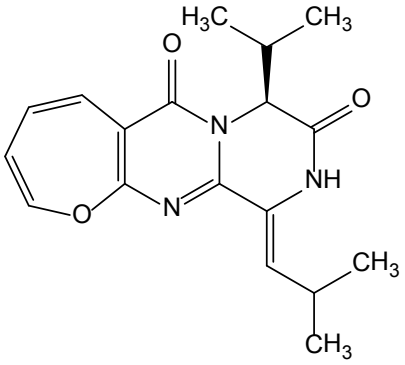

33

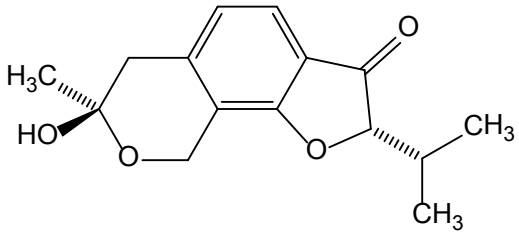

34

A fermentation extract from a *Chaetomium* sp. (ENDO-3063), isolated as a corn endophyte, showed modest antifungal activity against both *A. flavus* and *F. verticillioides*. The extract afforded multiple known compounds from the well-characterized chaetoglobosin family, including chaetoglobosins A (**35**)[141] and F (**36**).[141] Members of the chaetoglobosin family are well-known for having significant antifungal activity,[146] cytotoxicity,[147,148] antiinsectan activity,[149] and antibacterial effects.[146]

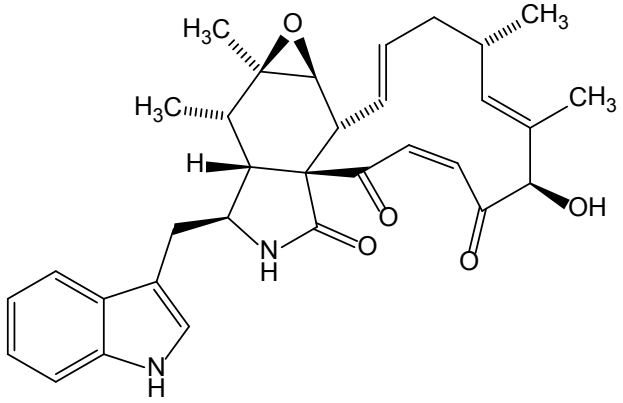

35

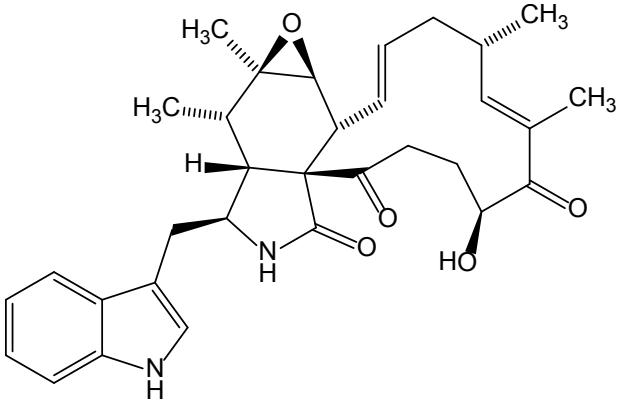

36

Investigations of an unidentified endophytic isolate (ENDO-3191) whose extract showed activity against *A. flavus* and *F. verticillioides* while reducing the growth rate of the fall armyworm by 50% were undertaken. The reversed-phase HPLC fractions of the acetonitrile-soluble portion of the initial partition contained significant amounts of equisetin (**37**), as indicated by ^{1}H NMR analysis.[150,151] Compound **37** is active against several strains of Gram-positive bacteria and at least one strain of Gram-negative bacteria (*Neisseria perflava*)[150] and reportedly has shown anti-HIV activity.[151] Compound **37**,

isolated from solid cultures of *Fusarium equiseti* FO-68, was also reported to possess antifungal activity against plant pathogenic fungi *in vitro* and *in vivo*.[152] The abundance of **37** in the extract is very likely to have been the cause of the moderate antifungal and antiinsectan activity observed in our assays.

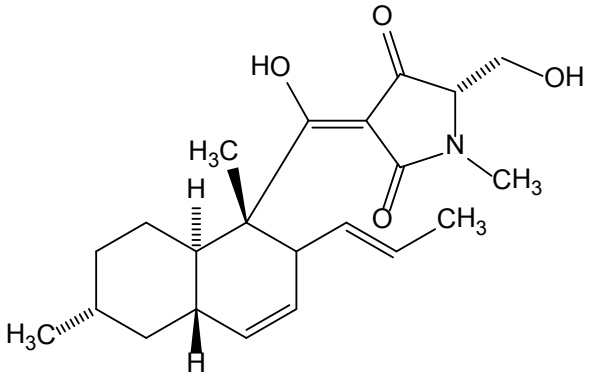

37

Studies of extracts of an unidentified fungicolous/mycoparasitic fungal isolate (MYC-1645) that showed modest activity against *F. verticillioides* resulted in the isolation of two known compounds; the cyclohexadepsipeptide pullularin A (**38**)[153] and verticillin D (**39**).[154] Compound **38** is known to display both antiplasmodial and antiviral activities.[153] Compound **39** showed antibacterial activity at 100 µg/disk in standard Petri-plate assays, causing inhibition zones ranging from 23 to 26 mm against *B. subtilis* (ATCC 6051) and 11 mm to 14 mm against *S. aureus* (ATCC 14053).[154] The compound responsible for the antifungal activity was not identified and further investigations were abandoned once these major components had been identified due to the limited activity seen in the crude extract.

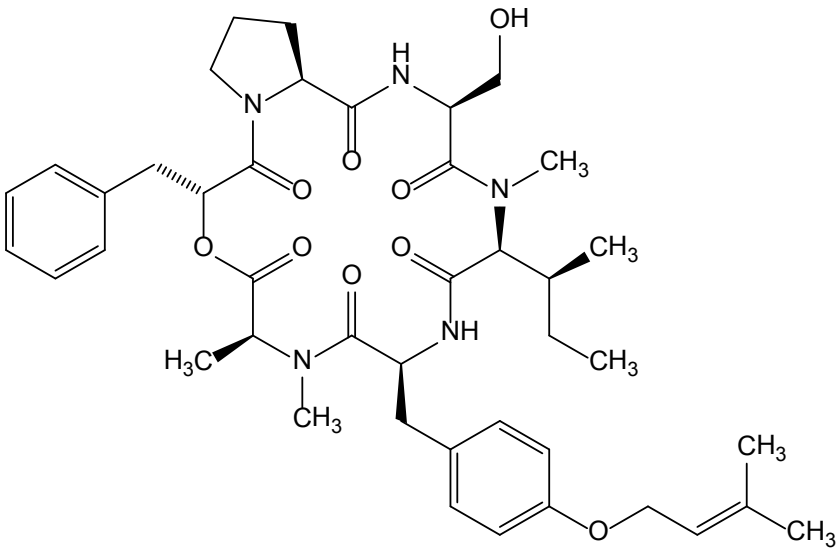

38

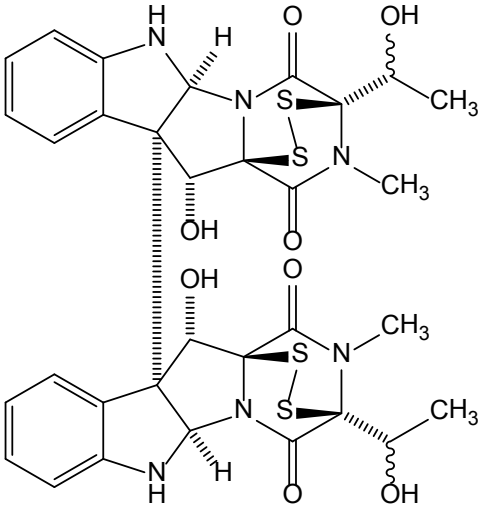

39

A *Penicillium* sp. isolate (MYC-2032) showed moderate antifungal activity against *A. flavus* and trace antifungal activity against *F. verticillioides*. Chemical investigations of this extract yielded the known compound cephalochromin (**40**).[155] Compound **40** comprised nearly the entire acetonitrile-soluble portion of the extract (870

mg). Cephalochromin (**40**) is a known compound that is often encountered during our research and it is known to possess antimicrobial activity against *S. aureus*, *B. subtilis*, and *Streptococcus pyogenes*.[155] However, to our knowledge, there have been no reports of antifungal activity for **40**. Compound **40** was not tested in our bioassays against fungi because the crude extract showed only relatively limited antifungal activity. While the presence of a minor component with antifungal activity is possible, the presence of such copious amounts of **40** in the extract would complicate their isolation and identification, therefore, further investigations were not pursued. The absolute configuration of **40**, only recently assigned, was established using the same TDDFT calculations described in Chapter 1 when compared to experimental ECD, optical rotation, and vibrational circular dichroism (VCD) data.[156]

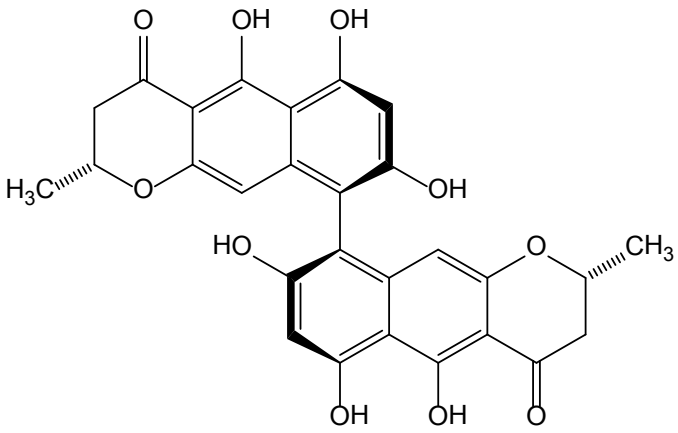

40

Chemical investigations of the extracts obtained from the other endophytic and fungicolous/mycoparasitic fungal isolates listed in Table 1 led to the isolation of novel metabolites, as well as some additional known compounds. The known compounds described here were identified through comparison of ^{1}H NMR, ^{13}C NMR, and/or MS data with literature values. Details of the isolation, structure elucidation, and biological

activities of the novel compounds from this research will be discussed in Chapters 3-6 of this thesis.

In addition to the work done with fungicolous/mycoparasitic and endophytic fungi, a collaboration with Dr. Victor Sobolev of the USDA National Peanut Research Laboratory yielded eight novel secondary metabolites from peanuts seeds. Two known metabolites that had not previously been reported as being produced by the peanut plant were also encountered. The structure elucidation and characterization of these metabolites will be discussed in detail in Chapters 7 and 8. The culturing and separation techniques used for the isolation of these metabolites are different from those employed in our own fungal metabolites work, and are also detailed in Chapter 10.

CHAPTER 3

ISOLATION AND CHARACTERIZATION OF AFLAQUINOLONES A–G: SECONDARY METABOLITES FROM FUNGICOLOUS AND MARINE ISOLATES OF *ASPERGILLUS* SPP.

Our long-term studies of fungi from a variety of ecological groups have resulted in the discovery of many new bioactive natural products.[6,111,120] Fungicolous and mycoparasitic isolates from Hawaii have been a productive source of such compounds over the last few years,[112-115] as have marine fungi. Chemical investigations of two isolates of *Aspergillus* sp. (Trichocomaceae) obtained from these two different habitats carried out independently in our laboratory and that of a collaborator led to the isolation of seven new dihydroquinolin-2-one-containing natural products that we named aflaquinolones A-G. These compounds are members of a known general class of fungal metabolites that includes aspoquinolones and penigequinolones.[157-159] Details of the isolation and structure elucidation of these compounds are presented here.

A culture of *Aspergillus* sp. (MYC-2048 = NRRL 58570) was obtained from a basidioma of *Rigdoporus microsporus* found on a dead hardwood branch in a Hawaiian alien wet forest. The fungus was cultured by solid-substrate fermentation on rice, and the EtOAc extract of the resulting fermentation mixture showed antifungal activity against *A. flavus* (NRRL 6541) and *F. verticillioides* (NRRL 25457) as well as the ability to reduce the growth rate of the fall armyworm (*S. frugiperda*) in a dietary assay. The extract was therefore subjected to chemical investigation (Figure 7), leading to the isolation of the known metabolites alantrypinone (**41**),[160] aspochalasins I (**28**) and J (**29**),[130] methyl-3,4,5-trimethoxy-2((2-((3-pyridinylcarbonyl)amino)benzoyl)amino)benzoate (**42**),[161] and *trans*-dehydrocurvularin (**25**),[127] all of which were identified by analysis of MS and NMR spectroscopic data in comparison with literature values.[127,130,160,161] Chemical

investigations also lead to the isolation of the novel compounds aflaquinolones A (**43**) and B (**44**).

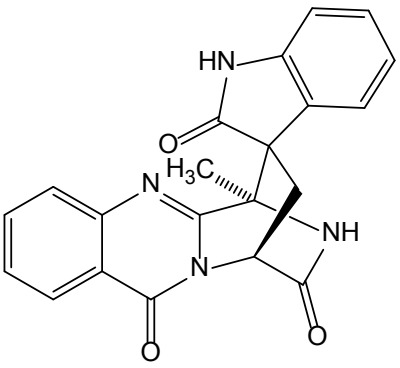

41

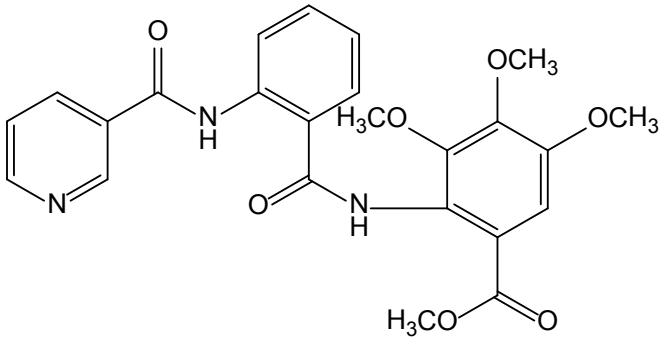

42

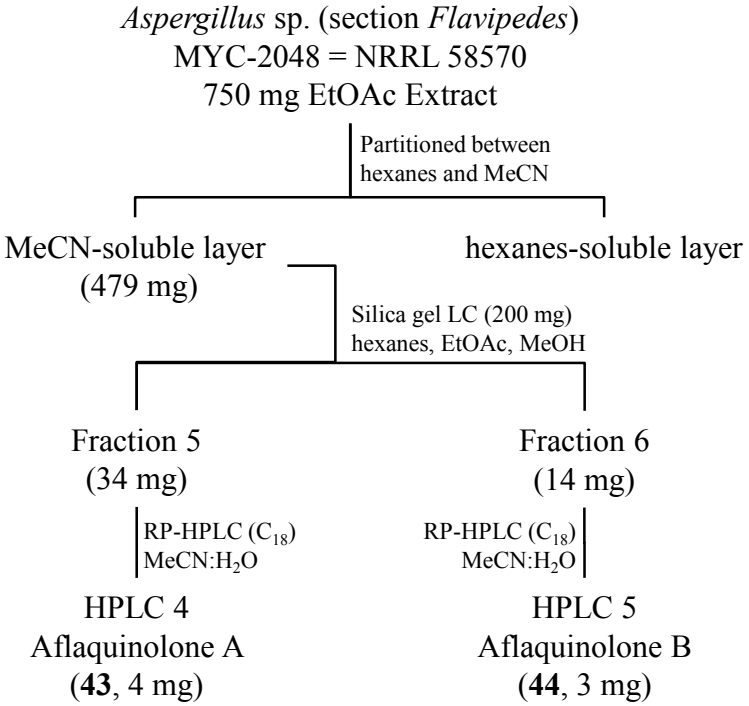

Figure 6. Isolation Scheme for Aflaquinolones A (**43**) and B (**44**).

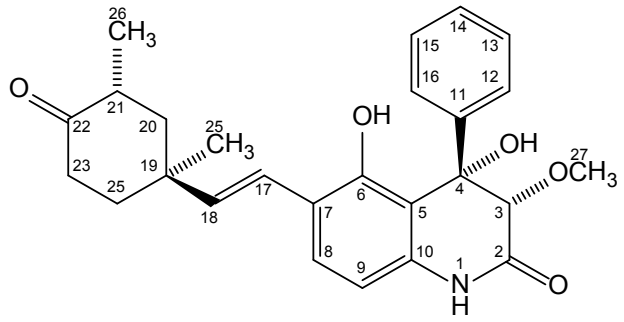

43

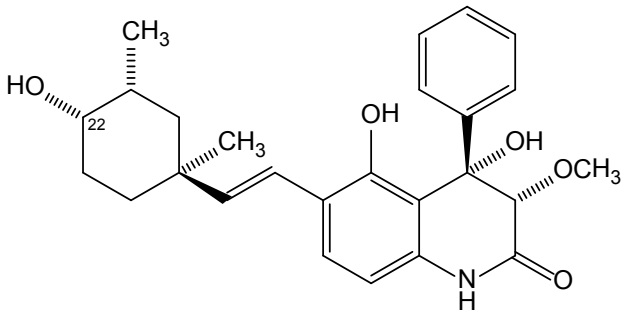

44

Structure Elucidation of Aflaquinolones A (**43**) and B (**44**)

Aflaquinolone A (**43**) was found to have the molecular formula $C_{26}H_{29}NO_5$ (13 unsaturations) on the basis of HRESITOFMS and NMR data. The ^{1}H NMR spectrum of **43** (Table 2) exhibited signals for a phenyl group, an isolated *trans* olefin unit, a pair of *ortho*-coupled aromatic protons indicative of a 1,2,3,4-tetrasubstituted benzene ring, an isolated amide NH, and three methyl groups, including one methoxy group. There were also numerous signals for diastereotopic methylene protons. ^{13}C NMR data (Table 2) revealed the presence of two carbonyl carbons (one ketone and one amide), 14 aromatic/olefinic carbons (corresponding to the two aromatic rings and the *trans* olefin), and two quaternary sp^3 carbons. Chemical shift data indicated that one of the aromatic ring carbons is oxygenated. The remaining eight carbon signals were located in the

aliphatic region of the spectrum. These units account for 11 degrees of unsaturation, requiring two additional rings to be present.

Table 2. ^{1}H and ^{13}C NMR Data for Aflaquinolones A (**43**) and B (**44**) in $CDCl_3$.[a]

	43		**44**	
position	δ_H (mult; J in Hz)	δ_C	δ_H (mult; J in Hz)	δ_C
1-NH	7.52 (br s)		7.44 (br s)	
2		165.1		165.2
3	3.67 (d, 1.5)	84.0	3.65 (d,1.5)	84.1
4		79.0		78.9
5		110.9		110.8
6		155.0		154.7
7		122.3		121.2
8	7.40 (d, 8.3)	127.2	7.35 (d, 8.3)	127.1
9	6.35 (d, 8.3)	106.9	6.32 (d, 8.3)	106.8
10		134.3		133.9
11		137.2		137.8
12/16	7.26 - 7.33 (m)	128.9	7.25 - 7.32 (m)	128.9
13/15	7.26 - 7.33 (m)	126.2	7.25 - 7.32 (m)	126.3
14	7.30 (m)	129.2	7.25 - 7.32 (m)	129.3
17	6.76 (d, 17)	122.5	6.58 (d, 17)	123.0
18	6.26 (d, 17)	135.9	6.06 (d, 17)	137.4
19		37.3		30.7
20_{eq}	2.09 (m)	47.5	1.32 - 1.45 (m)	40.0
20_{ax}	1.45 (t, 13)		1.32 - 1.45 (m)	
21	2.53 (dpent, 13, 6.0)	41.3	1.55 - 1.73 (m)	37.1
22[b]		213.7	3.72 (br q, 2.7)	70.1
23_{ax}	2.47 (ddd, 14, 14, 5.8)	38.6	1.55 - 1.73 (m)	32.4
23_{eq}	2.22 (ddd, 14, 4.5, 2.5)		1.55 - 1.73 (m)	
24_{eq}	2.13 (m)	38.4	1.55 - 1.73 (m)	31.7
24_{ax}	1.71 (td, 14, 4.5)		1.55 - 1.73 (m)	
25	1.09 (s)	30.4	1.01 (s)	30.1
26	0.96 (d, 6.4)	14.4	0.91 (d, 6.9)	18.3
27	3.60 (s)	58.9	3.59 (s)	58.9
4-OH	4.60 (s)		4.58 (s)	
6-OH	9.08 (s)		9.02 (s)	

[a]Data collected at 400 MHz (^{1}H) or 100 MHz (^{13}C). Carbon signal multiplicities were established by DEPT experiments and are consistant with the assignments. [b]A 22-OH signal for compound **44** was not observed in the ^{1}H NMR.

The structure of the dihydroquinolone portion of **43** was established by analysis of 2D NMR data and through comparison to a known series of compounds that includes the aspoquinolines and penigequinolones.[157-159] HMBC correlations from the H-12/H-16 signal for the phenyl group to C-4; from the isolated oxymethine H-3 to C-2, C-4, C-5, and C-11; and from the amide NH to C-5 and C-10 were consistent with the corresponding features of the structure of aspoquinolone C (**45**), albeit without the *para*-methoxy group on the aromatic ring substituent.[157]

The remaining portion of the structure was significantly different from those of the aforementioned compounds. HMBC correlations of H_3-25 to C-20 and C-24, and correlations of H_3-26 to C-20 and C-22, with the last remaining methylene unit (C-23) bridging C-22 and C-24, complete a cyclohexane ring, accounting for the remaining unit of unsaturation. This ring was connected to the *trans* olefin unit at C-18 on the basis of correlations of H-17 and H-18 to C-19, and of H_3-25 to C-18. Finally, the two main structural units of **43** were linked on the basis of HMBC correlations of both *trans* olefinic protons to C-7 to complete the gross structure as shown. Additional HMBC data were fully consistent with this conclusion. The differences in structures relative to those of the aspoquinolones led to the proposal of the distinct name aflaquinolone A for **43**. However, the numbering system shown is consistent with that of the aspoquinolones.[157]

Analysis of NOESY data and ^{1}H NMR *J*-values enabled assignment of the relative configuration of each half of **43**. The dihydroquinolone unit of **43** exhibited NMR shifts and *J*-values virtually identical to those of the aspoquinolones. In addition, the appearance of the H-3 signal as a doublet long-range-coupled to the NH (J = 1.5 Hz) matched a characteristic signal described for these compounds in the literature.[157] NOESY results for this structural unit were also analogous to those previously reported. Key NOESY data included correlations of H-3 with signals for both the phenyl group and the 4-OH (requiring H-3 to be pseudoequatorial), as well as a correlation from the methoxy group (C-27) to the 4-OH, all of which are consistent with literature

observations for molecules having the relative configuration shown for **43** at C-3 and C-4.[159] The relative configuration of the left-hand portion of **43** was assigned on the basis of NMR *J*-values (Table 2) and NOESY data (Figure 8). A NOESY correlation between H_3-26 and H-18 placed the C-26 methyl group and the *trans* olefin on the same face of the cyclohexanone ring, while H_{ax}-21 exhibited a large *trans*-diaxial coupling (J = 13 Hz) with H_{ax}-20, supporting this assignment. NOESY correlations involving H_{ax}-21, H_{eq}-20, and H_3-25 indicated that all three are on the same face of the ring, placing CH_3-25 in an axial orientation. Further correlations from H_{ax}-23 with both H_3-25 and H_{ax}-21 supported these conclusions. The equatorial protons at C-20 and C-24 showed correlations to H-17 and H-18, respectively, verifying their placement on the same face as the C-17/C-18 *trans* olefin unit. On the basis of these data, the cyclohexanone unit of **43** was assigned the relative configuration shown. However, no NOESY correlations were observed that enabled relative stereochemical correlation of the cyclohexanone and dihydroquinolone portions of the molecule.

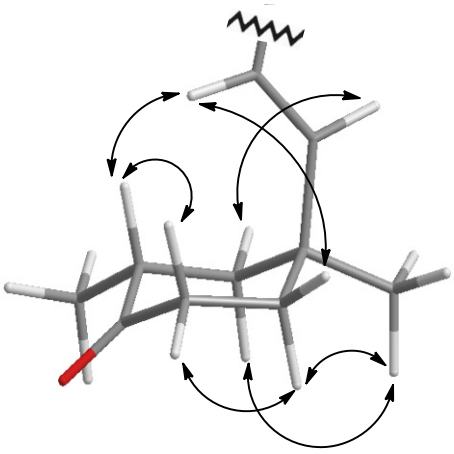

Figure 7. Key NOESY Correlations of the Cyclohexanone Unit of Aflaquinlone A (**43**).

Electronic circular dichroism (ECD) data were collected for **43** and matched closely with the spectrum of the literature compound peniprequinolone (**46**),[159] a member of this class with a simple prenyl substituent at C-7 and a *para*-methoxyphenyl group in place of the phenyl group of **43**. A simpler, co-occurring metabolite in the same report lacking the prenyl group also afforded an ECD curve of similar shape.[159]

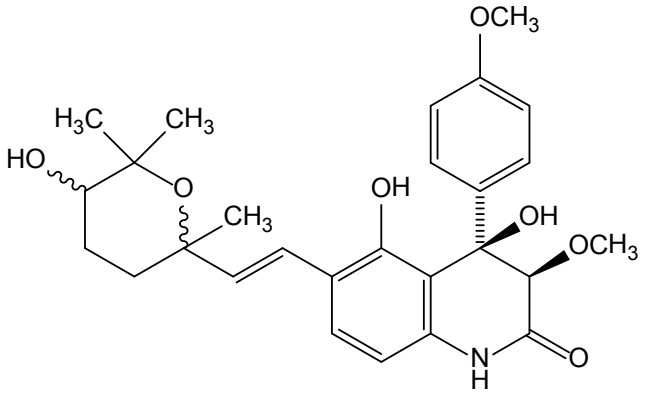

45

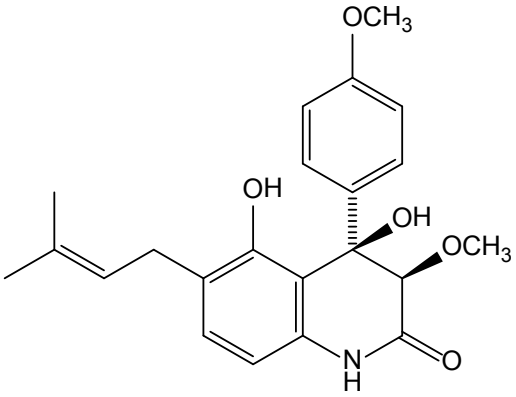

46

The similarity in ECD data among these compounds suggested that the shape of the ECD curve is dictated largely by the configuration of the dihydroquinoline unit, and that these three compounds all share the same absolute configuration in that portion of the molecule. However, the literature does not offer definitive assignment of absolute configuration for a member of this class, and the structure does not lend itself well to

stereochemical analysis by standard empirical methods. Ultimately, TDDFT computational methods proved to be helpful in making a stereochemical assignment.

After geometry optimization of each possible isomer of **43** to obtain minimum energy conformers, TDDFT-calculated, smoothed ECD spectra were generated for each and compared with the experimental data (Figure 9). Comparison of the experimental and calculated spectra for **43** showed excellent agreement for the 3*S*, 4*S*-absolute configuration at C-3 and C-4 in **43**, regardless of the choice of configuration for the cyclohexanone portion of the molecule. Both the calculated and experimental data spectra showed a pair of positive CEs above 275 nm, a negative CE near 250-260 nm, and a positive CE below 220 nm. These close similarities enabled assignment of the absolute configuration for the dihydroquinoline unit of **43** as shown. However, those of the remote terpenoid-derived portion could not be assigned by these methods. This issue is addressed further below.

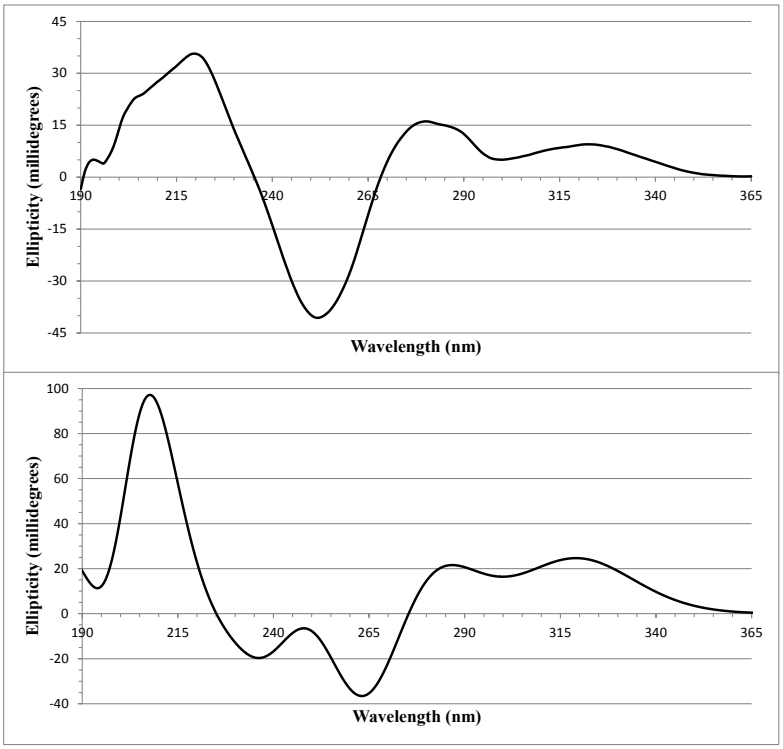

Figure 8. Experimental ECD Curve (Top) and TDDFT-Calculated ECD Curve (Bottom) for Aflaquinolone A (**43**).

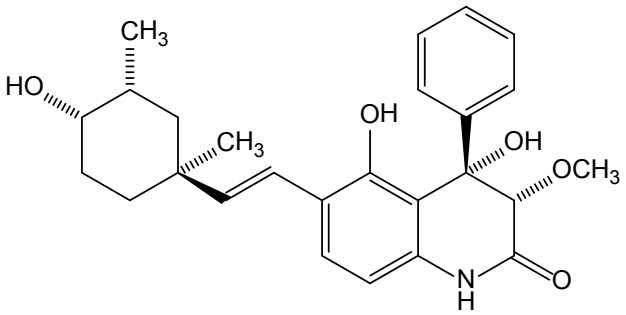

44

Compound **44** was assigned the molecular formula $C_{26}H_{31}NO_5$ (12 unsaturations) on the basis of HRESITOFMS and NMR data. The structure of **44** was nearly identical to that of **43**. The main difference was evident in the absence of a ketone signal in the ^{13}C NMR spectrum, the appearance of ^{1}H and ^{13}C NMR signals for an oxymethine unit (CH-22), and associated changes in shifts and multiplicities of nearby diastereotopic protons (Table 2). These observations indicated that **44** differs from **43** by reduction of the C-22 ketone unit to a secondary alcohol moiety. Some of the key ^{1}H NMR *J*-values were difficult to measure due to overlap in the upfield region, but a spectrum in acetone-d_6 afforded better resolution of these signals. The resulting data indicated that the axial proton at C-20 showed a large *trans*-diaxial-type coupling (13 Hz) to H-21, indicating that H-21 must be axially oriented, and placing the C-21 methyl group in an equatorial position. The oxymethine signal (H-22) shows only small couplings, with a large *trans*-diaxial coupling clearly absent, thereby placing H-22 in an equatorial position, and indicating that the new C-22 hydroxyl group adopts an axial orientation. A NOESY correlation between the axial H-21 with H-17 of the disubstituted olefin unit required these two units to be on the same face of the molecule, thereby setting the relative configuration at C-19. Other NOESY data (Figure 10) were consistent with these relative stereochemical assignments. The data also showed correlations for the dihydroquinolone

moiety that matched those observed for **43**, enabling assignment of the analogous relative configuration at C-3 and C-4.

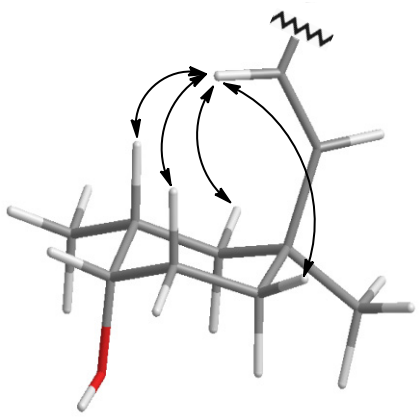

Figure 10. Key NOESY Correlations for the Cyclohexane Unit of Aflaquinolone B (**44**).

The ECD spectrum collected for **44** (Figure 11) was virtually identical to that of **43**, enabling assignment of the analogous 3*S*, 4*S*-absolute configuration to the dihydroquinolinone portion of the molecule. Unlike compound **43**, the presence of the secondary alcohol moiety on the terpenoid-derived unit of **44** suggested that the absolute configuration of this portion of the molecule could be assigned through the use of Mosher's method.[25] Treatment of **44** with *R*-(-)-MTPA-Cl (*R*-(-)-α-methoxy-α-(trifluoromethyl)phenylacetyl chloride) or *S*-(+)-MTPA-Cl (*S*-(+)-α-methoxy-α-(trifluoromethyl)phenylacetyl chloride) in the presence of dry pyridine-d_6 and $CDCl_3$ afforded the *S*-MTPA ester (**44a**) or *R*-MTPA ester (**44b**), respectively. Formation of the esters was confirmed by the significant downfield shift of the signal for H-22 in each case, and the appearance of the expected new aromatic and methoxy signals in the ^{1}H NMR spectra. The analysis was complicated somewhat by the formation of minor products arising from a second acylation at the phenolic OH group. However, assignment of ^{1}H NMR signals for relevant portions of **44a** and **44b** was accomplished by

comparison with the data for **44**, and verified by ^{1}H-^{1}H decoupling experiments. The resulting Δδ values observed for key signals of **44a** and **44b** (Figure 12) were consistent with the *S*-configuration at C-22, leading to assignment of the overall absolute configuration shown for **44**. The absolute configuration for the cyclohexanone unit of **43** was then proposed as shown by analogy to **44**. The name aflaquinolone B is proposed for compound **44**.

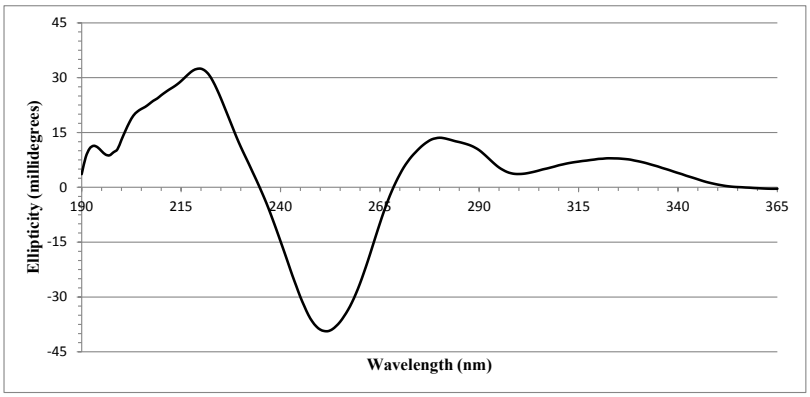

Figure 10. Experimental ECD Spectrum of Aflaquinolone B (**44**).

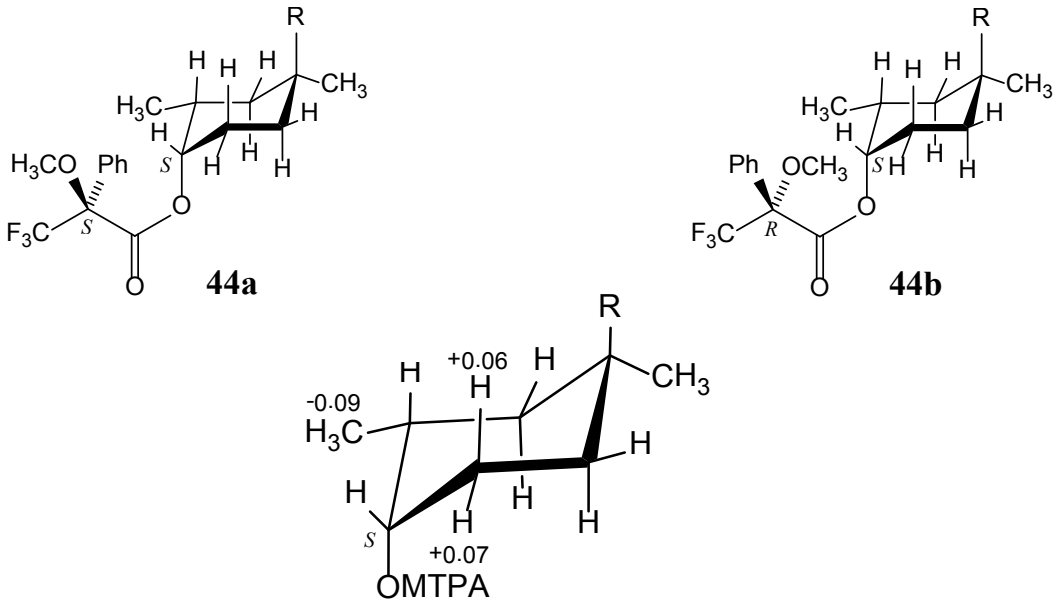

Figure 11. Observed Chemical Shift Differences ($\Delta\delta = \delta_S - \delta_R$, ppm; 400 MHz) for the *S*- (**44a**) and *R*-MTPA (**44b**) Esters of Aflaquinolone B (**44**).

In an effort to chemically correlate **43** and **44** to further support the above conclusions, attempts were made to oxidize **44** to **43** under mild conditions using TPAP/NMO. Unfortunately, the approaches employed led to decomposition and did not succeed in providing detectable product. More extensive efforts toward this end were hampered by sample limitations. However, treatment of **43** with $NaBH_4$ afforded a mixture of alcohol products, one of which gave NMR signals and chromatographic properties identical to those of **44**.

Structure Elucidation of Aflaquinolones C-G (**47-51**)

In the course of this work, it came to our attention that colleagues at another institution had independently encountered and identified members of the same class of compounds from a marine isolate of *Aspergillus* sp. (SF-5044), including one metabolite that initially appeared to be identical to **43**. Because of this overlap, a decision was made to pool our efforts in the characterization of these metabolites. Earlier studies of this marine isolate led to isolation of an unrelated set of compounds.[162]

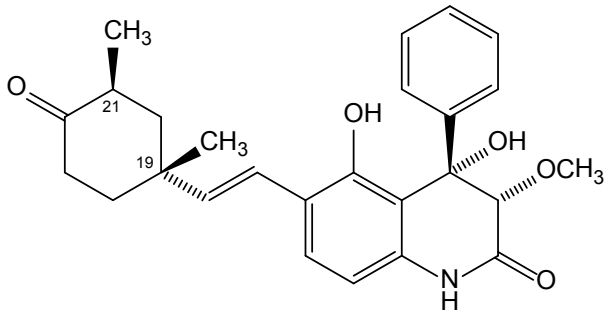

47

The first of these compounds, aflaquinolone C (**47**) was assigned the same molecular formula as **43** on the basis of HRESIMS data, and was initially thought to be identical to **43**, as the structure and relative configuration of the two stereochemically

insulated portions of the molecule were found to be identical to those of **43** by independent analysis of COSY, HMBC, and NOESY data, as well as ^{1}H NMR *J*-values. Moreover, direct comparison of the ^{1}H and ^{13}C NMR shifts for the two compounds (as measured for both samples in acetone-d_6) were identical (Table 3).

Table 3. NMR Spectroscopic Data for Aflaquinolones C (**47**) and D (**48**) in Acetone-d_6.[a]

	47		**48**
position	δ_H (mult; *J* in Hz)	δ_C	δ_H (mult; *J* in Hz)
1-NH	9.36 (br s)		9.40 (br s)
2		166.4	
3	3.67 (s)	85.8	3.66 (s)
4		80.1	
5		112.2	
6		156.1	
7		122.0	
8	7.52 (d, 8.3)	127.9	7.44 (d, 8.4)
9	6.60 (d, 8.3)	107.8	6.58 (d, 8.4)
10		137.2	
11		140.3	
12/16	7.34 - 7.37 (m)	129.6	7.31-7.38 (m)
13/15	7.34 - 7.37 (m)	127.5	7.31-7.38 (m)
14	7.34 - 7.37 (m)	129.8	7.31-7.38 (m)
17	6.83 (d, 17)	123.6	6.64 (d, 17)
18	6.44 (d, 17)	135.9	6.24 (d, 17)
19		37.9	
20_{eq}	2.13 (m)	48.3	1.89 (m)
20_{ax}	1.45 (t, 13)		1.54 (t, 13)
21	2.58 (dq, 13, 6.4)	41.7	2.69 (dq, 13, 6.6)
22		212.1	
23_{ax}	2.51 (dt, 14, 6.3)	39.1	2.62 (dt, 14, 7.3)
23_{eq}	2.15 (m)		2.17 (m)
24_{eq}	2.11 (m)	39.3	1.86 (m)[a]
24_{ax}	1.71 (dt, 14, 4.4)		1.81 (m)[a]
25	1.11 (s)	30.8	1.43 (s)
26	0.92 (d, 6.4)	14.9	0.94 (d, 6.6)
27	3.52 (s)	58.9	3.51 (s)

[a]Data collected at 400 MHz (^{1}H) or 100 MHz (^{13}C). [a]These assignments may be interchanged.

However, despite the virtually identical ECD spectra obtained for the two samples, the specific rotation values recorded under identical conditions were of somewhat different magnitudes and, more importantly, of opposite sign. These observations led to the hypothesis that **43** and **47** have the same dihydroquinolinone unit absolute configuration, and the same relative configuration in the cyclohexanone ring, but have opposite absolute configurations at both stereocenters in the latter unit. This would make the two compounds diastereomers of one another, but because the two stereogenic features in the structures are well insulated from one another, they might be expected to possess virtually identical NMR data. Their specific rotations might well differ, even though their ECD curves might match.

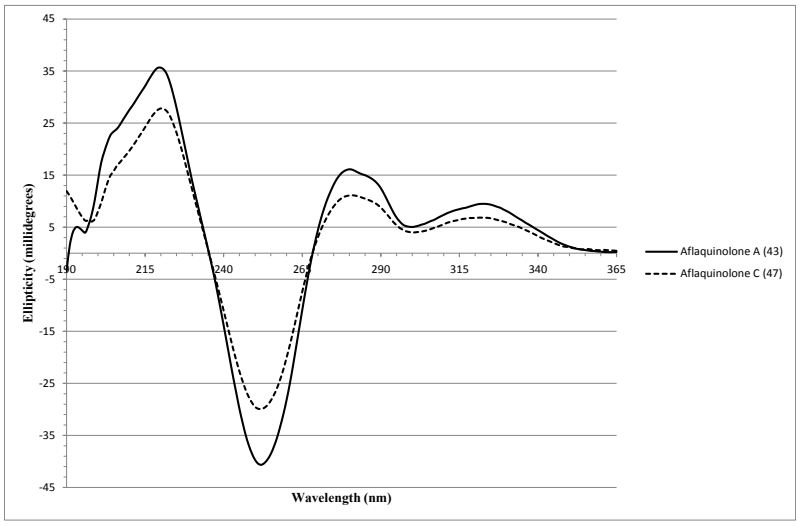

Figure 12. Combined Experimental ECD Curves for Aflaquinolone A (**43**) and C (**47**).

Indeed, a mixed sample of **43** and **47** gave a single ^{1}H NMR spectrum (acetone-d_6), as well as a single peak by HPLC analysis on three different stationary phases. While our inability to resolve the two isomers was unexpected, the reproducible difference in the sign (and magnitude) of optical rotation for **43** and **47**, together with the

accompanying virtually identical ECD spectra could not be explained in any other way. Isolation of reduced analogue **44** from the same source as **43**, and the assignment of its absolute configuration by Mosher's method as noted above led us to propose that **43** has the absolute configuration analogous to that of **44**, thereby enabling proposal of the opposite cyclohexanone unit absolute configuration for **47**, as shown.

The ^{1}H NMR spectrum of aflaquinolone D (**48**), another isomer of **43** and **47** as established by HRESIMS data, was almost identical to those of **43** and **47** except for some further chemical shift variations of signals corresponding to the C-17 to C-26 portion of the molecule (Table 3). Therefore, **48** was suggested to be another stereoisomer of compounds **43** and **47**.

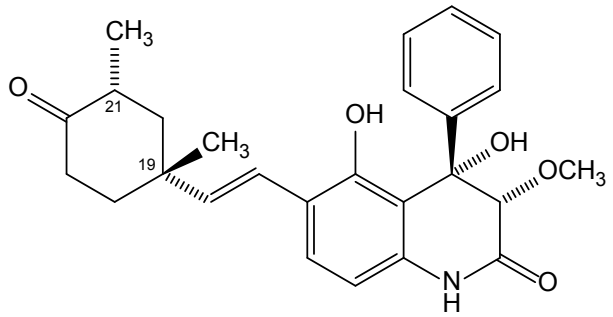

48

Detailed analysis of 1D- and 2D-NMR data supported the conclusion that **48** has the same planar structure as **43** and **47**, and NOESY correlation of H-3 with the aromatic protons of the phenyl group, along with ECD analysis, indicated that the quinolin-2-one unit in **48** has the same absolute configuration as in compounds **43**, **44**, and **47**. However, comparisons of the NOESY data and *J*-values of **48** with those of **43** and **47** revealed a difference in relative configuration in the cyclohexanone unit. A *trans*-diaxial *J*-value (13 Hz) for H-21 and H_{ax}-20 again indicated an axial orientation for H-21 and an

equatorial orientation for CH_3-26. However, in this instance, the H-21 signal showed a NOESY correlation with H_3-25, rather than H-17 as in **43**, **44**, and **47**, placing CH_3-25 in an axial orientation *cis* to H-21 and *trans* to CH_3-26. Correlations of H_{ax}-20 with H-18 and H_3-26 were consistent with location of all of these protons on the same face of the cyclohexanone ring. Therefore, aflaquinolone D (**48**) was assigned as a diastereomer of **43** and **47** possessing an inverted configuration at one of the centers in the cyclohexanone ring. The structure shown for **48** displays an inverted orientation at C-21 (α to the ketone carbonyl) relative to that of **47**, but the other possible diastereomer (i.e., with inversion at C-19 instead) could not be ruled out. Unlike the case for **43** and **47**, an isomer with the same relative configuration in the cyclohexanone unit that would have enabled an analogous comparison was not obtained from the fungicolous fungal culture, and sample limitations precluded further study of the issue for this compound.

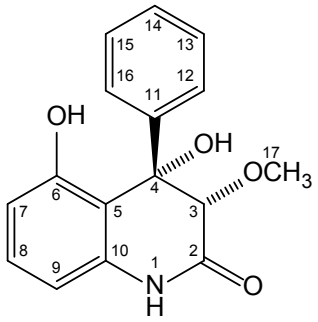

49

The molecular formula of aflaquinolone E (**49**) was established as $C_{16}H_{15}NO_4$ on the basis of HRESIMS analysis and NMR data, making it significantly smaller than compounds **43**, **44**, **47**, and **48**. Analysis of the ^1H and ^{13}C NMR data for **49** and comparison with those of compounds **43**, **44**, **47**, and **48** suggested that **49** retains the phenylquinolin-2-one skeleton, but lacks the terpenoid side-chain appended to the

aromatic ring in **43**, **44**, **47**, and **48**. The planar structure of **49** was readily determined by independent analysis of 1D- and 2D-NMR data (Table 4).

Table 4. ^{1}H and ^{13}C NMR Data for Aflaquinolones E-G (**49-51**) in CD_3OD.[a]

	49		**50**		**51**	
position	δ_H (mult; J in Hz)	δ_C	δ_H (mult; J in Hz)	δ_C	δ_H (mult; J in Hz)	δ_C
2		169.1		172.7		172.6
3	3.64 (s)	86.3	4.76 (s)	75.8	4.58 (s)	76.6
4		79.9		78.7		78.2
5		113.0		130.1		132.4
6		159.1	6.71 (dd, 7.8, 2.1)	130.1	7.53 (dd, 7.7, 1.2)	127.6
7	6.45 (d, 8.0)	108.1	6.90 (t, 7.8)	124.0	7.11 (t, 7.7)	124.8
8	7.14 (t, 8.0)	131.0	7.25 (dt, 7.8, 1.4)	130.6	7.29 (dt, 7.7, 1.2)	130.1
9	6.53 (d, 8.0)	113.2	6.95 (d, 7.8)	117.0	6.95 (d, 7.7)	116.8
10		138.1		138.4		136.7
11		140.9		143.2		141.5
12/16	7.24-7.29 (m)	127.6	7.51 (d, 7.5)	128.3	7.34 (d, 8.0)	128.6
13/15	7.26-7.31 (m)	129.6	7.39 (d, 7.5)	129.0	7.19-7.25 (m)	128.7
14	7.26-7.31 (m)	129.8	7.32 (t, 7.5)	128.4	7.19-7.25 (m)	128.7
17	3.52 (s)	59.2				

[a]Data collected at 400 MHz (^{1}H) or 100 MHz (^{13}C).

NOESY correlation of H-3 with the aromatic protons of the phenyl group again indicated that **49** possesses a relative configuration analogous to those found in the quinolin-2-one moieties of **43**, **44**, **47**, and **48**, and the ECD spectrum was again very similar to the same compounds, aside from a modest blue shift in wavelength values, indicating analogous absolute configuration as well. In fact, the similarity in ECD spectral shape among all five of these compounds strongly supports the conclusion that the quinolin-2-one moiety is dominant in dictating the shape of the ECD curve, regardless of the presence or absence of side-chains like those found in **43**, **44**, **47**, and **48** and any stereocenters that might be associated with them (Figure 14).

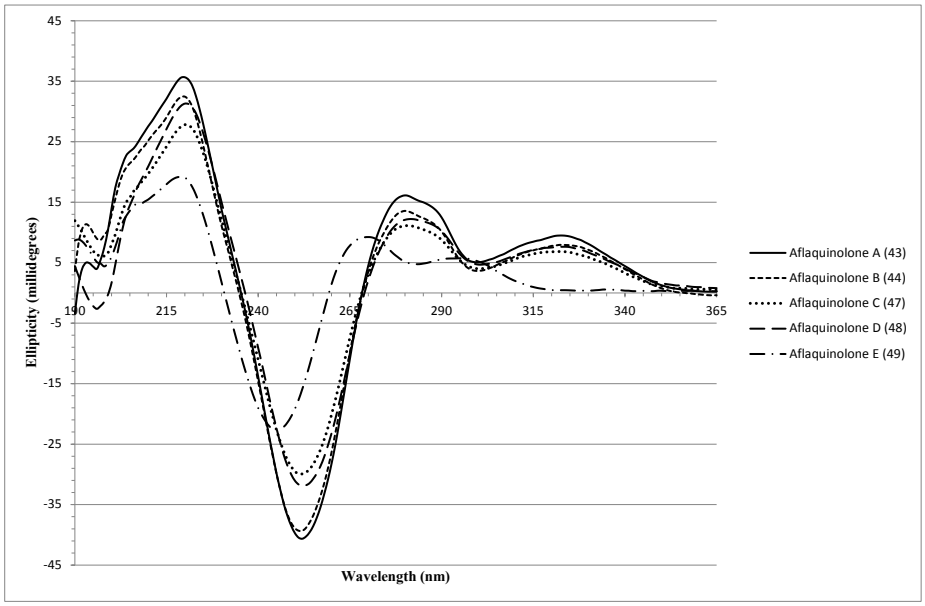

Figure 13. Combined Experimental CD Curves for Aflaquinolones A-E (**43**, **44**, **47**-**49**).

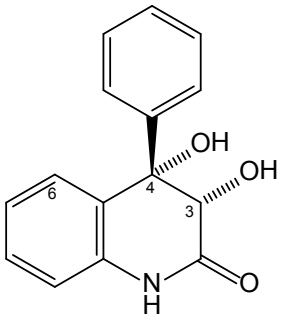

50

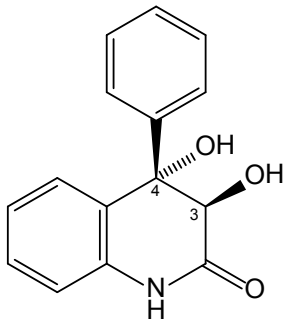

51

HRESIMS data established the molecular formula $C_{15}H_{13}NO_3$ for both aflaquinolones F (**50**) and G (**51**). ^{1}H and ^{13}C NMR data of **50** and **51** showed almost identical patterns with some minor chemical shift variations. Comparison of these data with the ^{1}H and ^{13}C NMR data for **49** indicated replacement of the phenolic OH group with an additional aromatic proton, and also revealed the absence of the methoxy group

(Table 4). These observations led to the proposal that **50** and **51** are diastereomers of one another, each having a 3,4-dihydroxy-4-phenyl-3,4-dihydro-2(1*H*)-quinolinone structure. Detailed analysis of 2D-NMR data confirmed this proposal. The relative configurations of **50** and **51** were determined by analysis of NOESY data. NOESY correlation of H-3 with the aromatic protons of the phenyl group in **50** indicated a *cis* arrangement of the two hydroxyl groups in **50**, thus leading to assignment of the same relative configuration found in the quinolin-2-one moieties of **43**, **44**, and **47**-**49**. In order for **51** to be a diastereomer of **50**, a *trans* orientation of the two hydroxy groups is required, and this assignment is consistent with the absence of a NOESY correlation between H-3 and the protons of the phenyl group in the data for **51**. A literature search revealed that similar spectroscopic patterns were observed for the two diastereomers of 3,4-dihydroxy-4-(4'-methoxyphenyl)-3,4-dihydro-2(1*H*)-quinolinone.[163]

Comparison of the ECD spectra of **50** and **51** with that of **49**, the closest relative among the other metabolites encountered, showed some differences in both cases. However, as might be expected given the relative configuration assignments for **50** and **51**, the data for **50** more closely resembled those of **49**, as both compounds show a positive CE at approximately 270 nm, a negative CE near 250 nm, and a strongly positive CE below 230 nm. By contrast, the ECD data for **51** included a negative CE at 286 nm not present in any of the spectra for compounds **43**, **44**, and **47**-**50**, although other ECD features retained some resemblance with those of **43**, **44**, and **47**-**50**. Thus, while the absolute configuration of **50** was assigned to match those of **43**, **44**, and **47**-**49**, that of **51** (the only metabolite encountered in this study with a *trans* orientation of the oxygen substituents at C-3 and C-4) could not be assigned with confidence by comparison of the experimental ECD curves. In an effort to resolve this ambiguity, we again employed computational methods to calculate ECD spectra for the two possible enantiomers of **51**. The results (Figure 15) showed a much better match for the C-3 epimer of **50** than for its enantiomer, resulting in assignment of the 3*R*,4*S*-configuration shown in **51**.

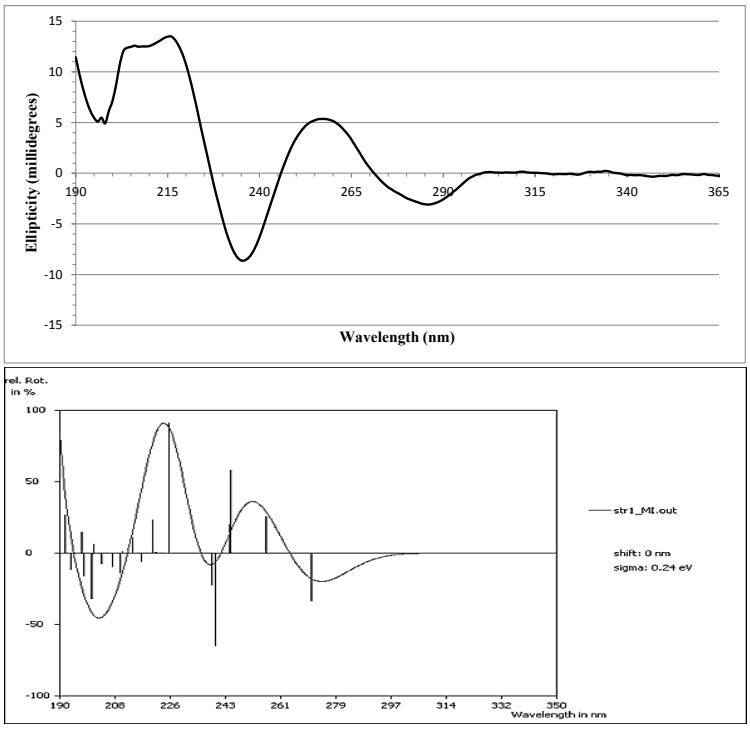

Figure 14. Experimental ECD Spectrum (Top) and TDDFT-Calculated ECD Spectrum (Bottom)for Aflaquinolone G (**51**).

Biogenetically, compounds **43**, **44**, and **47-49** appear likely to be derived from one unit each of anthranilic acid and phenylalanine, along with two isoprene units via processes analogous to those proposed for the aspoquinolones and the penigequinolones,[157-159] although these precedents would presumably incorporate tyrosine rather than phenylalanine, and also have some significant differences in the arrangement/cyclization of the ten-carbon unit appended to the aromatic ring of the quinolinone unit. Compounds **49-51** lack the prenyl units, but would otherwise be similarly constructed. In view of the results described here, it is likely that ECD could be readily applied to assignment of the absolute configuration of the dihydroquinolone portions of other members of this class. In some cases, comparison with data provided in

the literature now enable such an assignment.[159] However, establishment of the configurations of any centers that are remote from this unit remains a complicated issue, and would still require independent analysis on a case-by-case basis.

The fungicolous *Aspergillus* isolate from Hawaii (MYC-2048 = NRRL 58570) was initially suggested to be *Aspergillus flavipes* (section *Flavipedes*) on the basis of morphological characteristics. However, DNA sequence information and subsequent BLAST queries of GenBank produced a 100% match with an undescribed species of *Aspergillus* sp. NRRL 32683 (= MYC-1580 = NRRL 58569), another isolate from our own collection that was shown to be most closely related to *Aspergillus aureofulgens* section *Flavipedes* (NRRL 6326).[164] The NRRL 6326 isolate was originally described from truffle soil in France.[164] Its occurrence in truffle soil is intriguing because this environment is also suggestive of a possible fungicolous origin.

Neither compounds **43** nor **44** showed bioactivity that would account for the initial activity seen in the extract of the Hawaiian isolate. However, numerous known compounds were also encountered in the extract, including compounds **25**, **28**, **29**, **41**, and **42**.[127,130,160,161] The presence of these bioactive compounds, along with their abundance in the extract, likely explains the bioactivity originally observed. The aflaquinolones were evaluated for growth inhibitory activity against chronic myelogenous leukemia cells (K562), murine melanoma cells (B16F10), human acute promyelocytic leukemia cells (HL-60), human breast cancer adenocarcinoma cells (MDA-MB-231), and hepatocellular carcinoma cells (Hep3B) using *in vitro* cell viability assays, although **48** was not tested due to sample limitations. As shown in Table 5, aflaquinolone C (**47**) was the most active, showing weak inhibitory activity against all five cell lines, with IC_{50} values ranging from 36.4 to 62.2 μg/mL. On the other hand, the simpler quinolin-2-one analogues **49-51** showed little or no inhibitory activity against these cells up to the 100 μg/mL level, which may indicate that the terpenoid side chain plays an important role in the cytotoxicity of these compounds.

Table 5. Growth Inhibitory Activity of Compounds **43**, **44**, **47**, and **49-51** on Tumor Cell Lines.

	IC_{50} (μg/mL)[a]					
Cell Line	**43**	**44**	**47**	**49**	**50**	**51**
K562	63.9	> 100	62.2	> 100	> 100	82.5
B16F10	38.3	80.9	40.2	> 100	> 100	> 100
HL-60	72.2	> 100	36.4	> 100	89.8	80.7
MDA-MB-231	> 100	> 100	49.3	> 100	> 100	> 100
Hep3B	71.7	> 100	43.5	> 100	> 100	> 100

[a]The concentrations of compounds needed to inhibit cell growth by 50% relative to controls.

CHAPTER 4

CHEMICAL INVESTIGATIONS OF A CRYPTIC FUNGICOLOUS ISOLATE OF *ASPERGILLUS* SP. (SECTION *FLAVIPEDES*) (MYC-1580 = NRRL 58569)

Our ongoing studies of fungicolous and mycoparasitic fungi have resulted in the discovery of numerous novel bioactive natural products.[6,110,111] Hawaiian isolates have been a productive source of such compounds over the last few years.[112,115,138] Chemical investigation of an undescribed *Aspergillus* sp. (section *Flavipedes*) from Hawaii (MYC-1580 = NRRL 58569) led to the isolation of two novel peptides (**52** and **53**). Asperlarin A (**52**) incorporates an unusual 3-hydroxy-2-aminobenzoic acid (HABA) unit, and this uncommon unit is new among compounds isolated from fungi in our group and has rarely been reported as a constituent of any natural product.[165] Flavipeptide A (**53**) is a cyclic tetrapeptide peptide that bears close resemblance to the cyclic pentapeptide cycloaspeptide A (**24**).[125] Known bioactive metabolite PF1233B (**54**) was also isolated from the extract. Literature data for this compound were incomplete,[166] but complete data were gathered for our sample, and are presented here. In addition, alantrypinone (**41**),[160] aspochalasins I (**28**) and J (**29**),[130] curvularin (**55**),[167] four curvularin analogues (**25**, **56**-**58**),[127,168] and an asteriquinone-like compound (**42**)[161] were also encountered in the extract and identified by comparison of spectral data with literature values. Details regarding the isolation and structure elucidation of asperlarin A (**52**), flavipeptide A (**53**), and PF1233B (**54**) constitute the main focus of this chapter.

The fungicolous fungal isolate MYC-1580 was obtained from a basidioma of *Earliella scarbrosa* found on a dead hardwood branch collected in a Hawaiian alien wet forest. The fungus was cultured by solid-substrate fermentation on rice, and the EtOAc extract of the resulting fermentation mixture showed antifungal activity against *F. verticillioides* as well as the ability to reduce the growth rate of *S. frugiperda* (fall

armyworm). Due to these bioactivities, the extract was subjected to chemical investigation, leading to the isolation of **52**-**54** (Figure 15).

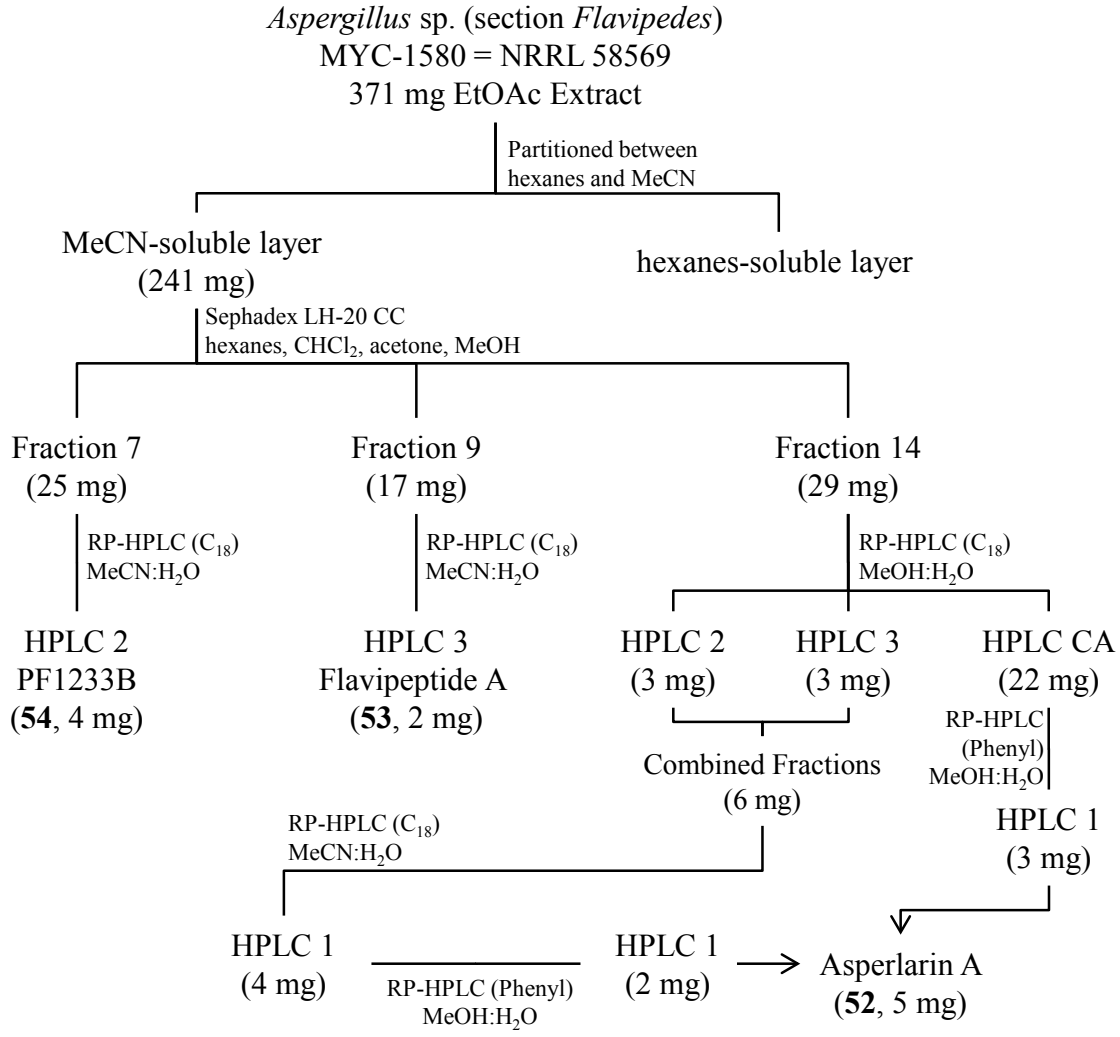

Figure 15. Isolation Scheme for Metabolites **52**-**54** from MYC-1580.

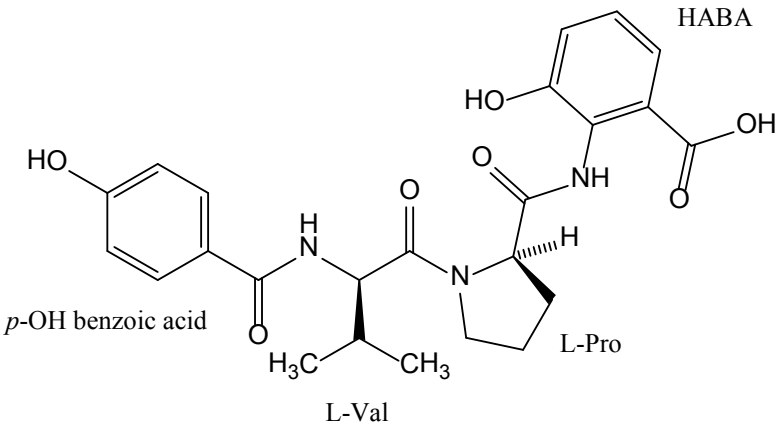

52

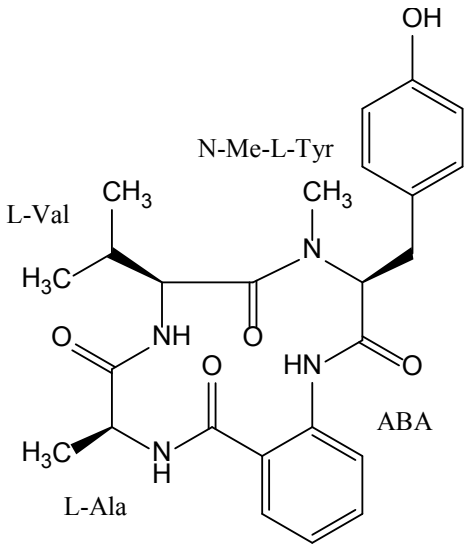

53

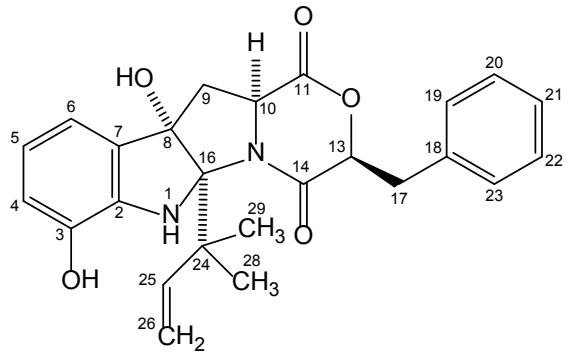

54

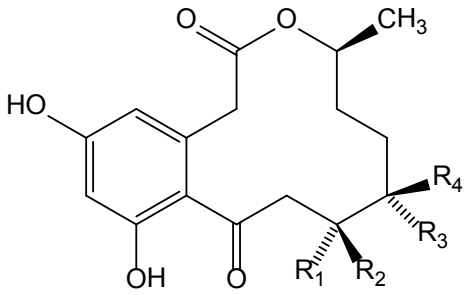

55: $R_1 – R_4 = H$
56: $R_1 = OH$, $R_2 – R_4 = H$
57: $R_1/R_3/R_4 = H$, $R_2 = OH$
58: $R_1/R_2 = H$, $R_3/R_4 = O$

Structure Elucidation of Asperlarin A (**52**) and Flavipeptide A (**53**)

Sequential application of solvent partitioning, Sephadex LH-20 column chromatography, and reversed phase HPLC (Figure 15), afforded novel compounds **52-54**. Compound **52** was found to have the molecular formula $C_{24}H_{27}N_3O_7$ (13 degrees of unsaturation) on the basis of NMR and HRESITOFMS data. The ^{1}H NMR spectrum of **52** (Table 6) exhibited signals for an oxygen-substituted *p*-disubstituted benzene ring, a 1,2,3-trisubstituted benzene ring, as well as signals characteristic of the common amino acids valine (Val) and proline (Pro). In addition to the signals expected for Val and Pro, the ^{13}C NMR spectrum (Table 6) revealed the presence of two carboxy carbonyl carbons and 12 aromatic carbons, two of which were oxygenated. These units account for all 13 degrees of unsaturation; indicating that **52** is a linear molecule.

HMBC data (Figure 16) and chemical shift considerations revealed the presence of a *p*-hydroxybenzoyl group which, in turn, acylates the Val unit. Determining the remaining connectivity of the molecule was hindered somewhat because the compound was insoluble in both $CDCl_3$ and acetone-d_6. Because we preferred not to risk sample loss by attempting to dissolve the compound in DMSO, **52** was dissolved in methanol-d_4 for analysis, resulting in the exchange of all hydroxyl and amide protons, making sequence-relevant 2D NMR correlations sparse. The only HMBC correlation observed (Figure 16) that assisted in connecting these units was a correlation between the α-proton of the Val unit (δ 4.62) to the carbonyl (δ 170.0) of the *p*-hydroxylbenzoyl unit. Other HMBC correlations helped to confirm the individual fragments and determine regiochemistry, including the regiochemistry of the 1,2,3-trisubstituted aromatic ring, which was established as the rare HABA unit on the basis of these HMBC correlations and considerations of the ^{1}H and ^{13}C NMR shift calculation estimates using the ChemDraw Ultra 12.0 Suite software.[165]

Table 6. ^{1}H and ^{13}C NMR Data for Asperlarin A (**52**) in CD_3OD.[a]

residue	position	δ_H (mult; J in Hz)	δ_C
p-Hydroxybenzoic Acid	C1		125.9
	C2/C6	7.74 (d, 8.8)	130.5
	C3/C5	6.82 (d, 8.8)	116.1
	C4		162.5
	CO		170.0
Valine	Cα	4.72 (d, 7.5)	58.3
	Cβ	2.31 (m)	31.7
	Cγ	0.98 (d, 6.8)	18.8
	Cγ	1.08 (d, 6.8)	19.9
	CO		171.0
Proline	Cα	4.62 (dd, 8.3, 5.1)	63.2
	Cβ	2.21 m	31.0
		2.37 m	
	Cγ	2.08 m	26.2
		2.08 m	
	Cδ	3.99 m	49.0
		3.46 m	
	CO		173.9
3-Hydroxy-2-Aminobenzoic Acid (HABA)	C1		123.0
	C2		128.1
	C3		150.3
	C4	6.94 (dd, 7.8, 1.6)	122.8
	C5	7.09 (t, 7.8)	126.5
	C6	7.56 (dd, 7.8, 1.6)	124.2
	CO		170.0

[a]Data collected at 400 MHz (^{1}H) or 100 MHz (^{13}C). ^{13}C NMR assignments were established by analysis of HMQC and HMBC data.

Because HMBC correlations were unable to determine the sequence of the structure HRESITOFMSMS data were employed to complete the gross structure of **52**. Key HRESITOFMSMS fragments corresponding to the loss of the *p*-hydroxylbenzoyl unit from the peptide (*m/z* 384.1572), as well as fragment ions corresponding to Val – Pro (*m/z* 195.1142), requiring the Pro unit to be acylated by the Val unit, and Pro – HABA (*m/z* 249.0885), requiring the HABA unit to be acylated by the Pro unit, were observed.

The linkage of the HABA unit with the Pro unit was determined to be through acylation of the HABA nitrogen atom based on a close similarity of both the ^{1}H and ^{13}C NMR calculations using the ChemDraw Ultra 12.0 Suite software to the experimental data (Table 6). These data confirmed the connectivity of the four units of **52** as shown.

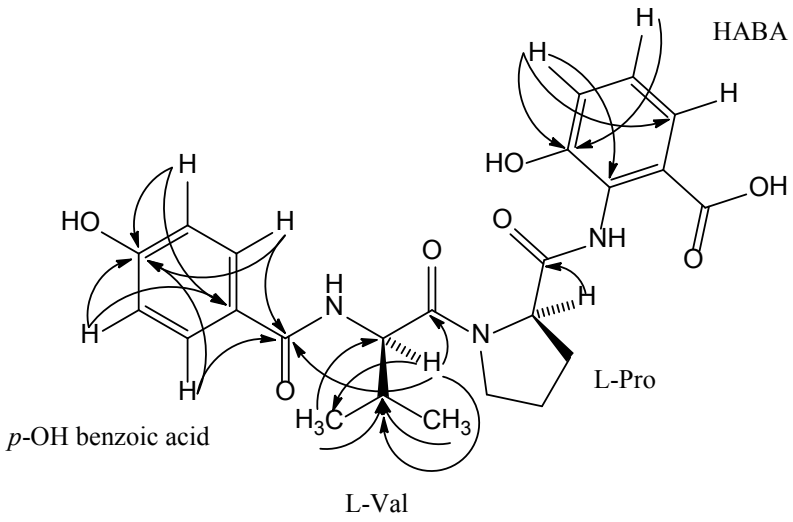

Figure 16: HMBC Correlations for Asperlarin A (**52**).

Acid hydrolysis of **52** was performed to afford a mixture of the individual amino acids present, and the absolute configurations of the resulting amino acids were determined by GCMS analysis of the corresponding trifluoroacetyl (+)-*S*-*sec*-butyl ester derivatives of the individual amino acids.

The hydrolyzate of **52** was treated with (+)-*S*-*sec*-butanolic HCl and then heated at 110°C for 30 min. The solvent was completely removed before the product was redissolved in CH_2Cl_2 and trifluoroacetic anhydride (TFAA), and then heated at 150°C for 5 min. The resulting solution was only partially evaporated before additional CH_2Cl_2

was added for GCMS analysis. The trifluoroacetyl (+)*S*-*sec*-butyl ester derivatives for D- and L-valine and D- and L-proline were also prepared in the same fashion as described. These derivatives served as the standards in the GCMS analysis of the derivatized hydrolyzate of **52**. The GCMS analysis of these derivatives and the corresponding D- and L- standards lead to the identification of peaks corresponding to L-valine and L-proline for **52**, thus assigning the absolute configuration shown. The name asperlarin A is proposed for compound **52**.

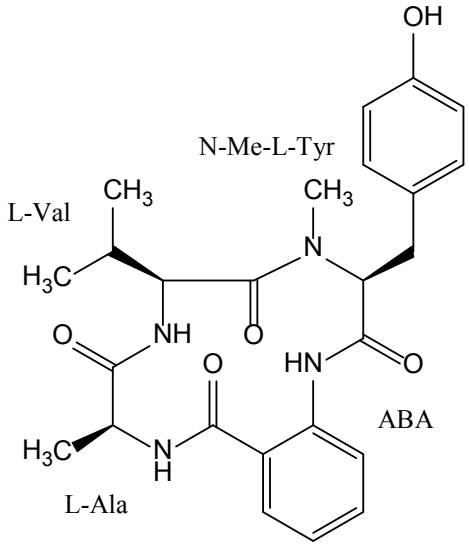

53

Compound **53** was determined to have the molecular formula $C_{25}H_{30}N_4O_5$ (13 degrees of unsaturation) on the basis of HRESITOFMS and NMR data. The ^{1}H NMR spectrum of **53** (Table 7) showed signals representative of N-methyl tyrosine (N-MeTyr), valine (Val), alanine (Ala), and *o*-aminobenzoic acid (anthranilic acid; ABA) units. The presence of these units was verified by GCMS analysis of the trifluoroacetyl (+)-*S*-*sec*-butyl ester derivatives of the individual amino acids prepared after the acid hydrolysis of **53**. The main question to be addressed in determining the structure of **53** was the order in

which the amino acyl units were connected. Due to the poor solubility of **53** in $CDCl_3$, HMBC data were collected in acetone-d_6, leading to gradual exchange of the NH protons. This gradual exchange of NH protons in acetone-d_6 could be seen most clearly in the Val α-proton signal at δ 4.49 which occurred as a doublet (for the exchanged version) overlapping with a triplet (for the non-exchanged proton). (Figure A17 and Table 7) Over time, this signal was gradually simplified to a doublet, indicating that the exchange of the NH proton had proceeded to completion.

Table 7. ^{1}H and ^{13}C NMR Data for Flavipeptide A (**53**) in Acetone-d_6.[a]

residue	position	δ_H (mult; J_H in Hz)	δ_C
N-Me Tyrosine	N-Me	2.94 (s)	40.8
	Cα	4.04 (dd, 11, 4.0)	70.2
	Cβ	3.37 (dd, 14, 4.0)	33.9
		3.17 (dd, 14, 11)	
	C1		131.0
	C2, C6	7.12 (d, 8.6)	131.8
	C3, C5	6.81 (d, 8.6)	116.3
	C4		157.5
	CO		169.0
	OH	8.19 (br s)	
o-Aminobenzoic acid	NH	9.79 (br s)[b]	
(ABA)	C1		128.8
	C2		139.0
	C3	8.42 (br d, 8.3)	121.9
	C4	7.46 (td, 8.3, 1.4)	132.5
	C5	7.09 (td, 7.6, 1.4)	123.5
	C6	7.57 (dd, 7.6, 1.4)	127.9
	CO		171.2
Alanine	NH	8.21 (br s)[b]	
	Cα	4.16 (dq, 1.5, 7.5)[b]	55.0
	Cβ	1.54 (d, 7.5)	16.6
	CO		173.5
Valine	NH	7.96 (br d)[b]	
	Cα	4.49 (t, 10)[b]	55.9
	Cβ	1.96 (dsep, 10, 6.8)	31.3
	Cγ	0.89 (d, 6.8)	18.9
	Cγ	0.93 (d, 6.8)	20.2
	CO		172.6

[a]Data were collected at 400 MHz (^{1}H) or 100 MHz (^{13}C). [b]Partially exchanged (see text).

Due in part to this gradual exchange of amide protons, there was only a single useful HMBC correlation to link to individual units together. The HMBC correlation from the N-methyl group of the N-MeTyr unit to the carbonyl carbon of Val indicated that the Val unit acylates the N-MeTyr unit, but ultimately, HMBC data were inconclusive in completing the structure of **53**. HRESITOFMSMS data were therefore again used to determine the remainder of the sequence. HRESITOFMSMS fragments corresponding to Val – N-MeTyr (*m/z* 277.1555), the connection which had previously been established via HMBC correlations, ABA – Ala (*m/z* 191.0825), accounting for the other two identified fragments, and N-MeTyr – ABA (*m/z* 297.1245), which indicated that N-MeTyr must acylate ABA. This, in turn, meant that ABA must acylate Ala based on the ABA – Ala fragment identified above. The only possible remaining connection for **53** is the one in which Ala acylates Val, thus completing the gross structure of **53** as shown. Interestingly, the assigned sequence matches that of the known fungal cyclic pentapeptide cycloaspeptide A (**24**), with the difference being the absence of the phenylalanine unit.[125] Even though compound **53** bears this similarity to **24**, compound **24** was not detected as a constituent of this extract. In fact, no other cyclic peptides were encountered in the extract.

Determination of the absolute configuration of compound **53** was accomplished through the same acid hydrolysis and trifluoroacetyl *S*-*sec*-butyl ester derivatization process that was used for **52**. GCMS analysis, and comparison to authentic D- and L-standards prepared in the same manner allowed for the assignment of the absolute configuration of each individual amino acid. Peaks corresponding to L-val, L-ala, and N-Me-L-tyr were observed, thereby enabling assignment of the absolute configuration of **53** as shown. The name flavipeptide A is proposed for compound **53**.

Structure Elucidation of PF1233B (**54**)

Compound **54**[166] was determined to have the molecular formula $C_{25}H_{26}N_2O_5$ (14 degrees of unsaturation) on the basis of NMR and HRESITOFMS data. The ^1H NMR spectrum of **54** (Table 8) exhibited signals for a phenyl group, a vinyl group, a 1,2,3-trisubstuted benzene ring, and two protons attached to heteroatom-bearing carbons. Two methyl singlets, two sp^3 methylene signals, and three exchangeable proton signals were also present in the spectrum. In addition to signals for the aforementioned units, the ^{13}C NMR spectrum (Table 8) contained four oxygenated sp^2 or carbonyl carbon signals, two downfield-shifted aromatic carbons, a downfield-shifted sp^3 carbon suggestive of multiple heteroatoms connected to a single carbon, and three aliphatic carbons. These units account for nine degrees of unsaturation. This requires the presence of three additional rings, and the four sp2 carbons noted above still needed to be assigned as either oxygenated or carbonyl carbons.

Two-dimensional NMR data (Table 8) were used to determine the structure of compound **54**. The phenyl group was located at C-17 on the basis of HMBC correlations of H_2-17 to C-18 and C-23. In turn, H_2-17 showed correlations to oxygenated sp^3 carbon C-13 and carbonyl carbon C-14. Correlations from H-13 to C-17 and C-14 confirmed this connection. H-13 also showed a correlation to another carbonyl carbon (C-11) requiring acylation of the C-13 oxygen to form an ester linkage. This portion of the molecule was extended by correlations from mutually coupled protons H_2-9 and H-10 to C-11. H-10 showed correlations to oxygenated carbon C-8, carbonyl carbon C-14, and heteroatom-bearing carbon C-16. Additional correlations from H_2-9 to quaternary carbons C-8 and C-16 were suggestive of a five-membered ring attached to a modified diketopiperazine ring system, completing two of the three additional rings that were needed for **52**.

Table 8. NMR Spectroscopic Data for PF1233B (**54**) in Acetone-d_6.

position	δ_H (mult; J in Hz)[a]	δ_C[a]	HMBC (H → C#)[b]
1-NH	6.43 (br s)		8
2		137.0	
3		144.9	
4	6.66 (dd, 7.9, 1.1)	116.6	2, 3, 6
5	6.58 (m)	120.8	2[c], 3, 6, 7, 8[c]
6	6.76 (dd, 7.4, 1.1)	116.4	2, 3[c], 4, 8
7		132.9	
8		88.9	
9	2.82 (dd, 14, 11)	37.7	7, 8, 10, 11
	3.24 (dd, 14, 2.0)		7, 8, 10, 11, 16
10	4.77 (dd, 11, 2.0)	57.6	8, 9, 14, 16
11		168.5	
13	5.21 (dd, 9.4, 3.6)	78.5	11, 14, 17, 18
14		167.0	
16		95.2	
17	2.74 (dd, 15, 9.4)	35.2	13, 14, 18, 19/23
	3.31 (dd, 15, 3.6)		13, 14, 18, 19/23
18		138.0	
19/23	7.14 - 7.27 (m)	130.0	
20/22	7.14 - 7.27 (m)	128.8	
21	7.14 - 7.27 (m)	127.0	
24		45.8	
25	6.51 (dd, 18, 11)	145.6	16, 24, 27, 28
26	5.05 (dd, 11, 1.6)	112.5	24, 25, 16[c]
	5.17 (dd, 18, 1.6)		24, 25, 16[c]
27	1.39 (s)	24.5	16, 24, 25, 26[c], 28
28	1.41 (s)	25.2	16, 24, 25, 26[c], 27
3-OH	4.46 (br s)		
8-OH	4.46 (br s)		

[a]Data collected at 400 MHz (^{1}H) or 100 MHz (^{13}C). Carbon signal multiplicities were established by DEPT experiments and are consistent with the assignments. [b]Data collected at 600 MHz. [c]Weak 4-bond HMBC correlations.

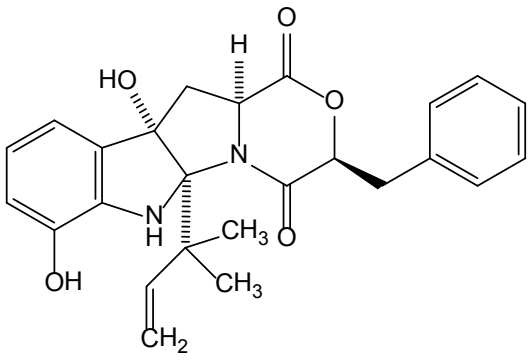

54

Two-dimensional NMR data (Table 8) were used to determine the structure of compound **54**. The phenyl group was located at C-17 on the basis of HMBC correlations of H_2-17 to C-18 and C-23. In turn, H_2-17 showed correlations to oxygenated sp^3 carbon C-13 and carbonyl carbon C-14. Correlations from H-13 to C-17 and C-14 confirmed this connection. H-13 also showed a correlation to another carbonyl carbon (C-11), requiring acylation of the C-13 oxygen to form an ester linkage. This portion of the molecule was extended by correlations from mutually coupled protons H_2-9 and H-10 to C-11. H-10 showed correlations to oxygenated carbon C-8, carbonyl carbon C-14, and heteroatom-bearing carbon C-16. These data, together with additional correlations from H_2-9 to quaternary carbons C-8 and C-16, were suggestive of a five-membered ring attached to a modified diketopiperazine ring system, completing two of the three additional rings that were needed for **54**.

Correlations from H-6 to C-8 and from H_2-9 to C-7 located the 1,2,3-trisubstituted aromatic ring by connecting it to the aforementioned unit via C-8. HMBC correlations within the 1,2,3-trisubstituted ring set the regiochemistry of the oxygenated aromatic carbon (C-3) and another downfield-shifted aromatic carbon (C-2). A correlation from an exchangeable signal (δ 6.43, NH-1) to C-8 completed a

dihydroindole-type structure and closed the final, required ring at C-16. Interestingly, one of the 1,2,3-trisubstituted aromatic ring protons (δ 6.58, H-5) exhibited a splitting pattern that was unusual for its location in **54**. (Figure A19) Due to its coupling with protons H-4 and H-6, H-5 was expected to be a triplet or a doublet of doublets, but it exhibited an unexpected additional small splitting. Decoupling experiments were unsuccessful in determining the source of the additional splitting, but it could be caused by long-range coupling to the hydroxyl proton (OH-3) or the amine proton (NH-1), both of which are broad singlets that could mask small splitting characteristics and slight changes expected during decoupling experiments. In either case, the connectivity proposed thus far for **54** is fully consistent with all of the other data obtained.

The remaining nitrogen was placed within the modified diketopiperazine ring system as shown, allowing for an amide linkage. This modification also explains the downfield-shifted nature of C-16, as it is linked to two heteroatoms. It also rationalizes the downfield shift of H-10 in the ^{1}H NMR spectrum. The remaining units of **54** were linked by HMBC correlations from the terminal olefinic signals (H_2-26) to C-24 and C-25, establishing a prenyl moiety. This prenyl group was attached to the core structure at C-16 via HMBC correlations from H-25, H_3-27, and H_3-28, thereby completing the gross structure of **54**. All of these conclusions were also supported by additional HMBC data. Once the structure had been established, an extensive literature search led to a match with compound **54**, called PF1233B, a bioactive metabolite previously described only briefly in a Japanese patent.[166] In this patent, PF1233B (**54**) is said to have the potential for use in treating an irregular heartbeat, as a pain reliever, as a sodium channel blocker, and for protection from seizures.[166]

The stereochemistry shown for **54** matches that of the structure from the literature because ^{1}H NMR *J*-values and $[\alpha]_D$ data were the same as those of the previously described sample.[166] Due to the inability to translate the Japanese patent information into English, the method in which the configuration, whether relative or absolute, for **54** was

assigned in the patent could not be determined. The patent literature for compound **54** provides ^{1}H NMR, ^{13}C NMR, UV, IR, HRFABMS, and rotational data, but it is incomplete with regard to the description of ^{1}H NMR multiplicities and *J*-values and does not provide ^{13}C NMR assignments. Thus, complete ^{1}H and ^{13}C NMR data for this metabolite are provided here.

Neither asperlarin A (**52**) nor flavipeptide A (**53**) showed antifungal activity against *A. flavus* or *F. verticillioides* at 100 µg/disk. Flavipeptide A (**53**) was not tested for activity against the fall armyworm, but asperlarin A (**52**) reduced the growth rate of the fall armyworm by 14% in a dietary assay at 100 ppm. PF1233B (**54**) was not tested against *A. flavus* and it did not show activity against *F. verticillioides*. However, compound **54** did show weak, but statistically significant activity against the fall armyworm at $P < 0.05$ (13% reduced growth rate) when it was incorporated into the diet at 160 ppm. Curvularin (**55**) and various curvularin derivatives (including **25**, **56**-**58**) have been isolated from various fungal species, including *Penicillium citreoviride* and *Eupenicillium* sp.,[133] and reported to possess antifungal, antitumor, and antibacterial activity against *Staphylococcus aureus*,[133] as well as cytotoxicity against sea urchin embryo cells.[168] Aspochalasins I (**28**) and J (**29**), originally reported from and isolate of *Aspergullus flavipes*, are reported to exhibit weak to moderate cytotoxicity against cancer cell lines, but no antifungal activity was described in the literature.[130] Alantrypinone (**41**) was originally reported from an isolate of *Penicillium thymicola*, with no biological activity data provided.[160] It was later described as an antiinsectan alkaloid that is highly selective for insect (vs. mammalian) GABA (γ-aminobutyric acid) receptors, an important site for insecticidal activity.[169] No antifungal activity has been reported in the literature for **41**. Compound **42** was isolated from an isolate of *Aspergillus terreus* and is said to exhibit contractive activity for smooth (bronchial and intestinal) muscles and cardinal muscles of guinea pigs, but no anti-inflammatory activity. No antifungal or antiinsectan activity was reported for **42**. Ultimately, the presence of these known

bioactive compounds (**25**, **28**, **29**, **41**, **42**, and **55-58**), along with their abundance in the extract, especially that of **25** and **56-58**, is likely to explain the moderate antifungal and antiinsectan activity originally observed for the crude extract.

CHAPTER 5

CHEMICAL INVESTIGATIONS OF AN ENDOPHYTIC ISOLATE OF *EMERICELLA NIDULANS* (ENDO-3111 = NRRL 58893)

By analogy to fungal endophytes found in corn plants, fungal endophytes of wheat (*Triticum aestivum*) could also play an important role in the health of these economically important crop plants. The U.S. wheat harvest in 2010 was valued at nearly $13 billion.[170] Like other plants, living wheat plants typically contain a host of fungal endophytes, and the metabolites they produce could conceivably be relevant to plant health, and could also affect livestock and humans, either directly or indirectly. Our research group has shown that fungal endophytes of corn are prolific producers of bioactive secondary metabolites,[118-120] and it is likely that fungal endophytes of wheat also produce a variety of active compounds. In the course of our ongoing project on endophytic fungi, we investigated a fungal endophyte of wheat identified as *Emericella nidulans* (anamorph: *Aspergillus nidulans*). This isolate (ENDO-3111) was obtained from a wheat seed that was collected in Arizona, and was fermented on rice for 30 days at 25 °C. The EtOAc extract of the resulting fermentation cultures displayed moderate antifungal activity against *A. flavus* and *F. verticillioides*, as well as the ability to significantly reduce the growth rate of the fall armyworm (*S. frugiperda*) and was therefore targeted for chemical investigation. Distinctive metabolites that exhibit biological activity have been isolated from *E. nidulans* before,[171] and the possibility that *E. nidulans* might produce additional novel bioactive metabolites was also a contributing factor in choosing this isolate for chemical investigation.

The initial crude extract (and later a subsequent scale-up fermentation) was partitioned between MeCN and hexanes, thereby removing most of the lipids, and the resulting MeCN-soluble layer was fractionated using silica gel chromatography and

reversed-phase HPLC techniques, ultimately yielding six known compounds and four novel compounds (Figure 17) that will be discussed in this chapter.

The six known compounds were identified by comparison of ^{1}H NMR, ^{13}C NMR, and MS data with literature values. They were determined to be sterigmatocystin (**59**),[172] emindole DA (**60**),[173] emestrin (**61**),[174] microperfuranone (**62**),[175] 3-benzyl-4-phenyl-2,5-furadione (**63**,an acid anhydride precursor of **62**),[176] and silvaticol (**64**),[177] also known as porriolide.[178] Sterigmatocystin (**59**) has been isolated from *E. nidulans* previously, and is a carcinogenic polyketide mycotoxin produced by many fungi. Sterigmatocystin (**59**) is considered to be a precursor to the more potent carcinogenic mycotoxins known as aflatoxins, which are among of the most widely studied fungal metabolites due to their considerable economic impact as crop contaminents.[179] In contrast to its activity as a carcinogenic mycotoxin, **59** has also been reported to possess antitumor activity against multiple human solid tumor cell lines.[180] Compound **59** is also reported to exhibit antiinsectan properties.[181] Emindole DA (**60**) has also been previously isolated from *E. nidulans*, and is also reported to exhibit antitumor activity against multiple tumor cell lines.[171] The literature does not describe the antifungal or antiinsectan activity for **60**. The known macrocyclic epidithiodioxopiperazine emestrin (**61**), biogenetically derived from the combination of benzoic acid and two units of phenylalanine, was a major constituent of this extract and is known to display a wide range of biological activities. Effects of **61** reportedly include acute poisoning in mice,[182] inducing DNA clevage,[183] ability of neutralizing the binding of ^{125}I-MCP (a chemoattractant protein) to the chemokine receptor CCR2, which is associated with inflammation in the lungs and several other organs,[184] and antifungal effects against *Gibberella zeae* and *Penicillium expansum* at concentrations of 1.0 µg/disk (MICs were 10 and 2.5 µg/mL, respectively).[185] In our own disk diffusion assays, **61** showed significant antifungal activity against both *A. flavus* and *F. verticillioides*, causing clear inhibition zones after two days with diameters of 23 and 33 mm, respectively, at 100 µg/disk. Compound **61**

also exhibited significant activity against the fall armyworm causing a 28% reduction in growth rate at the 100 ppm dietary level. Due to the abundance of **60** and **61** in the ENDO-3111 extract, the majority of antifungal and antiinsectan activity exhibited by the extract can be attributed to the presence of these bioactive metabolites.

Microperfuranone (**62**) was originally isolated from cultures of the ascomycete *Anixiella* micropertusa[175] and was tested for antibacterial, antifungal, and antialgal activity at 50 μg/disk in standard disk diffusion assays,[171] but it did not exhibit any effects. The acid anhydride **63**, originally isolated from the anamorph of *E. nidulans*, stimulated the elongation of the roots of radish and lettuce seedlings when tested at 100 μg/mL.[176] Silvaticol (**64**), originally isolated from the fungus *Aspergillus silvaticus*,[177] was also isolated from *Alternaria porri* (Ellis) Ciferri, the casual fungus of black spot disease in the stone-leek and onion, and mistakenly given a different name, porriolide.[178] Phthalide **64** exhibited minimal phytotoxicity against lettuce and stone-leek seedlings, inhibiting root elongation by 53 and 48%, respectively, when tested at 400 ppm,[178] but no discussion of antifungal or antiinsectan activity of this compound is reported in the literature.

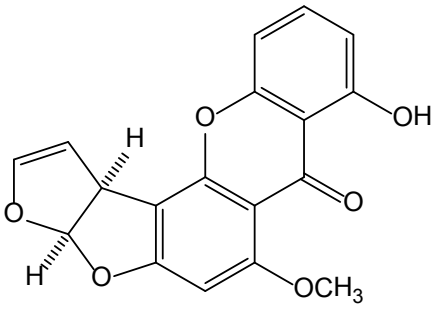

59

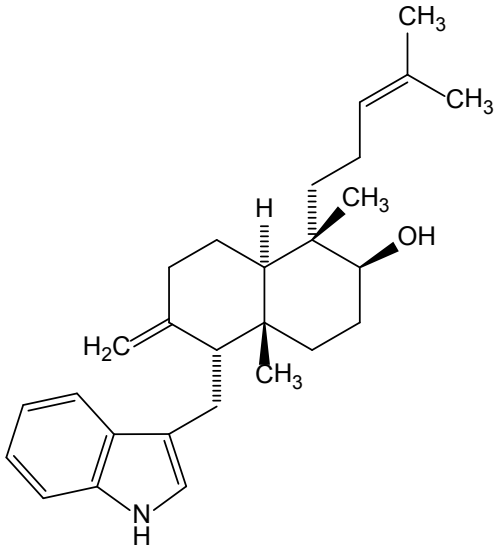

60

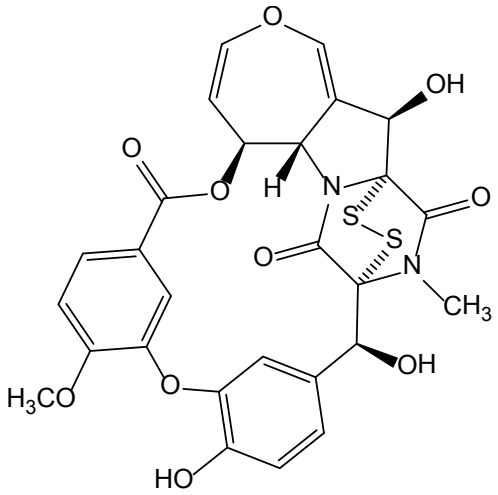

61

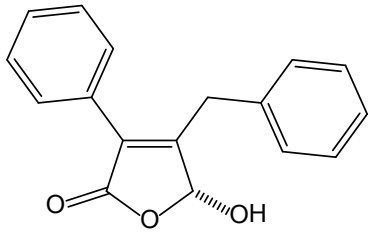

62

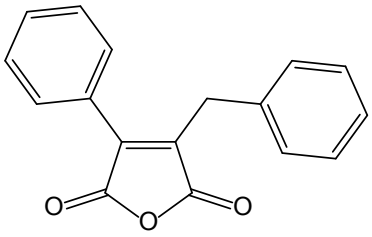

63

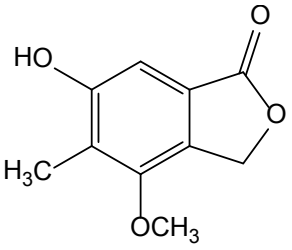

64

The novel secondary metabolites isolated from this extract were assigned the names emeridin A (**65**), O-methylsecoemestrin C_1 (**66**), 5-(hydroxymethyl)-2,4-dimethylbenzene-1,3-diol (**67**), and 5-(hydroxymethyl)-3-methoxy-2,4-dimethylphenol (**68**), and the details of the isolation (Figure 17) and structure elucidation of these new natural products are the focus of the remainder of this Chapter.

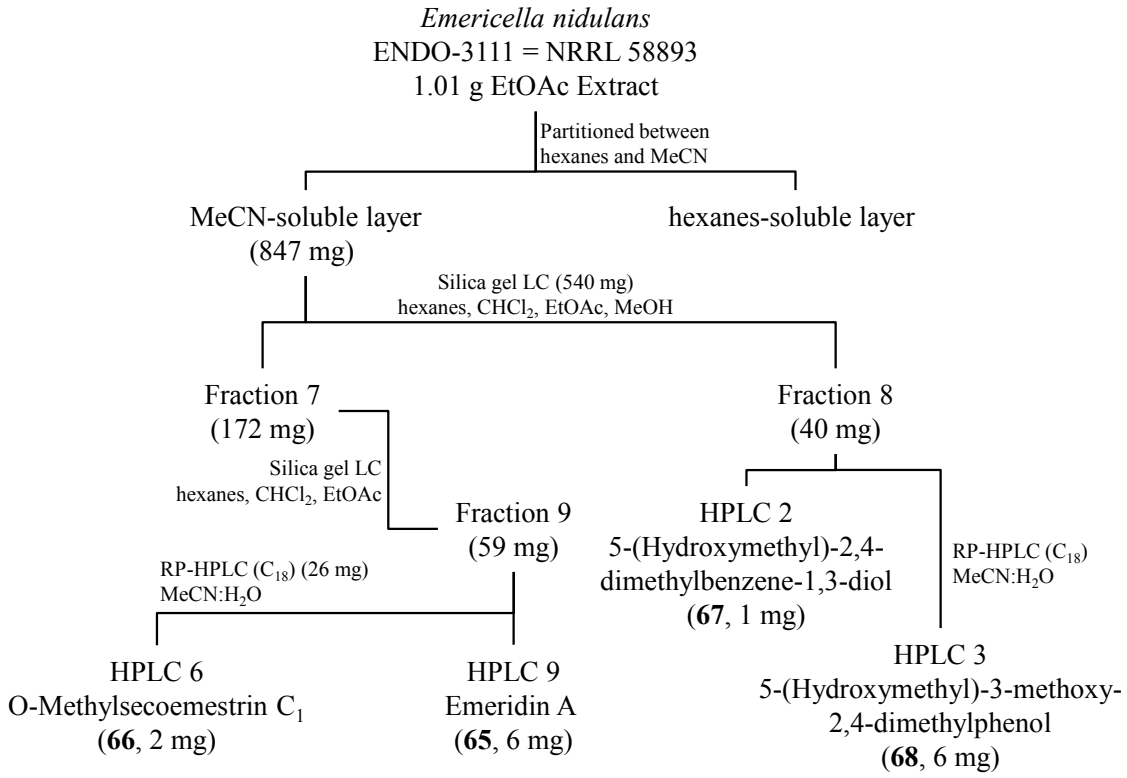

Figure 17. Isolation Scheme for Metabolites **65-68** from ENDO-3111.

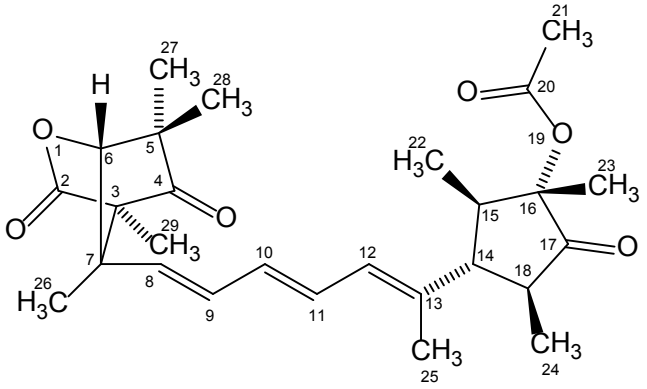

65

Structure Elucidation of Emeridin A (**65**)

Emeridin A (**65**) was found to possess the elemental composition $C_{27}H_{36}O_6$ (ten degrees of unsaturation) on the basis of NMR (Table 9) and HRESIMS data. The ^1H NMR spectrum of **65** contained resonances that corresponded to a conjugated triene system, three sp^3 CH protons, a single proton attached to an oxygenated carbon, and nine methyl groups, one of which (δ 1.74) was identified as an vinyl methyl, and another (δ 2.02) as an acetyl group methyl. Two of the remaining seven methyl signals were doublets (J = 7 Hz) while the last five were singlets representative of methyl groups attached to quaternary sp^3 carbons, one of which was an oxygenated sp^3 carbon. Of the remaining six carbons, two were quaternary sp^3 carbons and the others were identified as carbonyls, two of which were ketones and two of which were esters. The triene functionality was assembled as shown in **65** on the basis of ^1H, ^{13}C, HMQC, and HMBC NMR data. The corresponding J-values (11 to 16 Hz) established the *E* geometry of the two disubstituted olefinic moieties, while the C-12–C-13 double bond was identified as being trisubstituted, bearing the aforementioned vinyl methyl group.

All proton-bearing carbons were correlated to signals for their directly-connected protons using HMQC data and these assignments are reflected in Table 9. The cyclopentanone ring, on the right side portion of **65**, was assembled by analysis of HMBC correlations (Table 9). The previously identified acetyl methyl (H_3-21) was established as part of an acetate group due to its HMBC correlations to ester carbon C-20 and C-16, an oxygenated sp^3 carbon. HMBC correlations from H_3-23 to C-16, C-15, and ketone carbon C-17 located the only methyl group attached to an oxygenated sp^3 carbon as shown. HMBC correlations from H_3-24 to C-17, C-18, and C-14 indicated that the methine CH-18 connected to methyl group H_3-24 was attached to a quaternary sp^3 carbon, as well as to C-17. Methyl carbon H_3-22 exhibited correlations to C-14, quaternary sp^3 carbon C-15, and oxygenated carbon C-16. Together, these HMBC correlations required a cyclopentanone ring, with an acetate unit attached at C-16. The

structure of **65** was extended though correlations from H-13 to C-14 and from H-14 to olefinic carbons C-12 and C-13, indicating that the triene system was attached to the cyclopentanone ring via C-14. HMBC correlations from vinyl methyl H_3-25 to C-12, C-13, and C-14 confirmed this connection. The structure of **65** was extended at the opposite end of the triene system by HMBC correlations from olefinic proton H-8 to quaternary sp^3 carbons C-3 and C-7, oxygenated methine carbon C-6, and methyl carbon C-26. Correlations from H_3-26 to C-3, C-6, C-7, and C-8 confirmed its connection at C-7. Methyl group H_3-29 was attached at C-3 through is HMBC correlations to C-3, C-7, ester carbon C-2, and ketone carbon C-4. Additional HMBC correlations from H_3-27 to C-4, C-5, C-6, and C-28, and from H_3-28 to C-4, C-5, C-6, and C-27 indicate that the H_3-27 and H_3-28 methyl groups are both attached to the same quaternary sp^3 carbon (C-5), which is situated between ketone carbon C-4 and oxygenated carbon C-6. These correlations and the correlations from H-6 to ester carbon C-2, ketone carbon C-4, C-5, and to methyl groups C-27 and C-28 indicate a ketolactone ring. The last degree of unsaturation, as indicated by spectroscopic and HRESIMS data for **65**, was established by a strong HMBC correlation from H-6 to C-3, which indicated that C-7 a bridgehead carbon, forming the final ring. Additionally, H-6 also showed a weak long-range correlation to C-29, which would be consistent with such a bicyclic ring structure, as 2-type long-range couplings in such systems are often observed, thereby completing the gross structure of **65**. This type of bicyclic ring system has been previously described as being part of a bioactive natural product produced by *Penicillium rugulosum*, isolated by Jayasuriya and co-workers.[186] The numbering system of **65** is also based on this literature report.[186] All of these conclusions were supported by additional HMBC data.

Table 9. NMR Spectroscopic Data for Emeridin A (**65**) in $CDCl_3$.[a]

position	δ_H (mult; J in Hz)	δ_C	HMBC (H# → C#)[a]
2		172.5	
3		69.0	
4		210.8	
5		46.2	
6	4.42 (s)	89.2	2, 3, 4, 5, 26, 27, 29[b]
7		58.9	
8	5.40 (d, 16)	130.8	3, 6, 7, 9, 10, 26
9	6.20 (dd, 16, 11)	134.0	8, 10, 11
10	6.06 (dd, 15, 11)	130.6	8, 9, 12
11	6.48 (dd, 15, 11)	130.7	9, 10, 12, 13
12	5.95 (d, 11)	128.5	10, 14, 25
13		138.3	
14	1.77 (t, 12)	58.1	12, 13, 15, 18, 22, 24
15	2.70 (m)	38.5	14, 16, 17, 23, 22
16		84.5	
17		215.4	
18	2.68 (m)	44.4	13, 14, 17, 24
20		170.2	
21	2.02 (s)	21.1	16[b] 20
22	0.88 (d, 7.0)	11.0	14, 15, 16
23	1.12 (s)	17.2	15, 16, 17
24	0.97 (d, 7.0)	13.0	14, 16, 17, 18
25	1.74 (s)	12.5	12, 13, 14
26	1.36 (s)	18.7	3, 6, 7, 8
27	1.15 (s)	24.8	4, 5, 6, 28
28	1.25 (s)	23.3	4, 5, 6, 27
29	1.20 (s)	5.9	2, 3, 4, 7

[a]Data collected at 400 MHz (^1H) or 100 MHz (^{13}C). ^{13}C NMR assignments were confirmed by analysis of HMQC and HMBC data. [a]Data collected at 600 MHz. [b]Weak long-range HMBC correlations.

NOESY correlations were used to establish the relative configuration of the molecule. Figure 18 shows MM2 energy-minimized models of the two halves of the molecule (ChemDraw Ultra Suite 12.0) depicting key NOESY correlations. However, because the two ring systems are insulated from one another by the triene unit, the relative configurations of the individual ring systems could not be related to each other.

Due to the geometric constraints of the bridgehead carbon present in the bicyclic ring system, the relative configurations at C-3 and C-6 must be assigned as shown. Therefore, NOESY correlations are only needed to assign the relative configuration at the bridgehead carbon, C-7. NOESY correlations from H_3-28 to both H-8 and H-9 indicate that the triene system and the methyl groups at C-5 are orientated on the same side of the bridgehead carbon, C-7. This enables the assignment of the relative configuration at C-7 as shown in **65**. The relative configuration of the cyclopentanone ring in **65** was also assigned through a series of NOESY correlations (Figure 18). H-14 showed NOESY correlations to both H_3-22 and H_3-24, and H_3-22 showed a correlation to H_3-23, indicating that all of these hydrogens are on the same face of the ring. In addition, H-12 exhibited strong correlations to H-15 and H-18, confirming that H-14 is *cis* to both H_3-22 and H_3-24. This relationship was further supported by the typical large *trans* coupling exhibited by H-14 (J = 12 Hz) to both protons H-15 and H-18. On the basis of these data, the relative configuration of emeridin A (**65**) was assigned as shown.

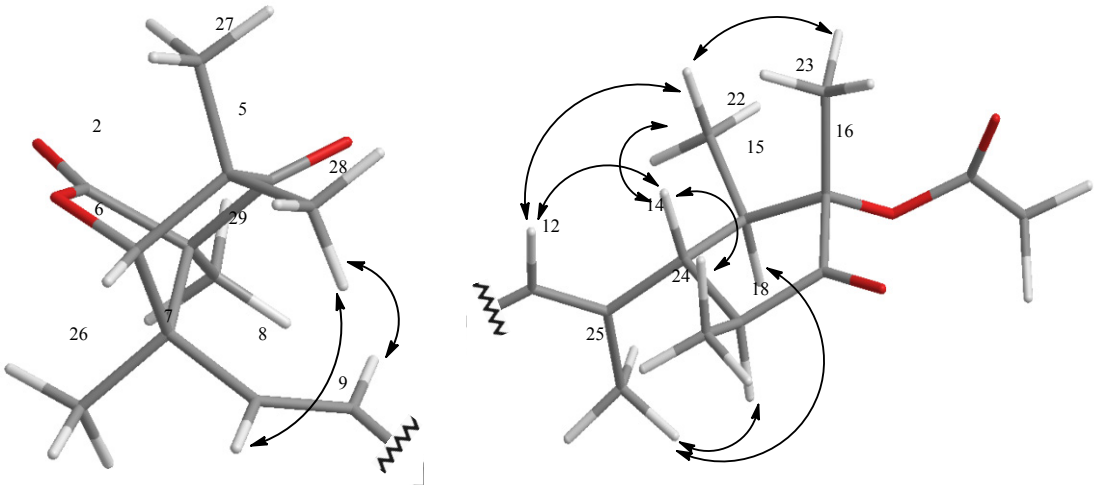

Figure 18. Key NOESY Correlations of the Bicyclic Ring System (A) and Cyclopentanone Ring (B) of Emeridin A (**65**).

Several strategies to assign the absolute configuration of compound **65** and to relate the relative configuration of the two halves of the molecule to one another were considered. Multiple attempts were made at crystallization, application of chemical degradation, and circular dichroism (CD) measurements. Noted above, the two ring systems are insulated from each other and no NOESY correlations between the two units were observed. Because of this, assignment of the absolute configuration of the molecule was expected to require assignment of the absolute configuration of each of the ring-containing subunits independently. In an effort to accomplish this, chemical degradation of the triene unit was attempted in order to separate the two halves. If the separation was successful, each portion could then be individually analyzed by CD (using empirical and/or semi-empirical approaches – see Chapter 1) and/or through the application of Mosher's method in an effort to assign the absolute configuration.

The initial attempt at chemical degradation involved reaction of **65** with excess OsO_4,[187,188] in an effort to generate a polyhydroxylation product, which could then undergo oxidative cleavage with $NaIO_4$ to afford products characteristic of the two halves (Scheme 2). However, after 24 hr of exposure to OsO_4, no reaction had taken place and only starting material **65** was recovered.

The next attempt at cleaving the triene involved treatment of the recovered **65** from the previous reaction with $NaHCO_3$ and $KMnO_4$ (Scheme 2).[189-191] After 24 hr, ^1H NMR analysis revealed that **65** has completely degraded, but there were no signals suggestive of products along the lines of those expected.

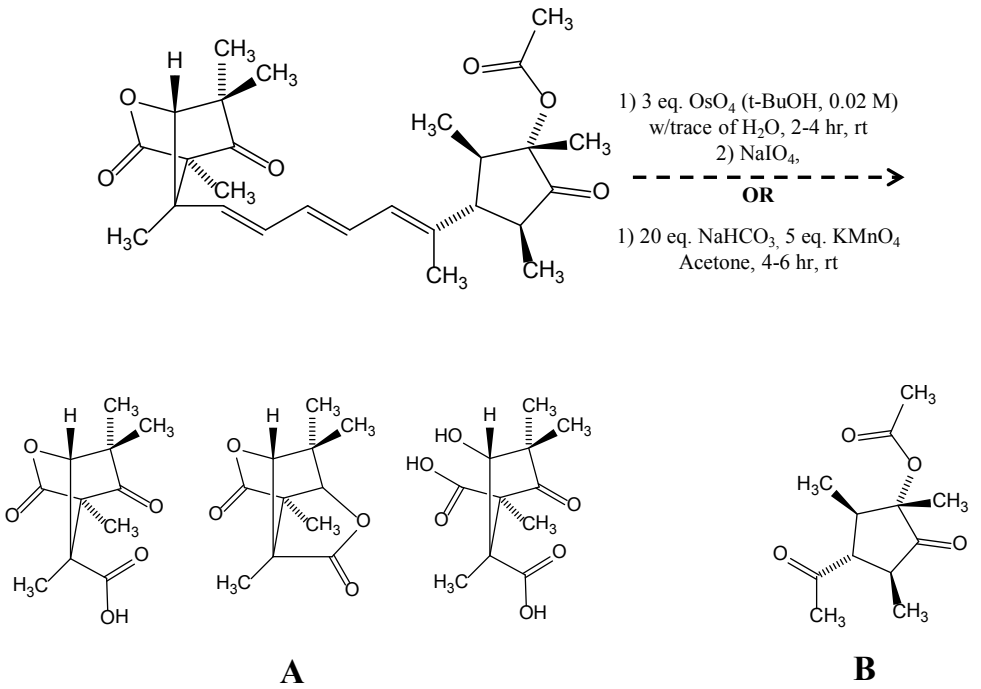

Scheme 2. Proposed $OsO_4/NaIO_4$ and $KMnO_4$ Oxidative Cleavage Reactions of Emeridin A (**65**) and the Potential Products.[187-191]

The next attempt employed ozone (O_3) as the oxidizing agent.[192-194] Another sample of **65** was dissolved in CH_2Cl_2 and a stream of O_3 was bubbled through the solution at low temperature. During this process, the solution was observed changing from a bright yellow to a completely colorless solution, suggesting that the conjugated olefins had reacted. Reductive work-up with Me_2S, afforded a product mixture that had characteristics expected for a successful degradation as depicted in Scheme 3. ^{1}H NMR analysis of the reaction mixture showed the absence of the olefinic signals observed for **65**, as well as the emergence of an aldehyde signal (δ 9.67) and a methyl group exhibiting a chemical shift characteristics of a ketone methyl (δ 2.24), while all other signals remained relatively unchanged, indicating that the chemical degradation had proceeded to completion. However, because the reductive work-up using Me_2S afforded the bicyclic aldehyde, rather than the corresponding carboxylic acid, a simple polar/non-polar

extraction process to separate the products from one another was not feasible. Due to sample limitations, no attempt was made to oxidize the corresponding aldehyde to the carboxylic acid, as any additional reaction upon the product mixture would be extremely difficult to control and could result in unwanted side-products and degradation of the other half. Unfortunately, extensive efforts to separate the products by HPLC using different mobile and stationary phases were unsuccessful in separating these two components of the product mixture.

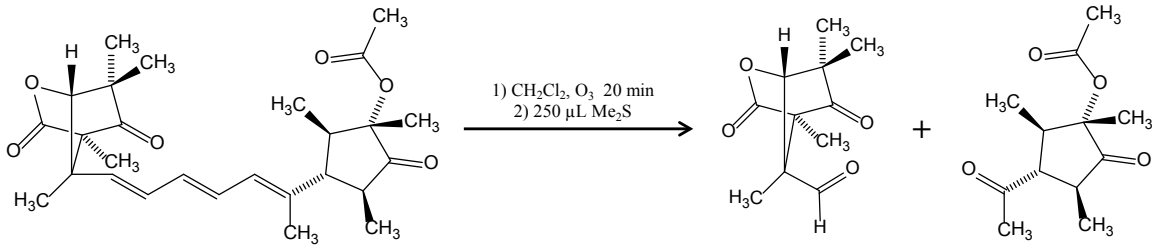

Scheme 3. Ozonolysis of Emeridin A (**65**) with Reductive Work-Up Using Me_2S.[192-194]

Even though the ozonolysis appeared to be successful, the inability to separate the products, together with sample limitations, did not allow for further stereochemical analysis of **65** and, therefore, only the relative configurations of the two subunits were assigned. Isolated from an extract of *Penicillium rugulosum*, Coccidiostatin A (**69**) is a previously reported compound that consists of the same type of ketolactone bicyclic ring system with a polyene system insulating another ring feature, similar to **65**,[186] but the literature did not provide any information regarding the assignment of the absolute configuration for **69**.[186] Compound **69** is reportedly active against *Eimeria acervulina* at 150 ppm in a MAC (mycobacterium avium complex) assay.

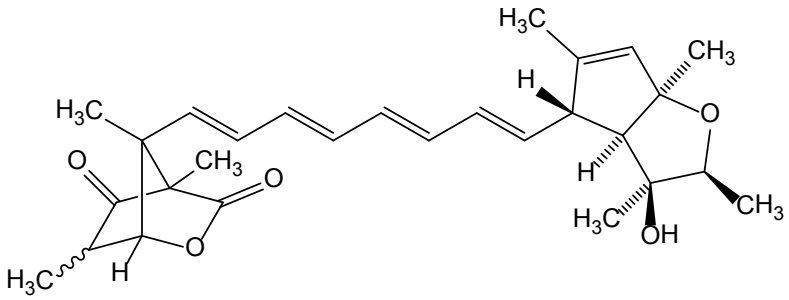

69

Acquiring additional starting material, through a third scale-up, would possibly be the best opportunity to gather any products of the ozonolysis reaction that could be used to assign the absolute configuration of **65**. Due to limited bioactivity exhibited by **65** (see below), no attempts were made at obtaining additional material in order to assign the absolute configuration of **65**. However, this is a chemically intriguing problem that deserves to be investigated further.

Emeridin A (**65**) exhibited modest activity against *F. verticillioides*, causing a mottled inhibition zone of 19 mm at a concentration of 200 µg/disk in a standard agar diffusion assay. In a dietary assay against the fall armyworm, compound **65** caused the death of 44% of test insects while causing 77% of the survivors to exhibit reduced growth rates compared to controls, albeit at a relatively high concentration (12,500 ppm).

Structure Elucidation of O-Methylsecoemestrin C_1 (**66**)

The new compound **66** was isolated from ENDO-3111 alongside **61**, the parent compound to this known family of metabolites, which was also the dominant metabolite in the extract. Compound **66** was identified as a new O-methylated analogue of the known compound, secoemestrin C_1 (**70**), which was originally isolated from the mycelium of a fungus isolated from musk ox dung collected in Alaska.[184] The structure elucidation of O-methylsecoemestrin C_1 (**66**) was carried out by analysis of HRESIMS

and 2D NMR data, and supported by comparisons to the data reported for **70**.[184] The ^{1}H, ^{13}C, and HMBC NMR data for **66** are summarized in Table 10.

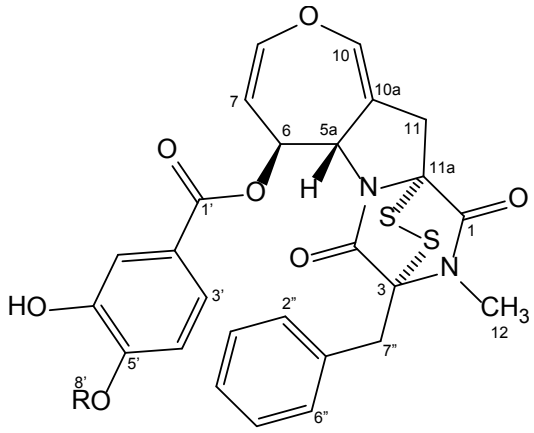

66: R = CH_3
70: R = H

Most of the ^{1}H NMR data for **66** were analogous to those of **70**. The only significant differences were the presence of an additional methoxy singlet at δ 3.95 and the appearance of two protons (H_2-7") that were resolved in the spectrum of **70**, showing germinal coupling (J = 16 Hz), but were coincident in the spectrum of **66**, occurring as a two-proton singlet at δ 3.65. The signal corresponding to H_2-7" in **66** exhibited a ^{1}H NMR shift that was the average of the two locations reported for **70** (δ 3.68 and 3.62).[184] An additional interesting feature of the ^{1}H NMR of **66** was the long-range coupling observed between H_2-11 and H-5a (J = 1.5 Hz). This small coupling was not directly measured for **70**, but the reported broadening of the proton signals for H_2-11 and H-5a in **70** indicate a similar effect was seen in **70** as in **66**. These observations, in conjunction with ^{13}C NMR data and an HMBC correlation (Table 10) from the new methoxy signal to C-5', allowed assignment of a methoxy group in **66** in place of the hydroxy group at C-5' in **70**. All of the HMBC data, including correlations from H_2-7" to C-3, C-4, C-1", and C-2"/6", were also consistent with assignment of the structure as shown in **66**.

Table 10. NMR Spectroscopic Data for O-Methylsecoemestrin C_1 (**66**) in $CDCl_3$.[a]

position	δ_H (mult; J in Hz)	δ_C[b]	HMBC (H# → C#)[c]
1		166.3	
3		78.5	
4		162.0	
5a	5.32 (br dq, 8.7, 1.5)	62.8	6, 7[c], 10, 10a, 11a
6	5.83 (dt, 8.7, 1.7)	70.4	5a, 7, 8, 1'[c]
7	4.66 (dd, 8.2, 1.7)	105.7	5a, 6, 8
8	6.30 (dd, 8.2, 2.2)	141.0	6, 7, 10
10	6.65 (q, 2.2)	139.2	5a, 8, 10a, 11
10a		113.4	
11	3.12 (dt, 18, 1.5)	35.2	5a, 10, 10a, 11a
	4.10 (ddd, 18, 2.2, 1.5)		1, 5a[c], 10, 10a, 11a
11a		73.2	
12	2.96 (s)	29.3	1, 3
1'		165.4	
2'		122.8	
3'	7.70 (dd, 8.4, 2,1)	123.5	1', 5', 7'
4'	6.87 (d, 8.4)	109.7	1'[c], 2', 5', 6', 7'[c]
5'		150.7	
6'		145.2	
7'	7.66 (d, 2.1)	116.2	1', 3', 5', 6'
8'	3.95 (s)	55.9	5'
1"		133.8	
2"/6"	7.21 (br d, 7.8)	129.6	2"/6", 4", 7"
3"/5"	7.06 (dd, 7.8, 7.2)	128.2	1", 2"/6", 3"/6"
4"	7.15 (br t, 7.2)	127.3	1"[c], 2"/6", 3"/5"[c]
7"	3.65 (s)	36.3	3, 4, 1", 2"/6"
6'-OH	5.60 (s)		

[a] ^1H NMR data were recorded at 400 MHz; ^{13}C NMR data were recorded at 150 MHz. [b] ^{13}C NMR assignments were established by analysis of HMQC and HMBC data. [c]Data collected at 600 MHz. [d]Weak, long-range HMBC correlations. The numbering system for **66** is consistant with those used for **70**.[187]

The known metabolite emestrin (**61**), originally reported from *Emericella striata*, and identified in ENDO-3111 through comparison of ^1H and ^{13}C NMR spectra to reported data,[174] was found to be the major constituent of this extract. Compound **61** reportedly displays a wide range of biological activities (see above). Even though O-

methylsecoemestrin C_1 (**66**) lacks the macrocycle present in **61**, it is presumably biosynthesized through a pathway analogous to that of **61** (see above). Due to antifungal properties already reported for **61**, it was not tested in our own assays against *A. flavus* and *F. verticillioides*. However, compound **66** exhibited reasonable antifungal activity against *F. verticillioides*, causing a mottled inhibition zone with a diameter of 35 mm at a concentration of 200 µg/disk. Compound **66** also exhibited antiinsectan activity against the fall armyworm by causing a 20% mortality rate ad a 78% reduced growth rate of the survivors compared to controls, at the 7,500 ppm dietary level.

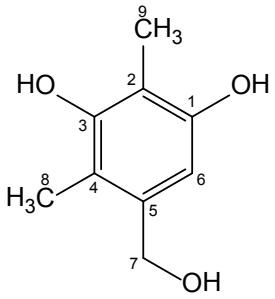

67

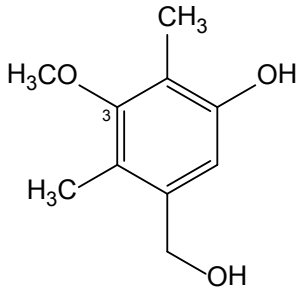

68

Structure Elucidation of Compounds **67** and **68**

The new compound **67** was found to have the molecular formula $C_9H_{12}O_3$ (four degrees of unsaturation) on the basis of HRESIMS and NMR data (Table 11). The ^1H NMR spectrum only showed four singlets, suggesting that this compound was a simple aromatic metabolite. The ^1H NMR spectrum indicated a single aromatic proton, an oxygenated CH_2 unit, and two methyl groups attached to a benzenoid aromatic ring, which would account for all of the unsaturations. The remaining two oxygen atoms, as indicated by the HRESIMS data, must be hydroxyl groups directly attached to the aromatic ring. HMQC and HMBC NMR experiments (Figure 19) were used to assign the ^{13}C NMR shifts (Table 11) as well as the regiochemistry of the molecule. Structure

67 was assigned on the basis of HMBC correlations observed from H-6 to C-4, and oxygenated carbons C-1 and C-7, from H_2-7 to C-4, C-5, and C-6, from H_3-8 to C-4, C-5, and oxygenated carbon C-3, and from H_3-9 to C-1, C-2, and C-3. Compound **67** was thus identified as 5-(hydroxymethyl)-2,4-dimethylbenzene-1,3-diol.

Table 11. ^{1}H and ^{13}C NMR Data for Compounds **67** and **68** in CD_3OD.[a]

	67		**68**	
position	δ_H (multiplicity)	δ_C	δ_H (multiplicity)	δ_C
1		154.6		155.1
2		112.1		117.5
3		153.4		158.8
4		115.2		120.3
5		138.2		139.1
6	6.42 (s)	107.9	6.64 (s)	111.5
7	4.50 (s)	63.5	4.50 (s)	63.4
8	2.11 (s)	11.0	2.14 (s)	10.9
9	2.05 (s)	8.9	2.10 (s)	9.3
10			3.65 (s)	60.4

[a]Data collected at 400 MHz (^{1}H) or 100 MHz (^{13}C). ^{13}C NMR assignments were established by analysis of HMQC and HMBC data.

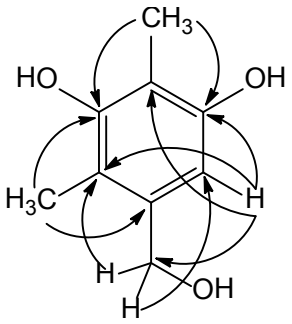

67

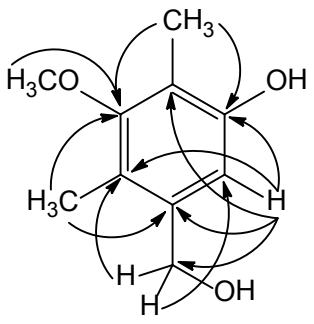

68

Figure 19. Key HMBC Correlations for Compounds **67** and **68**.

The ^{1}H NMR spectrum of an additional new compound (**68**) was similar to that of **67**, but contained an additional three-proton singlet at δ 3.65, indicating the presence of a

methoxy group. Analysis of HRESIMS data established the molecular formula of **68** as $C_{10}H_{14}O_3$ (four degrees of unsaturation), which is consistent with replacement of a phenolic OH group with a methoxy group when compared to **67**. The only question regarding the structure of **68** was the location of the new methyl group. HMBC correlations (Figure 19) from H-6 to C-2, C-4, C-5, and oxygenated carbons C-1 and C-7, from H_2-7 to C-4, C-5, and C-6, from H_3-8 to C-4, C-5, and oxygenated carbon C-3, from H_3-9 to C-1, C-2, and C-3, and from the new methoxy signal (H_3-10) to C-3, indicated that the new methyl group must be attached to the oxygen at C-3, establishing the structure shown for **68**, 5-(hydroxymethyl)-3-methoxy-2,4-dimethylphenol.

Although lacking a second ring, both **67** and **68** are similar to the fungal metabolite **64** in both simplicity and oxygenation pattern. Due to this similarity, both **67** and **68** would presumably possess a biogenetic origin similar to that of **64**, as well as related compounds described in the literature.[187] Compound **68** was tested for antifungal activity against *A. flavus* and *F. verticillioides,* causing zones of inhibition of 15 mm and 21 mm, respectively, against the two fungi at 200 µg/disk. Compound **68** also exhibited modest activity against the fall armyworm, reducing the growth rate by 54%, albeit at a rather high dietary concentration of 15,000 ppm. Compound **67** caused a clear inhibition zone of 15 mm in diameter at 200 µg/disk against *F. verticillioides* and, interestingly, caused an unusual enhanced growth rate (39%) when tested against the fall armyworm at 5,000 ppm.

All of the novel compounds identified from this *E. nidulans* isolate (**65**-**68**) exhibited some level of antifungal activity against *A. flavus* and/or *F. verticillioides*. The presence of these novel bioactive compounds, together with the previously described known carcinogenic mycotoxin **59**, the known anticancer metabolite **60**, and the abundant known bioactive compound **61**, would likely explain the bioactivity originally observed for the ENDO-3111 extract (Table 1).

CHAPTER 6
ADDITIONAL NEW SECONDARY METABOLITES OBTAINED FROM OTHER FUNGICOLOUS FUNGI

In addition to the metabolites described in detail in the preceding chapters, several additional new metabolites were isolated through investigations of additional isolates of fungicolous fungi. These metabolites, although new, were closely related to previously known compounds, so extensive analysis was not required in order to solve their structures. Details of the isolation and structure elucidation of these compounds are summarized in this chapter.

Chemical Investigation of a Fungicolous Isolate of *Trichoderma longibrachiatum* (MYC-1515 = NRRL 54514)

During the course of our ongoing studies of fungicolous fungi, we investigated cultures of a fungicolous isolate of *Trichoderma longibrachiatum* (MYC-1515) that was obtained from a basidioma of *Gloeophyllum trabeum* found growing on a dead hardwood branch on the island of Hawaii. The EtOAc extract of fermentation cultures of this isolate showed modest antifungal activity against *A. flavus* and *F. verticillioides*, as well as limited activity against the fall armyworm (*S. frugiperda*). This extract also exhibited activity in an anti-HIV assay that was conducted by researchers at the National Cancer Institute (NCI). Although the corresponding NCI assay program was terminated, so this activity could not be followed, this result was a contributing factor in the selection of this extract for further investigation. Such activity was not commonly observed among our extracts, suggesting that the effect might be due to the presence of an uncommon or novel compound. Sequential solvent partitioning, silica gel column chromatography, and reversed-phase HPLC (Figure 20) of this extract afforded one new metabolite,

tetrahydrosorbicillinol (**71**), and two previously reported metabolites, harzialactone A (**72**)[195] and bisorbibutenolide (**73**),[196] which were identified by comparison of ^{1}H NMR and/or ^{13}C NMR and MS data with reported values.

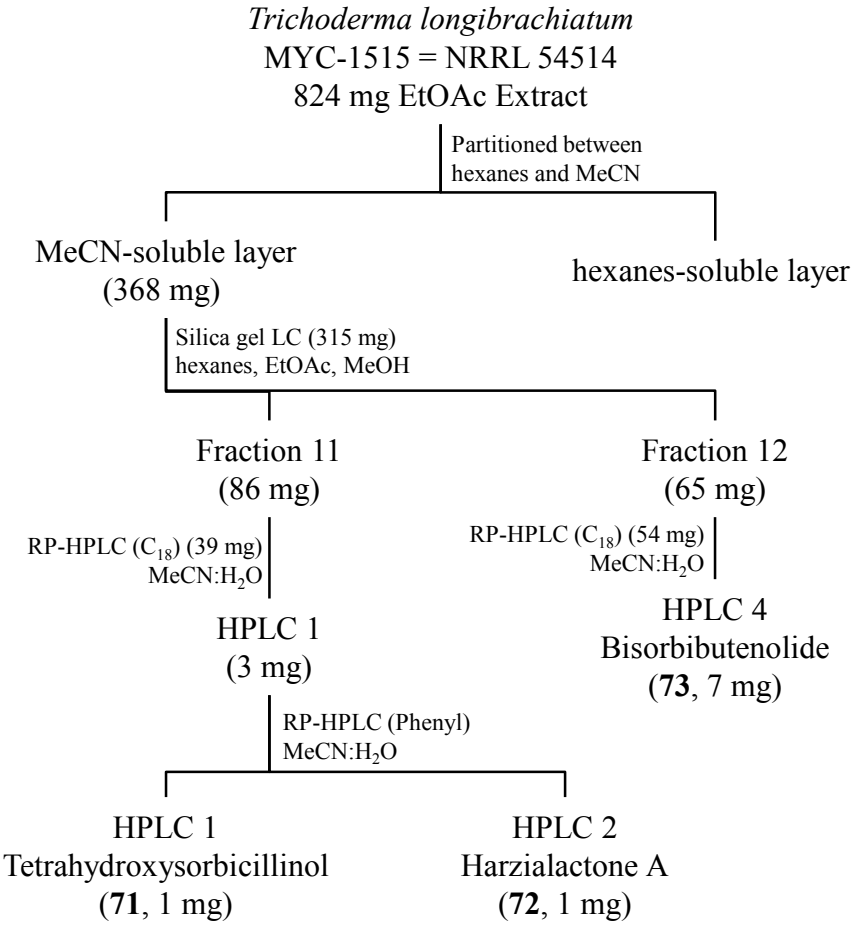

Figure 20. Isolation Scheme for Metabolites **71**-**73** from MYC-1515.

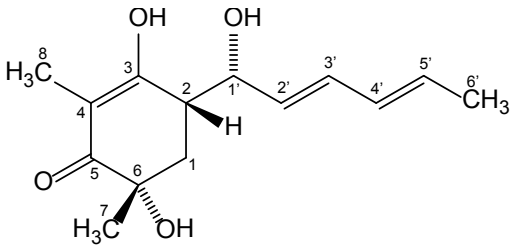

71

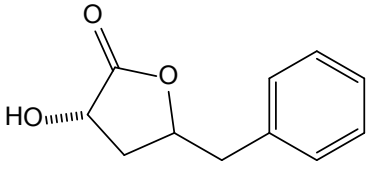

72

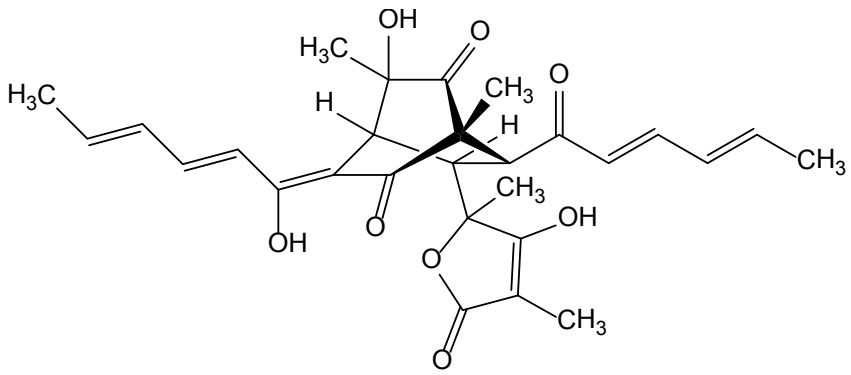

73

Structure Elucidation of Tetrahydrosorbicillinol (**71**)

Analysis of HRESIMS and ^{1}H NMR data established the molecular formula of compound **71** as $C_{14}H_{20}O_4$ (five degrees of unsaturation). The ^{1}H NMR spectrum (Table 12) revealed the presence of a conjugated diene system linked to a terminal vinyl methyl croup, an oxygenated CH unit, a CH_2CH unit, and two additional methyl groups, one of which was attached to a third double bond. Chemical shifts observed in the ^{13}C NMR spectrum (δ 192.1, 106.8, and 196.1) suggested that this third double bond was a tautomerized (i.e., enolized) β-diketone unit. These signals account for 12 of the 14 carbons and three of the five unsaturations. Due to sample limitations, the ^{13}C NMR signals were located and the connectivity of the molecule was assigned through the use of HMBC correlations (Table 12).

Olefinic proton H-3' showed correlations to C-1' and C-5', thereby linking the diene and terminal vinyl methyl unit to oxygenated carbon C-1'. H-1' showed correlations to non-protonated oxygenated olefinic carbon C-3, as well as C-2' and C-3', confirming the connection of the diene unit to C-1'. H_3-8 showed correlations to C-3, C-4, and C-5, confirming that the remaining double bond must be part of an α,β-unsaturated ketone unit, accounting for one of the two remaining unsaturations. Correlations from

H_2-1 to C-2, C-3, C-5, oxygenated quaternary sp^3 carbon C-6, and C-1' indicated that the last unsaturation was a cyclohexanone ring attached to C-1' via C-2. The cyclohexanone ring structure is confirmed by the correlations from H_3-7 to C-5, C-6, and C-7. A small long-range coupling observed for H_3-7 (δ 1.65, J = 0.7 Hz) w disappeared when the signal at δ 2.53 (H-2) was irradiated in a ^{1}H-^{1}H decoupling experiment. The three remaining hydrogen atoms required by the molecular formula must be present as hydroxyl groups. The only possible locations for these three hydroxyl groups are at C-3, C-6, and C-1', all of which were previously identified as oxygenated carbons.

Table 12. NMR Spectroscopic Data for Tetrahydrosorbicillinol (**71**) in CD_3OD.[a]

position	δ_H (mult; J_H in Hz)	δ_C[b]	HMBC (H → C#)[c]
1	1.90 (dd, 12, 5.1)	38.4	2[d], 3, 5, 6, 7
	1.56 (t, 12)		2[d], 6, 7, 1'
2	2.53 (m)	46.2	
3		192.1	
4		106.8	
5		196.1	
6		72.4	
7	1.65 (d, 0.7)	8.1	1, 5, 6
8	1.30 (s)	26.1	3, 4, 5
1'	4.35 (t, 7.4)	77.0	2, 2'[d], 3'
2'	5.49 (dd, 15, 7.5)	131.0	1', 4'
3'	6.21 (dd, 15, 11)	133.8	1', 5'
4'	6.09 (ddd, 15, 11, 1.2)	131.8	2', 6'
5'	5.73 (dq, 15, 6.8)	130.4	3', 6'
6'	1.74 (dd, 6.8, 1.2)	17.9	4', 5'

[a] ^{1}H NMR data were recorded at 400 MHz; ^{13}C NMR data were recorded at 150 MHz. [b] ^{13}C NMR assignments were established by analysis of HMQC and HMBC data. [c]Data collected at 600 MHz. [d]These entries indicate weak HMBC correlations.

The structure of **71** is similar to that of the polyketide-derived known compounds sorbicillinol (**74**) and oxosorbicillinol (**75**), both of which have also been isolated from *Trichoderma* spp.[197,198] The structure of **71** displays reduction of the side-chain carbonyl

carbon and the C-1–C-2 double bond when compared to **74**. The relative configuration of **71** at carbons C-2 and C-1' is based on the coupling constant observed for H-1' (J = 7.4). This J-value indicated that the vicinal angle between H-2 and H-1' was small, suggesting a *syn* relationship. The relative configuration at C-6 was proposed as shown based on analogy to the reported known compounds.[197,198]

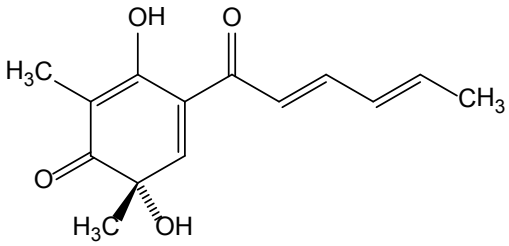

74

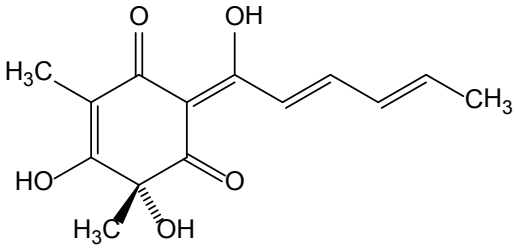

75

As previously discussed, these types of compounds are prone to tautomerization. When evaluating **71**, it was observed that oxygenated olefinic carbon C-3 and carbonyl carbon C-5 showed similar shifts (δ 192.1 and 196.1, respectively), and are consistent with such a system.[197,198] The literature reports of **74** and **75** do not mention the occurrence of tautomerization,[197,198] but clearly, all of these compounds could exist in different tautomeric forms. The choice of the form shown was based on the ^{13}C NMR shift of C-5 being somewhat closer to the shifts typical of ketones. Because C-5 exhibits HMBC correlations to both H_3-7 and H_3-8, the ketone must be in the position shown, as opposed to C-3, which would only correlate to H_3-8. Compound **71** was given the name tetrahydrosorbicillinol because it can be viewed as a reduced version of **74**.

When tested for antifungal activity against *A. flavus* and *F. verticillioides* in standard disk assays, compound **71** showed no activity at 200 µg/disk. No bioactivity has

been reported for either of the known compounds **72**[195] and **73**.[196] Compounds **72** and **73** have not yet been tested for bioactivity in our own assays, due to time limitations. Therefore, the metabolite(s) that were responsible for the modest bioactivity of the crude extract in this case have yet to be identified.

Chemical Investigations of a Fungicolous Isolate of *Stachybotrys parvispora* (MYC-2013 = NRRL 54531)

Stachybotrys parvispora Hughes (Dermatiaceae) is a relatively unexplored member of the *Stachybotrys* genus, as only a few prior reports of metabolites from this species, such as parvisporin (**76**), from this species have appeared.[199] By contrast, a more commonly explored species of this genus (*S. chartarum*) is known to produce mycotoxins known as satratoxins.[200] Satratoxins are known to cause pulmonary inflammation and hemorrhaging in infants when individuals are exposed to *S. chartarum* spores that have grown in damp structures.[200] A fungicolous isolate of *S. parvispora* (MYC-2013) was obtained from a white mycelial growth on the undersurface of a dead hardwood branch near Mackenzie State Park in Hawaii. The EtOAc extract of solid-substrate fermentation cultures of this isolate showed moderate antifungal activity against *F. verticillioides* in a disk diffusion assay. Chemical studies of this extract afforded a new metabolite that was named agistatine F (**77**). Compound **77** was obtained through silica gel chromatographic fractionation of the crude extract, followed by reversed-phase HPLC (Figure 21). In addition to **77**, a known compound from the same family, agistatine B (**78**) was also encountered in the extract. Parvisporicin (**79**), a metabolite previously isolated by a member of our group from a different isolate of *S. parvisporia*, was identified as the major component of the extract through ^{1}H NMR and ^{13}C NMR data analysis and by comparison to reported values.[201]

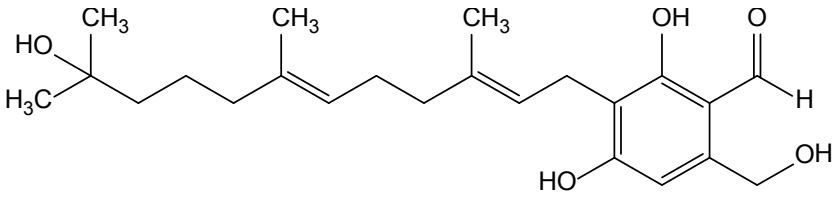

76

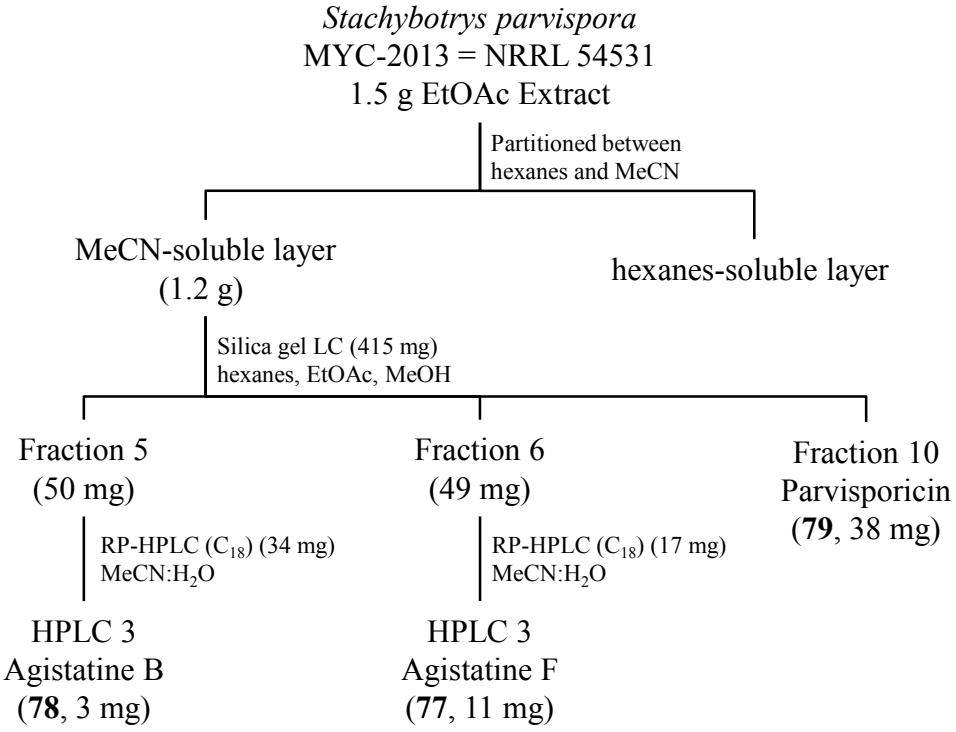

Figure 21. Isolation Scheme for Metabolites **77-79** from MYC-2013.

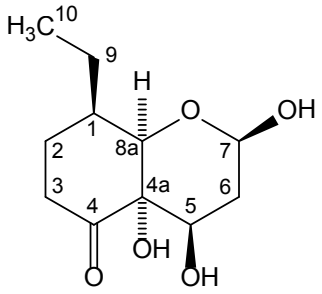

77

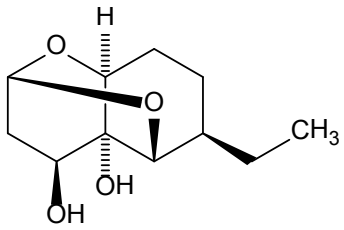

78

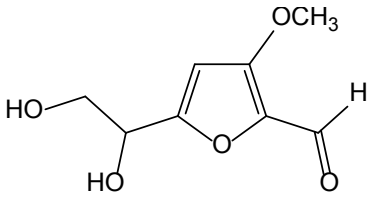

79

Structure Elucidation of Agistatine F (**77**)

The molecular formula of **77** was determined to be $C_{11}H_{18}O_5$ (three degrees of unsaturation) on the basis of NMR (Table 13) and HREIMS data. The ^{1}H NMR spectrum indicated the presence of four methylene units, one of which was coupled to a methyl group, and four methine protons, three of which were on oxygen-bearing carbons. The ^{13}C and DEPT NMR data showed signals for 11 carbons including a ketone, three oxygenated sp^3 methines, one oxygenated quaternary carbon, one non-oxygenated methine carbon, four methylene carbons, and a methyl group (Table 13). Comparison of the ^{1}H NMR and DEPT data with the molecular formula indicated that the three broad singlets from δ 3.10 to 3.40 must correspond to three free hydroxyl groups.

Table 13. NMR Spectroscopic Data for Agistatine F (**77**) in $CDCl_3$.

position	δ_H (mult; J_H in Hz)[a]	δ_C[b]	HMBC (H → C#)[a]
1	2.21 (m)	36.2	2[c], 9[c], 10[c]
2	1.83 (m)	26.5	1, 3, 4, 8a, 9
	1.71 (dq, 14, 4.3)		1, 3, 4, 8a, 9
3	2.81 (dt, 14, 6.5)	38.0	1, 2, 4, 4a
	2.28 (ddd, 14, 4.3, 2.6)		1, 2, 4, 4a
4		209.8	
4a		72.0	
5	4.18 (br t, 3.1)	67.1	4[c], 4a, 6, 8a
6	2.09 (br t, 3.1)	33.8	4a, 5, 7
7	5.25 (br s)	92.3	5, 8a
8a	4.28 (br s)	69.9	1, 2, 4, 4a, 7, 9
9	1.43 (m)	23.9	1, 2, 8a, 10
	1.38 (m)		1, 2, 8a, 10
10	0.95 (t, 7.5)	11.8	1, 9
4a-OH	3.10-3.40 (br s)		
5-OH	3.10-3.40 (br s)		
7-OH	3.10-3.40 (br s)		

[a]Data collected at 600 MHz. [b]Data collected at 100 MHz. ^{13}C NMR assignments were established by analysis of HMQC and HMBC data. [c]Weak HMBC correlations due to signal broadening.

Analysis of HMBC and ^1H-^1H NMR decoupling data confirmed the presence of a cyclohexanone-pyranacetal bicyclic ring system as shown in **77**. The decoupling experiments enabled establishment of two distinct spin-systems, which were then linked together by HMBC correlations (Table 13). The $CH_3CH_2CHCH_2CH_2$ spin-system corresponding to the C-1–C-3/ C-9–C-10 unit in **77** was established by a complete set of decoupling experiments, as was the OH–CH2CH–O spin-system corresponding to the C-5–C-7 unit. ^{13}C NMR shift data indicated that the carbons C-4a, 4, and 8a were all oxygenated, while C-7 was deoxygenated. Key HMBC correlations from H-3 to C-4 and C-4a; from H-5 to C-4 and C-4a; and from H-7 to C-8a interconnected these distinct spin systems in **77**.

Comparison with literature data showed that **77** is a new member of a class of known compounds called agistatines, which include compound **78**, agistatine A (**80**), and agistatine E (**81**).[202] The absolute configuration of the previously known agistatines was assigned by X-ray diffraction analysis of the 2-bromobenzoic acid derivative of **80**.[202] The relative configuration of **77** was assigned by analogy to these known compounds as well as relevant coupling constants observed in the ^{1}H NMR spectrum (Table 13).

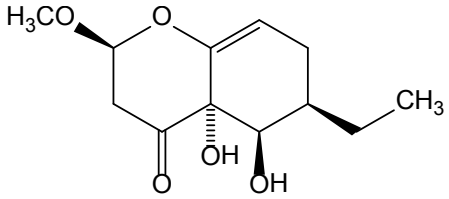

80

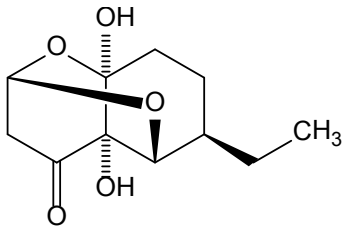

81

Compound **77** does display some differences relative to the other agistatines. The most obvious difference is the location of CH_2CH_3 side-chain, which is *para* to the ketone in **77**, rather than at C-6, which is the case with all other agistatines. Like the previously known agistatines, **77** seems likely to be polyketide-derived, however, no discussion of the biosynthetic pathway leading to the known agistatines has been provided in the literature.[202] The name agistatine F was proposed for **77** due to its resemblance to the known agistatines.

Although reportedly tested for antibacterial, anitfungal, antiviral, herbicidal, and insecticidal activity, the known agistatines did not exhibit any significant activity.[202] Similarly, compound **77** did not display any antifungal activity when tested at 200 µg/disk against *A. flavus* and *F. verticillioides*. Compound **77** did, however, exhibit limited antiinsectan activity, reducing the growth rate of the fall armyworm by 39% when

compared to controls, albeit at a very high concentration (17,500 ppm). Although parvisporicin (**79**) was obtained as the major metabolite of the MYC-2013 extract, it is also reported to display no antifungal activity against *A. flavus* or *F. verticillioides* in standard disk assays at similar levels.[201] The metabolite(s) responsible for the initial bioactivity of the crude extract were again, therefore, not identified.

Chemical Investigations of an Unidentified Fungicolous Fungus (MYC-1991)

The EtOAc extract of fermentation cultures of an unidentified fungicolous fungal isolate (MYC-1991) yielded a compound previously known as a synthetic product named dihydrosporothriolide (**82**).[203] However, it was isolated as a natural product for the first time from this extract. This fungal isolate was collected from the surface stromata of a Pyrenomycete that was found growing a dead hardwood branch on the island of Hawaii in November 2002. Extracts from fermentation cultures of the isolate exhibited modest antifungal activity against *F. verticillioides*. Compound **82** is reported to possess antifungal activity against *Ustilago violacea* and *Mycotypha microspora*, as well as herbicidal activity against *Medicago stiva* (Alfalfa).[203] The isolation (Figure 22) and characterization of **82** is described here.

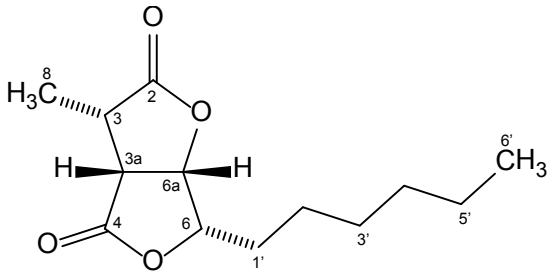

82

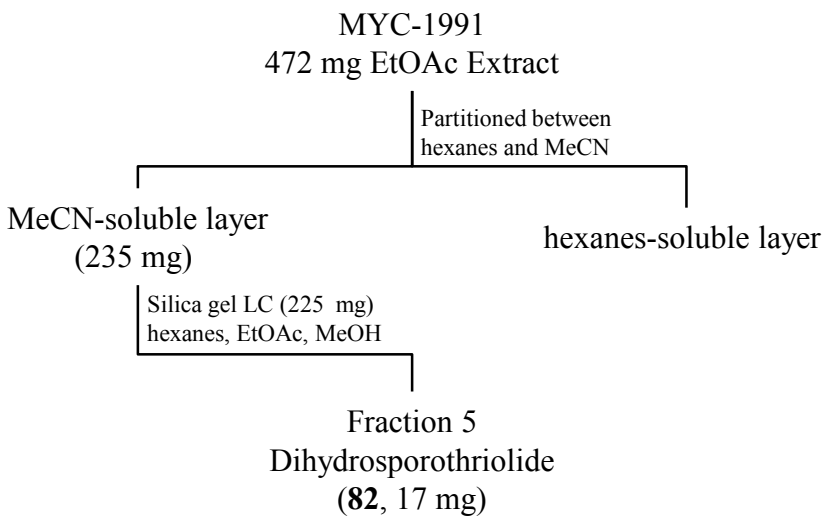

Figure 22. Isolation Scheme for Dihydrosporothriolide (**82**) from MYC-1991.

Structure Elucidation of Dihydrosporothriolide (**82**)

The molecular formula of compound **82** was determined to be $C_{13}H_{20}O_4$ (four degrees of unsaturation) on the basis of ^{1}H NMR and HRESIMS data. The ^{1}H NMR spectra exhibited signals (Table 14) corresponding to two methyl groups (one doublet and one triplet), two sets of overlapping aliphatic multiplets, one integrating to two protons, the other integrating to eight, and four sp^3 methine protons, two of which were on oxygen-bearing carbons. Comparison of HRESIMS data and partial structures obtained from ^{1}H NMR analysis to literature and database information initially yielded no known matches. Therefore ^{13}C, DEPT, and homonuclear decoupling NMR experiments were performed to elucidate the structure of **82**. Evaluation of the ^{13}C and DEPT NMR spectra (Table 14) accounted for all hydrogen atoms in the formula as CH-type hydrogens (requiring the absence of exchangeable hydrogens). These data also confirmed the presence of 13 carbons, including two ester carbonyl carbons (δ 176.3 and 172.2), two oxygenated sp^3 methine carbons (δ 81.9 and 78.1), two non-oxygenated sp^3 methine

carbons (δ 45.9 and 37.0), two methyl groups (δ 14.2 and 11.1), and five aliphatic methylene carbons (δ 35.5, 31.9, 29.0, 29.0, and 22.6).

Table 14. ^{1}H and ^{13}C NMR Data for Dihydrosporothriolide (**82**) in $CDCl_3$.[a]

position	δ_H (mult; J_H in Hz)	δ_C
2		172.2
3	3.02 (dq, 10, 7.5)	37.0
3a	3.40 (dd, 10, 6.0)	45.9
4		176.3
6	4.48 (ddd, 6.0, 4.0, 1.5)	78.1
6a	5.00 (dd, 6.0, 4.0)	81.9
8	1.45 (d, 7.5)	14.2
1'	1.85 (m)	31.9
2'	1.21-1.42 (m)	29.0
3'	1.21-1.42 (m)	29.0
4'	1.21-1.42 (m)	35.5
5'	1.21-1.42 (m)	22.6
6'	0.93 (t, 6.7)	11.1

[a]Data collected at 400 MHz (^{1}H) and 100 MHz (^{13}C).

Decoupling experiments were used to establish the connectivity of these units to determine the gross structure of **82**. Irradiating the muliplet at δ 1.85 (H_2-1') caused the signal at δ 4.48 (H-6, ddd) to sharpen and change to a doublet of doublets. Irradiation of H-6 caused the proton on oxygen-bearing carbon C-6a (H-6a , δ 5.00, dd) to collapse to a doublet. Decoupling H-6a resulted in simplification of H-3a (δ 3.40, dd) to a doublet and H-6 to a doublet of doublets. Irradiating H-3a simplified the signal for H-6a and caused the H-3 signal (δ 3.02, dq) to sharpen slightly. The final methyl doublet was attached to the core structure via CH-3, as irradiation of H-3 caused H_3-8 (δ 1.45, d) to collapse to a singlet. The last two unsaturations that had yet to be accounted for required the presence of two ester linkages (O-1 to C-6a and O-5 to C-6) in **82**. The resulting bicyclic ring

system structure was fully consistent with the decoupling results and with ^{13}C NMR and DEPT data.

Once the structure of **82** had been assigned, a full structure search was conducted and it was then discovered that this molecule was a previously known, but only as a hydrogenation product of the known fungal natural product sporpthriolide (**83**),[203] not as a natural product itself. Comparison of the ^{1}H NMR data of natural product **82** with the synthetic compound further confirmed the structure of **82**. The absolute configuration of the synthetic product, and by analogy, the naturally occurring compound **82**, was assigned by analogy to that previously established for **83**.[203] The *exo*-addition of hydrogen expected during hydrogenation of **83**, as well as the large coupling constant between H-3a and H-3 (J = 10 Hz), indicated a *cis* relationship of these protons, based on other γ-lactone precedent structures, thereby establishing the configuration for synthetic **82**.[203]

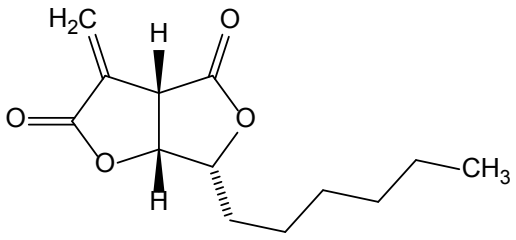

83

This is the first report of the isolation of compound **82** as a natural product. In addition, no ^{13}C NMR assignments were provided for **82** in the literature, so those assignments are also reported here for the first time. Synthetic **82** was reported to possess antifungal and herbicidal activity.[203] When tested in our own assays, **82** exhibited significant antifungal activity against both *A. flavus* and *F. verticillioides* at 200 μg/disk, showing clear inhibition zones of 17 mm in diameter against *A. flavus* and 25 mm in

diameter against *F. verticillioides* in standard disk assays. This bioactivity is most likely the cause of the activity of the crude extract against *F. verticillioides*, but interestingly, the crude extract did not show any antifungal activity against *A. flavus* even though **82** showed significant activity. Compound **82** also exhibited weak antiinsectan activity by reducing the growth rate of the fall armyworm by 62% when compared to controls, albeit again at a rather high concentration at a concentration (17,500 ppm).

The studies of new metabolites presented in this Chapter demonstrate that even close analogues of known compounds can be chemically interesting. In the case of **82**, a known compound was revealed to possess bioactivity that was not previously known, which can sometimes be as important as the initial isolation of the metabolite itself. The isolation of such analogues can add to the information about a family of compounds not only in their identification, but also to information about the types of compounds produced by fungi of certain taxa from specific environments.

CHAPTER 7

NEW STILBENE-DERIVED PHYTOALEXINS FROM PEANUT (*ARACHIS HYPOGAEA*) SEEDS CHALLENGED BY *ASPERGILLUS CAELATUS*

Peanut (*Arachis hypogaea*) is a plant endemic to South America that has been widely introduced and has become an economically and nutritionally important crop worldwide.[204] Peanuts are host to approximately 50 genera of fungi,[205] among which *Aspergillus* species, especially *A. flavus* and *A. parasiticus*, are of particular agricultural significance due to their ability to produce carcinogenic aflatoxins.[206] Under favorable conditions, the peanut plant can resist fungal attack by promptly producing stilbene-derived phytoalexins.[205,207-209] This natural phytotalexin-based mechanism of peanut disease resistance is attractive because, once understood, it may be possible to manipulate this mechanism of resistance to enhance natural peanut resistance to pests. Such knowledge may be valuable for breeding new fungi-resistant peanut cultivars.

A number of stilbene phytoalexins from peanuts have been reported.[100, 210-214] The pathway of formation of stilbenoids[214-218] as well as the occurrence of other stilbenoids in other plants[219-223] suggests that peanuts may be capable of producing other important bioactive stilbenoids. The purpose of this research was to isolate and characterize further new and/or known stilbenoids that may occur in peanut seeds and may act as phytoalexins.

More complex stilbenoid derivatives, such as those reported from other sources that are considered important factors in defense of the corresponding plants have not previously been found in peanuts.[221,223-228] For example, stilbene dimers and oligomers are known to possess biological activity.[227,229-235] The potential therapeutic value of stilbenoid dimers has promoted research activity on the occurrence of this class of compounds in various plants around the world.[221-235]

The research described here resulted in the isolation and identification of four new stilbene derivatives, called arahypins, that were isolated from peanut seeds challenged by an *Aspergillus caelatus* strain, along with two other stilbenoids, chiricanine A (**84**) and arahypin-2 (**85**), that were previously known from other plant sources, but had not been reported in peanuts. The new arahypins include araphypin-1 (**86**), arahypin-3 (**87**), arahypin-4 (**88**), and arahypin-5 (**89**). Together with these metabolites, several higher-molecular weight compounds with spectroscopic properties characteristic of stilbenoids were also detected. These metabolites were found to be a part of new dimeric stilbenoids, which were assigned the names arahypin-6 (**90**) and arahypin-7 (**91**). Details of the isolation (Figure 23) and structure elucidation of all of these metabolites are presented here.

Based on earlier results, as noted above, it was expected that challenged peanut seeds might produce stilbene phytoalexins, and initial HPLC separations of extracts made from seeds that were incubated with *A. caelatus* for 96 hr showed three major peaks correlating to known stilbene compounds. Several additional unidentified compounds (**84**-**89**) were thought to be stilbenoids based on their characteristic UV absorptions in the 281-313 or 308-339 nm range, as well as their HPLC-DAD-MS data.

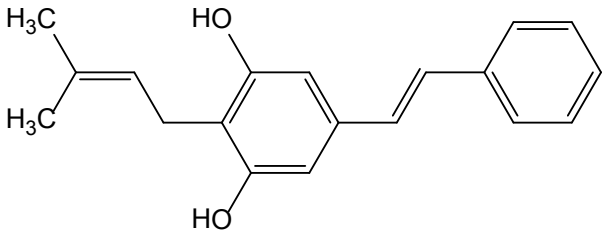

84

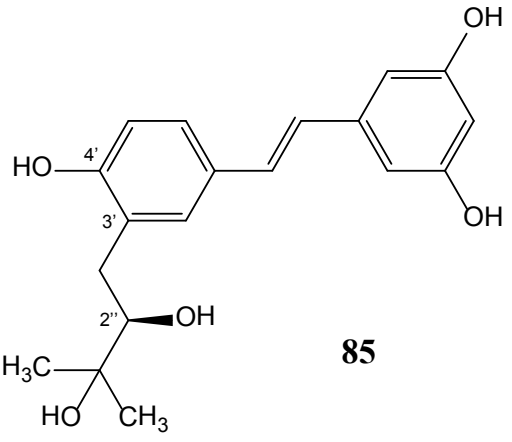

85

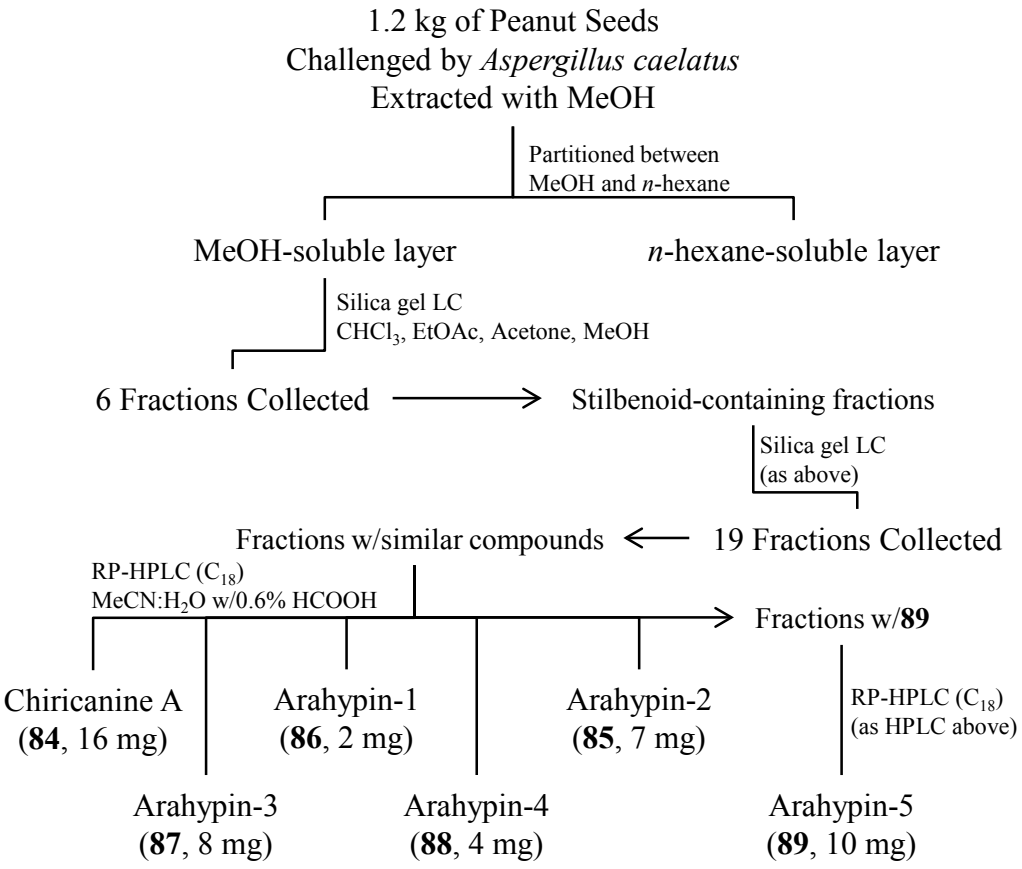

Figure 23. Isolation Scheme for the MeOH Extract of Peanut Seeds Challenged by *Aspergillus caelatus* that Yielded Stilbenoids **84-89**.

Structure Elucidation of Chiricanine A (**84**) and Arahypins 1-7 (**85-91**)

The APCI mass spectrum of **84** showed a molecular mass of 280 Da, and a characteristic loss of 56 Da, corresponding to a loss of C_4H_8, as is typical for prenylated stilbenes.[90] An absorption in the UV spectrum in the 301-312 nm range suggested the absence of a conjugated double bond in the prenyl side chain.[100,210,211] This was

supported by the ^{1}H NMR spectrum in which the methyl groups of the prenyl side chain were no longer doublets and were shifted slightly downfield. Upon further evaluation of the data, the structure of **84** was found to match that of chiricanine A, a compound previously reported from the root bark of the leguminous tree *Lonchocarpus chiricanus*.[219] Similarly, compound **85** (molecular mass 330 Da), whose structure was determined though ^{1}H NMR,^{13}C NMR, HMQC, HMBC, and HRESIMS data analysis, had been reported as a constituent of the evergreen tree *Artocarpus dadah*.[220] Compound **85** was not given a common name by the original authors, so the name arahypin-2 was proposed for it in order to reflect its relationship to other similar compounds encountered in this work. Neither of these compounds has been reported previously as a peanut metabolite. All of the new compounds described below are similar to these known compounds, and their structure assignments were facilitated by this resemblance.

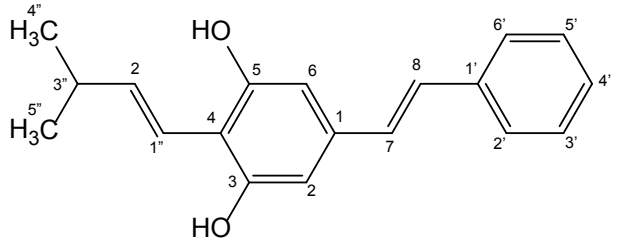

86

The APCI-MS data for **86** matched very closely with those of **84** which is an isomer of **86**. However, a UV absorption at 327 nm suggested the presence of a conjugated double bond in the side chain in the compound in this instance. Analysis of ^{1}H, ^{13}C, and DEPT NMR data (Tables 15 and 16) for **86**, when compared to **84**, confirmed very close structural similarities. Similarities included ^{1}H NMR signals consistent with a monosubstituted phenyl group, a symmetrical 1,3,4,5-tetrasubstituted benzene ring, a *trans* double bond, and two methyl groups. The difference between

the ^{1}H NMR spectra of **84** and **86** indicating the presence of a second *trans* double bond, and both of the methyl signals were now split into doublets (J = 7.2 Hz) in the spectrum of metabolite **86**. Interpretation of these data was straightforward and led to the confirmation that the structure of **86** differs from that of **84** only in that the side-chain olefin is located between C1" and C2", rather than between C2" and C3". This difference rationalizes the replacement of the NMR signals for the vinylic methyls, the trisubstituted olefin, and the adjacent methylene unit in the data for **84** with signals for an isopropyl group linked to a *trans*-oelefin unit in the spectra of **86** (Tables 15 and 16). Secondary metabolite **86** has not been previously reported and was given the common name arahypin-1.

Table 15. ^{1}H NMR Data (400 MHz) for Compounds **86-89**.

	δ_H (mult; J in Hz)			
position	**86**[a]	**87**[b]	**88**[b]	**89**[a]
2	6.63 s	6.52 s	6.56 s	6.57 (d, 1.4), 6.41 (d, 1.4)
7	6.93 (d, 16)[c]	6.76 (d, 17)[d]	6.97 (d, 16)[e]	6.75 (d, 16)
8	7.03 (d, 16)[c]	6.93 (d, 17)[d]	7.02 (d, 16)[e]	6.94 (d, 16)
2', 6'	7.46 (br d, 8.0)	7.34 (d, 8.5)	7.49 (dd, 7.4, 1.2)	7.34 (d, 8.4)
3', 5'	7.34 (t, 8.0)	6.76 (d, 8.5)	7.32 (t, 7.4)	6.79 (d, 8.4)
4'	7.24 (t, 8.0)		7.21 (dt, 7.4, 1.2)	
1"	6.27 (dd, 16, 1.6)	2.60 (dd, 14, 10)	2.62 (dd, 14, 10)	6.59 (d, 10)
		3.12 (dd, 14, 2.4)	3.13 (dd, 14, 2.3)	
2"	6.14 (dd, 16, 7.2)	3.55 (dd, 10, 2.4)	3.56 (dd, 10, 2.3)	5.58 (d, 10)
3"	2.55 (doct, 7.2, 1.6)			
4", 5"	1.13 (d, 7.2)	1.24 s	1.25 s	1.42 s
OHs	5.10 br s			4.81 br s, 4.86 br s

[a] In $CDCl_3$. [b] In CD_3OD. [c-e] Assignments with identical superscripts are interchangeable. Assignments for **87** were verified by analysis of HMBC data.

Table 16. ^{13}C NMR Data (100 MHz) for Compounds **86-89**.

position	**86**[a]	**87**[b]	**88**[b]	**89**[a]
1	146.2 s	138.6 s	138.9 s	138.6 s
2	105.8 d	106.3 d	106.5 d	105.9 d
3	153.8 s	157.8 s	157.9 s	155.3 s
4	111.8 s	114.3 s	115.0 s	109.0 s
5	153.8 s	157.8 s	157.9 s	151.2 s
6	105.8 d	106.3 d	106.5 d	107.1 d
7	127.8 d[c]	128.8 d[d]	128.4 d[e]	126.1 d
8	128.0 d[c]	130.5 d[d]	128.8 d[e]	128.4 d
1'	137.2 s	127.0 s	138.0 s	130.2 s
2'	126.7 d	128.7 d	127.4 d	115.6 d
3'	128.8 d	116.5 d	129.7 d	128.0 d
4'	129.3 d	158.3 s	129.9 d	154.1 s
5'	128.8 d	116.5 d	129.7 d	128.0 d
6'	126.7 d	128.7 d	127.4 d	115.6 d
1"	117.2 d	26.7 t	26.8 t	116.3 d
2"	137.8 d	80.9 d	80.9 d	128.4 d
3"	32.3 d	74.0 s	74.0 s	76.1 s
4"	22.4 q	25.5 q	25.5 q	27.8 q
5"	22.4 q	25.3 q	25.3 q	27.8 q

[a] In $CDCl_3$. [b] In CD_3OD. Chemical shift (δ) values presented in ppm. Carbon multiplicities are shown next to the shifts and were established by DEPT experiments. Position assignments were made on the basis of chemical shifts, multiplicities, comparisons with similar analogues in the literature, and/or HMBC data (for **89**). A different numbering system was used in ref 236 for a close analogue of **89**, but the shifts corresponding to C4 and C5 in this table were accidentally reversed in that reference. [c-e] Assignments with identical superscripts are interchangeable.

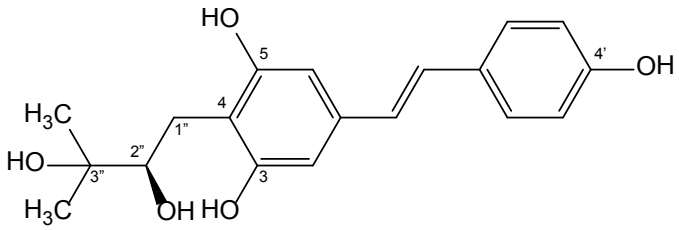

87

The UV and HRESI mass spectra of arahypin-3 (**87**) were similar to those of **85**. The molecular formula of **87** was determined to be $C_{19}H_{22}O_5$ (nine degrees of

unsaturation) on the basis of ^{1}H NMR,^{13}C NMR, DEPT, and HRESIMS data. Analysis of the ^{1}H, ^{13}C, and DEPT NMR data (Tables 15 and 16) revealed that **87** contained a dihydroxylated prenyl group identical to that of **86**. More specifically, this unit was recognized on the basis of NMR signals for a dimethylated oxygen-bearing quaternary carbon and an isolated CH_2–CHOH unit in place of signals corresponding to the prenyl groups found in the spectra of **84** and **86**. The NMR spectra for **87** also clearly indicated the presence of the *trans* olefin unit characteristic of a stilbene structure, an oxygenated *para*-substituted benzene ring, and the same type of symmetrical 1,3,4,5-tetrasubstituted ring found in **84** and **86**. These results indicate that the dihydroxylated prenyl group in **87** is located on the dihydroxylated ring, by analogy to both **84** and **86**, rather than on the monooxygenated ring, as in **85**. Compound **87** is also a novel natural product and was assigned the named arahypin-3.

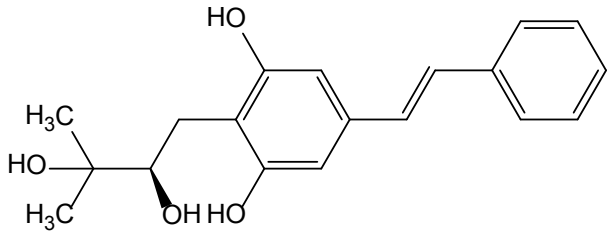

88

Compound **88** has a molecular formula of $C_{19}H_{22}O_4$ (nine degrees of unsaturation), as established by analysis of NMR (Tables 15 and 16) and HRESIMS data. It differs from **85** only in the absence of the hydroxyl group at C4'. The presence of one fewer oxygen atom in the molecular formula relative to that of **85**, together with the replacement of the *para*-disubstituted pattern present in the ^{1}H and ^{13}C NMR spectra of **85** with diagnostic monosubstituted phenyl group NMR signals in the data for **88**, made the assignment particularly straightforward. This structure assignment for **88** is

consistent with its significantly lower polarity, as reflected by a considerable difference in the retention times between **84** and **88**. Compound **88** is also a new natural product, and was assigned the name arahypin-4.

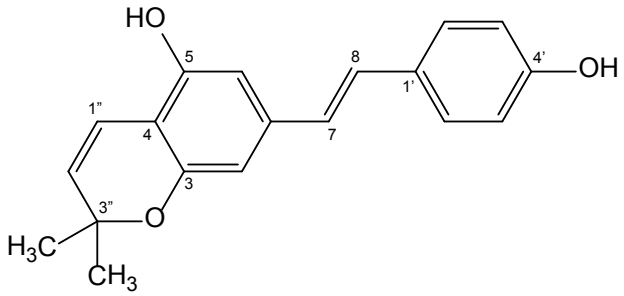

89

Compound **89** was assigned the molecular formula $C_{19}H_{18}O_3$ (11 degrees of unsaturation) by analysis of NMR and HRESIMS data and clearly contained a unit not found in any of compounds **84**-**88**. Unlike compounds **84** and **86**, which displayed a characteristic loss of 56 Da (C_4H_8) in the EI mass spectrum, and compounds **86** and **87**, each of which showed an abundant M-H_2O ion, compound **89** produced a highly fragmented mass spectrum that included a distinctive loss of 28 Da (CO or C_2H_4). In addition to signals indicating the presence of a *p*-disubstituted oxygenated benzene ring and a *trans* olefin stilbene bond, the ^{1}H NMR spectrum included signals representative of an isolated *cis*-olefin unit that was suggestive of the cyclization of a prenyl unit with an *ortho* position of the aromatic ring to form a dimethyl coumarin unit.[236] The location of this new ring was based on comparison of NMR data (Tables 15 and 16) with those of similar compounds,[236] together with the fact that all of the other stilbenoids in the mixture that have a prenyl group linked to the dihydroxylated ring place the group in a position analogous to that shown for **89**. In order to verify this regiochemical assignment and to enable unambiguous NMR shift assignments for all positions, an HMBC experiment was performed. As expected, the signal for the olefinic H-1" showed correlations to both of

the oxygenated carbons of the adjoining aromatic ring (C-3 and C-5), whereas both H-2 and H-6 (now two differently *meta*-coupled signals due to the less symmetrical structure) showed correlations to the C-7 carbon of the central olefin of the stilbene unit. These results confirmed the location of the new ring as shown in structure **89**. Compound **89** is also a previously unreported metabolite and was assigned the name arahypin-5.

Due to the ease with which stilbenoids are known to undergo olefin photoisomerization under particular conditions,[237] it should be noted that all of these stilbenoids were detected strictly in the *trans*-configuration on the basis of the large *J*-value (16–17 Hz) for the ^{1}H NMR signals at the central olefin unit in each case. For compounds **85**, **87**, and **88**, another stereochemical issue was raised by the presence of an sp^3 stereocenter in each side chain. Studies reported for known compound **85** afforded the intriguing result that **85** was originally reported as a 5:3 mixture of enantiomers favoring the *R*-isomer.[220] This enantiomeric mixture was observed when Kinghorn, *et al*. attempted to determine the absolute configuration of **85** by application of Mosher's Method, and unexpectedly observed pairs of signals for the reaction products obtained with both the *R* and *S* forms of the Mosher reaction. The relative integration of the separated signals, led to determination of the 5:3 ratio of *R*- to *S*-isomers.[220] Comparison of the specific rotation of the sample of **85** obtained in the current study (+8.1) with that of the sample previously described (+4.0) indicated that the sample of **85** obtained from peanuts is also not a pure enantiomer, but is instead present in approximately a 2:1 *R*-to-*S* ratio, rather than a 5:3 ratio. Compounds **87** and **88** also showed positive specific rotations and are presumed to favor the *R*-form over the *S*-form by analogy with the aforementioned example, but their enantiomeric identities and ratios were not rigorously determined.

Several additional stilbenoid-like compounds, with molecular masses significantly higher than the simple stilbenoid derivatives described above, were also detected in the course of this project. A second extract of inoculated peanut seeds, again challenged by

A. caelatus, was separated in the hopes of isolating these higher-mass stilbenoids in larger quantities (Figure 24), as the previous isolation scheme (Figure 23) failed to produce these larger stilbenoids in sufficient quantities for characterization. All of these higher mass compounds were eluted from an analytical reversed phase HPLC column after elution of all of the major simple stilbenoids. These compounds (**90** and **91**) were suggested to be stilbenoid derivatives based on their characteristic UV absorptions in the 340 nm region, as well as their HRESIMS data. Both ESI and APCI MS of **90** revealed a molecular weight of 606 Da and a characteristic loss of 56 Da (C_4H_8), as observed for several of the prenylated stilbene derivatives described above. The structure of **90** was ultimately deduced by detailed analysis of HRESIMS and NMR data.

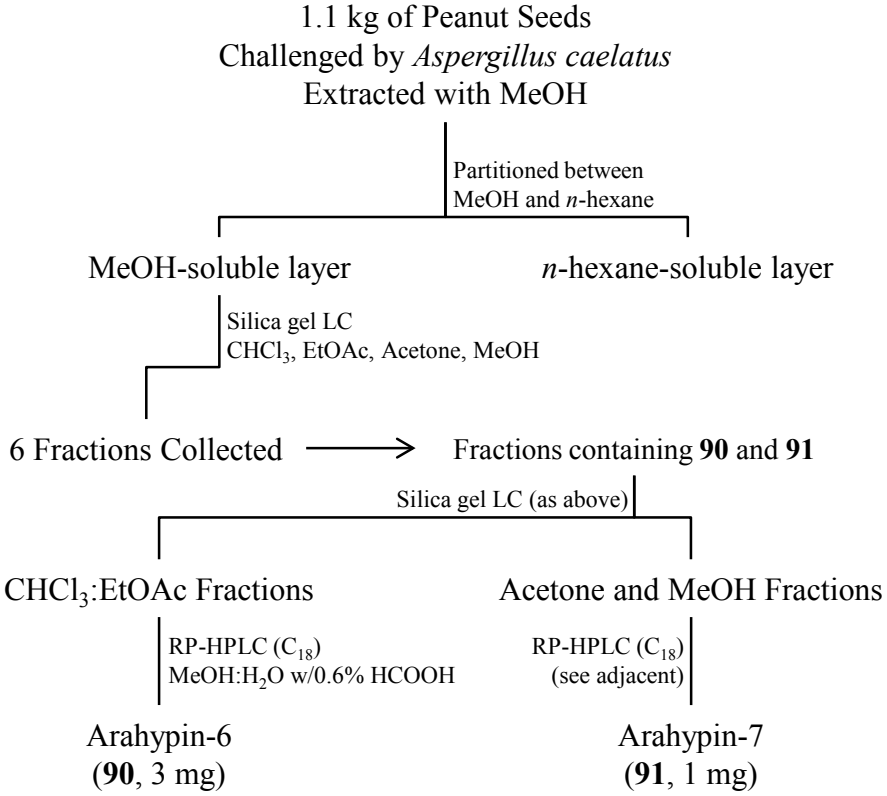

Figure 24. Isolation Scheme for the MeOH Extract of Peanut Seeds Challenged by *Aspergillus caelatus* that Yielded Dimeric Stilbenoids **90** and **91**.

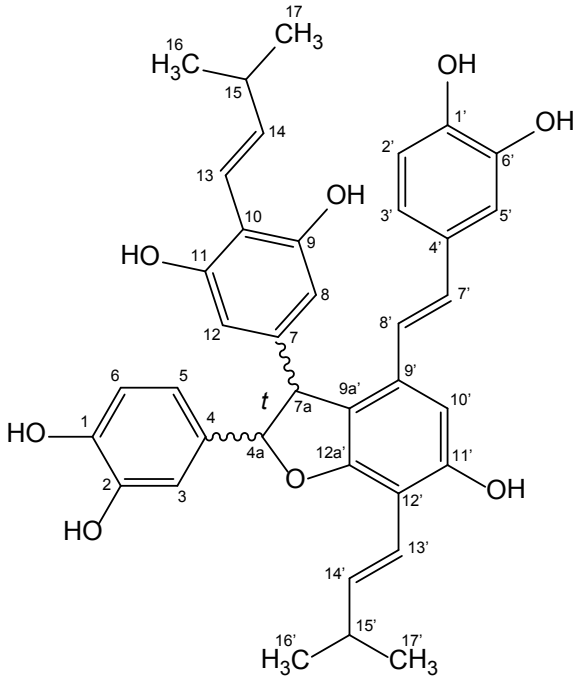

90

Compound **90** was assigned the molecular formula $C_{38}H_{38}O_7$ (20 unsaturations) by analysis of NMR and HRESIMS data. NMR data (Table 17) revealed the presence of two isolated *trans*-3-methyl-1-butenyl groups, an isolated *trans*-olefin unit, a monooxygenated *para*-disubstituted benzene ring, a *meta*-dioxygenated 1,2,3,5-tetrasubstituuted benzene ring with C2 symmetry, a *meta*-dioxygenated pentasubstituted benzene ring, and an *ortho*-dioxygenated 1,2,4-trisubstituted benzene ring. ^{1}H NMR signals corresponding to six phenolic OH groups were also observed, as well as resonances corresponding to an isolated OCH–CH system. This seventh and final oxygen atom must be present as an ether group involving this unit and one of the seven oxygenated aromatic carbons.

Table 17. NMR Spectroscopic Data for Arahypin-6 (**90**) in $CDCl_3$.[a]

position	δ_H (mult; J in Hz)	δ_C[b]	HMBC (H# → C#)
1	5.12 s, OH	143.8	1[c]
2	5.13 s, OH	143.8	2[c]
3	6.83 (d, 2.0)	112.5	1, 5
4		135.2	
4a	5.45 (d, 5.3)	92.7	3, 5, 7, 12a'
5	6.76 (dd, 8.3, 2.0)	118.2	1, 2 wk, 3
6	6.82 (d, 8.3)	115.5	2, 4
7		144.5	
7a	4.36 (d, 5.3)	56.6	4, 4a, 7, 8/12, 9a', 12a'
8, 12	6.30 s	107.0	7, 8/12, 9/11, 10
9, 11	5.08 s, OH	154.2	8/12, 9/11, 10[c]
10		111.0	
13	6.24 (dd, 17, 1.2)	117.2	9/11, 15
14	6.10 (dd, 17, 6.7)	146.0	10, 13, 15, 16/17
15	2.54 m	32.3	
16	1.102 (d, 6.8)	22.7	14, 15, 16/17
17	1.106 (d, 6.8)	22.7	14, 15, 16/17
1'	4.71 s, OH	155.5	
2', 6'	6.70 (d, 8.7)	115.5	1', 2'/6', 4'
3', 5'	7.09 (d, 8.7)	127.8	1', 3'/5', 7'
4'		130.3	
7'	6.79 (d, 16)	129.0	4', 3'/5', 9'
8'	6.510 (d, 16)	122.8	4', 7', 9a', 10'
9'		133.5	
9a'		119.2	
10'	6.66 s	104.0	8', 9a', 11', 12'
11'	5.14 s, OH	154.0	
12'		108.0	
12a'		159.0	
13'	6.512 m[d]	117.2	11', 12a', 14', 15'
14'	6.512 m[d]	142.7	12', 15', 16'/17'
15'	2.54 m	32.7	
16', 17'	1.11 (d, 6.8)	22.4	14', 15', 16'/17'

[a] ^1H NMR data were recorded at 400 MHz; ^{13}C NMR data were recorded at 150 MHz. [b] ^{13}C NMR assignments were established by analysis of HMQC and HMBC data. [c]These entries indicate correlations from the corresponding phenolic OH signal. [d]These signals are coincident in the spectrum, resulting in an apparent doublet.

HMQC and HMBC NMR data (Table 17) were used to establish the connectivity of these units. One of the *para*-disubstituted ring ^{1}H NMR signals (H-3'/H-5') correlated to C-7' of the isolated olefin unit in the HMBC spectrum, linking the *para*-disubstituted benzene ring to the isolated double bond. H-8' of the same olefin unit showed correlations to C-9a' and C-10' of the pentasubstituted benzene ring, while H-7' showed a correlation to C-9. These data required the connection of C-8' to C-9'. The oxygenated carbons of the pentasubstituted ring (C-12a' and C-11') were correlated with an olefinic proton signal of one of the 3-methyl-1-butenyl side-chains (H-13'), thereby locating this side-chain at C-12'. The other 3-methyl-1-butnyl side-chain showed a correlation from one of its olefin protons (H-13) to the oxygenated carbon signals of the symmetrical 1,2,3,5-tetrasustituted benzene ring (C-9/C-11), thereby locating the second side-chain at C-10 in **90**. The sp^3 methine H-7a showed correlations to C-8/C-12 of this same symmetrical benzene ring, requiring its attachment to C-7. H-7a also showed correlations to C-9a' and C-12a', linking C-7a to the pentasubstitiuted benzene ring at C-9a'. The remaining 1,2,4-trisubstituted benzene ring was connected to the oxygenated carbon (C-4a) of the OCH–CH system on the basis of correlations of H-4a to C-3 and C-5. The presence of an ether unit linking C-4a and C-12a' was established on the basis of an HMBC correlation of H-4a with C-12a'. This requires all of the other oxygen atoms to be present as OH groups, thereby enabling completion of the assignment of the structure as shown in **90**. Only four of the six phenolic OH signals showed HMBC correlations to nearby carbons, but all observed correlations were consistent with the proposed structure. Compound **90** appears to be comprised of one unit each of arachidin-1 and arachidin-3.

The relative configuration of **90** at C-7a and C-4a was determined on the basis of the corresponding vicinal ^{1}H NMR *J*-value of 5.3 Hz, which is indicative of a *trans* orientation in a ring system of this type.[238] In contrast, the *J*-value for a *cis* orientation has been reported as 8.3 Hz.[239] Compound **90** is a new natural product, for which the common name arahypin-6 is proposed.

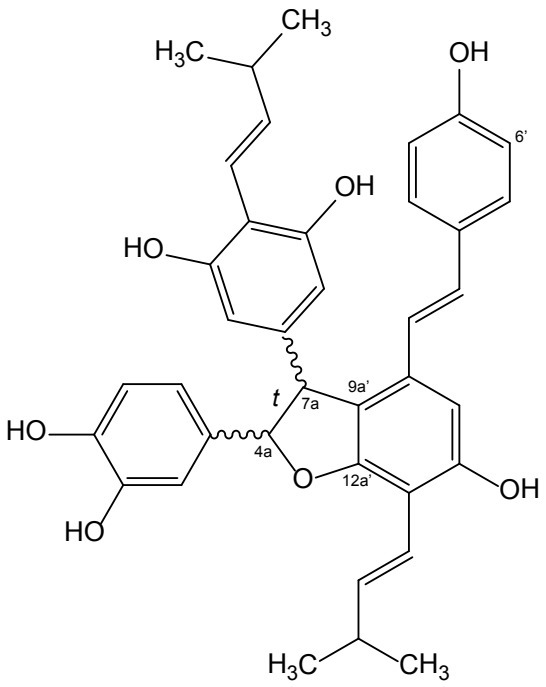

91

Compound **91** has the molecular formula $C_{38}H_{38}O_8$ (20 unsaturations), differing from that of **90** by addition of an oxygen atom, as established by analysis of NMR and HRESIMS data. The MS^2 data for **91** displayed several ions of similar relative abundance that were also observed in the data for **90**, indicating close structural similarities between the two compounds. The NMR data for **90** and **91** were also very similar, although the aromatic and olefinic signals in the ^1H NMR spectrum of **91** showed much more overlap, regardless of which NMR solvent was used. Even so, the data for **91** clearly lacked the *para*-disubstituted aromatic ring signals, replacing them instead with signals for a second *ortho*-dioxygenated 1,2,4-trisubstituted benzene ring. Thus, the structure of **91** was presumed to differ from that of **90** by addition of one OH group at position 6' on the *para*-disubstituted aromatic ring of **90**. This relationship was consistent with the very similar HPLC behavior of **90** and **91** (6 seconds between peak apexes, with compound **91** eluting first). Although the degree of overlap in the ^1H NMR

spectrum did not permit complete assignment of all of the signals for **91**, key signals that did resolve were fully consistent with the proposed structure, which is essentially a dimer of arachidin-1 formed in a process directly analogous to the formation of **90**. Due to the severe overlap, together with difficulties of completely purifying **91**, the structure of **91** was verified by synthetically preparing **91** though an oxidative coupling of two units of arachidin-1. The oxidative coupling reaction was performed by treatment of arachidin-1 with $FeCl_3$. The resulting products were separated via a silica gel column and fractions containing **91** were recombined and subsequently purified via HPLC. Compound **91** is another novel metabolite and was assigned the common name arahypin-7.

Experimental data do not permit a conclusion as to whether stilbenoid dimers **90** and **91** are produced by peanuts *in vivo* or whether they would perhaps be formed *in vitro* from simple peanut stilbenoids under favorable incubation conditions. However, no significant optical rotation values were observed for samples of **90** and **91** isolated from challenged peanut extracts, and the CD curves for the samples were comparable to those of MeOH blanks (Figure 25). The *t*-designations shown in the structures of **90** and **91** indicate that the relative configuration has determined to be *trans* in each case, but because the compounds are racemic, their formation is likely to have been nonenzymatic.

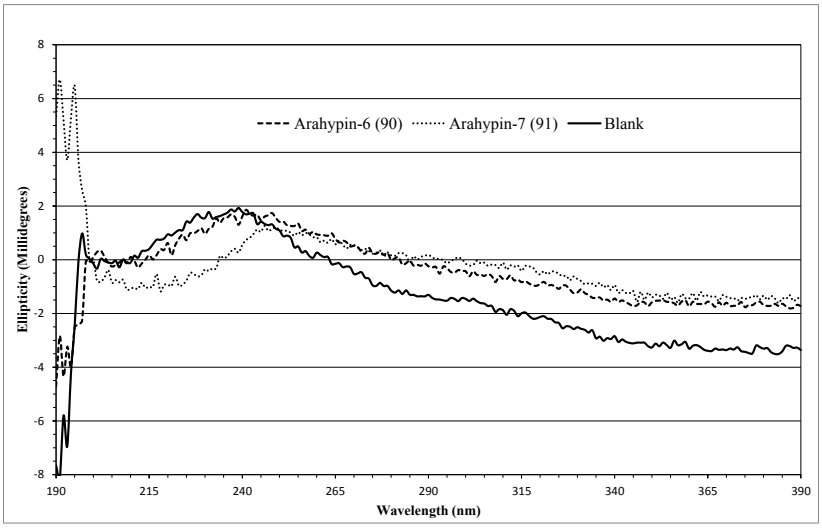

Figure 25. Experimental ECD Spectra of **90**, **91**, and a MeOH Blank.

Stilbene derivatives in general are known for their biological activity.[102,207,240,241] The prior literature report of compound **84** indicated that it shows antifungal effects against *Cladisporium cucumerinum*, exhibiting a MIC value of 30 μg/mL, and toxicity toward the yellow fever-transmitting mosquito *Aedes aegypti* by killing 100% of the larvae within 24 h at only 6 ppm.[219] It was also demonstrated that the presence of the prenyl chain in **84** was required for the antifungal properties of this metabolite.[219] It seems likely that prenylated compound **86** may possess antifungal properties as well, since other prenylated stilbenes, which differ from each other only in the position of the side-chain double bond, as do **84** and **86**, possess antifungal properties and inhibit spore germination and hyphal extension of *A. flavus*.[102] A similar comparison may be valid for **87** and **88**, which bear the same dihydroxydimethylpropyl group as compound **85**. Compound **85** reportedly demonstrated inhibitory effects against cyclooxygenases, particularly against cyclooxygenase-1.[220]

Stilbenoid dimers that show similarities to **90** and **91** are known, and represent the most abundant group in the class of stilbenoid-derived oligomers. Such compounds are known to show antifungal, antinematodal, antioxidant, cancer chermopreventive, anti-inflammatory, anti-HIV, antimutagenic, cytotoxic, hepatoprotective, blood glucose reductive, and tyrosinase inhibitory effects.[225,227-231,233,234,242] Based on the similarity of structures **90** and **91** with known natural oligomers, it is likely that **90** and **91** would show some of the same kinds of biological activities. Taking into account the importance of knowledge about natural plant defense mechanisms, as well as these published biological activities of known stilbenoid oligomers, a systematic study of the biological activity of compounds **90** and **91** is underway.

Arahypins 1-5 (**85-89**), as well as chiricanine A (**84**) were tested in a variety of assays, including tests for antifungal effects against *Botrytis cinera*, *Colletotrichum acutatum*, *C. fragariae*, *C. gloeosporioides*, *Phomopsis viticola*, *P. pnscurans*, and *Fusarium oxysporum*, cytotoxic activity against four human tumor cell lines and

noncancerous cell lines, anti-inflammatory activity, opioid receptor activity, and mosquito larvae toxicity.[93] Log *P* values were also established (through the comparison to standards) for each of the tested compounds. Log *P* values (in the octanol/H_2O system) quantitatively determine the difference in affinity of a molecule for the lipophilic octanol/H_2O system over the hydrophilic H_2O/octanol system. Presumably, the higher the log *P* value of an individual molecule, the easier it should be for that molecule to penetrate microbial cell membranes, thereby fostering biological effects. The log *P* values for **84**-**89** are given here in parentheses and were determined to be: **84** (3.46), **85** (1.36), **86** (3.71), **87** (1.59), **88** (2.59), and **89** (3.34). These numbers suggest that the analogues possessing the dihydroxy prenyl group are less likely to result in biological activity that is equivalent to the other compounds.

Of the compounds tested for antifungal activity, only compounds **84**, **86**, and **89** were active, showing effects against *P. obscurans*, *P. viticola*, and *B. cinera* (Figure 26). This is consistent with the log *P* values (< 3) for these compounds, which is considered to be an indicator of potential activity in such assays.

When tested up to 25 μg/mL, none of these compounds inhibited NF-κB, a protein that controls the transcription of DNA. There was also no statically relevant activity seen in the cytotoxicity assays against the human cell lines (both cancerous and noncancerous) at similar concentrations. However, compounds **85**-**89** did demonstrate significant antioxidant properties comparable to the standard, Trolox.[93] Trolox demonstrated antioxidant activity at an IC_{50} of 0.11 μg/mL, compounds **85**-**89** showed IC_{50} values of 0.35, 0.19, 0.4, 9.5, and 1.3 μg/mL, respectively.[93]

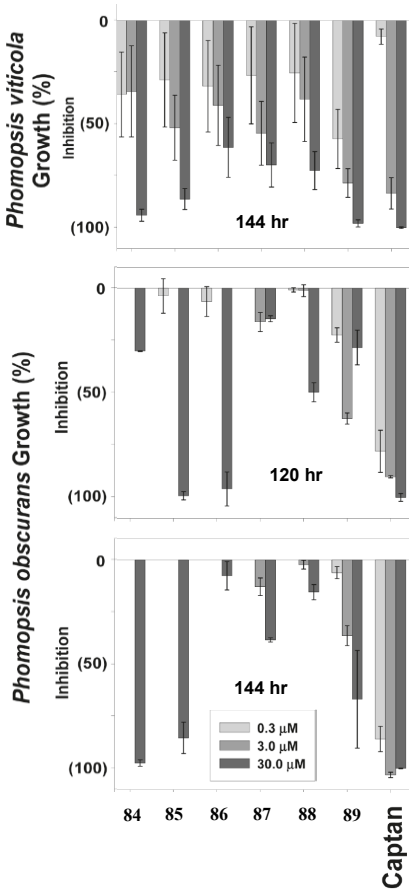

Figure 26. Antifungal Properties of Compounds **84-89** against *P. viticola* and *P. obscurans*. Captan is Used as the Standard. Antifungal Assays were Performed (and Charts Produced) by D. E. Wedge and Co-Workers.[93]

None of the compounds showed any significant activity in assays for insecticidal activity against mosquito larvae and adult mosquitos. This was also the case when the compounds were tested for effects on opioid receptors (Δ, μ, and κ).[93]

In addition to the novel stilbene-derived compounds described in this Chapter, additional stilbene-derived compounds with different structural features were encountered in further experiments and they will be discussed in the next Chapter.

CHAPTER 8

NEW PTEROCARPENES ELICITED FROM PEANUT (*ARACHIS HYPOGAEA*) SEEDS UPON COLONIZATION BY *ASPERGILLUS CAELATUS*

Under favorable conditions, the leguminous peanut plant (*Arachis hypogaea* L.), when infected by a fungal pathogen, is capable of producing stilbene-derived phytoalexins, which have been considered the backbone of the plant's inducible chemical defenses.[90,100,101,211-214] Peanut leaves infected with the early leaf-spot fungus *Cercospora arachidicola* reportedly produce two pterocarpanoids, medicapin (**16**) and a degradation product, demethylmedicapin.[98] Although accumulation of the pterocarpanoid and isoflavone phytoalexins is a common reaction of several leguminous plants to challenge by host-pathogenic fungi,[243] **16** is the only induced pterocarpanoid previously detected in peanut leaves. Increased concentrations of **16** were found only in infected leaves. This compound has therefore been suggested to play a defensive role as a phytoalexin.[92]

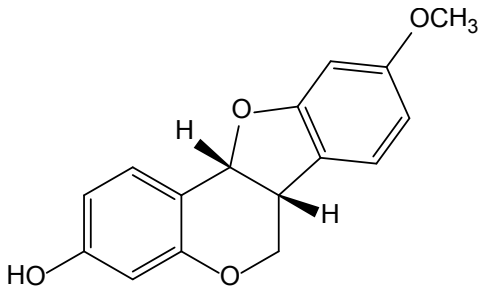

16

Pterocarpanoids and isoflavones represent the most abundant class of isoflavonoid phytoalexins produced by leguminous plants.[243] Pterocarpans contain a tetracyclic ring system that is derived from the basic isoflavonoid skeleton; more specifically, pterocarpans are isoflavans in which a furan ring is formed through generation of an ether

linkage between the chromane and the 3-phenyl unit (Figure 27). Pterocarpans generally tend to possess the highest antifungal activity among the leguminous plant phytoalexins in the flavonoid-based class of compounds.[244] In addition to their defensive antifungal functions, pterocarpans display other diverse biological effects, such as antibacterial,[244-248] anti-inflammatory,[249,250] antitumor,[251,252] antioxidant and antiallergenic,[253] and antiparasitic activities,[254,255] as well as activity against *Anopheles gambiae* adult mosquitoes[256] and the common cutworm, *Spodoptera litura.*[257]

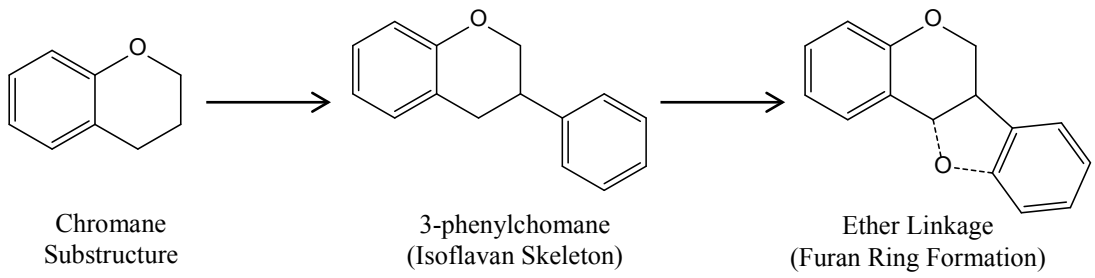

Figure 27. Formation of a Pterocarpan Skeleton.

Pterocarpenes differ from pterocarpans by incorporation of a double bond between C-6a and C-11a (Figure 27). In contrast to hundreds of pterocarpans known from various plant sources,[243,244,258] only six members of the pterocarpene (pterocarp-6a-ene) group were known just 10 years ago.[243] A few more pterocarpenes have been isolated since that time, and the biological activities of some of these have been investigated.[245-247,249,259] Antibacterial activity similar to that of pterocarpans seems to be the most common and important quality of pterocarpenes described to date. Despite their scarce distribution in plants, pterocarpenes may play important roles in the disease resistance of plants in which they are produced due to the bioactivities they display.

An *Aspergillus caelatus* strain (NRRL 25528, ex type) was chosen as a biotic phytoalexin elicitor because it demonstrated a high growth rate and rapid stimulation of phytoalexin biosynthesis in previous experiments.[92] Compared to other strains, *A. caelatus* produced only a few known secondary metabolites under the conditions employed, which were easily detected and did not interfere with detection of elicited peanut metabolites. The compounds of interest in this study were initially detected in earlier experiments with wounded, challenged peanut seeds. In this contest, the concept of "challenging" refers to inoculating with a fungus to purposefully infect a host in hopes that it will produce metabolites that fend off the infection.[92] Because the compounds were observed only in inoculated seed extracts, they were suspected as possible phytoalexins. When the experimental conditions were changed from high temperature – short incubation time to low temperature – long incubation time, the production of the two major compounds of this type increased significantly. These two compounds, ultimately identified as aracarpene-1 (**92**) and aracarpene-2 (**93**), were targeted for further investigation and isolated from the extracts by column chromatography and reversed-phase HPLC (Figure 28).

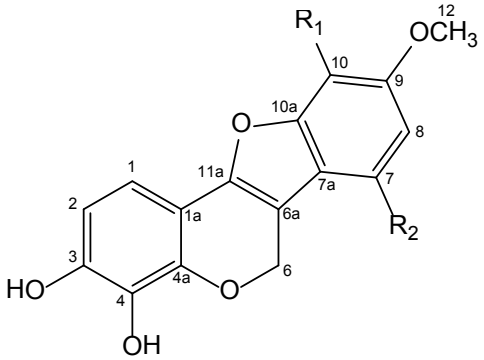

92: R_1 = OH, R_2 = H
93: R_1 = H, R_2 = OH

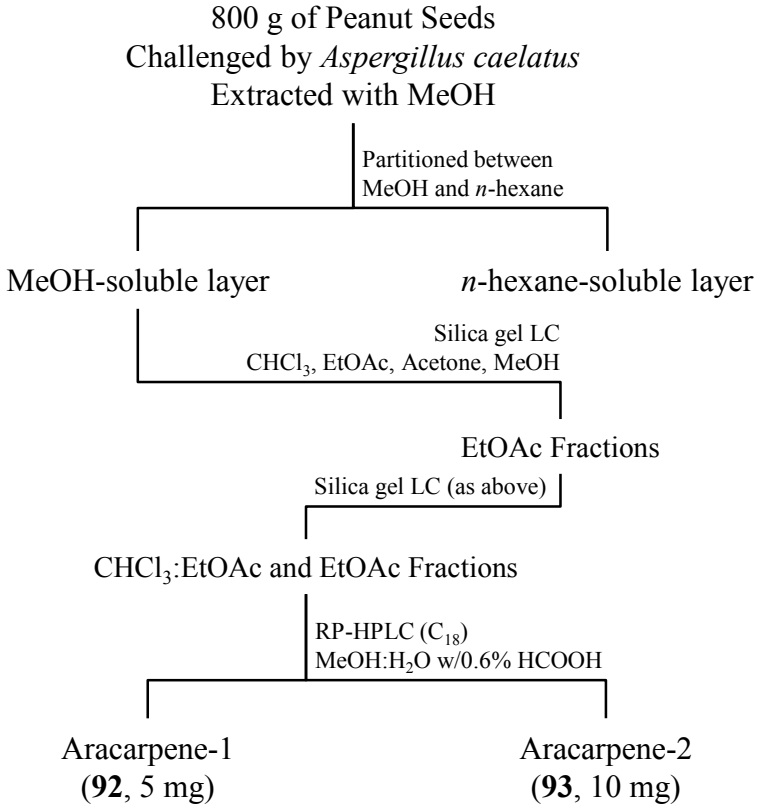

Figure 28. Isolation Scheme for the MeOH Extract of Peanut Seeds Challenged by *Aspergillus caelatus* that Yielded Compounds **92** and **93**.

Structure Elucidation of Aracarpenes 1 (**92**) and 2 (**93**)

Aracarpene-1 (**92**) was assigned the molecular formula $C_{16}H_{12}O_6$ (11 unsaturations) by analysis of NMR and HRMS data. NMR spectroscopic data (Table 18) indicated the presence of two 1,2,3,4-tetrasubstituted aromatic rings (both 1,2,3-trioxygenated according to ^{13}C NMR shift data), an isolated CH_2O unit, a tetrasubstituted double bond, and a methoxy group. ^1H NMR signals corresponding to three phenolic OH groups were also observed. The number of sp^2 carbons present in combination with the formula required a tetracyclic structure. A literature search suggested that **92** was likely to be a pterocarpene derivative.[245,246,253,260] The ESIMS^2 data bore some resemblance to

spectra reported for 3,9-dihydroxypterocarp-6a-ene[261] and were also consistent with such a structure. More specifically, the units present and the molecular formula were consistent with a pterocarpene system substituted with three OH groups and a methoxy group.

HMQC and HMBC NMR spectroscopic data (Table 18) were used to independently verify this conclusion, to determine the substitution pattern, and to locate the methoxy group on compound **92**. The methoxy signal at δ 3.94 showed an HMBC correlation to an oxygenated aromatic carbon (C-9) which was also correlated with a phenolic OH at δ 5.70. This phenolic OH showed additional HMBC correlations to C-10 and C-10a, both of which are also oxygenated aromatic carbons of the same 1,2,3-trioxygenated aromatic ring. One of the aryl protons of this ring (H-7) showed strong correlations to two of the oxygenated carbons (C-9 and C-10a) and a weak correlation to the third (C-10), which is *para* to H-7. H-8 (*ortho*-coupled to H-7) also shows strong correlations to two of the oxygenated carbons (C-9 and C-10) and a weak correlation to the third (C-10a), which is *para* to H-8. The remaining carbon of this ring (C-7a) was located via its correlations with H-7 and H-8. C-7a was further linked to a sp^2 carbon C-6a on the basis of a strong correlation of H-7 to C-6a. The isolated CH_2–O (CH_2-6) was connected to C-6a by virtue of it correlations to C-6a and C-7a. H_2-6 also showed strong correlations to two other oxygenated sp^2 carbons, which must correspond to C-4a and C-11a in **92**, although these two assignments could not be distinguished. Even so, these data require C-6 to be connected to the second aromatic ring via an ether linkage. The signals for the second tetrasubstituted aromatic ring could be assigned on the basis of HMBC correlations of H-1 and H-2 (Table 18). Strong correlations of H-1 to two other oxygenated carbons, aside from C-3 and C-4, required C-1a to be connected to an additional oxygenated sp^2 carbon. This was supported by weak correlations of H-2 to the same two carbons. The only ambiguity was the assignment of C-4a and C-11a. Although these two signal assignments were interchangeable, the formula requires

connection of O-11 to C-11a to complete the structure of **92**. Compound **92** has not been previously reported in the literature, and the 3,4,9,10-oxygenation pattern shown in **92** has been described only once previously (in bryacarpene-4, a trimethoxymonohydroxy pterocarpene derivative obtained from heartwood of *Brya ebenus*).[260] The common name aracarpene-1 was assigned to **92**.

Table 18. NMR Spectrocopic Data for Aracarpene-1 (**92**) and Aracarpene-2 (**93**).

	92[a]			**93**[b]		
position	δ_H (multiplicity, J_{HH})	δ_C[c]	HMBC (H# → C#)	δ_H (multiplicity, J_{HH})	δ_C[c]	HMBC (H# → C#)
1	7.09 d (8.4)	112.7	3, 4[e], 4a, 11a	6.83 d (8.4)	111.5	1a[e], 3, 4[e], 4a, 11a
1a		109.0			110.9	
2	6.57 d (8.4)	108.6	1a, 3, 4, 4a[e]	6.51 d (8.4)	109.2	1a, 3, 4, 4a[e]
3	5.36 br s, OH	145.5		7.86 br s, OH	147.9	
4	5.27 br s, OH	131.9		7.78 br s, OH	134.4	
4a		141.0			142.5	
6	5.59 s	66.0	1a[e], 4a, 6a, 7a, 10a[e], 11a	5.62 s	66.7	1a[e], 4a, 6a, 7a, 11a
6a		105.8			106.5	
7a		121.8			110.0	
7	6.80 d (8.3)	108.5	6a, 7a, 9, 10[e], 10a	8.93 br s, OH	152.0	
8	6.87 d (8.3)	108.2	6a[e], 7, 7a, 9, 10, 10a[e]	6.33 d (1.9)	98.6	6a[e], 7, 7a, 9, 10
9		144.5			160.0	
10	5.70 s, OH	131.8	9, 10, 10a[d]	6.68 d (1.9)	89.2	7[e], 7a, 8, 9, 10a
10a		143.0			158.5	
11a		148.5			146.7	
12	3.94 s	57.3	9	3.80 s	56.1	9, 10[e]

^{1}H NMR data were recorded at 400 MHz; ^{13}C NMR data were recorded at 150 MHz. [a]In $CDCl_3$. [b]In acetone-d_6. [c]Carbon assignments were established using HMQC and HMBC data. [d]These three entries indicate correlations from the corresponding phenolic OH signal. [e]These entries indicate weak HMBC correlations.

Aracarpene-2 (**93**) was recognized as an isomer of **92** by analysis of NMR and HRMS data. Close similarities in the UV and NMR spectroscopic data with those of **92** indicated that **93** is also a pterocarpene derivative. The main difference relative to **92** is that the ^{1}H NMR data of **93** (Table 18) indicated a different substitution pattern for one of the tetrasubstituted aromatic rings. While **92** has two sets of *ortho*-coupled protons, compound **93** shows one pair that is *ortho*-coupled and one pair that is *meta*-coupled (J = 1.9 Hz). The observed ^{13}C NMR shifts also show that one of the aromatic rings in **93** is a

1,3,5-trioxygenated aromatic ring. Once again, HMBC NMR data were used to determine the substitution pattern of **93**. The methoxy group (δ 3.80) showed a correlation to C-9, an oxygenated carbon of the 1,3,5-trioxygenated aromatic ring, as well as a weak correlation to C-10, a protonated aromatic carbon. H-10 was also strongly correlated with two oxygenated carbons (C-10a and C-9) and two non-oxygenated carbons (C-7a and C-8), and (weakly) to a third oxygenated carbon (C-7), which is *para* to H-10. H-8 was correlated with two oxygenated carbons (C-7 and C-9) and two non-oxygenated carbons (C-7a and C-10), but lacked a weak correlation to the third oxygenated carbon (C-10a). H-8 did, however, show a weak correlation to non-oxygenated sp^2 carbon C-6a. Other correlations were analogous to those described above for **92**.

Thus, compound **93** differs from **92** only in that one of the OH groups is located at C-7 rather than C-10. No other pterocarpene skeleton with a 3,4,7,9-tetraoxygenated substitution pattern has been previously reported in the literature.

Because compounds **92** and **93** did not display potent antifungal activity and showed only minimal activity against *Phomopsis viticola* and *Phomopsis obscurans*, it was suggested that they may possess antibacterial activity. In standard Petri plate disk assays against *Bacillus subtilis* (ATCC 6051) and *Staphylococcus aureus* (ATCC 29213) at 100 μg/disk, compound **93** showed zones of inhibition with diameters of 13 and 10 mm, respectively. By comparison, a gentamicin standard afforded zone sizes of 21 and 35 mm in these assays, respectively, at a concentration of 25 μg/disk. Interestingly, compound **92** showed no activity in either assay at the 100 μg/disk level, in spite of the close resemblance to **93**. In order to explore this further, a more quantitative method to investigate the antimicrobial activity was chosen to test compounds **92** and **93**.[262] Aracarpene-2 (**93**) was found to possess significant antibacterial properties (Figure 29) against gram-positive and gram-negative bacteria. It was especially active against *B. subtilis* and *S. aureus* with 100% loss of viability observed at 10 and 15 μM, respectively.

A concentration of 20 µM was needed to obtain 100% viability loss of *Escherichia coli* (ATCC 700728). Compound **92** displayed relatively weak antibacterial properties against these bacteria, which was consistent with the initial Petri plate assay results. Both compounds were inactive *A. flavus* at all levels tested (Figure 29).

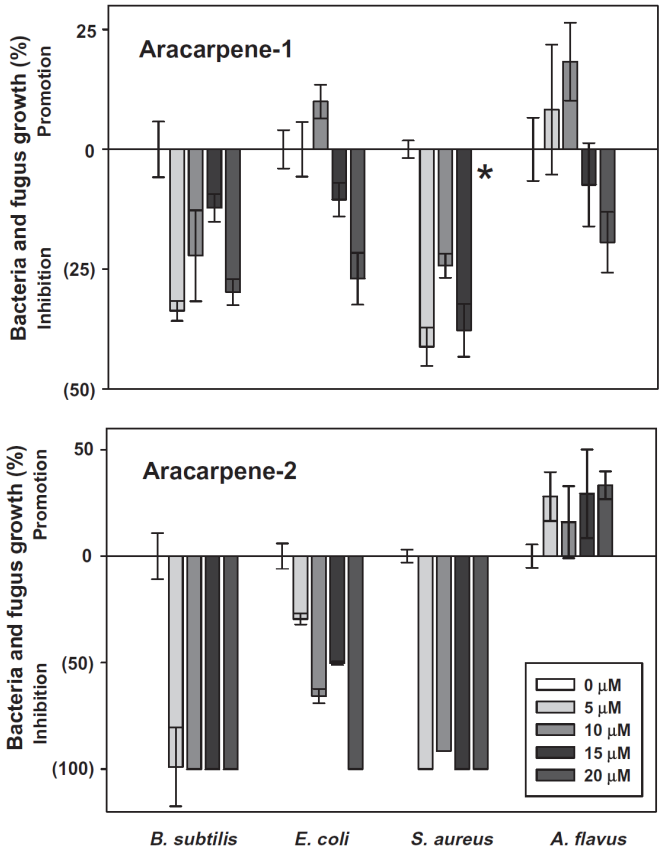

Figure 29. Antimicrobial Properties of Aracarpenes 1 (**92**) and 2 (**93**) against *Bacillus subtilis*, *Escherichia coli*, *Staphylococcus aureus*, and *Aspergillus flavus*. *Data were not Collected at 20 µM. Antifungal Tests were Performed (and Charts Produced) by A. J. De Lucca and Co-Workers.[92]

The higher biological activity observed for **93** compared to **92** may be due to the greater lipophilicity of **93**. Despite close structural similarities, **93** has a significantly

higher log *P* value (2.28) than **92** (1.47), as determined by an HPLC method using additional standards with known log *P* values. This means that **93**, when compared to **92**, has about 6.5 times greater affinity for the lipophilic octanol/H_2O system than the hydrophilic H_2O/octanol system. Presumably, the high lipophilicity of **93** would make it easier for **93** to penetrate microbial cell membranes and exert biological effects. Compounds **92** and **93** were also tested for anti-inflammatory, cytotoxic, and antioxidant activities, but were found to be inactive in all of the assays employed.[92]

The detection of **92** and **93** in peanut seeds challenged by a fungus, but not in uninoculated controls, suggests that these pterocarpenes may be biosynthesized in addition to the stilbene phytoalexins (Chapter 7) to jointly fight invasion by microorganisms. Interestingly, these antimicrobial compounds did not show activity against an Aspergillus species, even though a member of the group was uses as the "challenger". Although some limited antifungal effects were observed against a pair of Phomopsis species, it was not clear why challenge by a fungal species would stimulate production of additional compounds. Perhaps such compounds might be synergistic with other metabolites present and could act against a fungal invasion in that sense, but this concept has not been investigated. In any event, these results are consistent with previously published data, and support the idea that pterocarpenes **92** and **93** represent a new class of low-molecular weight peanut compounds that could play defensive roles against pathogenic microorganisms.

CHAPTER 9
SUMMARY AND CONCLUSIONS

This thesis describes chemical investigations of three distinct sources that yielded structurally interesting, and biologically relevant, secondary metabolites: endophytic fungi, fungicolous/mycoparasitic fungi, and peanut seeds.

The two fungal niche groups were selected for investigation based on the fact that such organisms engage in complex interactions with other host organisms that may be linked in some respects to their chemistry, and similar organisms have proven to produce bioactive secondary metabolites that have interesting and/or unique structural features. The preceding chapters describe the chemical investigation of 28 fungicolous or endophytic fungal isolates from which 50 fungal secondary metabolites were identified. Seventeen of these secondary metabolites were determined to be new compounds.

Most of the fungicolous/mycoparasitic fungi described here were obtained from the nutrient-rich fruiting bodies of wood-decay fungi (polypores) that were collected on the island of Hawaii. The endophytic fungi were obtained from corn (*Zea mays*), wheat (*Triticum aestivum*), or sorghum (*Sorghum vulgare*) plants that were growing in Arizona, Illinois, Kentucky, or Nebraska, or under controlled conditions at the NCAUR plot in Peoria, IL. Isolates of both fungal types were selected for chemical investigation on the basis of antifungal and antiinsectan activities of their crude fermentation extracts against *Aspergillus flavus*, *Fusarium verticillioides*, and *Spodoptera frugiperda* (the fall armyworm). In addition to the known antifungal and antiinsectan agents that were isolated, several of the new secondary metabolites that were tested also exhibited antifungal and/or antiinsectan activity.

In some cases, the antifungal or antiinsectan activity observed for the crude fungal metabolite extracts could be accounted for by the effects of known compounds. However, this was not the case in all instances. If the activity of an extract cannot be

attributed to novel or known compounds encountered, there are various reasons that could explain a lack of activity after separation. First, the active compound(s) could be present in vanishingly small quantities and it therefore might not have been possible to identify or isolate them under the conditions used. Alternatively, the active components could decompose during what is often a lengthy isolation process. It is also possible that the initial activity could have been the result of synergistic effects of a combination of multiple components present, and not caused by a single compound.

Identification of known metabolites was generally achieved through database searches in combination with preliminary NMR and/or MS data. Structure elucidation of novel compounds required application of more advanced NMR techniques such as HMQC, HMBC, and NOESY. Assigning absolute configuration was often the most difficult task in characterizing individual metabolites. To assign absolute configuration of the novel peptides encountered, a process of a hydrolysis, derivatization of the resulting amino acids, and subsequent analysis of the products by GCMS in comparison to standards was employed.

In two other cases, non-traditional methods for assigning the absolute configuration were required. Unlike the analysis of a single-crystal X-ray diffraction by incorporating a "heavy" atom, which can enable assignment of absolute configuration of an entire molecule, independent analysis of structurally insulated parts of the same molecule was required on multiple occasions. For alflaquinones A (**43**) and B (**44**), each region of the compound was separately and independently evaluated, with the absolute configuration of one portion assigned by using Mosher's Method, while the absolute configuration of the other was assigned by using CD measurements in comparison to calculated CD data on energy-minimized models. Chemical interconversion was also helpful in one case. Some of the aflaquinolones were also evaluated using theoretical optical rotation calculations in an effort to assist in the absolute configuration assignment.

Another novel compound that required extensive efforts to assign absolute configuration was emeridin A (**65**). A successful ozonolysis was carried out on a subsample of the isolated material to effectively divide the molecule in half, but efforts to separate the resulting products by HPLC were unsuccessful. Thus, only the relative configuration of **65** has been assigned at this point, but it is noted that the relative configurations of the two halves of the molecule could not be related to one another, leaving an additional undefined element. Other research groups reporting similar compounds also failed to establish the absolute configuration.

Previous members of our research group have occasionally collaborated with Dr. Sobolev in the characterization of secondary metabolites from *Arachis hypogaea* (peanut) seeds. However, this the first time that the extent of such work has risen to the level of inclusion in a thesis from a member of our group. Metabolites characterized in this portion of the research described here were isolated from peanut seeds challenged by *Aspergillus caelatus*, which were grown under controlled conditions at the USDA National Peanut Research Laboratory in Dawson, GA. Chapters 7 and 8 include the discovery and characterization of eight new metabolites, along with two additional previously known metabolites that were reported for the first time from peanut seeds. All of the compounds encountered exhibited similar structural features, as all are stilbene-derived, and all approximately were of similar molecular size, except for two dimeric compounds.

While the three main projects described in this thesis are distinct from one another, the common theme is that fungi can both produce or elicit secondary metabolites that are novel, interesting, and biologically active. Because fungicolous/mycoparasitic and endophytic fungi are underexplored, the likelihood of discovering new bioactive metabolites from such fungi remains high. Even when novel compounds were isolated that were not especially active in our assays, the new chemistry encountered posed challenges in structure determination that had to be overcome.

CHAPTER 10

EXPERIMENTAL

General Experimental Procedures

Solvents and Reagents

Solvents used for partitioning and chromatographic purposes were purchased from Fisher Scientific. General lab procedures were undertaken using reagent grade solvents, whereas analytical separations on HPLC instrumentation employed HPLC-grade solvents. Distilled water for HPLC applications was purified using a SYBRON/Barnstead NANOpure system with a pre-treatment cartridge (catalog number D08350, two ultra-pure cartridges (D0809), and a 0.2-μm hollow fiber filter (D3750). All HPLC solvents were degassed under vacuum using a Branson 1510 sonicator prior to use. Reagents and deuterated solvents were purchased from either Aldrich Chemical Company or Cambridge Isotope Laboratories.

Mass Measurements

Masses of reagents, crude extracts, partitions, column fractions, and pure compounds were measured using either a Mettler AE 160 or Mettler AE 200 balance. All before and after measurements were performed on the same balance.

Evaporation

Removal of solvents was primarily accomplished by evaporation under a flow of air. Prolonged exposure to airflow was necessary during periods of higher humidity during the course of a year. Occasionally, partial evaporations were carried out on a Büchi RE-11 Rotavapor with assistance from an antifreeze-filled Neslab RTE-110.

General Chromatography Information

Silica gel TLC separations were carried out using pre-coated plastic sheets (Sorbent Technologies, 200-µm thickness silica gel with fluorescent indicator, 40 × 80 mm). TLC spots were visualized by exposure to UV light at 254 nm or 365 nm, as well as exposure to iodine vapor. Column chromatography and VLC separations were performed with Scientific Adsorbent, Inc. 63-200-µm silica gel or with J.T. Baker 40-µm silica gel. VLC separations were conducted using a column with a ground-glass fitting, side arm, and a frit that was, in turn, secured onto a 500-mL round-bottom flask. Gel filtration column chromatography was accomplished using Sephadex LH-20 (Sigma). Fractions from column chromatography were collected manually using beakers.

Semipreparative reversed-phase HPLC separations were performed using one of two Beckman Instrument systems: (1) System Gold 125 solvent delivery module, with a photodiode array detector, model 168, both of which were controlled by System Gold 32 Karat software using an IBM 300PL PC; (2) System Gold 127P solvent delivery module with a model 166P variable wavelength UV detector, both controlled by System Gold software (version 5.1). Both of the described HPLC systems employed Rheodyne model 7725 injectors, which were used in conjunction with Hamilton syringes (100- or 500-µL, blunt). Separations were conducted using an Alltech HS Hyper Prep 100 BDS C_{18} (8-µm particle size, 250 × 10.0 mm), Alltech Apollo Phenyl (5-µm particle size, 250 × 10.0 mm), Alltech Platinum CN 100A (5-µm particle size, 250 × 10.0 mm), or Grace Apollo C_{18} (5-µm particle size, 250 × 10.0 mm) columns at a flow rate of 2.0 mL/min; or Grace Adsorbosphere HS C_{18} (5-µm particle size, 250 × 4.6 mm) column at a flow rate of 1.0 mL/min. All HPLC chromatograms were recorded using a Linear model 1200 chart recorder, and were monitored at selected wavelengths, typically between 210-260 nm.

Chromatography of Plant Metabolites – Chiricanine A (**84**) and Arahypins 1-5 (**85-89**)

HPLC-DAD-MS Analyses

Analyses were performed using an HPLC system equipped with a model LC-10ATvp pump (Shimadzu), a model SPD-M10Avp DAD covering the 200-600 nm range with Shimadzu Client/Server software, version 7.3, and a model 717 plus autosampler (Waters). Separations of seed extracts and purified stilbenoids were performed on a 50 mm x 4.6 mm i.d., 2.5 µm, XTerra MS C_{18} analytical column (Waters). H_2O (A), MeOH (B), 2% HCOOH in H_2O (C), and MeCN (D) were used in the following gradient (mobile phase 4): initial conditions 67% A/30% B/3% C, changed linearly to 2% A/95% B/3% C in 12 min, held isocratic for 4 min, and then changed to initial conditions in 0.01 min. The flow rate was 1.3 mL/min. The column was maintained at 40 °C in a model 105 column heater (Timberline Instruments, Boulder, CO). For tandem HPLC-MS analyses, a Surveyor HPLC system equipped with MS Pump Plus, Autosampler Plus, a PDA Plus Detector (Thermo Electron Corp., San Jose, CA) and a 50 mm x 4.6 mm i.d., 2.5 µm, XTerra MS C_{18} analytical column (Waters) was used. The column was maintained at 40 °C. The same solvents that were used to mobile phase 4 were used for the HPLC-MS analyses. The solvents were mixed in the following gradient: mobile phase 5, initial conditions 67% A/30% B/3% C, changed linearly to 2% A/95% B/3% C in 12 min, held isocratic for 2 min, changed to initial conditions in 0.01 min, mobile phase 6, initial conditions 70% A/27% B/3% C, changed linearly to 2% A/95% B/3% C in 12 min, held isocratic for 2 min, changed to initial conditions in 0.01 min. The flow rate for both systems was 0.8 mL/min.

Preparative HPLC Separations

Preparative HPLC separations for the stilbenoids were performed using a 100 mm x 19 mm i.d., 5-µm XTerra Prep RP_{18} OBD column (Waters). The column temperature was 40 °C. The following isocratic mobile phases were used: mobile phase 1, 74%

MeCN, 3% of 2% HCOOH in H_2O and 21% of H_2O; mobile phase 2, 55% MeOH, 5% of 2% HCOOH in H_2O, and 40% H_2O; mobile phase 3, 55% MeCN, 3% of 2% HCOOH in H_2O, and 42% H_2O. The flow rate was 8.0 mL/min.

Chromatography of Plant Metabolites – Arahypins 6-7 (**90** and **91**)

HPLC-DAD-MS Analyses

Separations of seed extracts and purified stilbenoids were performed using a tandem HPLC-MS Surveyor system equipped with MS Pump Plus, Autosampler Plus, a PDA Plus Detector (Thermo Electron Corporation, San Jose, CA), and a 50 mm x 4.6 mm i.d., 2.5 µm XTerra MS C_{18} analytical column (Waters). H_2O (A), MeOH (B), and 2% HCOOH in H_2O (C) were used in the following gradient: initial conditions 68% A/ 30% B/ 2% C, increased linearly to 0% A/ 98% B/ 2% C in 12 min, held isocratic for 5 min, decreased to initial conditions in 0.01 min (mobile phase 7). The flow rate was 0.8 mL/min. The column was maintained at 40 °C.

Preparative HPLC Separations

Preparative HPLC separations for the dimeric stilbenoids were performed using a 100 mm × 19 mm i.d., 5-µm XTerra Prep RP_{18}OBD preparative column (Waters). The column temperature was 40 °C. The following isocratic mobile phases were used: mobile phase 8, 75% MeCN, 3% of 2% HCOOH in H_2O, and 22% H_2O; mobile phase 9, 60% MeCN, 3% of 2% HCOOH in H_2O, and 37% H_2O; mobile phase 10, 70 % MeOH, 3% of 2% HCOOH in H_2O, and 27% H_2O. The flow rate was also 8.0 mL/min.

Chromatography of Plant Metabolites – Aracarpenes 1-2 (**92** and **93**)

HPLC-DAD-MS Analyses

Analyses of seed extracts and purified substituted pterocarpenes were performed using a tandem HPLC-MS Surveyor HPLC system equipped with MS Pump Plus, Autosampler Plus, a PDA Plus Detector (Thermo Electron Corp., San Jose, CA), and an XBridge C_{18} analytical column (2.5-µm, 3.0 x 50 mm; Waters). H_2O (A), MeOH (B), and 2% HCOOH in H_2O (C) were mixed in the following gradient: initial conditions,

68% A/30% B/2 % C, increased linearly to 0% A/98% B/2% C in 12 min, held isocratic for 5 min, decreased to initial conditions in 0.01 min (mobile phase 11). The flow rate was 0.5 mL/min. The column was maintained at 40 °C in a column heater (model 105, Timberline Instruments). Retention times of **92** and **93** were 3.3 and 5.4 min, respectively.

Preparative HPLC Separations

Preparative HPLC separations were performed using an XTerra Prep RP18 OBD (5-μm, 19 x 100 mm; Waters). The column temperature was maintained at 40 °C. The following mobile phases were used: initial conditions, 57% A/40% B/3% C, increased linearly to 7% A/90% B/3% C in 12 min, held isocratic for 3 min, decreased to initial conditions in 0.01 min (mobile phase 12); 34% A/63% B/3% C (mobile phase 13). The flow rate was 8.5 mL/min.

General Spectroscopic Information

Optical rotations were measured with a Rudolph Research Autopol III automatic polarimeter. Melting points were obtained on a Fisher-Johns micro melting point apparatus, and are uncorrected. UV Spectra were recorded using either a Hewlett Packard 8453 UV-Visible or a Varian Cary 100 Bio UV-Visible spectrophotometer. Low-resolution EI mass spectra, including those obtained by GC-MS, were acquired at 70 eV on a Thermo Voyager single-quadrupole mass spectrometer. Low-resolution ESIMS data were obtained using a Thermo LCQ Deca quadrupole ion trap spectrometer. MS facility personnel (Mr. Vic Parcell or Dr. Lynn Teesch) recorded all high-resolution EI and ESI mass spectra. HREIMS data were acquired on a Waters Autospec double-focusing magnetic-sector Waters mass spectrometer. HRESIMS and HRESIMSMS data were acquired on a Waters Q-ToF Premier mass spectrometer.

^{1}H NMR data were recorded on Bruker Avance III-600 (1.77-mm probe), Avance-600, Avance-400, DRX-400, or Avance-300 spectrophotometers (5-mm probes)

at room temperature unless otherwise noted. ^{13}C NMR and DEPT experiments were performed on either the DRX-400 or Avance-400 instruments. Homonuclear decoupling and COSY experiments were performed on the DRX-400 instrument. NOESY experiments were performed on the DRX-400, Avance-400, Avance-600, or AvanceIII-600 instruments. The Avance-300, DRX-400, and Avance-600 instruments were controlled by Bruker TopSpin 1.3 software. The Avance-400 instrument was controlled by TopSpin 2.1 software. The Avance III-600 instrument was controlled by TopSpin 3.0 software. Some early homonuclear decoupling experiments on the DRX-400 were performed using the XWinNMR 3.5 software. Both the Avance III-600 and Avance-600 NMRs operate at ^{1}H and ^{13}C frequencies of 600.1422 and 150.9203 MHz, respectively. ^{1}H NMR and inverse detection experiments (HMBC and HMQC) were recorded on the Avance-600 instrument using a 5-mm inverse probe (BBI) and on the Avance III-600 instrument using a 1.77-mm inverse probe (TXI). The DRX-400 spectrometer operates at a proton frequency of 400.1355 MHz and a carbon frequency of 100.6230 MHz using a 5-mm multinuclear broadband probe (BBO). The Avance-400 spectrometer operates at ^{1}H and ^{13}C frequencies of 400.1320 and 100.6230 MHz, respectfully, and also utilizes a 5-mm, BBO probe. The Avance-300 spectrometer operates at a proton frequency of 300.1675 MHz and a carbon frequency of 75.4786 MHz, and it utilizes a 5-mm proton-carbon-phosphorus probe (HCFP).

All NMR spectra were recorded in the deuterated equivalents of $CHCl_3$, acetone, MeOH, DMSO, MeCN, or benzene, and the chemical shifts (δ) are reported in ppm downfield from TMS, with the appropriate residual protonated solvent peaks used as internal reference standards (δ_H/δ_C, 7.24/77.16, 2.05/29.84 or 206.26, 3.31/49.0, 2.50/39.51, 1.94/1.32 or 118.26, and 7.16/128.06, respectively). 2D NMR data were processed using XWinNMR 3.1 on a Silicon Graphics workstation (SGI O2) or using TopSpin versions 1.3, 2.1, or 3.0. 1D NMR data were processed using the NUTS program (Acorn NMR Inc., version 5.02). Five-mm 535-PP and 5-mm 528-J4-7 NMR

tubes purchased from the Wilmad Glass Company were among the NMR tubes used for analysis. Microprobe (1.77-mm) NMR tubes were purchased from Bruker Instruments. Appropriate NMR tube ratings were met or exceeded for each experiment performed on a given spectrometer.

GCMS Conditions for Amino Acid Derivative Analysis

A Thermo Voyager single quadrupole mass spectrometer interfaced with a Trace2000 GC, equipped with an Agilent Technologies DB-1701 capillary column (30 m x 0.25 mm ID; 0.25 μm film) was used for GC-MS analysis. The GC temperature program started at 70°C for one minute then ramped up at 10°C/min to 280°C and was held there for 18 minutes. Helium was used as the GC carrier gas (1 mL/min flow rate). The GC inlet temperature was set at 280°C. The attached autosampler was set to inject 1 μL for each sample and standard. EIMS data (70 eV) were collected over the mass range 50-700 Da. Thermo's Xcalibur 1.4 software was used for data acquisition and processing.

Electronic Circular Dichroism (ECD) Analysis

ECD analysis was carried out on an Olis Cary 17 instrument. Samples analyzed on the ECD instrument were prepared in such a way that the maximum UV absorbance was one (1) absorbance unit (AU).

Additional Details of Spectroscopic Measurements in Studies of Marine *Aspergillus* sp. Isolate (Chapter 3)

Optical rotations were recorded on a Perkin Elmer 341 digital polarimeter. NMR spectra were recorded using a JEOL JNM ECP-400 spectrometer (400 MHz for ^{1}H and 100 MHz for ^{13}C), and chemical shifts were referenced relative to relative to the corresponding residual solvents signals (acetone-d_6: δ2.05/29.9; CD_3OD: δ3.31/49.0).

HMQC and HMBC experiments were optimized for $^{1}J_{CH}$ = 140 Hz and $^{n}J_{CH}$ = 8 Hz, respectively. ESIMS data were obtained using a Q-TOF micro LC-MS/MS instrument (Waters, USA) at Korea University, and a hybrid ion-trap time-of flight mass spectrometer (Shimadzu, Japan) at the Korean Basic Science Institute (KBSI).

Additional Details of Spectroscopic Measurements in Studies of Plant Metabolites – Chiricanine A (**84**), Arahypins 1-7 (**85**-**91**), and Aracarpenes 1-2 (**92** and **93**)

UV measurements were performed with a Varian Cary 100 Bio UV-Visible spectrophotometer. APCI-MS^n data were obtained on a Finnigan LCQ Advantage MAX ion trap mass spectrometer equipped with and APCI interface and operated with Xcalibur, version 1.4, software (Thermo Electron Corp.). All data were acquired in the full-scan positive polarity mode from *m/z* 100 to 2000. Capillary temperature was 165 °C, APCI vaporizer temperature 240 °C, sheath gas flow 55 units, auxiliary/sweep gas flow 5 units, source voltage 6 kV, and source current 6 μA. In MS^2 analyses using the Finnigan LCQ, the $[M + H]^+$ ions observed for each chromatographic peak in full-scan analyses were isolated and subjected to source collision-induced dissociation (CID) using He buffer gas. In all CID analyses, the isolation width, relative fragmentation energy, relative activation *Q*, and activation time were *m/z* 2.8, 35%, 0.25, and 30 ms, respectively. Concentrations of compounds of interest were approximated by reference to peak areas of corresponding pure compounds. The results of APCI-MS^2 experiments are represented in the discussion of peanut metabolites (Chapters 7 and 8) in the following format: *m/z aaa@bb*: *aaa*, *ccc*, *ddd*, where *aaa* is the parent ion, *bb* is normalized collision energy (%), and *ccc* and *ddd* are fragment ions.

General Procedures for Individual NMR Experiments

DEPT Experiment

DEPT experiments were used to establish carbon multiplicities. Data were recorded on either the DRX-400 or Avance-400 spectrometer using a file size of 64k and a suitable RG for a carbon spectrum. The results of a DEPT-135 experiment depict CH and CH_3 carbons as positive signals and CH_2 carbons as negative signals in the observed spectrum. Experimental parameters were preset for the DRX-400 instrument (Bruker software, version 1.3) using the program DEPT135 and for the Avance-400 instrument (Bruker software, version 2.1) using the program AA_13C-DEPT. Once the program is loaded, a suitable number of scans are entered and typing "zg" starts the experiment.

Homonuclear Decoupling Experiment

This experiment was used to determine which protons were mutually coupled within a molecule and/or to help establish ^{1}H-^{1}H coupling constants for individual proton signals. These experiments were carried out exclusively on the DRX-400 spectrometer. A preloaded program, AA_HomoDecouple, with standard experimental parameters in the XwinNMR software (version 3.1) was used. Alternatively, the preloaded program zghd.2 was used with the Bruker TopSpin software (version 1.3) that achieved the same results. A standard proton spectrum was initially obtained with a suitable number of scans and saved as the file entry "1" in the cell labeled EXPO. The frequencies (O2 values in Hz) of all proton signals to be irradiated were recorded. Multiple files were created in accordance with the number of protons to be irradiated and saved with successive numbers entered in the EXPO cell. The decoupling power, P24, was set between 50 and 70, usually 55 to 60, and the frequency to be irradiated was then entered for each EXPO experiment. The entire experiment was initiated in EXPO 2 by typing "xau", which opens a new cell requesting the number of experiments to be strung together, which must

be equivalent to the number of proton signals to be irradiated. Each experiment employs the same number of scans used for the standard ^{1}H NMR spectrum in EXPO 1. The resulting data were processed using the NUTS software (Acorn NMR Inc., version 5.02).

NOESY Experiment

The relative configuration of certain compounds could sometimes be determined based on the results of NOESY experiments. This 2D version of the NOE experiment provides through-space ^{1}H-^{1}H correlations based on the nuclear Overhauser effect. Either the DRX-400 or the Avance-600 spectrometers were used to carry out NOESY experiments. The procedure starts by properly tuning the NMR probe, followed by obtaining a well-shimmed ^{1}H NMR spectrum. Suitable SW and O2 values can be calculated from the ^{1}H NMR spectrum. A proton pulse calibration was then carried out using the pulse program "zg" (Bruker TopSpin, version 1.3 software), from which the parameters P0 (90° pulse), P1 (90° pulse), and P2 (180° pulse) were determined. A second pulse calibration was done using the pulse program "t1ir1d" to determine the appropriate mixing time by varying the parameter D7 to nullify the spectrum. Once done, D8, the mixing time, is set to the value of D7/0.7. The following parameters were then set with the "noesyph-i" pulse program: D1 (relaxation delay, RD) = 4 sec, D8 = value determined by pulse calibration, TD = 2k or 4k, NS = 8,16, or 32, DS = 16. The DW is a preexisting parameter and the IN_010 parameter is set at double the value of the DW. The dimensional parameter was then changed from 1D to 2D, changing ND_010 = 1 and FnMODE = TPPI. After verifying that the SW in Hz (SWH) is the same for both F1 and F2, and setting TD in F1 to 256 or 512, acquisition is initiated by typing "zg."

HMQC Experiment

The HMQC experiment is used to provide one-bond proton to carbon correlations. This method relies on indirect detection of ^{13}C nuclei by observing their effects on the

more sensitive ^{1}H nuclei to which they are coupled; an inverse detection method. HMQC experiments were conducted both on the Avance III-600 and on the Avance-600 spectrometers using the BBI and TXI inverse detection probes, respectively. After loading the sample, the probe was tuned and matched for both the ^{1}H and ^{13}C nuclei. This process was automated when using the Avance III-600 NMR. For the Avance-600 NMR, the spinner was engaged and a well-shimmed proton NMR spectrum was acquired. For the Avance III-600 NMR, these shimming and data acquisition steps were automated. The resulting ^{1}H NMR spectrum was used as a reference for projection of the ^{1}H dimension during processing (F2). The following parameters were set for a proton pulse calibration using the pulse program "zg" (Bruker TopSpin, versions 1.3 and 3.0 software): OFSX1 = 20 Hz, SFO = 152.92 MHz, DS = 0, N = 1, S1 = 16k, P0/P1 (90° transmitter high-power pulse) and P2 (180° transmitter high-power pulse). The following parameters were set with the pulse program "hmqcgpnd1d" on the Avance-600 NMR: D1 = 4 sec, D2 [$1/(2 \times J_{XH})$] = 3.33 sec (if experiment is optimized for J = 150 Hz), D13 = 3 μsec, DS = 4, NS = 16, and TD = 8k. After the acquisition was completed, the command "fmc" was entered in order to observe the signals of protons bound to ^{13}C atoms and determine signal intensity (allowing for a prediction of the NS needed for the actual HMQC experiment). When using the Avance III-600 NMR, all parameters were preset by the Bruker TopSpin 3.0 software pulse program.

The HMQC experiment was then conducted using the pulse program "hmqcgpqf" with multiple parameter changes on the Avance-600 NMR. Once the mode was switched from 1D to 2D, the following parameters were used for the experiment: FnMODE = QF, F1 Nucleus set to ^{13}C, DS = 96, TD = 2k or 4k, NS = any multiple of 8, RG = 16k, TD (F1 dimension) = 256 or 512, SI = 1k, SFO (F1 dimension) = 150.92, ND_010 = 2, IN_010 = 15 μsec, and O2P = 80. The HMQC acquisition was initiated by typing "zg." As with the pulse calibration, the parameter changes were preset by the Bruker TopSpin

3.0 software when using the Avance III-600 NMR instrument with the pulse program simply named HSQC.

HMBC Experiment

Long-range two-, three-, and occasionally four-bond ^{1}H to ^{13}C correlations were obtained from this type of experiment. The experiment was conducted on both the Avance-600 as well as the Avance III-600 spectrometers using a 5-mm (BBI) or 1.77-mm (TXI) inverse detection probe, respectively. The pulse program used for the HMBC experiment on the Avance-600 was labeled "hmbcgplpndqf." The parameters for the HMBC experiment were nearly identical to those of the HMQC, with the exception of changing IN_010 to 13 μsec if ^{13}C peaks were expected past 200 ppm and changing the O2P parameter to 100. The D6 parameter was used to optimize the experiment for the desired *J*-value. In most cases, a typical value of 8 Hz was used, corresponding to a D6 value of 60 msec. As with the HMQC parameters and pulse calibrations, the Avance III-600 NMR, controlled by Bruker TopSpin 3.0, had many of these parameters preset in the selected program simply named HMBC.

General Procedures for Solid-Substrate Fermentations

Fermentations of mycoparasitic/fungicolous and endophytic fungi were conducted in the laboratory of Dr. D. T. Wicklow of the Mycotoxin Research Unit, Agricultural Research Service, NCAUR, USDA in Peoria, Illinois. The fungal strains were cultured on slants of PDA at 25 °C for 14 days. Spore inoculum from these slants was suspended in sterile distilled water to give a final spore/cell suspension of 1×10^{6}/mL. Fermentaion was typically carried out in duplicate 2.8 L Fernbach flasks, each containing 100 g of rice. Distilled water (200 mL) was added to each flask and the contents were soaked overnight before autoclaving at 15 lb/in^{2} for 30 min. After cooling to rt, each was inoculated with 3.0 mL of the spore inoculum and incubated at 25 °C for 15-30 days.

After incubation, the fermented substrate was mechanically fragmented and extracted with EtOAc (3 × 500 mL). The combined EtOAc extracts were filtered and concentrated under vacuum to give a crude extract. In cases where additional material was needed, this process was scaled up using a greater number of flasks in an effort to obtain a targeted amount of crude extract for a given species.

General Procedures for Antifungal Assays

Antifungal assays against *Aspergillus flavus* (NRRL 6541) and *Fusarium verticillioides* (NRRL 25457) were conducted in the laboratory of Dr. Donald T. Wicklow of the NCAUR. A portion of the crude EtOAc extract of the solid-substrate fermentation cultures (approximately 6 mg) was redissolved in EtOAc. One-mg and 0.5-mg equivalents of extractable residue were pipetted into individual Petri dish lids and dried for 30 min in a laminar flow hood. After each disk was allowed to dry, up to four disks were placed equidistant from one another on the surface of freshly poured and solidified yeast-malt-glycerol (YMG) agar that was seeded with a spore suspension of *A. flavus* (NRRL 6541) conidia to give a final spore suspension of 100 cells per mL. Bioassay plates were incubated at 25 °C for four days and any inhibition of *A. flavus* was indicated by the presence of a cz, mz, or rg region around the disk (see Table 1 for zone definitions), which is indicative of the inhibition of germination and/or a measure of fungistatic activity (observations were typically noted after two and four days). An analogous procedure was employed for the assay against *F. verticillioides* (NRRL 25457).

Antifungal assays against *Candida albicans* (ATCC 10231) were conducted in our own laboratory. *C. albicans* test plates were freshly prepared as needed. One *C. albicans* BBL Quali Swab (Becton Dickinson) was used to inoculate 50 mL of sterile (MarketForge Sterilmatic Autoclave) Difco yeast maintenance broth. The culture was allowed to aerate on an orbital shaker at 150 rpm at rt for 36-48 hr. One hundred mL of

Tryptic soy agar (Difco) was prepared according to the product instructions, sterilized by autoclaving, and cooled to ~45 °C. One mL of the *C. albicans* inoculum suspension was transferred to the warm agar and mixed thoroughly by gently swirling to avoid bubbles. The inoculated agar was then poured into Petri plates (100 × 15 mm). The plates were allowed to set and were then stored in a refrigerator at 4 °C.

In conducting the disk diffusion assay, each filter paper disk (6.25 mm in diameter) was impregnated with the sample to be tested (25 or 100 µg/disk). After evaporation of the solvent, the disk was placed on the agar surface and incubated at rt for 24-96 hr. This same solvent was also used as a control blank for each test. Activity was reported by measuring the diameter (in mm) of the inhibition zone around each disk. A stock solution of the control antifungal agent filipin (Sigma Chemical Co.) was used as a positive control at a level of 25 µg/disk.

General Procedures for Antiinsectan Assays

Antiinsectan assays were developed and conducted by Dr. P. F. Dowd of the NCAUR. Selection of crude extracts for chemical investigation in search of antiinsectan metabolites was based on bioactivity against the fall armyworm, *Spodoptera frugiperda*.

The diet used to feed *S. frugiperda* was a standard pinto bean diet, consisting of the following ingredients: 120 g dried pinto beans, 43 g wheat germ, 28 g brewer's yeast, 8 g Vanderzant's vitamin mis, 2.8 g ascorbic acid, 1.75 g methylparaben, 0.9 g sorbic acid, 12 g sugar, 12 g formaldehyde (39%), 1.5 mL propionic-phosphoric acid solution (42 % propionic acid, 4.2 % phosphoric acid), and 550 mL of water. Crude extracts were incorporated into the diet at levels of at least 200 ppm. If deemed necessary, column fractions and pure compounds were sometimes tested at levels of 1000 ppm or more (wet weight). The samples were added in 125-µL of acetone to test tubes (100 × 16 mm) containing 5-mL aliquots of molten diet (60 °C). The mixture was then blended with a vortex mixer for 20 seconds. The diets were dispensed into Petri plates, allowed to cool

to rt, and placed in a fume hood for *ca.* 20 min to remove residual solvent. The diet was cut into equal blocks (*ca.* 250 mg each). Each block was placed into a well of a 24-well immunoassay plate, and then a single neonate *S. frugiperda* was added to each well. To prevent desiccation of the diet, a sheet of Parafilm, a sheet of cardboard, and a plastic cover covered the plate. The cover was secured with rubber bands. A solvent blank under the same conditions was used as a control.

Bioassays were conducted at 27 °C for seven days at 40% humidity with a 7:5 (light:dark) photoperiod. The insects were inspected at two, four, and seven days for mortality, and seven-day survivors were weighed. Each sample was tested on a total of 40 nenoate larvae. Antiinsectan activity was measured by comparison of the test larval weights relative to those of the controls. Data were reported as present reduction in weight gained relative to controls. Percent mortality was recorded in cases where mortality was observed.

General Procedures for Antibacterial Assays

Bacillus subtilis

Bacillus subtilis (ATCC 6051) assay plates were prepared every 14 days during heavy testing cycles or as needed during slow cycles. A sterile spore suspension of *B. subtilis* (1 mL sterile H_2O added to vial containing a pellet of *B. subtilis* – LyfoCults by PMLmicrobiologicals) was prepared. A 250-µL portion of this spore suspension was then pipetted directly into 100 mL of sterile Penassay seed agar (Difco – prepared as per product instructions) in a 250-mL Erlenmeyer flask once the agar had cooled to ~ 45 °C. The flask was gently swirled by hand to mix the spore suspension thoroughly. The agar was then poured into Petri plates (100 × 15 mm, approximately 5 mL each) and allowed to solidify before being stored in a refrigerator at 4 °C.

In conducting the assay, sterile filter paper disks (6.25 mm in diameter) were impregnated with 25 or 100 µg of sample. The solvent used to dissolve the sample was

evaporated and the disks were placed on the agar surface of the *B. subtilis*-seeded Petri dish. This same solvent was also used as a control blank for each test. The test plates were incubated at rt for 24-72 hr. The control antibiotic agent gentamycin (Sigma Chemical Co.) was used as a control at a level of 25 µg/disk.

Staphylococcus aureus

Staphylococcus aureus (ATCC 29213) plates were prepared as needed. A sterile spore suspension of *S. aureus* (1 mL sterile H_2O added to vial containing a pellet of *S. aureus* – LyfoCults by PML Microbiologicals) was prepared. A 250-µL portion of this spore suspension was then pipetted directly into 100 mL of sterile Tryptic soy agar (Difco – prepared as per product instructions) in a 250-mL Erlenmeyer flask once the agar had cooled to ~45 °C. The assay was otherwise conducted and evaluated in the same manner as the *B. subtilis* assay.

Escherichia coli

Escherichia coli (ATCC 25922) plates were prepared as needed. One *E. coli* bactrol disk (Difco) was dissolved in 50 mL of sterile Difco nutrient broth in a 250 mL Erlenmeyer flask and the culture was then aerated at 150 rpm for 36-48 hr at rt. One hundred mL of sterile Tryptic soy agar (Difco) was prepared according to the product instructions and then cooled to ~45 °C. Two mL of the *E. coli* inoculum suspension was transferred to the warm agar and the flask was gently swirled by hand to mix the spore suspension thoroughly. The assay was otherwise conducted and evaluated in the same manner as the *B. subtilis* assay.

In all of the above antibacterial assays, the antimicrobial activity of the sample was reported by measuring the diameter (in mm) on the inhibition zone around the disk in which no growth of the test organism was observed.

General Procedures for Cell Proliferation Assay

Chronic myelogenous leukemia (K562, 3×10^4 cell per well), murine melanoma (B16F10, 3×10^3 cell per well), human acute promyelocutic leukemia cells (HL-60, 1×10^5 cell per well), human breast cancer adenocarcinoma (MDA-MB-231, 5×10^3 cell per well) and hepatocellular carcinoma (Hep3B, 5×10^3 cell per well) cells were seeded on 96-well microplate. Test compounds were dissolved in DMSO at appropriate concentrations and were treated for 48 hr. Cell proliferation assays were carried out using the Enhanced Cell Viability Assay Kit EZ-CyTox (Daeil Lab Service Co., Ltd. Korea) protocol. The absorbance (450 nm) of each well was measured using a Power WaveX 340 (Bio-Tek Instruments, Winooski, VT).

Procedures for the Isolation and Characterization of Metabolites from Fungicolous and Marine Isolates of *Aspergillus* spp. (MYC-2048 = NRRL 58570 and *Aspergillus* sp. SF-5044)

Fungicolous Fungal Material

MYC-2048 (= NRRL 58570) was originally obtained by D.T.W. from a basidioma of *Rigidoporus microsporus* found on a dead hardwood branch in an alien wet forest near milepost 7 on Scenic Route 19, Onomea Bay, Hawaii Co., HI, in November, 2002. This isolate was initially identified as *Aspergillus flavipes* (section *Flavipedes*) based on *in vitro* colony growth and micromorphology. The culture was subjected to partial sequence analysis of the internal transcribed spacer region (ITS) and domains D1 and D2 of the nuclear large subunit (28S) rDNA gene using ITS5 and NL4 as polymerase chain reaction and sequencing primers.[263,264] A nucleotide-to-nucleotide BLAST query of the GenBank database (http://www.ncbi.nlm.nih.gov/BLAST) recovered EF669595 *Aspergillus* sp. NRRL 32683[164] (= MYC-1580; NRRL 58569) as the closest match to the ITS rDNA of NRRL 58570 (100%). This undescribed species of *Aspergillus* (section

Flavipedes) was also initially identified as *A. flavipes* and also came from our Hawaiian collection (isolated by D.T.W. from a basidioma of *Earliella scabrosa* found on a dead hardwood branch, alien wet forest, Hilo Zoo, Hawaii Co., HI). It was shown to be a sibling species to the clade containing *Aspergillus aureofulgens* NRRL 6326, which, in turn, was originally described from a single known isolate obtained from truffle soil in France.[164] The occurrence of this taxonomically related isolate in truffle soil is intriguing because this environment is also suggestive of a possible fungicolous origin. These results suggest that NRRL 58570 and NRRL 32683 represent separate Hawaiian isolates of the same undescribed species of *Aspergillus* (section *Flavipedes*). Because the isolate that matched has not been taxonomically described, we characterize this isolate at present only as "*Aspergillus* sp."

Marine Fungal Material

Aspergillus sp. SF-5044 (deposited at the College of Medical and Life Sciences fungal strain repository, Silla University) was isolated from an intertidal sediment sample collected from Dadaepo Beach, Busan, Korea in April, 2006 using procedures that have been described.[162] Analysis of 28S rRNA sequences (Genbank accession number FJ935999) and a subsequent GenBank search indicated *Aspergillus protuberus* (FJ176897) and *Aspergillus asperescens* (EF652495) as the closest matches, showing sequence identities of 99.64% and 98.22%, respectively. Therefore, the marine-derived fungal strain SF-5044 was identified as an *Aspergillus* sp., but could not be assigned to species, and is not the same species as the Hawaiian isolate.

Aspergillus sp. MYC-2048 was grown in 2.8 L Fernbach flasks on 100 g of autoclaved rice for 30 days at 25°C. The EtOAc extract (802 mg) of the resulting fermentation mixture showed antifungal activity against *A. flavus* and *F. verticillioides*. The extract also caused significant reduction in the growth rate of the fall armyworm. This fungicolous isolate yielded aflaquinolones A (**43**) and B (**44**). *Aspergillus* sp. SF-5044 was cultured on 110 petri plates (90-mm), each containing 20 mL of PDA with 3%

NaCl. Plates were individually inoculated with 2 mL seed cultures of the fungal strain and incubated at 25 °C for a period of 10 days. Extraction of the combined agar media with EtOAc (2 L) provided an organic phase, which was then concentrated *in vacuo* to yield 2.0 g of an extract. This marine isolate yielded aflaquinolones C-G (**47**-**51**).

Extraction and Isolation of Metabolites

The extract from *Aspergillus* sp. MYC-2048 (= NRRL 58570) was partitioned between MeCN and hexanes (~8 mL of MeCN and 3 to 4 successive washes of ~8 mL of hexanes to remove the fat). A portion (200 mg) of the resulting MeCN fraction (478 mg) was then chromatographed on a silica gel column using a hexanes/EtOAc/MeOH step gradient (hexanes, hexanes:EtOAc, EtOAc, EtOAc:MeOH, and MeOH, ratios used: hexanes, 3:1, 1:1, 1:3, 100% EtOAc, 99:1, 49:1, 19:1 9:1, and 100% MeOH) to give 15 100-mL fractions. Fraction 5 (34 mg), eluted with 1:1 hexanes:EtOAc, was further separated by reversed-phase HPLC (C_{18}; 25-100% MeCN in H_2O over 25 min with UV detection at 244 nm) to afford *trans*-dehydrocurvularin (**25**, 15 mg, t_R 19.0 min),[127] aflaquinolone A (**43**; 4 mg, t_R 20.4 min), and an additional sample of compound **44** (1 mg, t_R 17.0 min). Fraction 6 (14 mg), eluted with 1:1 hexanes:EtOAc, was further separated by reversed-phase HPLC (C_{18}; 25-100% MeCN in H_2O over 25 min with UV detection at 250 nm) to afford aflaquinolone B (**44**; 4 mg, t_R 17.8 min), aspochalasin J (**29**, 3 mg, 24.0 min),[130] and additional material of compound **43** (2 mg, t_R 20.9 min). Fraction 8 (19 mg), eluted with 1:3 hexanes:EtOAc, was further separated by reversed-phase HPLC (C_{18}, 25-100@ MeCN in H_2O over 25 min with UV detection at 244 nm) to afford alantripinone (**41**, 1 mg, t_R 14.1 min)[160] and methyl-3,4,5-trimethoxy-2((2-((3pyridinylcarbonyl)amino)benzoyl)amino)benzoate (**42**, 2 mg, t_R 22.2 min).[161] Fraction 10 (17 mg), eluted with 100% EtOAc, contained only aspochalasin I (**28**).[130]

The EtOAc extract (2.0 g) of the marine *Aspergillus* sp. isolate was subjected to C_{18} flash column chromatography (5 × 26 cm), eluting with a stepwise gradient of 20%, 40%, 60%, 80%, and 100% (v/v) MeOH in H_2O (500 mL each). The fraction eluted at

60% MeOH was re-subjected to C_{18} flash column chromatography (4.5 × 12 cm), eluting with a stepwise gradient of 20-70% MeOH in H_2O (250 mL each, 10% increment from 20%, to 50%, followed by two additional 50% MeOH fractions, 60% MeOH, and 70% MeOH). The fraction eluted with the first 50% MeOH in H_2O elution solvent (29.9 mg) was further purified by semi-preparative reversed-phase HPLC eluting with a gradient from 30-60% MeOH in H_2O (0.1% formic acid) over 40 min to yield **48** (3.5 mg, t_R 30.9 min). The fraction eluted with the second 50% MeOH elution solvent (35 mg) was purified by semi-preparative reversed-phase HPLC eluting with a gradient from 45-65% MeOH in H_2O (0.1% formic acid) over 65 min to yield compounds **47** (3.4 mg, t_R 27.5 min) and **49** (16 mg, t_R 25.1 min). The fraction from C_{18} flash column chromatography on the crude extract eluted at 80% MeOH (261 mg) was subjected to silica flash column chromatography (3.5 × 10 cm), eluting with a stepwise gradient of 0% to 20% (v/v) MeOH in CH_2Cl_2 (200 mL each, 1% increment for each fraction). The fraction eluted with 1 % MeOH (30 mg) was further purified by semi-preparative reversed-phase HPLC eluting with 75% MeOH in H_2O (0.1% formic acid) to yield **50** (3.0 mg, t_R 19.5 min). Compound **51** was purified from reversed -phase HPLC of the fraction collected between 1 to 10 min of the above HPLC procedure using a gradient from 50 to 100% MeOH in H_2O (0.1% formic acid) over 50 min (1.5 mg, t_R 33.5 min).

All of the known metabolites (**25**, **28**, **29**, **41**, and **42**) were identified by comparison of their ^{1}H NMR, ^{13}C NMR, and/or MS data with literature values.

Aflaquinolone A (**43**): pale orange amorphous solid; $[\alpha]^{22}_D$ +14 (c 0.19, MeOH); UV (MeOH) λ_{max} (log ε) 213 (4.3), 233sh (4.2), 278 (4.1), 324 (4.1) nm; CD (MeOH) Δε 220 (+36), 252 (-41), 280 (+16), 286 (+15), 323 (+9.5); ^{1}H and ^{13}C NMR data ($CDCl_3$), see Table 2; ^{1}H and ^{13}C NMR (400 MHz, acetone-d_6) data were the same as **47**; HMBC data (600 MHz, $CDCl_3$): NH → C-2, 3, 5, 9, 10; H-3 → C-2, 4, 5, 11; H-8 → C-5, 6, 7, 10, 17; H-9 → C-4, 5, 6, 7, 10; H-12/16 → C-11, 12/16, 13/15, 14; H-13/15 → C-11, 12/16, 13/15, 14; H-14 → C-11, 12/16, 13/15; H-17 → C-6, 7, 8, 18, 19, 25; H-18 → C-

7, 19, 20, 25; H_{ax}-20 → C-18, 19, 21, 22, 25, 26; H_{eq}-20 → C-19, 21, 22, 24; H-21 → C-20, 22, 26; H_{ax}-23 → C-22, 24; H_{eq}-23 → C-19, 21, 22; H_{ax}-24 → C-19, 23, 25; H_{eq}-24 → C-19, 21, 22; H_3-25 → C-18, 20, 23, 24; H_3-26 → C-20, 21, 22; H_3-27 → C-3; Key NOESY data (400 MHz, $CDCl_3$): 4-OH ↔ H_3-27; 4-OH ↔ H-3; H-3 ↔ H-12/16, H_{ax}-20 ↔ H_3-25; H_{eq}-20 ↔ H-18; H-21 ↔ H-17; H_{ax}-24 ↔ H_{eq}-23; H_{ax}-24 ↔ H_3-25; H_{eq}-24 ↔ H-17; HRESITOFMS obsd *m/z* 458.1941 $[M+Na]^+$, calcd 458.1943 for $C_{26}H_{29}NO_5Na$ $[M+Na]^+$.

Aflaquinolone B (**44**): pale yellow amorphous solid; $[\alpha]^{22}_D$ +20 (c 0.14, MeOH); UV (MeOH) λ_{max} (log ε) 213 (4.3), 233sh (4.1), 278 (4.0), 288sh (3.9), 324 (4.0) nm; CD (MeOH) Δε 220 (+32), 252 (-39), 280 (+14), 286 (+12), 323 (+7.9); ^1H and ^{13}C NMR data ($CDCl_3$), see Table 2; Key NOESY data (400 MHz; acetone-d_6): H-3 ↔ H-12/16; H-17 ↔ H_{eq}-20; H-17 ↔ H-21; H-17 ↔ H_{ax}-23; H-17 ↔ H_{eq}-24; Additional NOESY data (400 MHz; $CDCl_3$): 4-OH ↔ H_3-27; 4-OH↔H-3; HRESITOFMS obsd *m/z* 460.2089 $[M+Na]^+$, calcd 460.2091 for $C_{26}H_{31}NO_5Na$ $[M+Na]^+$.

Aflaquinolone C (**47**): pale yellow solid; $[\alpha]^{25}_D$ -33 (c 0.30, MeOH); UV (MeOH) λ_{max} (log ε) 203 (4.2), 212sh (4.1), 235sh (4.0), 278 (3.8), 324 (3.8) nm; CD (MeOH) Δε 220 (+28), 252 (-30), 281 (+11), 286 (+10), 322 (+6.8); ^1H and ^{13}C NMR data, see Table 3; HMBC data: H-3 → C-2, 4, 5, 6, 11, 27; H-8 → C-5, 6, 10, 11; H-9 → C-4, 5, 6, 7, 10; H-12/16 → C-4; H-17 → C-6, 8, 19, 25; H-18 → C-7, 19, 20, 24, 25; H_2-20 → C-18, 19, 21, 25, 26; H-21 → C-20, 22, 26; H_2-23 → C-22, 24; H_2-24 → C-18, 19, 25; H_3-25 → C-18, 19, 20, 24; H_3-26 → C-20, 21, 22; H_3-27 → C-3; NOESY data: H-3 ↔ H-12/16; H-17 ↔ $H\text{-}23_{ax}$, H-21; $H\text{-}23_{ax}$ ↔ $H\text{-}24_{ax}$, H_3-25, H_3-26; HRESIMS obsd *m/z* 434.1954 $[M-H]^-$, calcd for $C_{26}H_{28}NO_5$, 434.1967.

Aflaquinolone D (**48**): pale yellow solid; $[\alpha]^{25}_D$ -10 (c 0.10, MeOH); UV (MeOH) λ_{max} (log ε) 204 (4.3), 212sh (4.3), 235sh (4.2), 278 (4.0), 323 (4.0) nm; CD (MeOH) Δε 220 (+31), 252 (-32), 282 (+12), 286 (+12), 324 (+7.6); ^1H NMR data, see Table 3;

NOESY data: H-3 ↔ H-12/16; H-17 ↔ H-20_{ax}; H-20_{ax} ↔ H_3-26; H-21 ↔ H_3-25; H-23_{ax} ↔ H_3-25; HRESIMS obsd *m/z* 434.1954 $[M-H]^-$, calcd for $C_{26}H_{28}NO_5$, 434.1967.

Aflaquinolone E (**49**): white solid; $[\alpha]^{25}_D$ -41 (c 1.1, MeOH); UV (MeOH) λ_{max} (log ε) 208 (4.2), 252 (3.5), 295 (3.5) nm; CD (MeOH) Δε 218 (+19), 245 (-23), 270 (+9.2), 295 (+5.7); ^1H and ^{13}C NMR data, see Table 4; HMBC data: H-3 → C-2, 4, 5, 6, 11, 27; H-7 → C-5, 6; H-8 → C-5, 6, 7, 10; H-9 → C-5, 6, 7, 10; H-12/16 → C-4, 11, 14; H_3-17 → C-3; HRESIMS obsd *m/z* 308.0893 $[M+Na]^+$, calcd for $C_{16}H_{15}NO_4Na$, 308.0899.

Aflaquinolone F (**50**): white solid; $[\alpha]^{25}_D$ +10 (c 0.19, MeOH); UV (MeOH) λ_{max} (log ε) 208 (4.2), 252 (3.6), 295 (3.5) nm; CD (MeOH) Δε 200 (-9.5), 223 (+13), 252 (-3.2), 269 (+2.1), 290 (+0.8); ^1H and ^{13}C NMR data, see Table 4; HMBC data: H-3 → C-2, 4, 5, 11; H-6 → C-4, 8, 10; H-7 → C-6, 9; H-8 → C-6, 10; H-9 → C-5, 7; H-12/16 → C-4; H-13/15 → C-11, 12/16; H-14 → C-12/16; HRESIMS obsd *m/z* 256.0975 $[M+H]^+$, calcd for $C_{15}H_{14}NO_3$, 256.0974.

Aflaquinolone G (**51**): white solid; $[\alpha]^{25}_D$ -6 (c 0.18, MeOH); UV (MeOH) λ_{max} (log ε) 208 (4.2), 253 (3.7), 285sh (3.3) nm; CD (MeOH) Δε 206 (+13), 216 (+14), 235 (-8.6), 257 (+5.4), 286 (-3.1); ^1H and ^{13}C NMR data, see Table 4; HMBC data: H-3 → C-2, 4, 11; H-6 → C-4, 8, 10; H-7 → C-5, 6, 9, 10; H-8 → C-6, 9, 10; H-9 → C-5, 7; H-12/16 → C-4, 13/15; HRESIMS obsd *m/z* 278.0788 $[M+Na]^+$, calcd for $C_{15}H_{13}NO_3Na$, 278.0793.

Sodium Borohydride Reduction of Aflaquinolone A (**43**)

A 0.7-mg sample of aflaquinolone A (**43**) was transferred to a 0.5-mL Reacti-vial. To this vial, 0.75 mg of $NaBH_4$ and 75 μL of MeOH were added, and small triangular stir bar was placed into the vial. The vial was then sealed under Ar and monitored by TLC (9:1 Et_2O:MeOH). After 1 hr, all of the starting material had reacted. The solvent was then evaporated with air flow and worked-up using aqueous NH_4Cl and ether. The ether layer was collected and evaporated to dryness. ^1H NMR analysis of the ether-

soluble material indicated the presence of a mixture of products, which was separated by reversed-phase HPLC (C_{18}, column: 4.6 x 250 mm, 1.0 mL/min, 50 - 100% ACN in H_2O over 25 min), resulting in the collection of two peaks (t_R = 11.2 and 12.8 min, respectively). ^{1}H NMR analysis of the first fraction to elute exhibited signals matching those of aflaquinolone B (**44**), indicating that reduction of **43** to **44** had occurred. HPLC co-injection with a sample of **44** supported this conclusion.

Preparation of Aflaquinolone B (**44**) Mosher Esters

A solution of **44** (0.2 mg) in $CDCl_3$ (100 μL) was treated with dry pyridine-d_6 (10 μL) and *R*-(-)-α-methoxy-α-(trifluoromethyl)phenylacetyl chloride (*R*-MTPA-Cl, 5 μL). The mixture was allowed to react at rt for 24 hr in a Teflon-lined screw-cap vial, resulting in the *S*-MTPA ester **44a**. An additional 500 μL of $CDCl_3$ was then added directly to the vial and the resulting solution was placed in a NMR tube for analysis. Analogous treatment of an additional portion of **44** (0.2 mg) using *S*-MTPA-Cl afforded the *R*-MTPA ester **44b**. In both reactions, the pyridine-d_6 and MTPA-Cl were in excess.

S-MTPA ester **44a**: faint purple oil; Key ^{1}H NMR data (400 MHz, $CDCl_3$) δ 0.736 (d, J = 6.9 Hz, H_3-26), 1.29 (m, H_{ax}-23), 1.71 (m, H_{eq}-23).

R-MTPA ester **44b**: faint purple oil; Key ^{1}H NMR data (400 MHz, $CDCl_3$) δ 0.822 (d, J = 6.9 Hz H_3-26), 1.23 (m, H_{ax}-23), 1.64 (m, H_{eq}-23).

Precise δ values for other potentially relevant signals (e.g., H-21) could not be established due to signal overlap for both **44a** and **44b**.

Energy Minimizations and ECD Calculations

All geometry optimizations were performed in gas phase using resolution-of-identity (RI) approximation and BP functional,[58,59] combined with SV(P) basis set[265] and the corresponding auxiliary basis set.[266,267] No symmetry constraints were used during the optimization. Electronic circular dichroism (ECD) spectra were calculated for geometries obtained from the RI-BP/SV(P) calculations. Time-dependent density functional (TDDFT) calculations were used with B3LYP functional[268,269] using

RIJCOSX approximation[270] and TZVP basis set[265] with the corresponding auxiliary basis set.[266,267] in gas phase and in MeOH solution (COSMO solvation model).[271] A total of 80 excited states were calculated and only singlet excited states were considered. All of the quantum chemical calculations were performed with ORCA version 2.8.[272] ECD spectra were obtained using SpecDis version 1.50 software.[273] A broadening factor of 0.24 was used in an effort to match the resolution level of the experimental data as closely as possible.

Procedures for the Isolation and Characterization of Metabolites from a Cryptic Fungicolous Isolate of *Aspergillus* sp. (section *Flavipedes*; MYC-1580 = NRRL 58569)

Fungal Material

The isolate for this study (MYC-1580) was obtained by Dr. D. T. Wicklow from a basidioma of *Earliella scabrosa* on a dead hardwood branch that was collected from an alien wet forest near Hilo Zoo, Hawaii Co., Hawaii on November 12, 2002. Initially, this isolate was identified as *Aspergillus flavipes* based on cultural characteristics and micromorphology following the protocol of Raper and Fennell.[274] It was then deposited with ARS Culture Collection and given the number NRRL = 58569. MYC-1580 was an undescribed, or cryptic, *Aspergillus* sp. (section *Flavipedes*) that is closely associated with *Aspergillus aureofulgens* and *Aspergillus terreaus*.[164] Fermentation conditions are described above and lasted for 30 days at 25 °C. The resulting culture material was then extracted with EtOAc, affording 371 mg of crude extract upon evaporation of the solvent. The EtOAc extract showed moderate antifungal activity against *F. verticillioides*. The extract also caused significant reduction in the growth rate of fall armyworm when the crude extract was incorporated into the worm's diet, compared to controls.

Extraction and Isolation of Metabolites

The extract was partitioned between MeCN and hexanes (~8 mL of MeCN and 3 to 4 successive washes of ~8 mL of hexanes to remove the fat). The resulting MeCN fraction (241 mg) was then chromatographed on a Sephadex LH-20 column (Sigma) using a hexanes/CH_2Cl_2/acetone/MeOH step gradient (hexanes, hexanes:CH_2Cl_2, CH_2Cl_2:acetone, and MeOH, ratios used: hexanes, 1:4 hexanes:CH_2Cl_2, 3:2 CH_2Cl_2:acetone, 1:4 CH_2Cl_2:acetone, and 100% MeOH) to give 14 50-mL fractions. The entire fraction 1 (7 mg), eluted with 1:4 hexanes:CH_2Cl_2, was determined to be the known compound methyl-3,4,5-trimethoxy-2((2-((3-pyridinylcarbonyl)amino)benzoyl) amino)benzoate (**42**).[161] Fraction 4 (12 mg), also eluted with 1:4 hexanes:CH_2Cl_2, was found to consist of a sample of the known compound aspochalasin J (**29**).[130] Fraction 7 (25 mg), eluted with 3:2 CH_2Cl_2:acetone, was further separated by reversed-phase HPLC (C_{18}; 45-100% MeCN in H_2O over 25 min at 2.0 mL/min with UV detection at 236 nm) to afford *trans*-dehydrocurvularin (**25**, 3 mg, t_R 14.2 min)[127] and PF1233B (**54**, 4 mg, t_R 15.5 min). Fraction 8 (67 mg), eluted with 3:2 CH_2Cl_2:acetone, was further separated by reversed-phase HPLC (C_{18}; 25-100% MeCN in H_2O over 25 min at 2.0 mL/min with UV detection at 244 nm) to afford alantrypinone (**41**, 2 mg, t_R 13.7 min),[160] additional **25** (10 mg, t_R 17.1 min), and aspochalasin I (**28**, 17 mg, t_R 20.5 min).[130] Fraction 9 (17 mg), eluted with 3:2 CH_2Cl_2:acetone, was further separated by reversed-phase HPLC (C_{18}; 25-100% MeCN in H_2O over 30 min at 2.0 mL/min with UV detection at 244 nm) to afford flavipeptide A (**53**, 2 mg, t_R 14.1 min). Fraction 12 (8 mg), eluted with 1:4 CH_2Cl_2:acetone, was further separated by reversed-phase HPLC (C_{18}; 25-100% MeCN in H_2O over 35 min at 2.0 mL/min with UV detection at 224 nm) to afford 12-oxocurvularin (**58**, 1 mg, t_R 14.2 min)[168] and curvularin (**55**, 1 mg, t_R 15.9 min).[167] Fraction 13 (16 mg), eluted with 1:4 CH_2Cl_2:acetone, was further separated by reversed-phase HPLC (C_{18}; 25-100% MeCN in H_2O over 25 min at 2.0 mL/min with UV detection at 266 nm) to afford HPLC fraction 2 (6 mg, t_R 11.6 min) which was a mixture

of α-11-hydroxycurvularin (**56**) and β-11-hydroxycurvularin (**57**)[168] along with an additional sample of **25** (1 mg, t_R 19.0 min). Fraction 14 (29 mg), eluted with the MeOH wash, was further separated by reversed-phase HPLC (C_{18}, 50-100% MeOH in H_2O over 10 min, 100% MeOH isocratic for 8 min at 2.0 mL/min with UV detection at 308 nm) yielding four subfractions. HPLC subfractions two and three were recombined (6 mg) and further separated by reversed-phase HPLC (C_{18}; 70-100% MeOH in H_2O over 20 min at 1.0 mL/min with UV detection at 248 nm) yielding two fractions. Subsequent HPLC subfraction one (4 mg) was further purified by additional reversed-phase HPLC (Phenyl; 50-100% MeOH in H_2O over 25 min at 2.0 mL/min with UV detection at 254 nm) to afford asperlarin A (**52**, 2 mg, t_R 8.0 min). Sephadex fraction 14, subfraction four (22 mg), was further separated by reversed-phase HPLC (C_{18}; 50-100% MeOH in H_2O over 25 min at 2.0 mL/min with UV detection at 232 nm) to afford and additional sample of asperlarin A (**52**, 3 mg, t_R 6.4 min) material.

All of the known compounds (**25**, **28**, **29**, **41**, **42**, and **55-58**) were identified by comparison of their ^{1}H NMR, ^{13}C NMR, and/or MS data with literature values.

Asperlarin A (**52**): light brown oil; $[\alpha]^{22}_D$ -55 (c 0.11), MeOH); UV (MeOH) λ_{max} (log ε) 204 (4.3), 253 (4.0), 309 (3.3) nm; ^{1}H and ^{13}C NMR data, see Table 6; HRESITOFMS obsd *m/z* 468.1773 $[M-H]^-$, calcd for $C_{24}H_{26}N_3O_7$, 468.1770.

Flavipeptide A (**53**): white amorphous solid; $[\alpha]^{22}_D$ -60 (c 0.10, MeOH); UV (MeOH) λ_{max} (log ε) 217sh (4.3), 248 (3.9), 286 (3.5) nm; ^{1}H and ^{13}C NMR data, see Table 7; HRESITOFMS obsd *m/z* 467.2300 $[M+H]^+$, calcd for $C_{25}H_{31}N_4O_5$, 467.2294.

PF1233B (**54**): yellow oil; $[\alpha]^{22}_D$ +70 (c 0.20, MeOH); UV (MeOH) λ_{max} (log ε) 209 (4.4), 235sh (3.7), 245sh (3.5), 300 (3.2) nm; ^{1}H, ^{13}C, and HMBC NMR data, see Table 8; HRESITOFMS obsd *m/z* 435.1921 $[M+H]^+$, calcd for $C_{25}H_{27}N_2O_5$, 435.1920.

Amino Acid Analysis of Asperlarin A (**52**) and Flavipeptide A (**53**)

Acid hydrolysis of Asperlarin A (**52**) and Flavipeptide A (**53**).

In separate vacuum-sealed hydrolysis tubes, solutions of **52** (0.3 mg) and **53** (0.3 mg) were dissolved in 1.0 mL of 6 N HCl and heated at 110°C for 24 hr. After completion, each tube was cooled in ice and the solutions were dried down directly in the hydrolysis tube under a flow of air.

Preparation of trifluoroacetyl (+)-*S*-*sec*-butyl ester derivatives.

The absolute configuration of the constituent amino acids of **52** and **53** were determined by GCMS analysis of the trifluoroacetyl (+)-*S*-*sec*-butyl ester derivatives when compared to authentic D- and L- standards prepared under the same conditions. The hydrolyzate of **52**, still in the hydrolysis tube, was treated with ~1.0 mL of (+)-*S*-*sec*-butanolic HCl. (Preparation of (+)-*S*-*sec*-butanolic HCl: 1.0 mL (+)-*S*-*sec*-butanol and 35 µL acetyl chloride mixed directly in the hydrolysis tube.) The tube was sealed under vacuum and the sample was then heated at 110°C for 30 min, cooled in ice, and then dried down directly in the hydrolysis tube. The product mixture was then dissolved in 1.0 mL of CH_2Cl_2 and 500 µL of trifluoroacetic anhydride (TFAA), sealed under vacuum, and then heated at 150°C for 5 min. The resulting solution was removed from the hydrolysis tube, placed into a vial, and dried to near-completion before 1 mL of CH_2Cl_2 was added to prepare for GCMS analysis. The procedure for preparing the derivatives of the amino acids in the hydrolysate of **53** was exactly the same as above.

The trifluoroacetyl (+)-*S*-*sec*-butyl ester derivatives for L-valine and L-proline (for **52**) and L-valine, L-alanine, and N-Me-L-tyrosine (for **53**), and well as the D- and L- mixtures of the corresponding amino acids were also prepared as described above (except that the acid hydrolysis step was not necessary). The derivatized D- and L- mixtures of the individual standards resulted in two resolved peaks in the GCMS data for each form of amino acid. Retention times for the appropriate amino acids include: Alanine (D t_R = 7.90 min, L t_R = 8.00 min), Proline (D t_R = 11.86 min, L t_R = 11.93 min), N-Me Tyrosine

(D t_R = 16.60 min, L t_R = 16.67 min), and Valine (D t_R = 9.10 min, L t_R = 9.23 min). Co-injection of the L- form of each amino acid with its corresponding D- and L- mixture enabled identification of the specific form of each amino acid. These derivatives served as the standards for the GCMS analysis of the derivatized hydrolyzates of **52** and **53**.

Procedures for the Isolation and Characterization of Metabolites from an Endophytic Isolate of *Emericella nidulans* (ENDO-3111 = NRRL 58893)

Fungal Material

The isolate for this study (ENDO-3111) was obtained by Dr. D. T. Wicklow on July 7, 2005 from a wheat seed of the variety "WH-3" produced in Patagonia, Arizona. The gain sample was purchased from Native Seeds Search in Tucson, Arizona in 2005. The culture was subsequently identified as *Emericella nidulans* and was deposited with the ARS Culture Collection and assigned the accession number NRRL = 58893. Fermentation conditions are described above and lasted for 30 days at 25 °C. The resulting culture material was then extracted with EtOAc, affording 442 mg of crude extract upon evaporation of the solvent. The EtOAc extract showed moderate antifungal activity against *A. flavus* and *F. verticillioides*. The extract also caused significant reduction in the growth rate of fall armyworm when compared to controls when crude extract material was incorporated into the diet.

Extraction and Isolation of Metabolites

The extract was partitioned between MeCN and hexanes (~8 mL of MeCN and 3 to 4 successive washes of ~8 mL of hexanes to remove the fat). The resulting MeCN fraction (245 mg) was then chromatographed on a silica gel column using a hexanes/CH_2Cl_2/EtOAc/MeOH step gradient (hexanes, hexanes:CH_2Cl_2, CH_2Cl_2, CH_2Cl_2:EtOAc, EtOAc, EtOAc:MeOH, and MeOH, ratios used: hexanes, 3:1, 1:1, 1:3, 100% CH_2Cl_2, 3:1, 1:1, 1:3, 100% EtOAc, 32:1, 19:1, 9:1, 5:1, and 100% MeOH) to give

14 150-mL fractions. Fraction 2 (25 mg), eluted with 3:1 hexanes:EtOAc, was further separated by reversed-phase HPLC (C_{18}; 100% MeCN held isocratically for 15 min at 2.0 mL/min with UV detection at 212 nm) to afford 3-benzyl-4-phenyl-2,5-furadione (**63**, 1 mg, t_R 6.8 min).[176] Fraction 2, HPLC subfraction 5 (10 mg), was again separated by reversed-phase HPLC (Phenyl, 50-100% MeCN in H_2O over 25 min at 2.0 mL/min with UV detection at 240 nm) to afford emindole DA (**60**, 4 mg, t_R 20.8 min).[173] Fraction 3 (68 mg), eluted with 3:1 hexanes:EtOAc, was subsequently separated on a similar silica gel column using a hexanes/CH_2Cl_2/EtOAc step gradient (hexanes, hexanes:CH_2Cl_2, CH_2Cl_2, CH_2Cl_2:EtOAc, and EtOAc, ratios used: hexanes, 19:1, 9:1, 4:1, 3:2, 1:1, 1:3, 1:4, 100% CH_2Cl_2, 3:1, 1:1, 1:3, 100% EtOAc) to give 13 50-mL fractions. The 9th subfraction (10 mg) from the silica gel column separation of fraction 3, eluted with 100% CH_2Cl_2, was identified as an additional sample of **60**. The 10th subfraction (26 mg) from the silica gel separation of fraction 3, eluted with 1:3 EtOAc:CH_2Cl_2, was further separated by reversed-phase HPLC (C_{18}; 60-100% MeCN in H_2O over 25 min and 100% MeCN isocratic for 10 min at 2.0 mL/min with UV detection at 234 nm) to afford microperfuranone (**62**, 2 mg, t_R 13.6 min),[175] sterigmatocystin (**59**, 3 mg, t_R 17.2 min),[172] and an additional sample of **60** (6 mg, t_R 31.2 min). The 11th subfraction (13 mg) from the silica gel separation of fraction 3, eluted with 1:1 CH_2Cl_2:EtOAc, was further separated by reversed-phase HPLC (C_{18}; 50-100% MeCN in H_2O over 25 min at 2.0 mL/min with UV detection at 254 nm) to afford silvaticol (**64**, 2 mg, t_R 10.4 min).[177,178] Fractions 5 (38 mg), eluted with 1:1 hexanes:EtOAc, and 6 (10 mg), eluted with 1:3 hexanes:EtOAC, were both identified as containing pure emestrin (**61**).[174] Fraction 7 (172 mg), eluted with 1:1 CH_2Cl_2:EtOAc, was further separated on a similar silica gel column, as described above, using a hexanes/CH_2Cl_2/EtOAc step gradient (hexanes, hexanes:CH_2Cl_2, CH_2Cl_2, CH_2Cl_2:EtOAc, and EtOAc, ratios used: hexanes, 9:1, 5:1, 1.5:1, 1:1, 1:3, 1:4, 100% CH_2Cl_2, 3:1, 1:1, 1:3, and 100% EtOAc) to give 12 100-mL fractions. A portion (26 mg) of subfraction 9 (59 mg) was further separated by reversed-

phase HPLC (C_{18}; 50-100% MeCN over 25 min and 100% MeCN isocratic for 10 min at 2.0 mL/min with UV detection at 240 nm) to afford O-methylsecoemestrin C_1 (**66**, 2 mg, t_R 18.8 min) and emeridin A (**65**, 6 mg, t_R 25.2 min). Original silica gel fraction 8 (40 mg) was separated using reversed-phase HPLC (C_{18}; 40-100% MeCN over 25 min at 2.0 mL/min with UV detection at 242 nm) to afford 5-(hydroxymethyl)-2,4-dimethylbenzene-1,3-diol (**67**, 1 mg, t_R 5.6 min) and 5-(hydroxymethyl)-3-methoxy-2,4-dimethylphenol (**68**, 6 mg, t_R 9.6 min).

All of the known metabolites (**59-64**) were identified by comparison of their ^{1}H NMR, ^{13}C NMR, and/or MS data with reported values.

Emeridin A (**65**): bright yellow amorphous solid; $[\alpha]^{22}_D$ -73 (c 0.13, MeOH); UV (MeOH) λ_{max} (log ε) 289 (4.4) nm; ^{1}H, ^{13}C, and HMBC NMR data, see Table 9; HRESITOFMS obsd *m/z* 457.2593 $[M+H]^+$, calcd for 457.2590, $C_{27}H_{37}O_6$.

O-Metylsecoemestrin C_1 (**66**): pale yellow amorphous solid; $[\alpha]^{22}_D$ -10 (c 0.40, MeOH); UV (MeOH) λ_{max} (log ε) 206 (4.6), 218sh (4.5), 256 (4.1), 296 (3.8), 330sh (3.3) nm; ^{1}H, ^{13}C, and HMBC NMR data, see Table 10; HRESITOFMS obsd *m/z* 575.0924 $[M+Na]^+$, calcd for $C_{27}H_{24}N_2O_7S_2Na$, 575.0923.

5-(Hydroxymethyl)-2,4-dimethylbenzene-1,3-diol (**67**): pale brown oil; UV (MeOH) λ_{max} (log ε) 209 (4.2), 263 (3.4), 278sh (3.4), 302sh (3.0) nm; ^{1}H and ^{13}C NMR data, see Table 11.

5-(Hydroxymethyl)-3-methoxy-2,4-dimethylphenol (**68**): pale brown glass; UV (MeOH) λ_{max} (log ε) 208 (4.2), 222sh (3.9), 279 (3.3) nm; ^{1}H and ^{13}C NMR data, see Table 11; HRESITOFMS obsd *m/z* 165.0919 $[M-H_2O+H]^+$, calcd for $C_{10}H_{13}O_2$, 165.0916.

Attempted Chemical Degradations of Emeridin A (**65**) using OsO_4 and $KMnO_4$

The attempted oxidative cleavage of **65** using OsO_4 was performed on 0.7 mg of **65**. This material (0.0015 moles) was combined with 3 eq. of OsO_4 (0.0046 moles; 230 μL of 0.02 M OsO_4 in t-BuOH) and a trace of H_20 and then placed into a Teflon-capped

vial. The mixture was stirred for approximately 26 hr without any visual indications that a reaction had occurred. The mixture was dried down and analyzed by ^{1}H NMR, which indicated that the starting material of **65** went unreacted. This recovered material was used for the attempted $KMnO_4$ reaction described below.

The attempted oxidative cleavage of **65** using $KMnO_4$ was performed on 0.7 mg of **65**. This material (0.0015 moles) was dissolved in 1.5 mL of acetone and placed into a vial. Approximately 20 eq of $NaHCO_3$ was then added to the solution and stirred vigorously. $KMnO_4$ (5 eq.; 0.00765 moles, 1.21 mg) was then added and the mixture was allowed to stir at rt. The initial purple color was expected to dissipate over time, creating a black precipitate, however no color change or precipitate was observed. The reaction was allowed to continue for 24 hr, resulting in no visual change. The reaction was quenched with isopropyl alcohol and filtered through a small silica gel column using approximately 2 mL of isopropyl alcohol followed by careful addition of 1 mL of a 95% acetone/5% acetic acid solution. Each of the solvent fractions were collected in separate vials. ^{1}H NMR analysis of the separated material indicated that the original **65** material was completely degraded, but no relevant signals for expected products were observed in either ^{1}H NMR spectrum.

Ozonolysis of Emeridin A (**65**)

A portion of **65** (0.7 mg) was dissolved in ~4 mL of CH_2Cl_2 and placed into a small (15 mL) conical flask. The flask was then chilled to approximately -15 °C in an NaCl/Ice bath. Working in a hood and behind a blast shield, pure oxygen was bubbled into the solution for 20 min before the ozonator was enabled. The ozonolysis of **65** was performed using a Welsbach Ozonator T-408 (115 V, 2.4 A, 60 Hz; Welsbach Ozone Systems Corp., Philadelphia, PA.). Once the ozonator was switched on, O_3 was bubbled into the solution for 5 min. The ozonator was then switched off and O_2 was allowed to bubble into the solution for 2 min, thus purging any remaining O_3. The ozonolysis products then underwent a reductive work-up with the addition of ~0.5 mL of Me_2S to

the cold solution. The worked-up solution was swirled for 5 min and then evaporated under a stream of air. The resulting ^{1}H NMR spectrum strongly suggested that the products present in the mixture were the products expected (see Scheme 3). For example, all olefinic signals were absent. Instead, an aldehyde signal was present at δ 9.67, which would correspond to the anticipated bicyclic subunit product, and the methyl group H_3-25 was shifted downfield to δ 2.40, as would be expected for a methyl ketone that would arise from the cyclopentanone portion. Unfortunately, efforts to separate this mixture by HPLC were unsuccessful.

Procedures for the Isolation and Characterization of Metabolites from Other Fungicolous Fungi (MYC-1515 = NRRL 54514, MYC-2013 = NRRL 54531, and MYC-1991)

MYC-1515 (= NRRL 54514) Fungal Material

The isolate for this study (MYC-1515) was obtained by Dr. D. T. Wicklow from a basidioma of *Gloephyllum trabeum* that formed on a dead hardwood branch in a Subalpine Dry Forest Pu'u la'au near milepost 43 on Highway 200, Mamane (Sophora), Hawaii Co., Hawaii on November 12, 2002. The isolate was identified as *Trichoderma longibrachiatum* based on cultural characteristics and micromorphology following the protocol of Samuels,[275] and confirmed by a DNA BLAST search. It was deposited with ARS Culture Collection and assigned the accession number NRRL = 54514. Fermentation conditions are described above and lasted for 30 days at 25 °C. The resulting culture material was then extracted with EtOAc, affording 824 mg of crude extract upon evaporation of the solvent. The EtOAc extract showed modest antifungal activity against *A. flavus* and *F. verticillioides*. The extract also caused reduction in the growth rate of fall armyworm when compared to controls.

Extraction and Isolation of Metabolites

The extract was partitioned between MeCN and hexanes (~8 mL of MeCN and 3 to 4 successive washes of ~8 mL of hexanes to remove the fat). A portion (315 mg) of the resulting MeCN fraction (368 mg) was then chromatographed on a silica gel column using a hexanes/CH_2Cl_2/MeOH step gradient (hexanes, hexanes:CH_2Cl_2, CH_2Cl_2, CH_2Cl_2:MeOH, and MeOH, ratios used: hexanes, 12:1, 6:1, 4:1, 1.2:1, 1:4, 100% CH_2Cl_2, 99:1, 66:1, 32:1, 13:1, 7:1, 4:1, and 100% MeOH) to give 14 200-mL fractions. A portion (39 mg) of fraction 11 (86 mg), eluted with 13:1 CH_2Cl_2:MeOH, was further separated by reversed-phase HPLC (C_{18}; 60-100% MeCN over 25 min at 2.0 mL/min with UV detection at 248 nm) to give nine subfractions. HPLC subfraction 1 (3 mg) was purified using an additional reversed-phase HPLC separation (Phenyl; 50-100% MeCN over 25 min at 2.0 mL/min with UV detection at 212 nm) to afford tetrahydrosorbicillinol (**71**, 1 mg, t_R 8.8 min) and the known metabolite harzialactone A (**72**, 1 mg, t_R 10.3 min).[195] Fraction 12 (7 mg), eluted with 7:1 CH_2Cl_2:MeOH, contained only the known compound bisorbibutenolide (**73**).[196]

Both of the known compounds (**72** and **73**) were identified by comparison of their ^{1}H NMR, ^{13}C NMR, and/or MS data with literature values.

Tetrahydrosorbicillinol (**71**): pale yellow oil; $[\alpha]^{22}_D$ +6 (c 0.04, MeOH); UV (MeOH) λ_{max} (log ε) 228 (3.7), 264 (3.4), 325sh (2.7) nm; ^{1}H, ^{13}C, and HMBC NMR data, see Table 12; HRESITOFMS obsd *m/z* 2.75.1247 $[M+Na]^+$, calcd for $C_{14}H_{20}O_4Na$, 275.1259.

MYC-2013 (= NRRL 54531) Fungal Material

This isolate (MYC-2013) was obtained by Dr. D. T. Wicklow from a white mycelial growth on the undersurface of a dead hardwood branch in the Costal Mesic Forest, Casurina, Mackenzie State Park, Puna District, Hawaii on November 5, 2002. It was identified as *Stachybotrys parvispora* based on cultural characteristics and micromorphology following the protocol of Ellis.[276] It was then deposited with ARS

Culture Collection and assigned the accession number NRRL = 54531. Fermentation conditions are described above and lasted for 30 days at 25 °C. The resulting culture material was then extracted with EtOAc, affording 1492 mg of crude extract upon evaporation of the solvent. The EtOAc extract showed moderate antifungal activity against *F. verticillioides*.

Extraction and Isolation of Metabolites

The extract was partitioned between MeCN and hexanes (~8 mL of MeCN and 3 to 4 successive washes of ~8 mL of hexanes to remove the fat). A portion (415 mg) of the resulting MeCN fraction (1203 mg) was then chromatographed on a silica gel column using a hexanes/EtOAc/MeOH step gradient (hexanes, hexanes:EtOAc, EtOAc, and MeOH, ratios used: hexanes, 3:1, 1:1, 1:3, 100% EtOAc, and 100% MeOH) to give 11 150-mL fractions. Fraction 5, eluted with 1:1 hexanes:EtOAc, was further separated by reversed-phase HPLC (C_{18}; 100% MeCN isocratic for 10 min at 2.0 mL/min with UV detection at 248 nm) to afford agistatine B (**78**, 3 mg, t_R 7.4 min).[202] A portion (17 mg) of fraction 6 (51 mg) was further separated by reversed-phase HPLC (C_{18}; 100% MeCN isocratic for 10 min at 2.0 mL/min with UV detection at 248 nm) to yield three subfractions. HPLC subfraction 3 contained the new metabolite agistatine F (**77**, 11 mg, t_R 7.2 min). Fraction 10 (38 mg), eluted with 100% EtOAc, was identified as the known compound parvisporicin (**79**).[201]

Both of the known metabolites (**77** and **79**) were identified by comparison of their ^{1}H NMR, ^{13}C NMR, and/or MS data with reported values.

Agistatine F (**77**): colorless oil; $[\alpha]^{22}_D$ +82 (c 0.55, MeOH); UV (MeOH) λ_{max} (log ε) 202 (2.7), 243sh (2.5) nm; ^{1}H, ^{13}C, and HMBC NMR data, see Table 13; HREIMS obsd *m/z* 230.1169 $[M\cdot]^+$, calcd for $C_{11}H_{18}O_5$, 230.1154.

MYC-1991 Fungal Material

The fungal isolate MYC-1991 was isolated by Dr. D. T. Wicklow from black stroma of a Pyenomycete found on a dead hardwood branch in the Costal Mesic Forest,

Casuarina, Mackenzie State Park, Puna District, Hawaii on November 5, 2002. The isolate is unidentified because the initial culture was found to have died in storage, and thus could not be sequenced for species identification. Fermentation conditions are described above and lasted for 30 days at 25 °C. The resulting culture material was then extracted with EtOAc, affording 472 mg of crude extract upon evaporation of the solvent. The EtOAc extract showed modest antifungal activity against *F. verticillioides*.

Extraction and Isolation of Metabolites

The extract was partitioned between MeCN and hexanes (~8 mL of MeCN and 3 to 4 successive washes of ~8 mL of hexanes to remove the fat). The resulting MeCN fraction (235 mg) was then chromatographed on a silica gel column using a hexanes/EtOAc/MeOH step gradient (hexanes, hexanes:EtOAc, EtOAc, EtOAc:MeOH, and MeOH, ratios used: hexanes, 3:1, 1:1, 1:3, 100% EtOAc, 99:1, 49:1, 19:1, 9:1, and 100% MeOH) to give 15 100-mL fractions. Fraction 5 (17 mg), eluted with 1:1 hexanes:EtOAc, afforded the synthetically known compound dihydrosporothriolide (**82**).[203]

Dihydrosporothriolide (**82**): yellow-orange oil; $[\alpha]^{22}_{D}$ +7 (c 0.90, MeOH); UV (MeOH) λ_{max} (log ε) 201 (2.8), 221 (2.7), 258sh (2.1), 310sh (2.0) nm; ^{1}H and ^{13}C NMR data, see Table 14; HRESITOFMS obsd *m/z* 241.1440 $[M+H]^{+}$, calcd for $C_{13}H_{21}O_4$, 241.1440.

Procedures for the Isolation and Characterization of Pseudocitreoindole (**23**) from MYC-1805 (*Penicillium* sp.)

Fungal Material

The fungal isolate MYC-1805 was isolated by Dr. D. T. Wicklow from an area of red mycelial growth on the undersurface of a dead hardwood branch in a Subalpine dry forest, Pu'u la'au Highway 200 (near milepost 43), Hawaii Co., HI on November 4, 2002. Fermentation conditions are described above and lasted for 30 days at 25 °C. The

resulting culture material was then extracted with EtOAc, affording 1.202 g of crude extract upon evaporation of the solvent. The EtOAc extract showed modest antifungal activity against both *A. flavus* and *F. verticillioides*, as well as significant ability to reduce the growth rate of the fallarmyworm (Table 1).

Isolation and Characterization of Pseudocitreoindole (**23**)

The crude extract (1.202 g), was partitioned between MeCN and hexanes (~8 mL of MeCN and 3 to 4 successive washes of ~8 mL of hexanes to remove lipids). A portion (177 mg) of the resulting MeCN fraction (277 mg) was then chromatographed on a silica gel column using a hexanes/EtOAc/MeOH step gradient (hexanes, hexanes:EtOAc, EtOAc, EtOAc:MeOH, and MeOH, ratios used: hexanes, 3:1, 1:1, 1:3, 100% EtOAc, 99:1, 49:1, 32:1, 19:1, 9:1, and 100% MeOH) to give 15 100-mL fractions. Fraction 9 (26 mg), eluted with 100% EtOAc, was further separated by reversed-phase HPLC (C_{18}: 25-100% MeCN in H_2O over 25 min at 2.0 mL/min with UV detection at 238 nm) to afford pseudocitreoindole (**23**, 3 mg, t_R 22.4 min). Pseudocitreoindole (**23**) was identified by comparison of ^{1}H NMR, ^{13}C NMR, and MS data to reported values.[124]

In order to unambiguously distinguish **23** from the structurally and spectroscopically similar known metabolite citreoindole,[124] acid hydrolysis was performed on a portion (0.5 mg) of **23** and the resulting hydrolyzate was derivatized to afford trifluoroacetyl *n*-butyl esters of any amino acids present. Conditions for the preparation of the trifluoroacetyl *n*-butyl ester derivatives were analogous to those described above. Through GCMS analysis and comparison to phenylalanine (Phe) and β-Phe standards, derivatized in the same manner, it was determined that both Phe and β-Phe were present in the sample of **23**, thus distinguishing it from citreoindole, which contains two units of Phe and no β-Phe unit.

Procedures for the Isolation and Characterization of Stilbene-Derived Phytoalexins Chiricanine A (**84**) and Arahypins 1-5 (**85-89**)

All manipulations of plant material, including the growth of material, inoculation of peanut seeds by the fungal strains, extractions of viable and nonviable seeds, and all purifications were performed by Dr. Victor S. Sobolev at the USDA National Peanut Research Laboratory in Dawson, GA. Structure elucidation and characterization (except for acquisition of APCI-MS^n data) of all purified stilbenoids were performed at the University of Iowa.

Plant Material

The plant material examined in this study came from the 31-1314 peanut runner breeding line, 2007 harvest, from the National Peanut Research Laboratory (Dawson, GA). In order to elicit phytoalexins production from the peanuts, spores of an *Aspergillus caelatus* NRRL 25528 (ex type) fungal culture were used. Peanut seeds were allowed to imbibe distilled water for 16 hr at rt. They were then chopped with a sharp hand cutter into 3-6 mm pieces, washed with distilled water, blotted with a paper towel, air-dried to the condition where sliced peanuts did not leave water spots on filter paper, and placed on stainless steel trays so that the thickness of the layer did not exceed 1 cm. The trays were evenly sprayed with the fungal spores (see above), placed into autoclave bags, and incubated at 30 °C for 96 hr. To obtain nonviable peanut material as a control, a portion of the sliced seeds were placed into distilled boiling water for 90 s, blotted with a paper towel, and air-dried under sterile conditions. Viable peanut material, as a second control, was prepared as previously described;[217] whole axenic peanut seeds were aseptically sliced. Nonviable (inoculated and uninoculated) and viable (inoculated and unincoculated) peanut material was placed into Petri dishes in triplicate (12 dishes total) and incubated in the same autoclave bag at 30 °C for 96 hr. ^{1}H, MS, and UV-guided fractionation and identification of this plant material lead to the isolation of the four new

compounds (**86-89**) and identification of two compounds (**84** and **85**) not reported from peanuts.

Uninoculated peanut material, the control, was prepared as follows: whole kernels from the same batch of seeds that were previously used were surface-sterilized by shaking for 2 min with 2% NaOCl, rinsed three times with sterile distilled H_2O, blotted with a sterile paper towel, and aseptically sliced into 2-3 mm pieces. Control peanut material was placed into Petri dishes in triplicate and incubated in an autoclave bag at 30 °C for 96 hr. A portion of untreated sliced peanuts, a 2nd control, was kept frozen at -28 °C until the analysis.

Extraction and Isolation

For analytical purposes, 6 g of inoculated and incubated peanut seeds was aseptically collected from the trays every 24 hr and extracted with 30 mL of MeOH in a high-speed blender for 1 min. Filtered aliquots of the extracts were then used for direct determination of target constituents by HPLC. A similar extraction procedure was applied to the nonviable and viable control sliced seeds.

For preparative isolation of stilbenoids, 1.2 kg of inoculated and incubated peanut seeds was extracted with 6.0 L of MeOH in a high-speed blender for 1 min (300 mL for each portion of 60 g of seeds). The combined mixture was filtered through filter paper under reduced pressure. The solid residue was resuspended in 1.5 L of MeOH, and the extraction procedure was repeated twice. The combined extracts were filtered through filter paper and defatted three times with *n*-hexane. The MeOH layer was evaporated to dryness. The residue was redissolved in $CHCl_3$ and applied to a chromatographic column (34 mm i.d.) packed with silica gel. The column was subsequently eluted with 0.3 L of $CHCl_3$, 1.2 L of EtOAc, 1.2 of acetone, and 1.2 L of MeOH. Six fractions were collected from the column and analyzed by HPLC. HPLC fractions containing similar stilbenoids of interest were recombined and subjected to further purification on another silica gel column. This column was eluted with 0.3 L of $CHCl_3$, 1.2 L of $CHCl_3$:EtOAc

(1:1), 1.5 L of EtOAc, 0.7 L of acetone, and 0.3 L of MeOH, resulting in nineteen fractions. Combined fractions containing compounds **84** and **86**, **85** and **87**, and **88** were evaporated to dryness on a rotary evaporator, redissolved in MeOH, filtered, and subjected to purification by preparative HPLC using isocratic mobile phase 1 (see above) for compounds **84** and **86**, mobile phase 2 (see above) for compounds **85** and **87**, and mobile phase 3 (see above) for compound **88**, respectively. Combined fractions containing **89** were dried, redissolved in $CHCl_3$, and subjected to purification on a silica gel column using the following solvents: 500 mL $CHCl_3$, 250 + 50 mL hexane/acetone, 250 + 70 mL hexane/acetone, 500 + 200 mL hexane/acetone, 250 + 250 mL hexane/acetone, and 250 + 250 acetone/MeOH. Combined fractions containing purified compound **89** were dried, redissolved in MeOH, and purified on a prep-HPLC column using mobile phase 1 (see above). All pure fractions were transferred to separate vials, dried with a stream of N_2, and then placed into a lyophilizer for 2 hr at rt to remove all traces of solvent.

All manipulations of purified compounds from this source were carried out under minimal lighting conditions to avoid any possible photoisomerization of the stilbenoid olefinic double bond.

Chiricanine A (**84**): slightly yellowish oil; UV (mobile phase 4) λ_{max} (nm) 209, 301sh, 312, 326sh; ^{1}H and ^{13}C NMR data, see Tables 15 and 16; APCI-MS, *m/z* 281 ([M + H]$^+$; rel int 100), 225 (17), APCI-MS^2, *m/z* 281@35: 281 ([M + H]$^+$; rel int 4), 225 (100). The UV, MS, and NMR values agree with published values.[222]

Arahypin-1 (**86**): yellowish oil; UV (mobile phase 4) λ_{max} (nm) 217, 327; ^{1}H and ^{13}C NMR data, see Tables 15 and 16; APCI-MS, *m/z* 281 ([M + H]$^+$; rel int 100), 225 (21); APCI-MS^2, *m/z* 281@35: 281 ([M + H]$^+$; rel int 3), 225 (100); HRESIMS, obsd *m/z* 279, 1387, calcd for $C_{19}H_{20}O_2$ – H, 279.2385.

Arahypin-2 (**85**): yellowish oil; UV (mobile phase 4) λ_{max} (nm) 213, 229sh, 296sh, 306, 217; $[\alpha]^{22}_D$ +8.1 (*c* 0.45; MeOH); ^{1}H and ^{13}C NMR data, see Tables 15 and

16; APCI-MS, *m/z* 331 ($[M + H]^+$; rel int 100), 327 (38), 313 (68), 295 (58), 241 (4); APCI-MS^2, *m/z* 331@35: 313 ($[M + H - H_2O]^+$; rel int 100), 295 (11); UV, MS, and NMR data matched published values.[223]

Arahypin-3 (**87**): yellowish crystals from EtOAc; mp 213-216 °C; UV (mobile phase 4) λ_{max} (nm) 210, 230sh, 298sh, 306, 320, 335sh; $[\alpha]^{22}_D$ +20 (*c* 0.49; MeOH); ^1H and ^{13}C NMR data, see Tables 15 and 16; APCI-MS, *m/z* 331 ($[M + H]^+$; rel int 100), 313 (28), 295 (5), 241 (18); APCI-MS^2, *m/z* 331@35: 313 ($[M + H - H_2O]^+$; rel int 100), 241 (11); HRESIMS, obsd *m/z* 329.1390, calcd for $C_{19}H_{22}O_5 - H$, 329.1389.

Arahypin-4 (**88**): yellowish oil; UV (mobile phase 4) λ_{max} (nm) 206sh, 226sh, 234sh, 301sh, 311, 327sh; $[\alpha]^{22}_D$ +9.5 (*c* 0.25; MeOH); ^1H and ^{13}C NMR data, see Tables 15 and 16; APCI-MS, *m/z* 315 ($[M + H]^+$; rel int 100), 297 (28), 279 (7), 225 (15); APCI-MS^2, *m/z* 315@35: 297 ($[M + H - H_2O]^+$; rel int 100), 225 (7); HRESIMS, obsd *m/z* 313.1439, calcd for $C_{19}H_{22}O_4 - H$, 313.1440.

Arahypin-5 (**89**): off-white oil; UV (mobile phase 4) λ_{max} (nm) 217, 270, 339, 346sh; APCI-MS, *m/z* 295 ($[M + H]^+$; rel int 100); ^1H and ^{13}C NMR data, see Tables 15 and 16; Key HMBC correlations, H-2 → C-3, C-4, C-6, and C-7; H-6 → C-2, C-3, C-4, C-5, and C-7; H-7 → C-1, C-2, and C-6; H-8 → C-1', C-2', and C-6'; H-1" → C-3, C-4, C-5, C-3", C-4", and C-5"; H-2" → C-3, C-4, C-3", C-4", and C-5 "; H_3-4" → C-1", C-2", C-3", and C-4; H_3-5" → C-1", C-2", C-3", and C-4; APCI-MS^2, *m/z* 295@35: 295 ($[M + H]^+$; rel int 100), 267 (36), 253 (16), 201 (47), 175 (4), 159 (5), 107 (5); HRESIMS, obsd *m/z* 293.1175, calcd for $C_{19}H_{18}O_3 - H$, 293.1178.

Procedures for the Isolation and Characterization of Stilbenoid Dimers **90** and **91**

Plant Material

The plant material examined in this study again came from the 31-1314 peanut runner breeding line, 2007 harvest, from the National Peanut Research Laboratory

(Dawson, GA). The process in which phytoalexin production was elicited from the peanut seeds is analogous to process previously described for compounds **84-89** above.

Extraction and Isolation

For preparative isolation of the stilbenoid dimers, 1.1 kg of inoculated and incubated peanut seeds was extracted with 5.4 L of MeOH (300 mL for each portion of 60 g of seeds) in a high-speed blender for 1 min. The combined mixture was filtered through a filter paper under reduced pressure. The solid residue was resuspended in 1.4 L of MeOH, and the extraction procedure was repeated two more times. The combined extract solutions were filtered through a filter paper and defatted three times with 500 mL of n-hexane. The MeOH layer was then evaporated to dryness. The residue was redissolved in $CHCl_3$ and applied to a silica gel column. The column was subsequently eluted with 250 mL of $CHCl_3$ (1 fraction), 1.3 L of EtOAc (3 fractions), 1.1 L of acetone (1 fraction), and 1.0 L of MeOH (1 fraction). Fractions eluted with EtOAc, containing dimers **90** and **91**, were separately combined, dried, and subjected to further purification on a similar silica gel column to the one described above. This 2nd column was eluted with 250 mL of $CHCl_3$, 1.4 L of $CHCl_3$:EtOAc (1:1), 1.2 L of EtOAc, 750 mL of acetone, and 300 mL of MeOH. One of the fractions from this 2nd column, eluted with 1:1 $CHCl_3$:EtOAc contained **90** and was subjected to a 3rd silica gel column like the one above. This 3rd column was eluted portion wise (350 mL each) with hexane:acetone (7:1, 6:1, 5:1, 4:1, 3:1, 2:1; 1:1, and 100% acetone), respectively. Combined fractions eluted from the 3rd column with hexane:acetone 4:1 through 2:1 and containing compound **90** were dried, redissolved in MeOH, filtered, and subjected to prep-HPLC column using isocratic mobile phase 8 (see above). Combined fractions eluted from the 2nd column with acetone and MeOH, containing compound **91**, were dried, redissolved in MeOH, filtered, and subjected to prep-HPLC column using isocratic mobile phase 9 (see above). Fractions from the HPLC and containing pure compounds **90** and **91** were separately

dried under streams of N_2 after transfer to vials. The vials were then placed into a lyophilizer for 2 hr at rt to remove any traces of solvent.

Arahypin-6 (**90**): yellow-brownish glass; UV (CH_3OH) λ_{max} (nm) (log ε) 224 (4.71), 272 (4.41), 339 (4.43); ^1H, ^{13}C, and HMBC NMR data, see Table 17; ESI-MS, obsd *m/z* 607 ($[M + H]^+$; rel int 100); HREIMS, *m/z* 606.2615 $[M]^+\cdot$; calcd for $C_{38}H_{38}O_7$, 606.2616.

Arahypin-7 (**91**): yellow-brownish glass; UV (CH_3OH) λ_{max} (nm) (log ε) 224 (4.71), 270 (4.47), 310sh (4.17), 347 (4.42); ^1H NMR (acetone-d_6, 400 MHz) δ 6.27 (s, H_2-8/12), 5.43 (d, J = 4.3 Hz, H-4a), 4.37 (d, J = 4.3 Hz, H-7a), 2.46 (m, H-15'), 2.39 (m, H-15), 1.09 (d, J = 6.7 Hz, H_3-17), 1.08 (d, J = 6.7 Hz, H_3-16), 1.047 (d, J = 6.7 Hz, H_3-16'), 1.046 (d, J = 6.7 Hz, H_3-17'). The remaining signals in the ^1H NMR spectrum were severely overlapped in the region from δ 6.61 to 6.84 and could not be distinguished for accurate assignments. However, integration of this region indicated that the appropriate number of protons in present. ESIMS, obsd. *m/z* 623 ($[M + H]^+$; rel int 100); HRESIMS, obsd. m/z 623.2641 $[M + H]^+$; calcd for $C_{38}H_{38}O_8$ + H, 623.2644.

Procedures for the Isolation and Characterization of Pterocarpenes **92** and **93**

Plant Material

The plant material examined in this study came from the 31-1314 peanut runner breeding line, 2007 harvest, from the National Peanut Research Laboratory (Dawson, GA). The process in which phytoalexin production was elicited from the peanut seeds is analogous to process previously described for compounds **84**-**89** above.

Extraction and Isolation

Inoculated and incubated peanut seeds (0.8 kg) were extracted with 4 L of MeOH (250 mL for each 50 g portion of seeds) in a high-speed blender for 1 min. The combined mixture was filtered through filter paper under reduced pressure. The solid

residue was resuspended in MeOH (1.5 L), and the extraction procedure was repeated twice. The combined extract solutions were filtered through filter paper and defatted twice with *n*-hexane (400 mL). The MeOH was then evaporated to dryness. The residue was resuspended in $CHCl_3$ and applied to a chromatographic column (34 mm i.d.) and packed with silica gel. The column was subsequently eluted with $CHCl_3$ (200 mL), $CHCl_3$:EtOAc (500 mL) (1:1), EtOAc (1.0 mL), EtOAc:acetone (600 mL) (1:1), acetone (1.4 L), and MeOH (800 mL). Fractions eluted with EtOAc and containing **92** and **93** were combined, evaporated to dryness with a rotary evaporator, and subjected to further purification on a second silica gel column. This column was subsequently eluted with $CHCl_3$ (100 mL), $CHCl_3$:EtOAc (3:1, 2.5:1, 2:1, respectively), EtOAc (300 mL), EtOAc:acetone (1:1), acetone (100 mL), and MeOH (300 mL). Three fractions from this second column with $CHCl_3$/EtOAc and EtOAc, containing **92** and **93**, were evaporated to dryness on a rotary evaporator, redissolved in MeOH, filtered, and subjected to a final purification on a preparative HPLC column. Compound **92** was isolated using mobile phase 12 (see above) and **93** was isolated using mobile phase 13 (see above).

Fractions obtained from HPLC and containing chromatographically-pure **92** were evaporated with a rotary evaporator to near complete dryness. The remaining aqueous mixture containing **92** was extracted four times with EtOAc (H_2O/EtOAc, 3:2). The combined EtOAc layers were evaporated nearly to dryness. The residue was transferred into a 16 mL vial with MeOH and dried under a stream of N_2. The residues were redissolved in acetone, filtered, transferred into a 4 mL vial, and once again dried under a stream of N_2. The vial was then placed into a lyophilizer for 2 hr at rt to remove traces of solvent, affording **92** (5 mg) as a yellowish glass.

HPLC fractions containing chromatographically-pure **93** were concentrated with a rotary evaporator to near dryness. Compound **93** gradually emerged as an off-white solid precipitate. The solution was placed into a refrigerator at 4 °C for 6 hr, and then the resulting precipitate was collected, resuspended in H_2O, and transferred into a 16 mL

vial. The vial was centrifuged at 4000 rpm for 10 min, the supernatant was decanted, and the precipitate was collected into a small vial, which was placed in a freezer for 2 hr. The frozen suspension of **93** in water was lyophilized overnight to obtain a pure sample of **93** (10 mg) as a fluffy off-white solid.

Aracarpene-1 (**92**): yellowish glass; UV (mobile phase 12): λ_{max} (nm) 217, 243sh, 314, 327, 342sh, 380, 670; UV (MeOH) λ_{max} (log ε) 227 (4.29), 250sh (4.10), 319sh (4.23), 330 (4.27), 345sh (4.07); ^{1}H, ^{13}C, and HMBC NMR data, see Table 18; Positive ESIMS *m/z* 302 (rel int 14%), 301 ($[M + H]^+$; 80), 300 (100), 299 (29), 285 (15). Positive ESIMS^2 *m/z* 301@38: 301 ($[M + H]^+$; rel int 17%), 286 (23), 285 (100), 283 (25); Negative ESIMS^2 *m/z* 299@35: 299 ($[M - H]^-$; rel int 15%), 284 (100); Positive ESIMS^3 m/z 301@40 → 285@40: 285 (rel int 35), 266 (16), 257 (22), 240 (18), 239 (100); Negative ESIMS^3 *m/z* 299@40 → 284@40: 284 (rel int 100), 256 (96), 228 (37); HRESIMS $[M]^+\cdot$ at *m/z* 300.0629, calcd for $C_{16}H_{12}O_6$, 300.0633.

Aracarpene-2 (**93**): off-white powder; UV (mobile phase 13): λ_{max} (nm) 314, 326, 342sh, 402, 639; UV (MeOH) λ_{max} (log ε) 223 (4.40), 313 (4.26), 329 (4.35), 346 (4.24); ^{1}H, ^{13}C, and HMBC NMR data, see Table 18; Positive ESIMS *m/z* 302 (rel int 11%), 301 ($[M + H]^+$; 82), 300 (100), 299 (41), 97 (26); Positive ESIMS^2 *m/z* 301@40: 301 ($[M + H]^+$; rel int 54%), 300 (21), 299 (100), 286 (10), 285 (41), 284 (12), 283 (41), 282 (23), 272 (9), 255 (9), 254 (12), 245 (8); Negative ESIMS^2 m/z 299@40: 299 ($[M – H]^-$; rel int 26%), 284 (100), 271 (48), 256 (7), 243 (5); Positive ESIMS^3 m/z 301@40 → 285@40: 285 (rel int 26), 255 (20), 239 (100); Negative ESIMS^3 m/z 299@40 → 284@40: 284 (rel int 84), 256 (100), 240 (10), 228 (62), 227 (28); HRESIMS $[M]^+\cdot$ at *m/z* 300.0636, calcd for $C_{16}H_{12}O_6$, 300.0633.

APPENDIX

SELECTED NMR SPECTRA

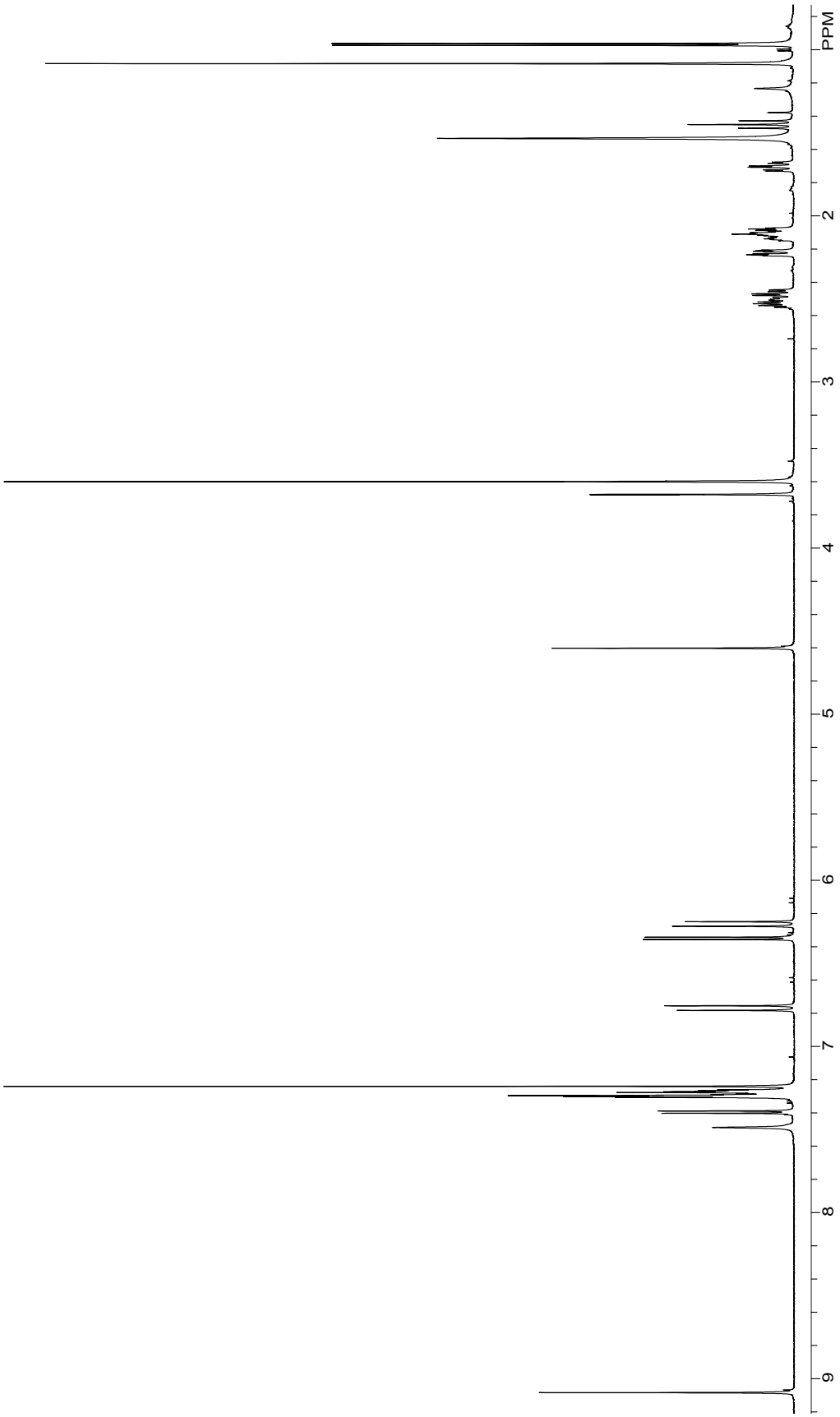

Figure A1. ^{1}H NMR Spectrum of Aflaquinolone A (**43**; 600 MHz, $CDCl_3$)

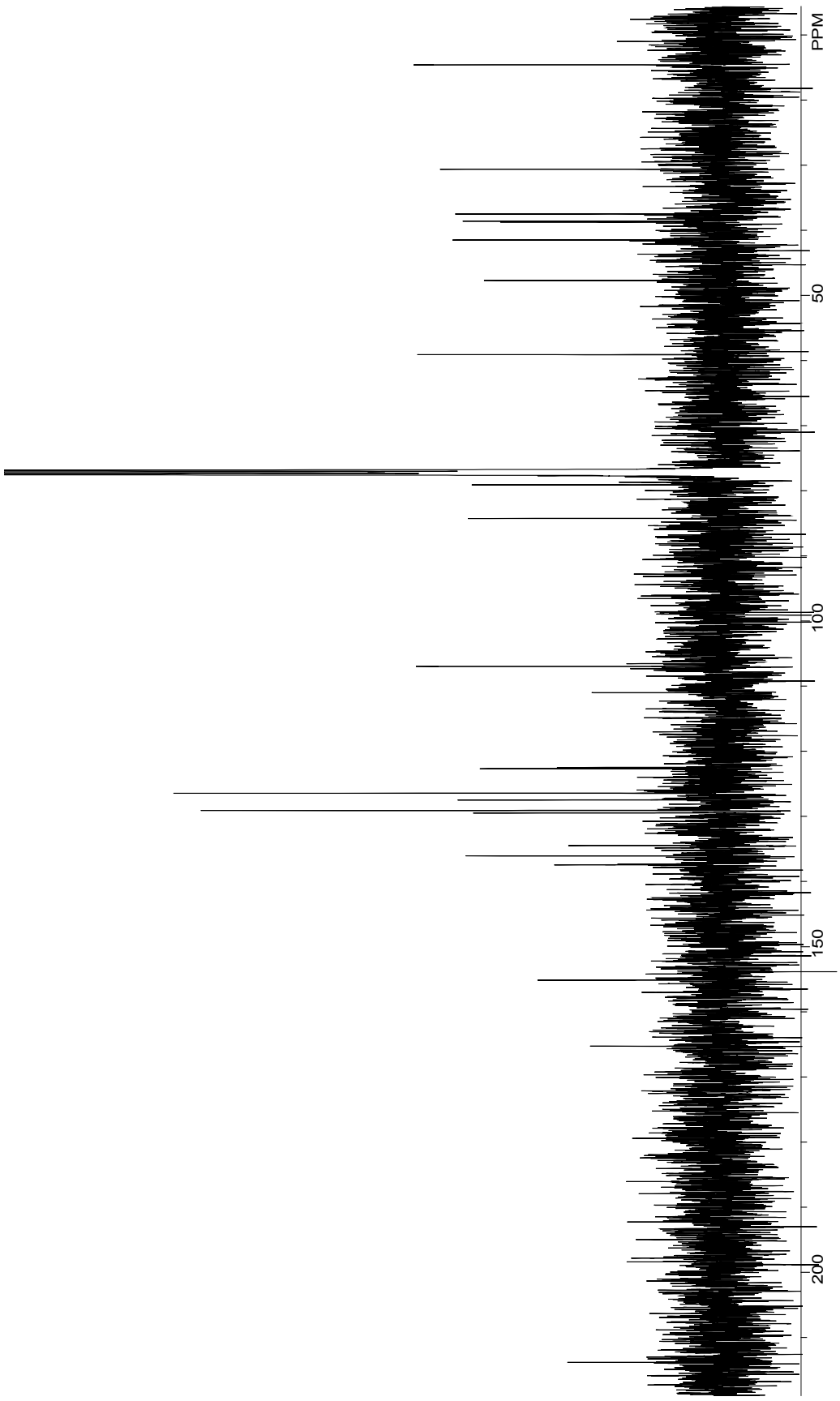

Figure A2. ^{13}C NMR Spectrum of Aflaquinolone A (**43**; 100 MHz, $CDCl_3$)

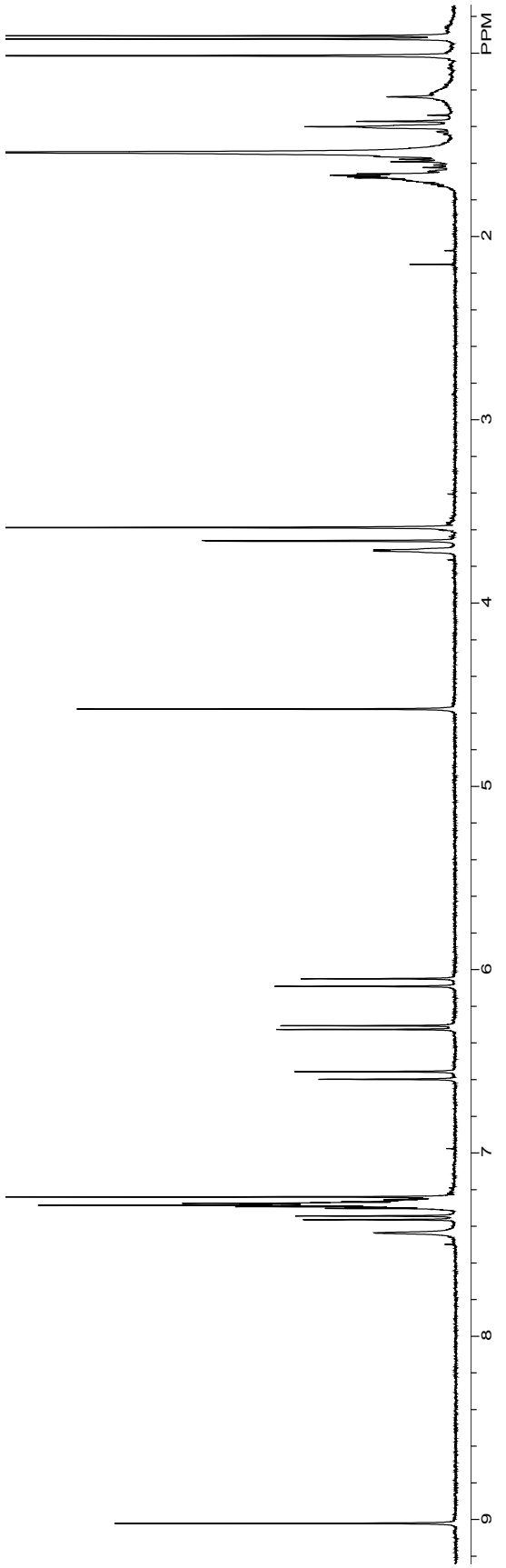

Figure A3. ^{1}H NMR Spectrum of Aflaquinolone B (**44**; 400 MHz, $CDCl_3$)

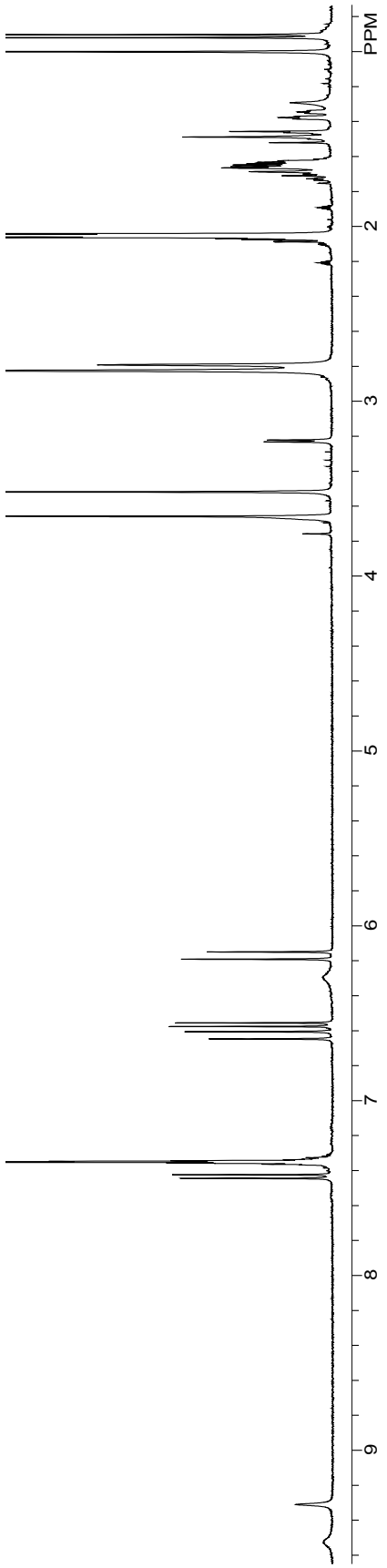

Figure A4. ^{1}H NMR Spectrum of Aflaquinolone B (**44**; 400 MHz, Acetone-d_6)

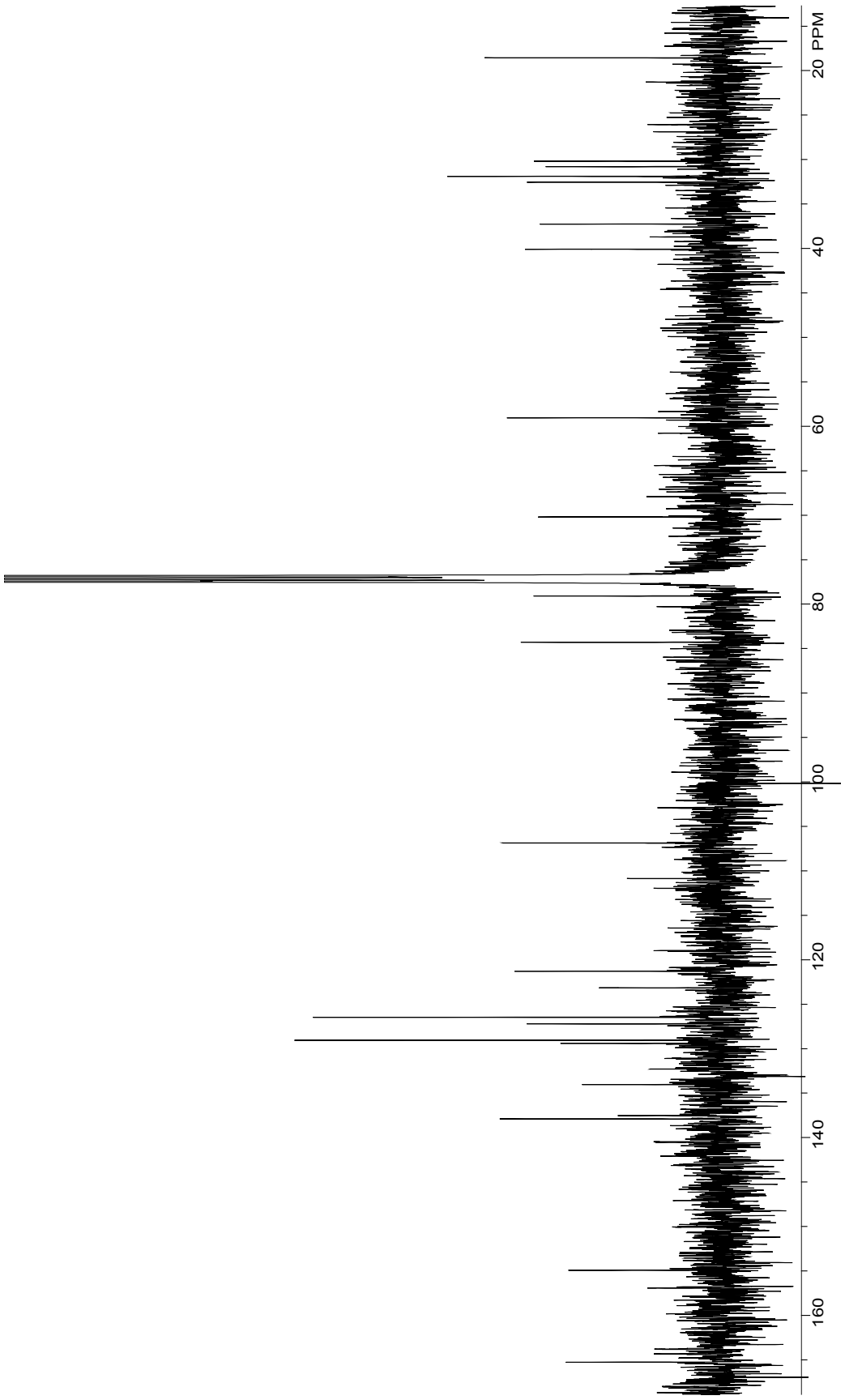

Figure A5. ^{13}C NMR Spectrum of Aflaquinolone B (**44**; 100 MHz, $CDCl_3$)

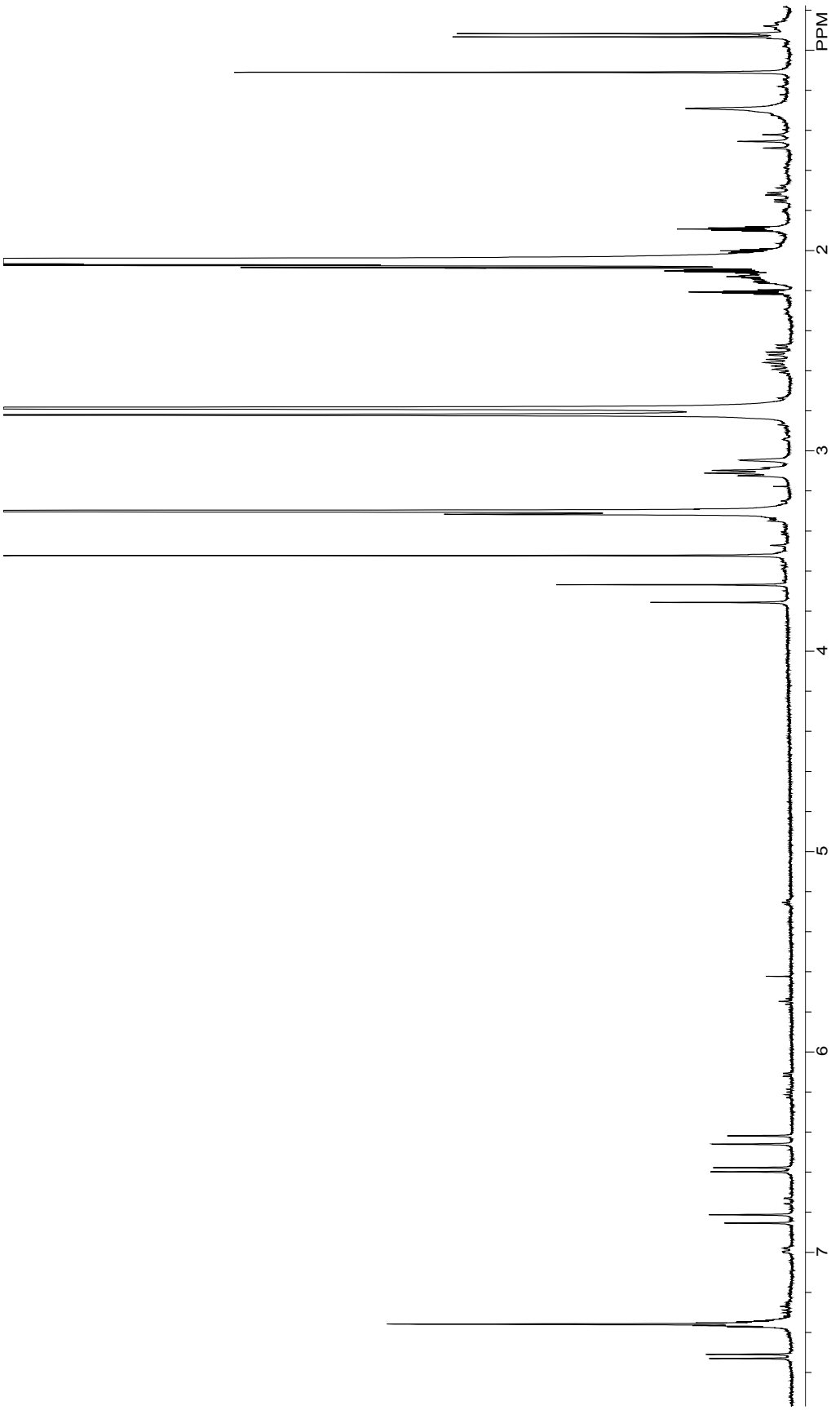

Figure A6. ^{1}H NMR Spectrum of Aflaquinolone C (**47**; 400 MHz, Acetone-d_6)

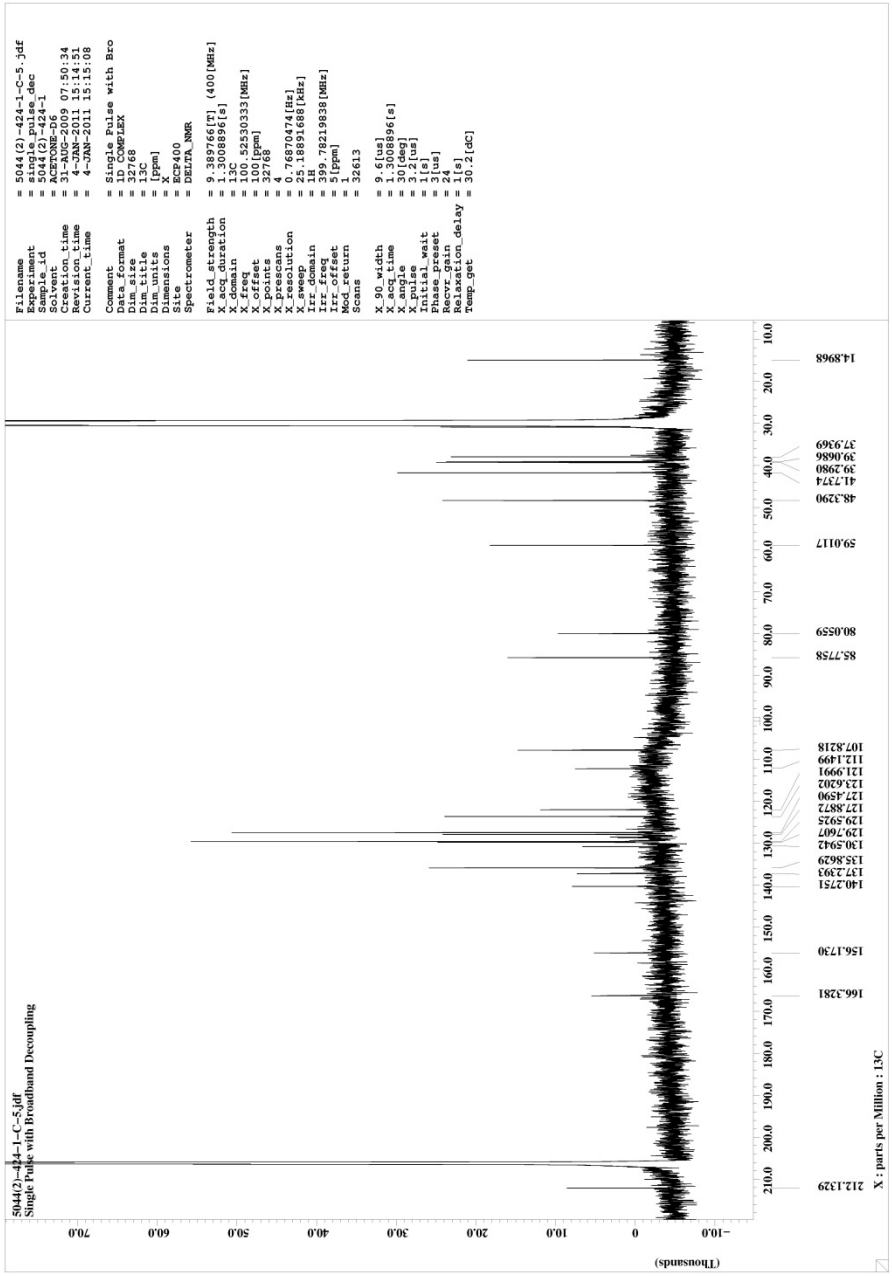

Figure A7. ^{13}C NMR Spectrum of Aflaquinolone C (**47**; 100 MHz, Acetone-d_6)

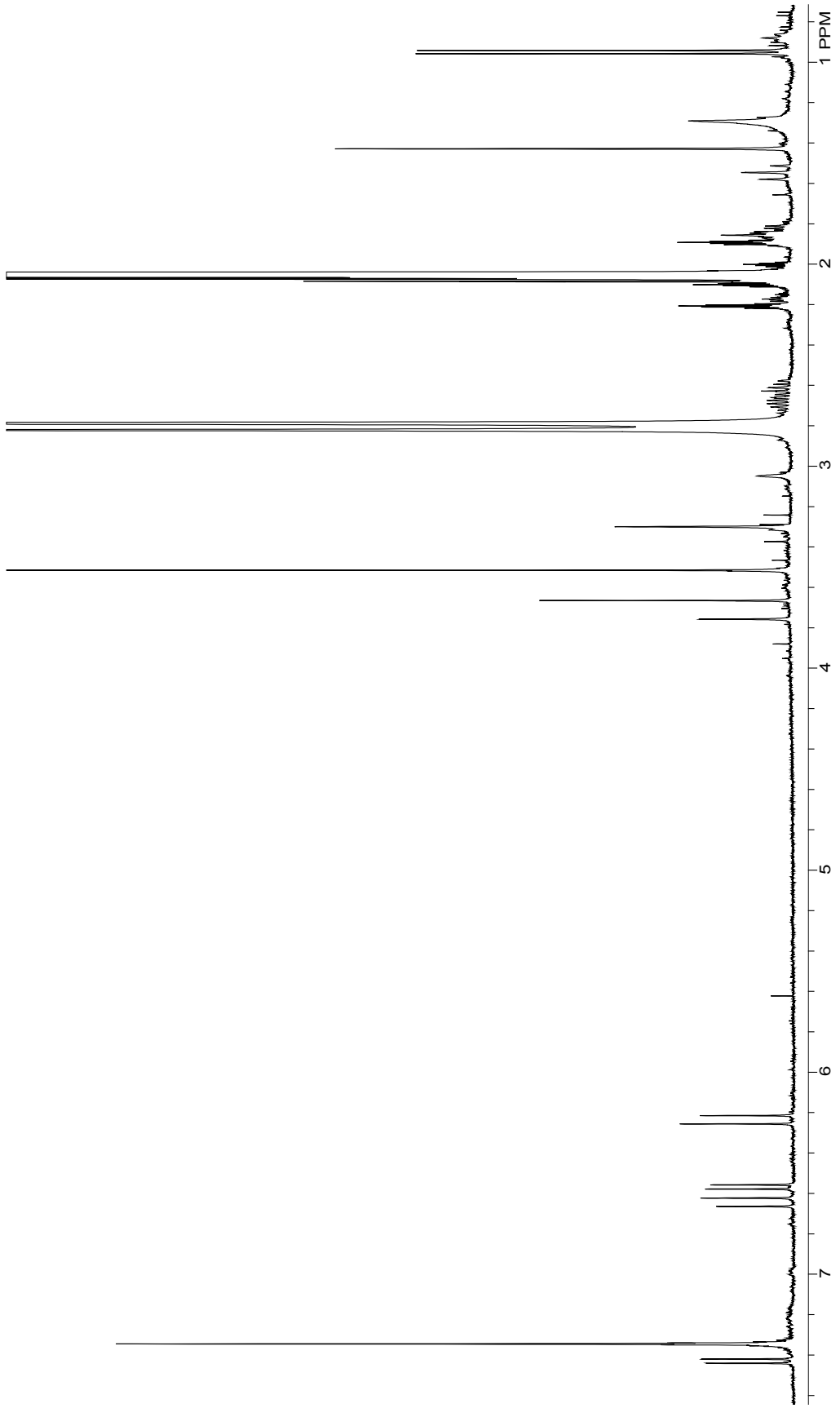

Figure A8. ^{1}H NMR Spectrum of Aflaquinolone D (**48**; 400 MHz, Acetone-d_6)

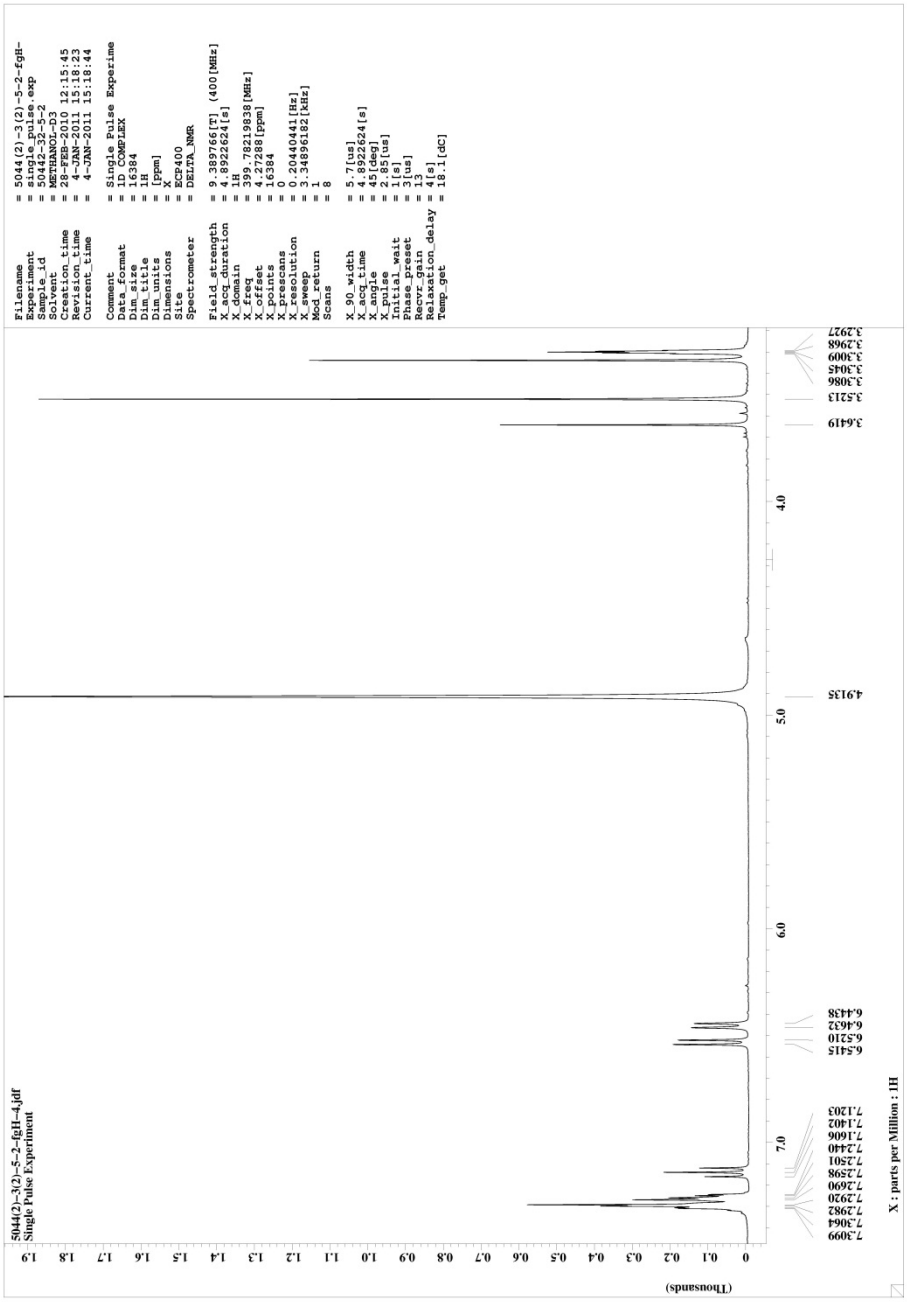

Figure A9. ^{1}H NMR Spectrum of Aflaquinolone E (**49**; 400 MHz, CD_3OD)

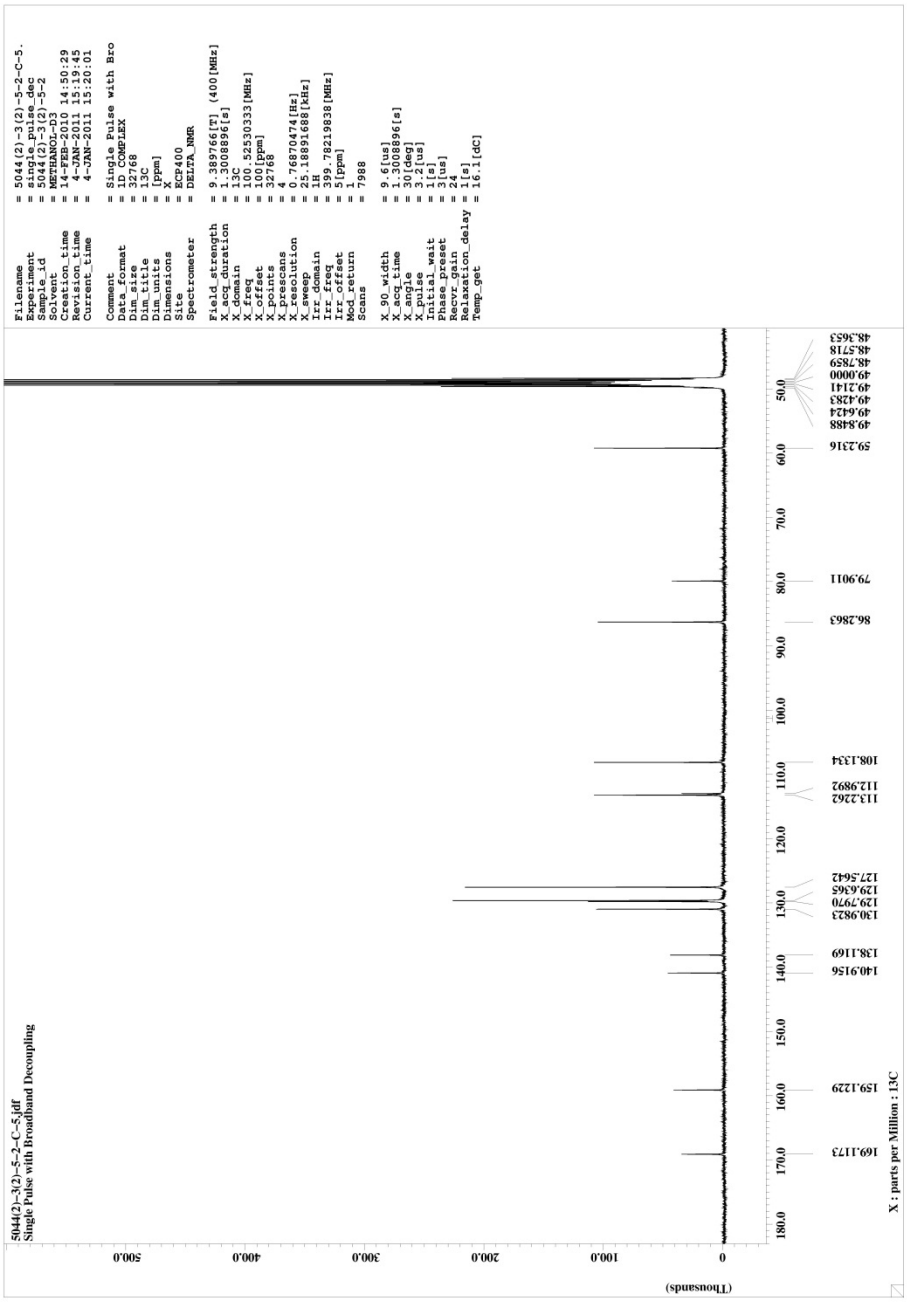

Figure A10. ^{13}C NMR Spectrum of Aflaquinolone E (**49**; 100 MHz, CD_3OD)

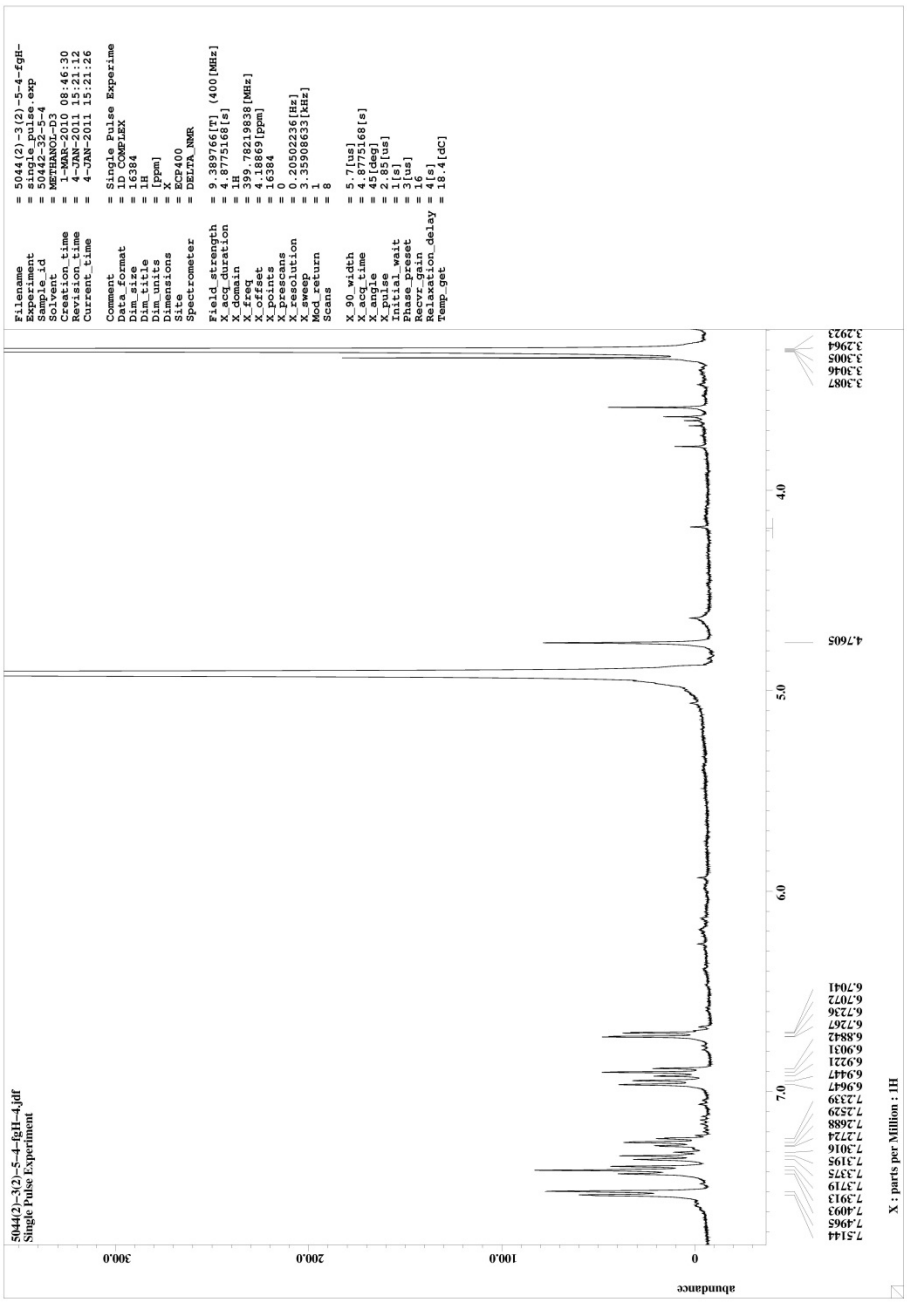

Figure A11. ^{1}H NMR Spectrum of Aflaquinolone F (**50**; 400 MHz, CD_3OD)

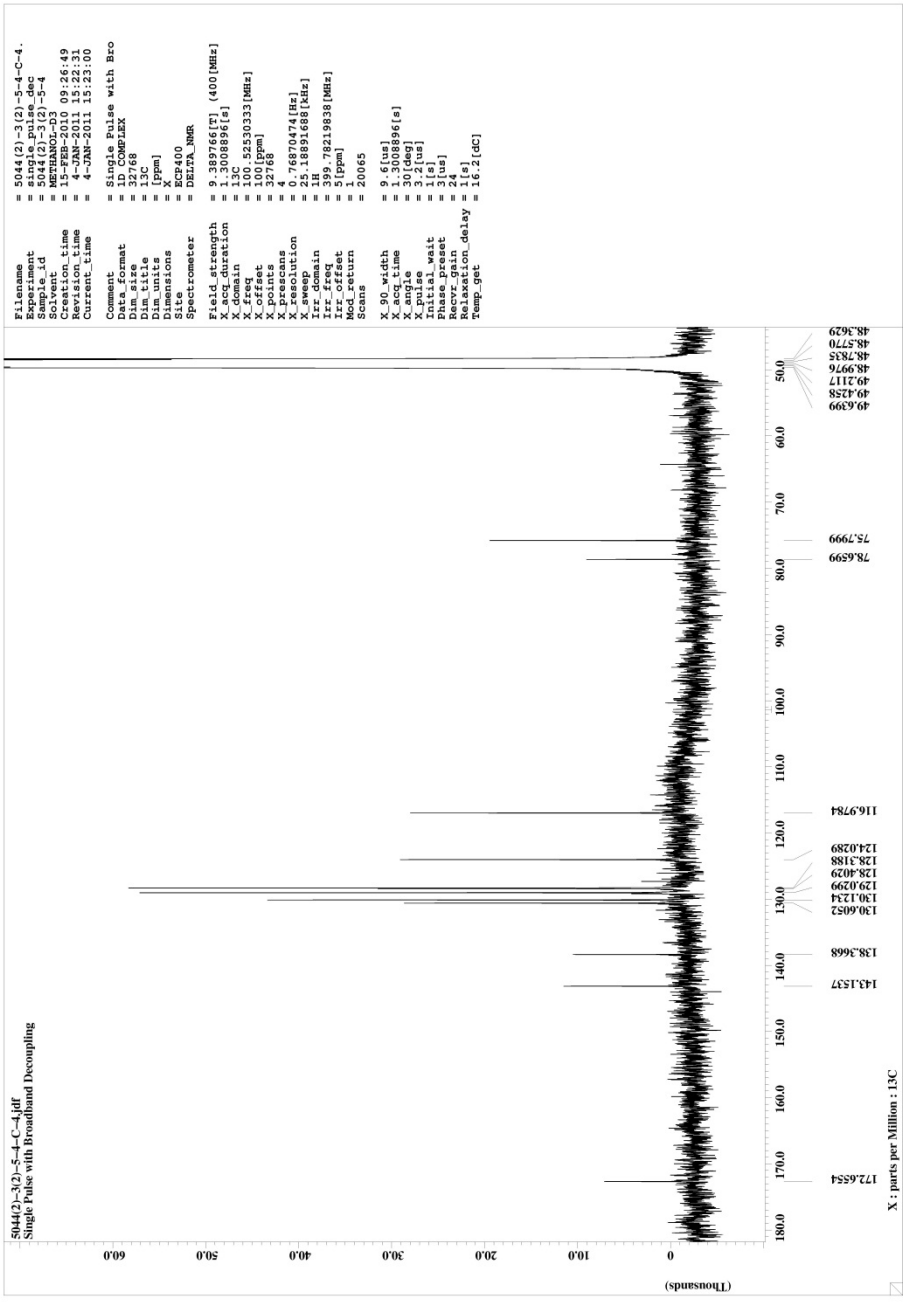

Figure A12. ^{13}C NMR Spectrum of Aflaquinolone F (**50**; 100 MHz, CD_3OD)

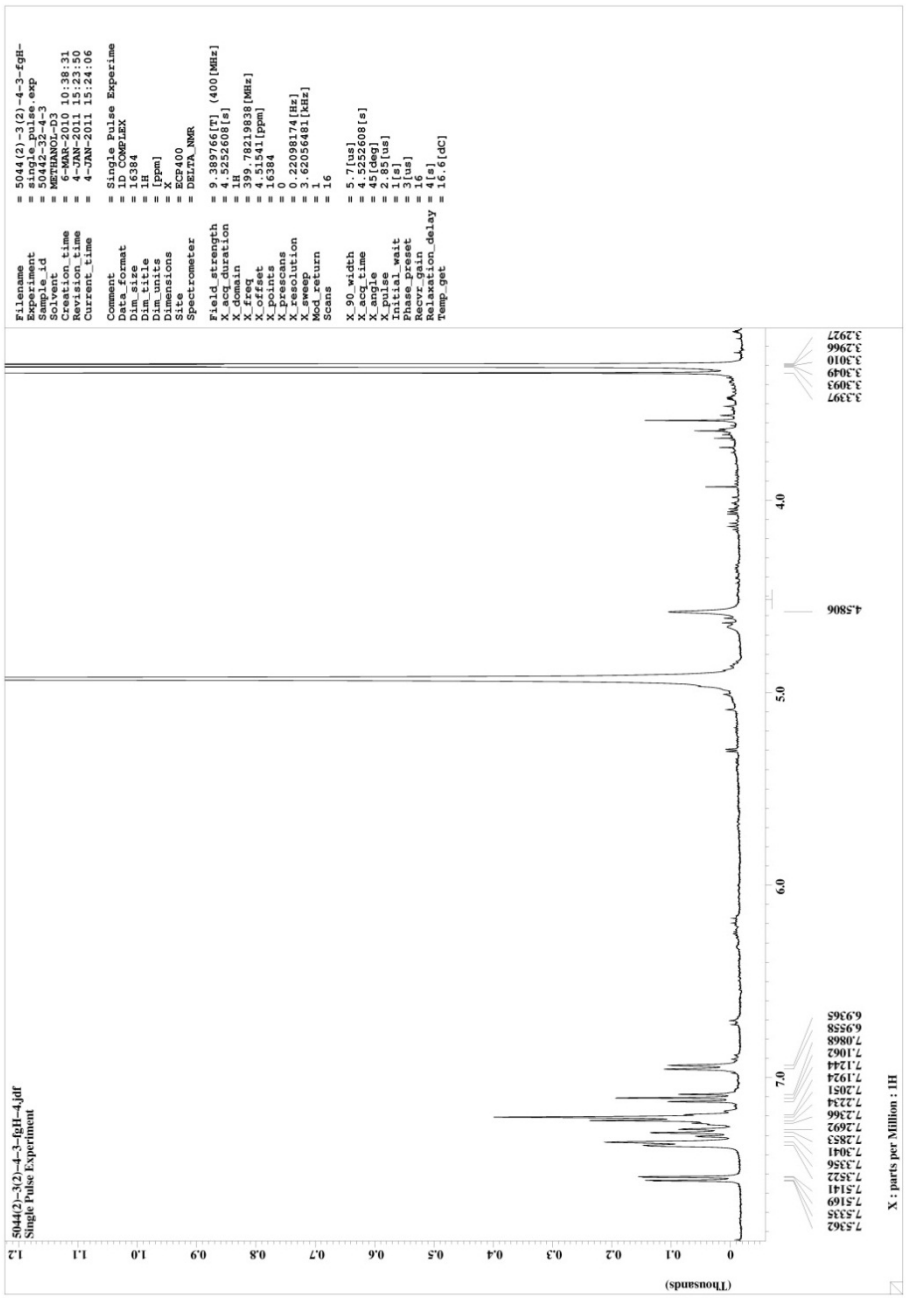

Figure A13. ^{1}H NMR Spectrum of Aflaquinolone G (**51**; 400 MHz, CD_3OD)

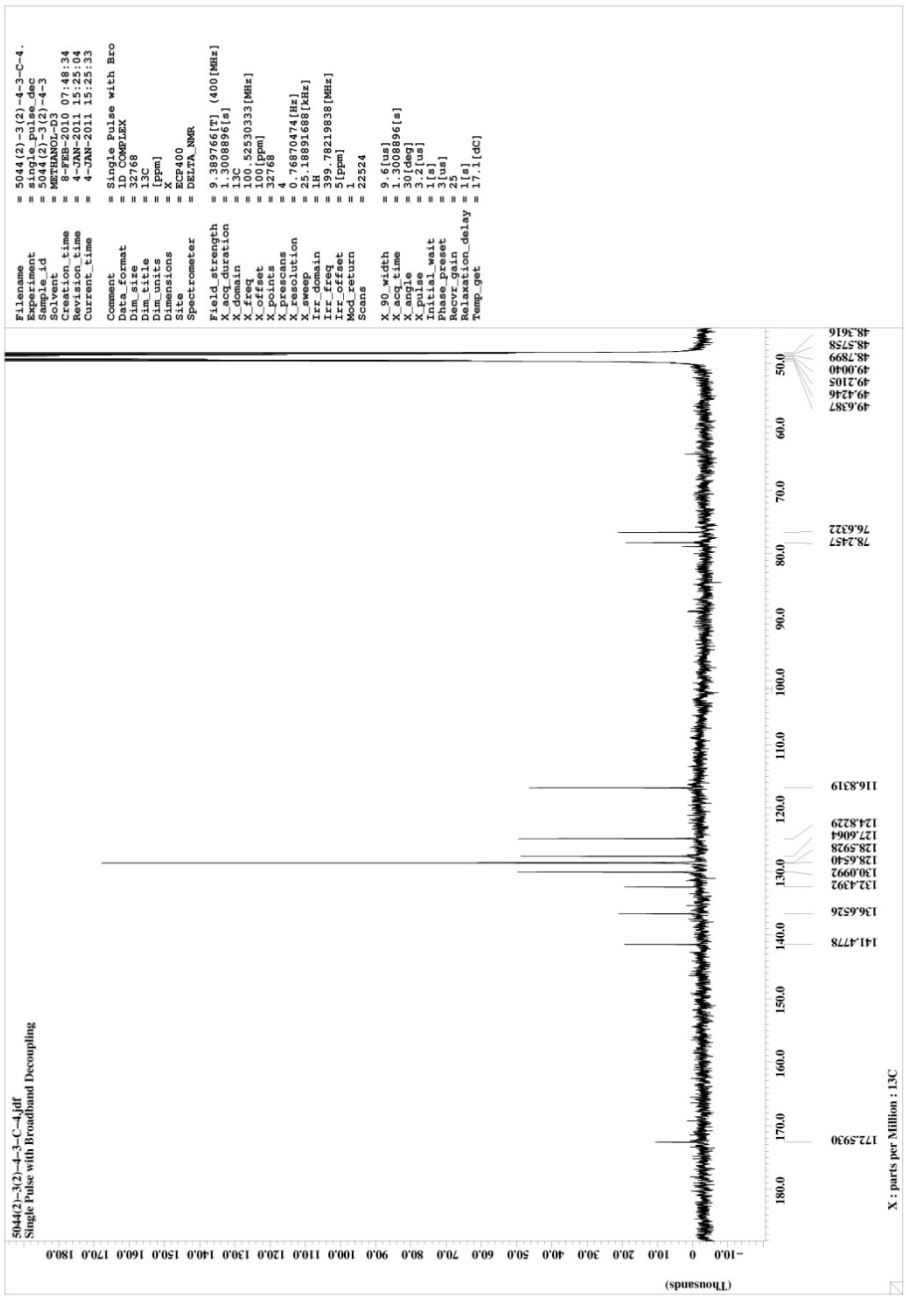

Figure A14. ^{13}C NMR Spectrum of Aflaquinolone G (**51**; 100 MHz, CD_3OD)

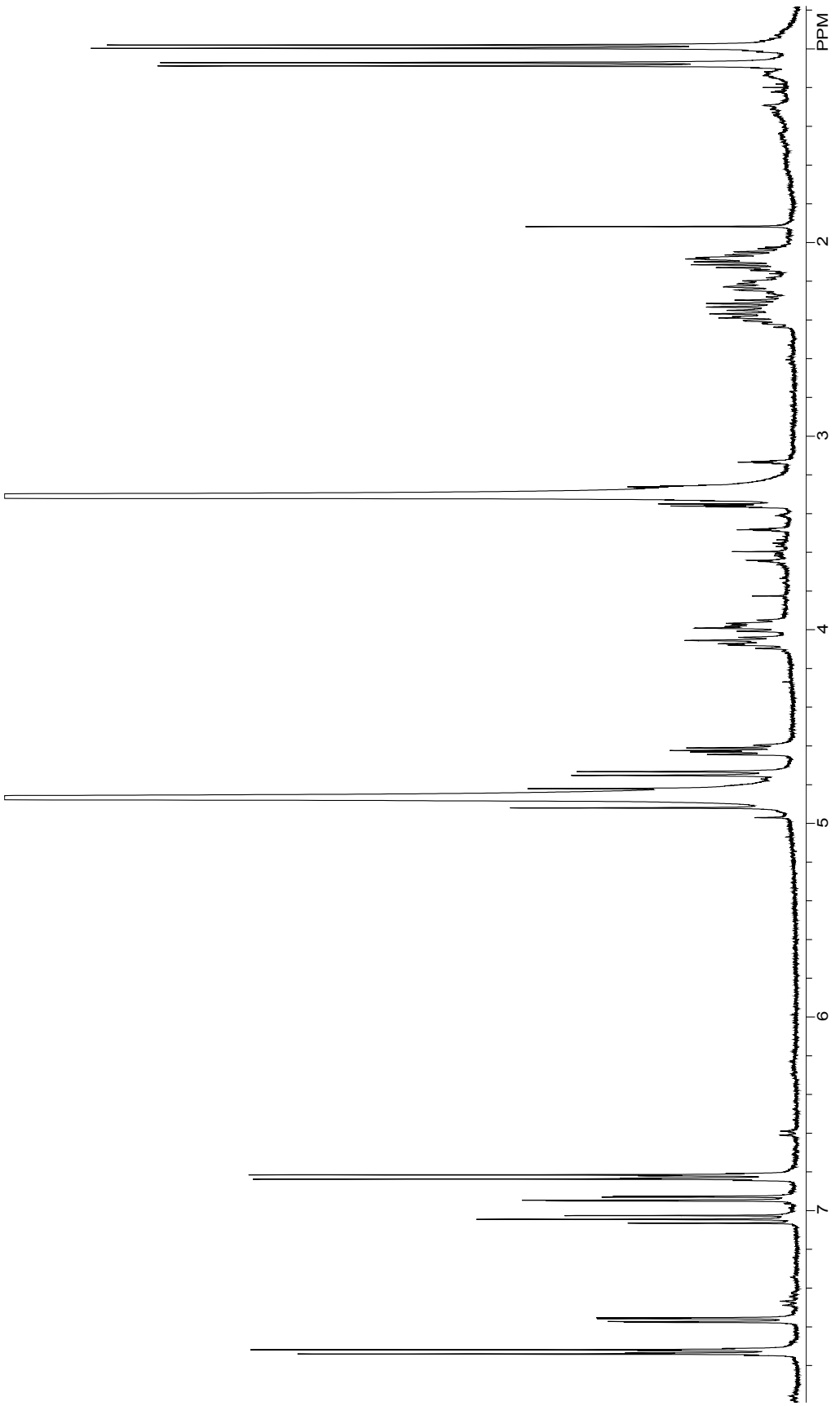

Figure A15. ^{1}H NMR Spectrum of Asperlarin A (**52**; 400 MHz, CD_3OD)

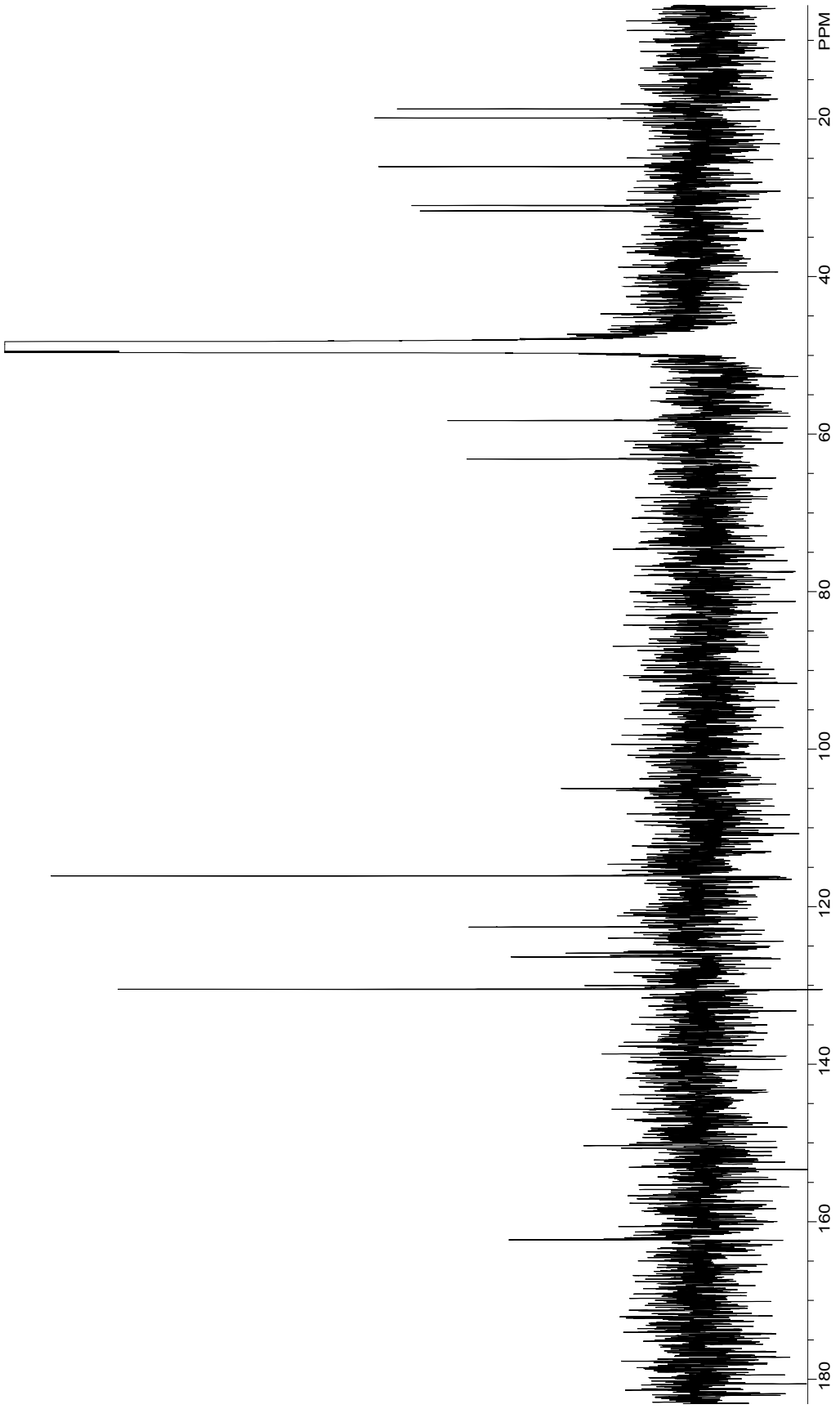

Figure A16. ^{13}C NMR Spectrum of Asperlarin A (**52**; 100 MHz, CD_3OD)

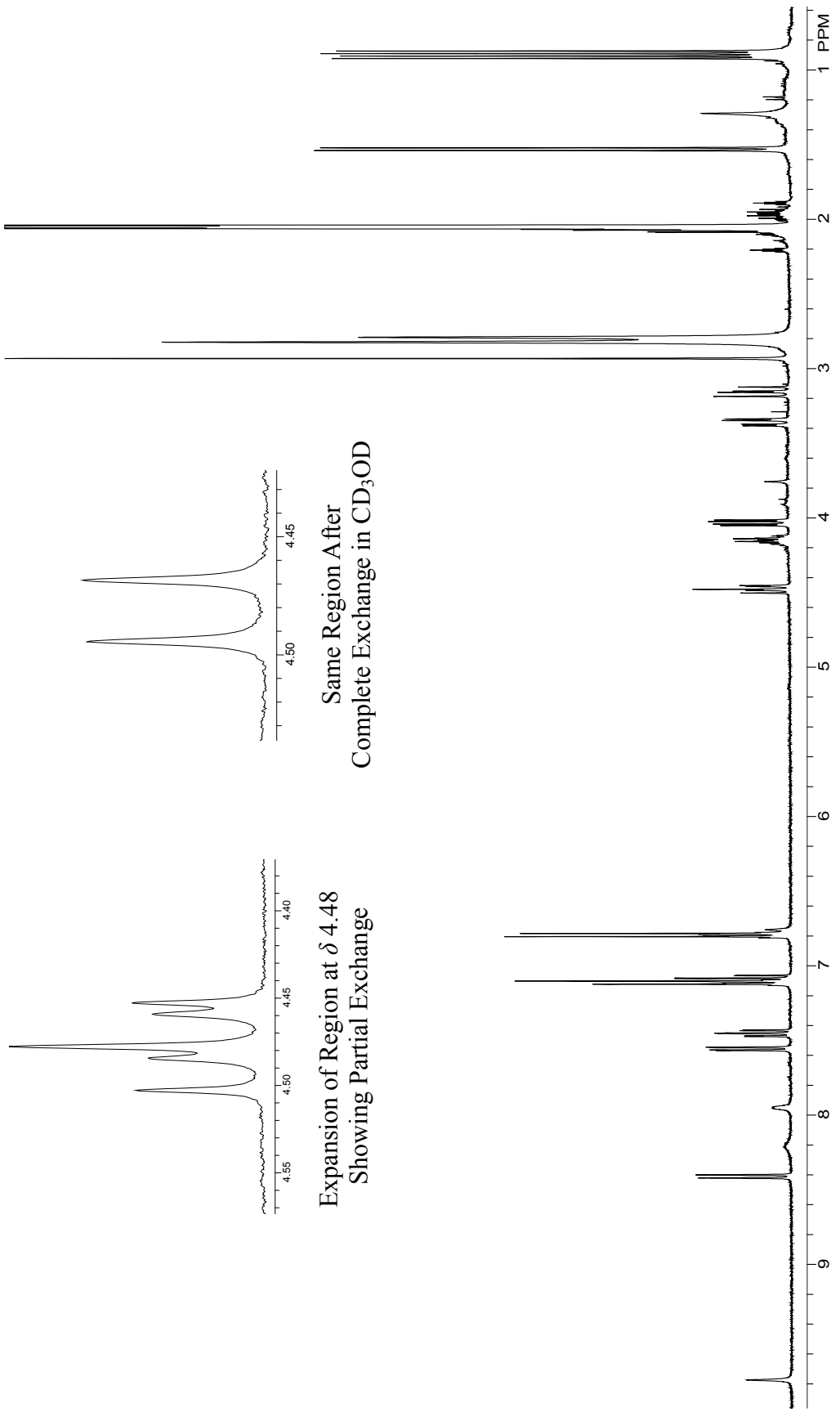

Figure A17. ^{1}H NMR Spectrum of Flavipeptide A (**53**; 400 MHz, Acetone-d_6)

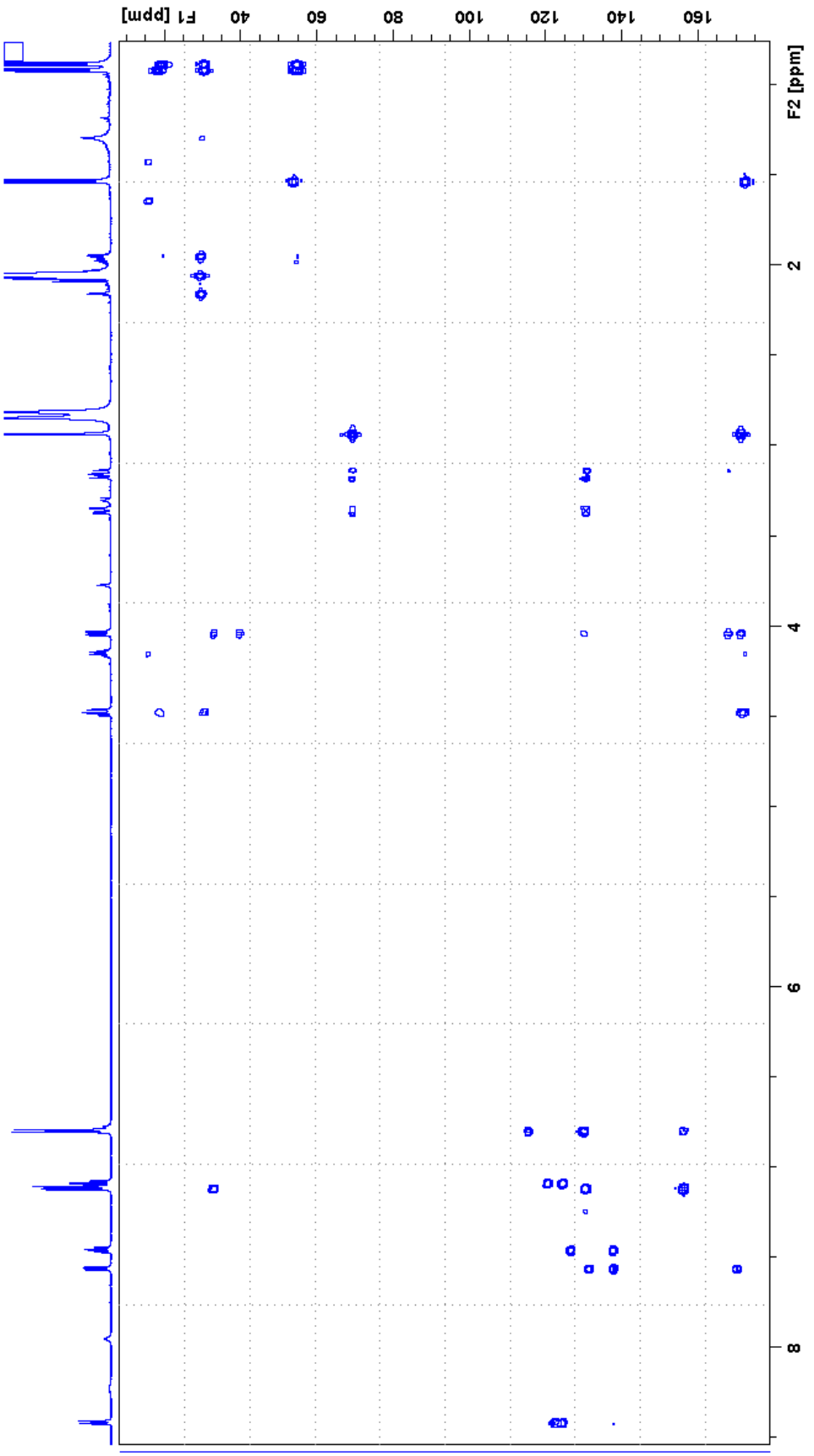

Figure A18. HMBC Spectrum of Flavipeptide A (**53**; 600 MHz, Acetone-d_6)

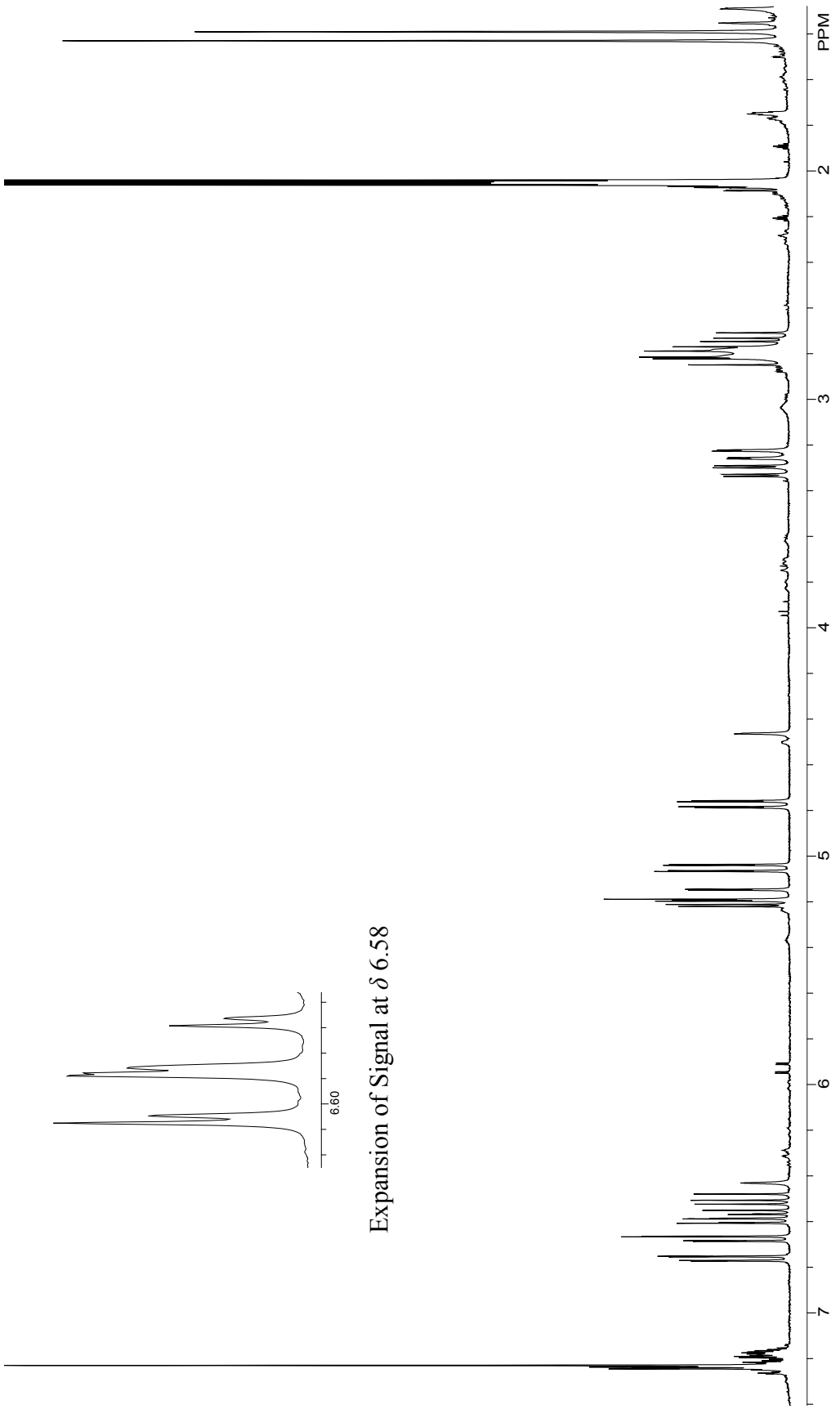

Figure A19. ^{1}H NMR Spectrum of PF1233B (**54**; 400 MHz, Acetone-d_6)

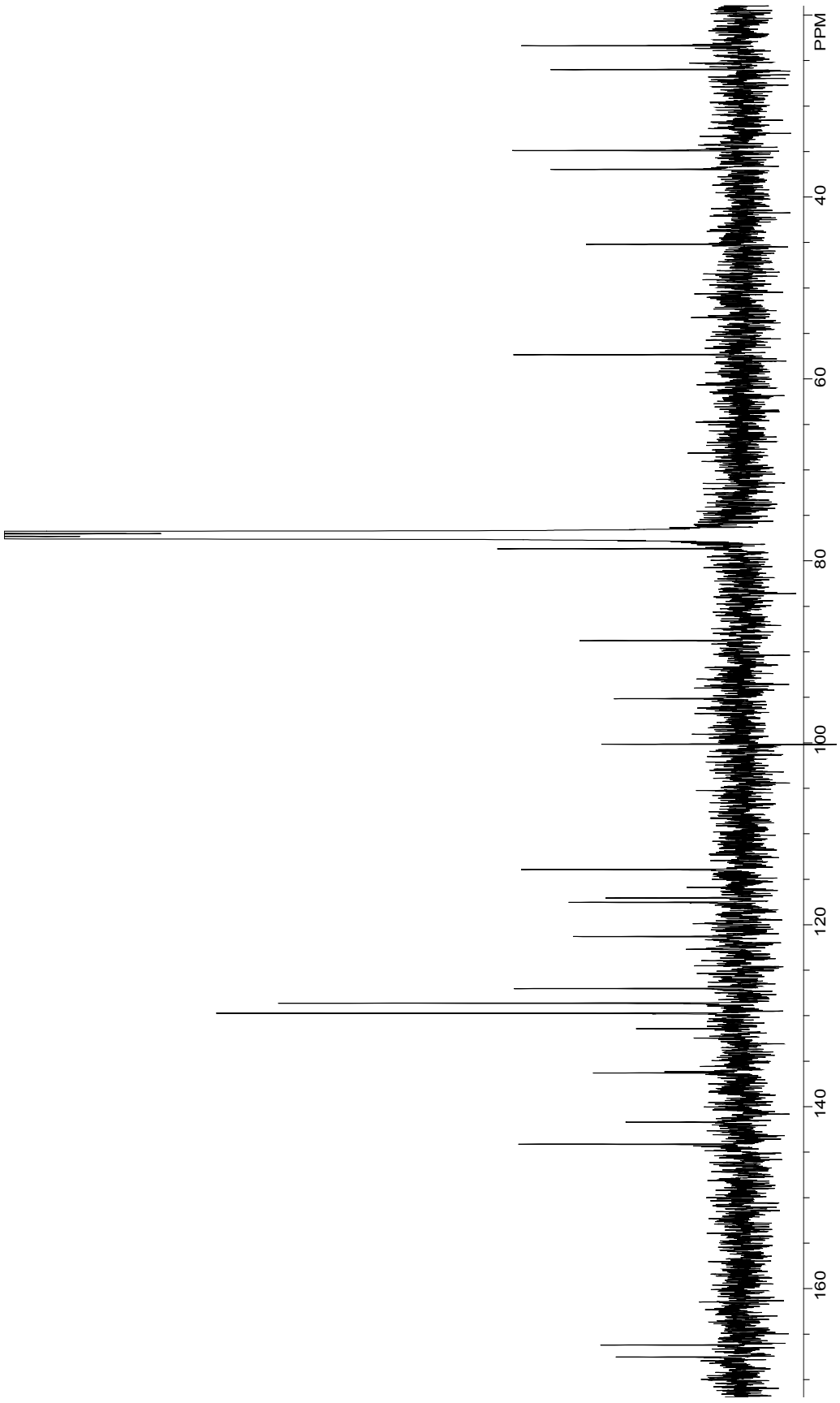

Figure A20. ^{13}C NMR Spectrum of PF1233B (**54**; 100 MHz, $CDCl_3$)

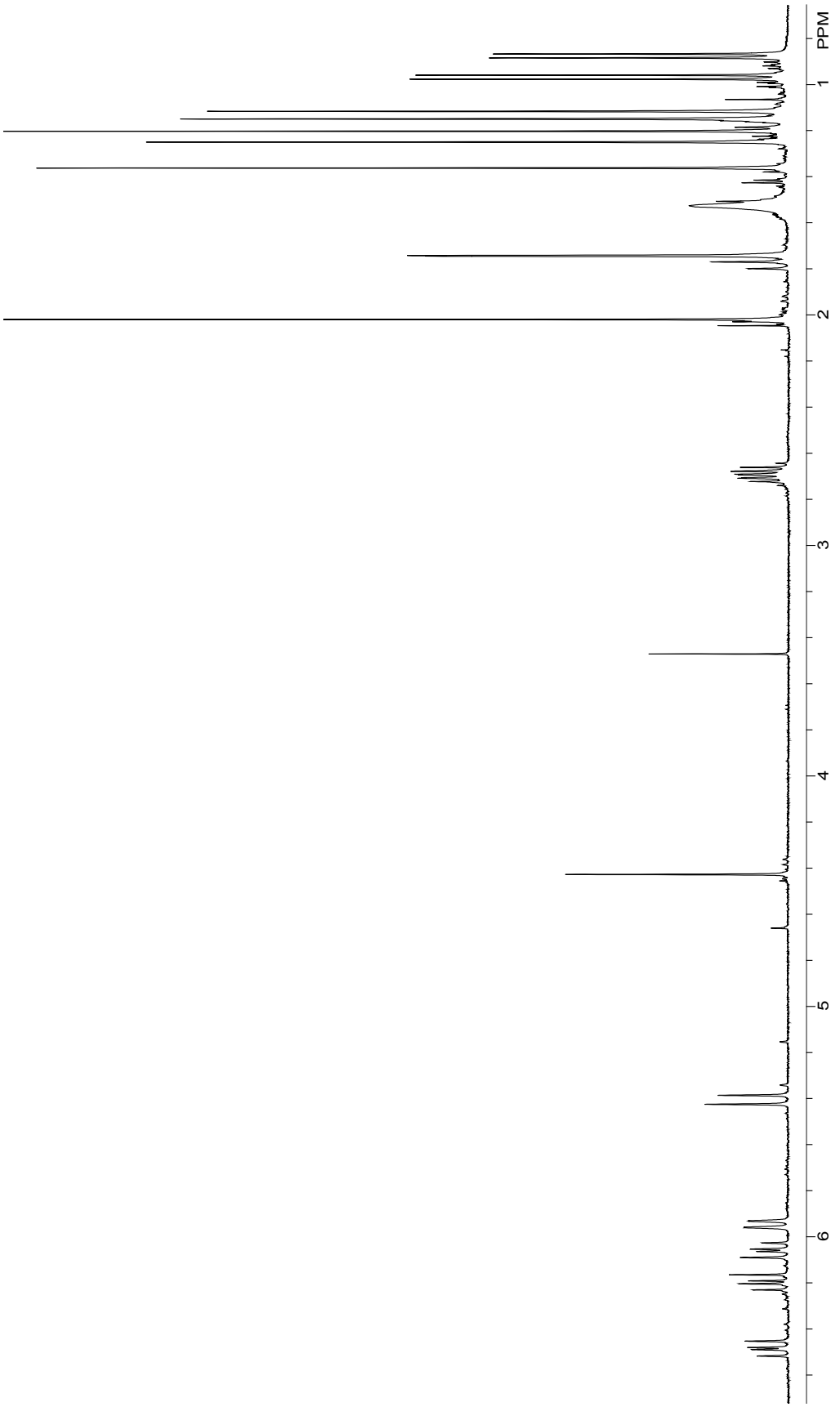

Figure A21. ^{1}H NMR Spectrum of Emeridin A (**65**, 400 MHz, $CDCl_3$)

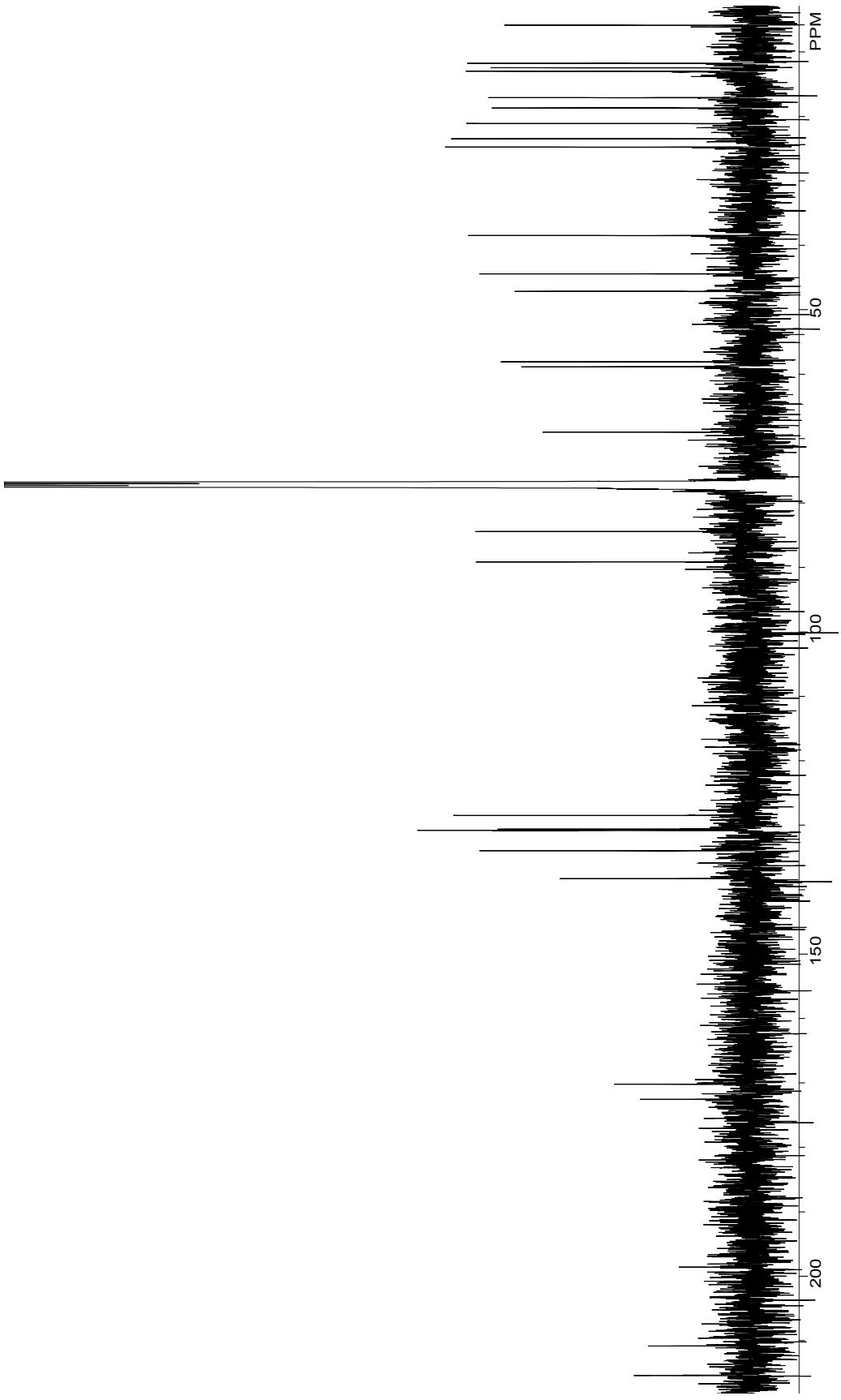

Figure A22. ^{13}C NMR Spectrum of Emeridin A (**65**; 100 MHz, $CDCl_3$)

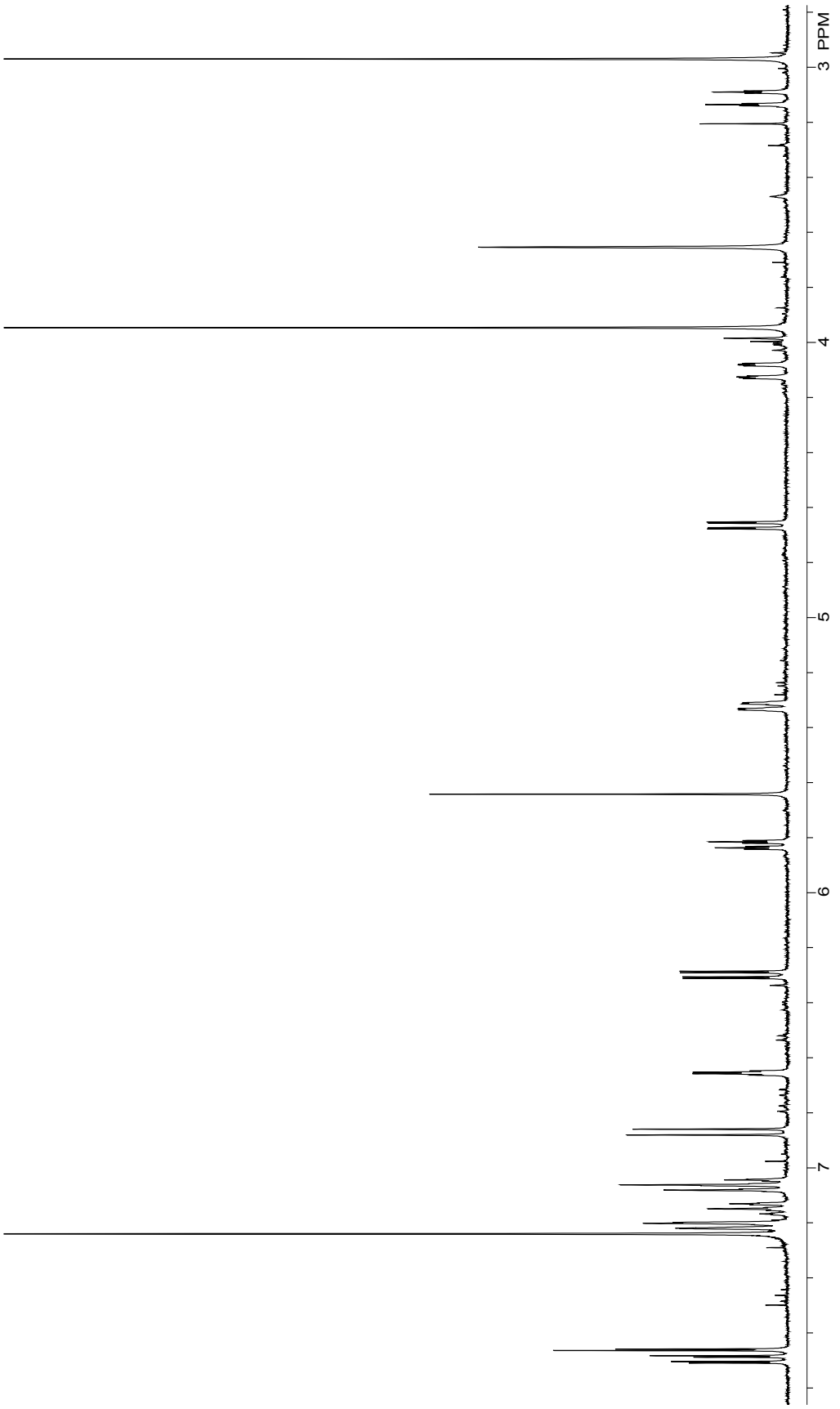

Figure A23. ^{1}H NMR Spectrum of O-Methylsecoemestrin C_1 (**66**; 400 MHz, $CDCl_3$)

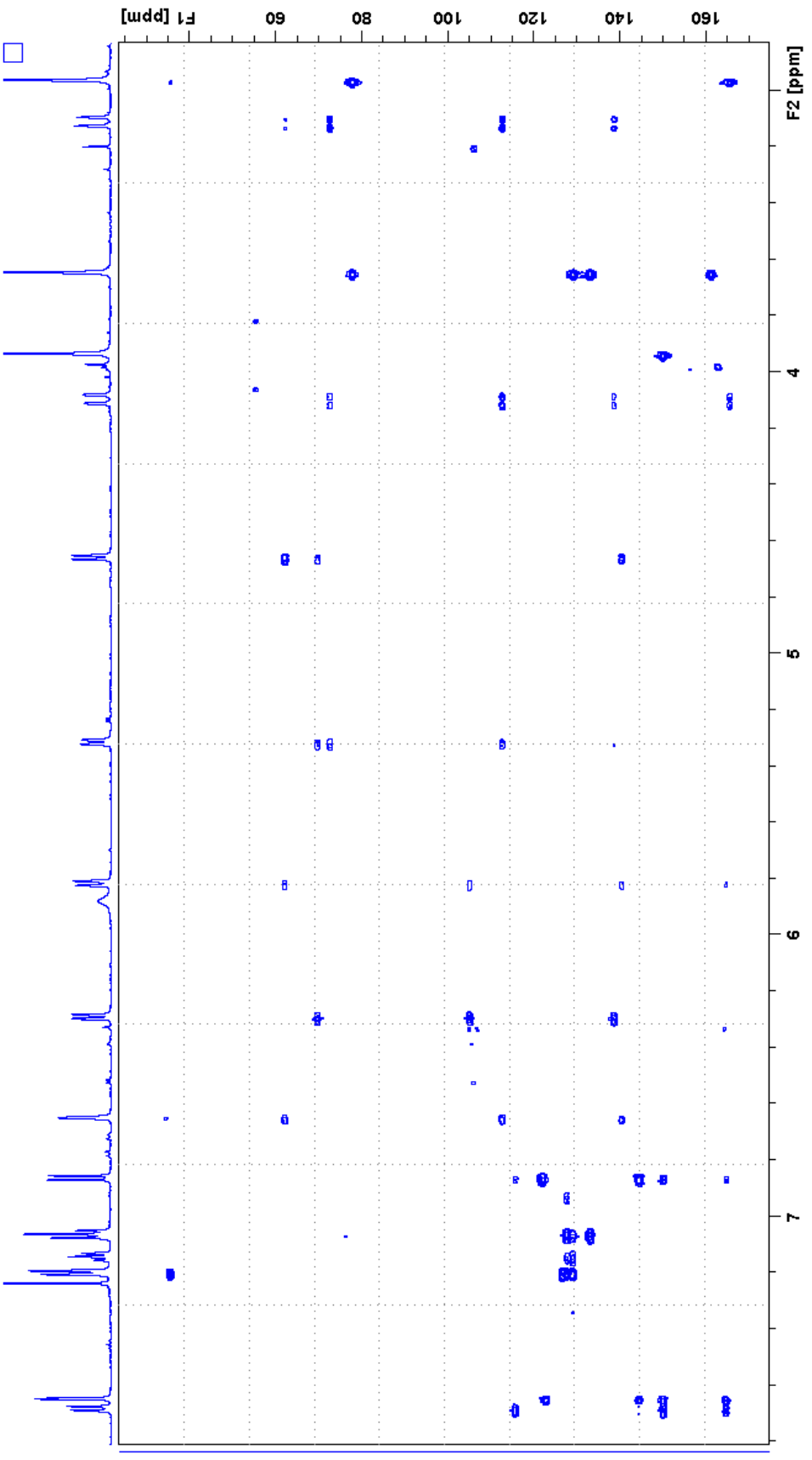

Figure A24. HMBC Spectrum of O-Methylsecoemestrin C_1 (**66**; 600 MHz, $CDCl_3$)

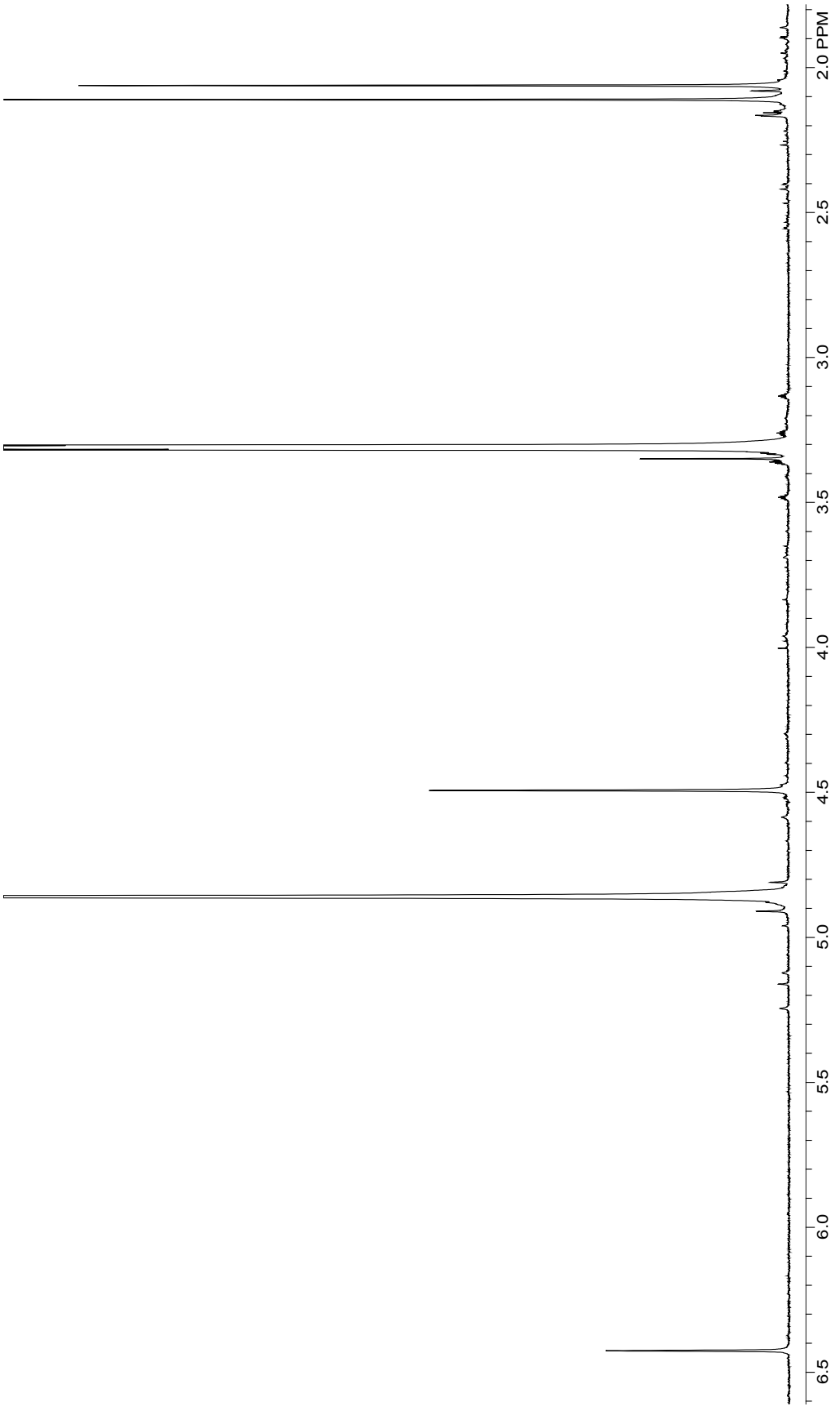

Figure A25. ^{1}H NMR Spectrum of 5-(Hydroxymethyl)-2,4-dimethylbenzene-1,3-diol (**67**; 400 MHz, CD_3OD)

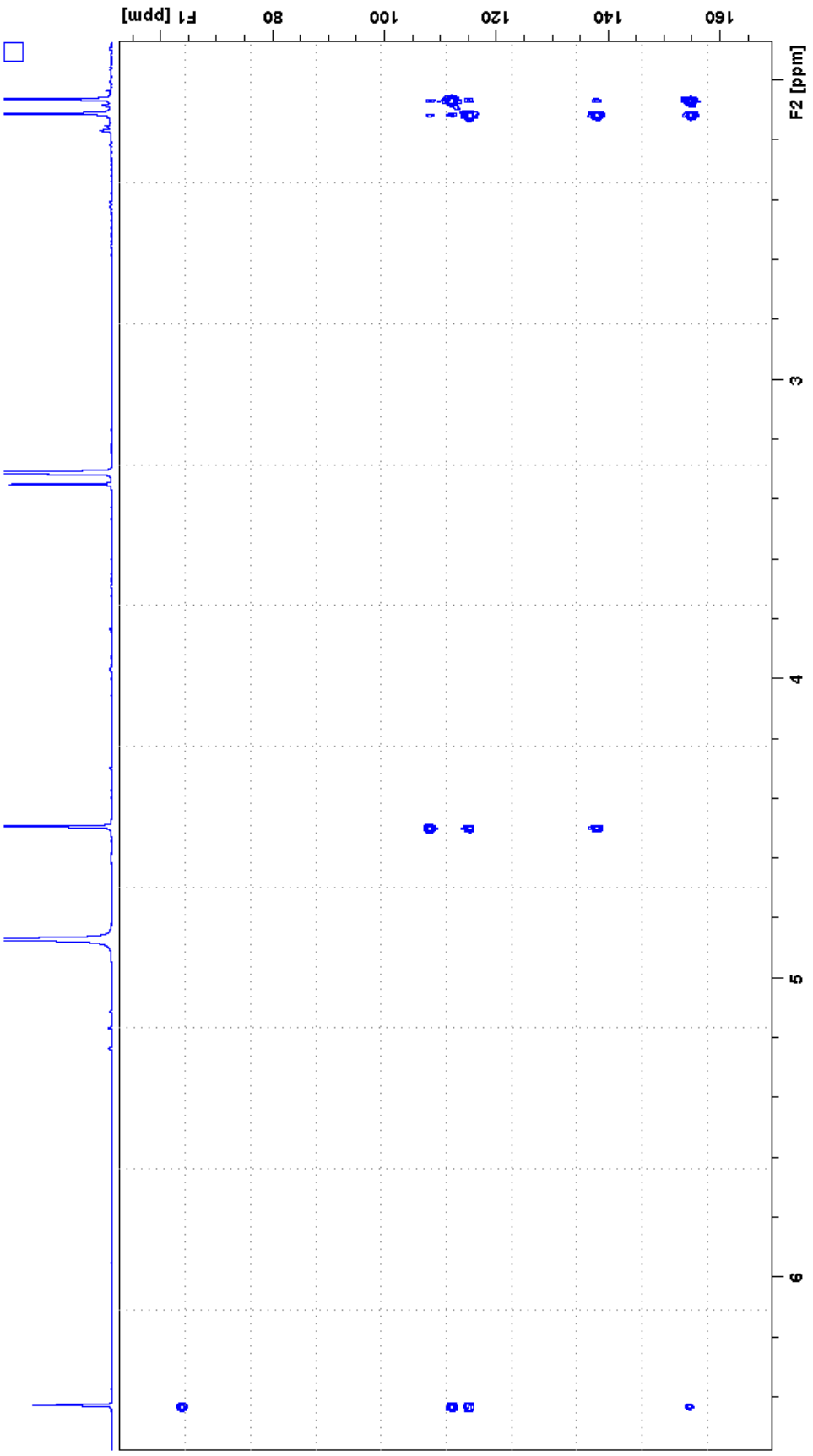

Figure A26. HMBC Spectrum of 5-(Hydroxymethyl)-2,4-dimethylbenzene-1,3-diol (**67**; 600 MHz, CD_3OD)

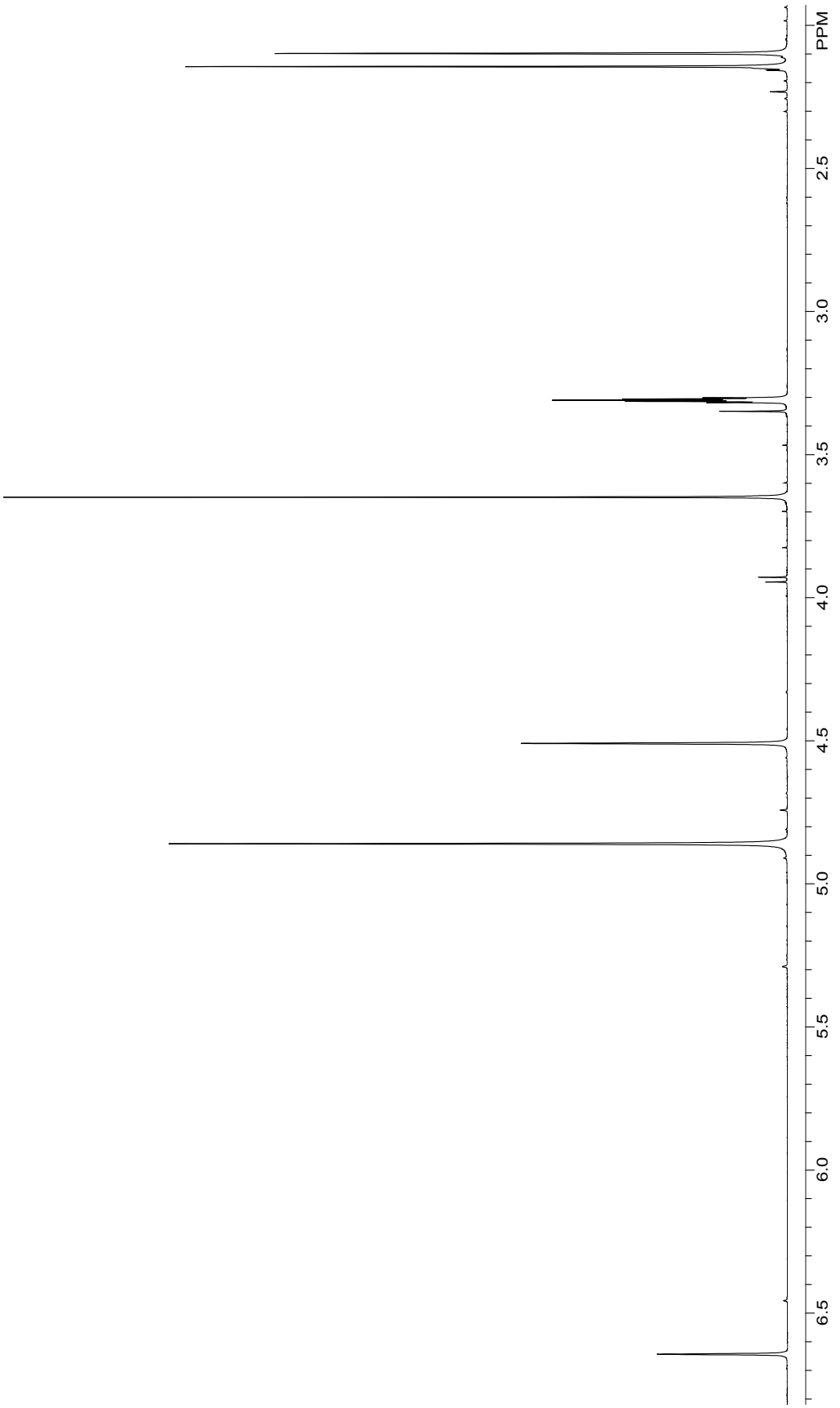

Figure A27. ^{1}H NMR Spectrum of 5-(Hydroxymethyl)-3-methoxy-2,4-dimethylphenol (**68**; 400 MHz, CD_3OD)

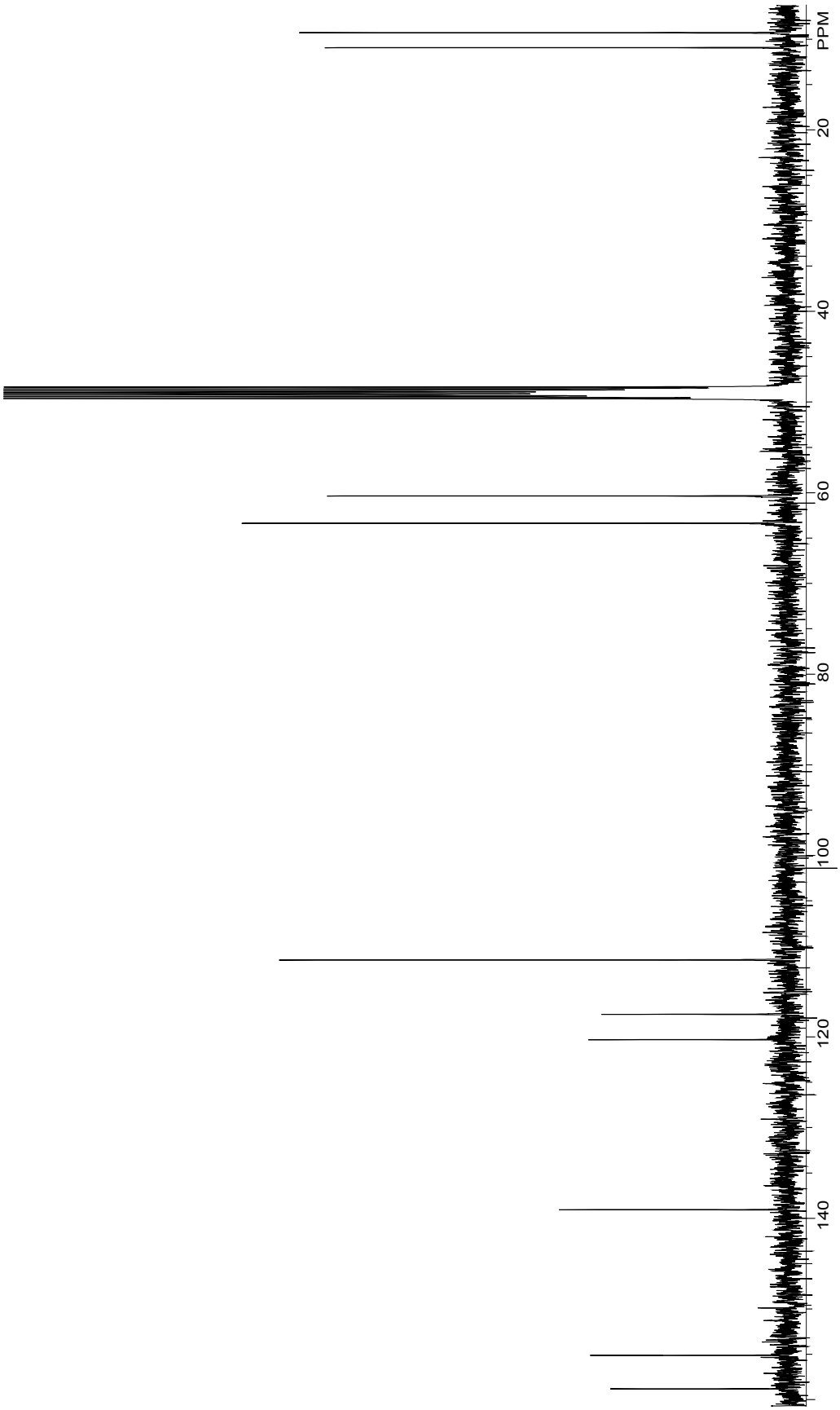

Figure A28. ^{13}C NMR Spectrum of 5-(Hydroxymethyl)-3-methoxy-2,4-dimethylphenol (**68**; 100 MHz, CD_3OD)

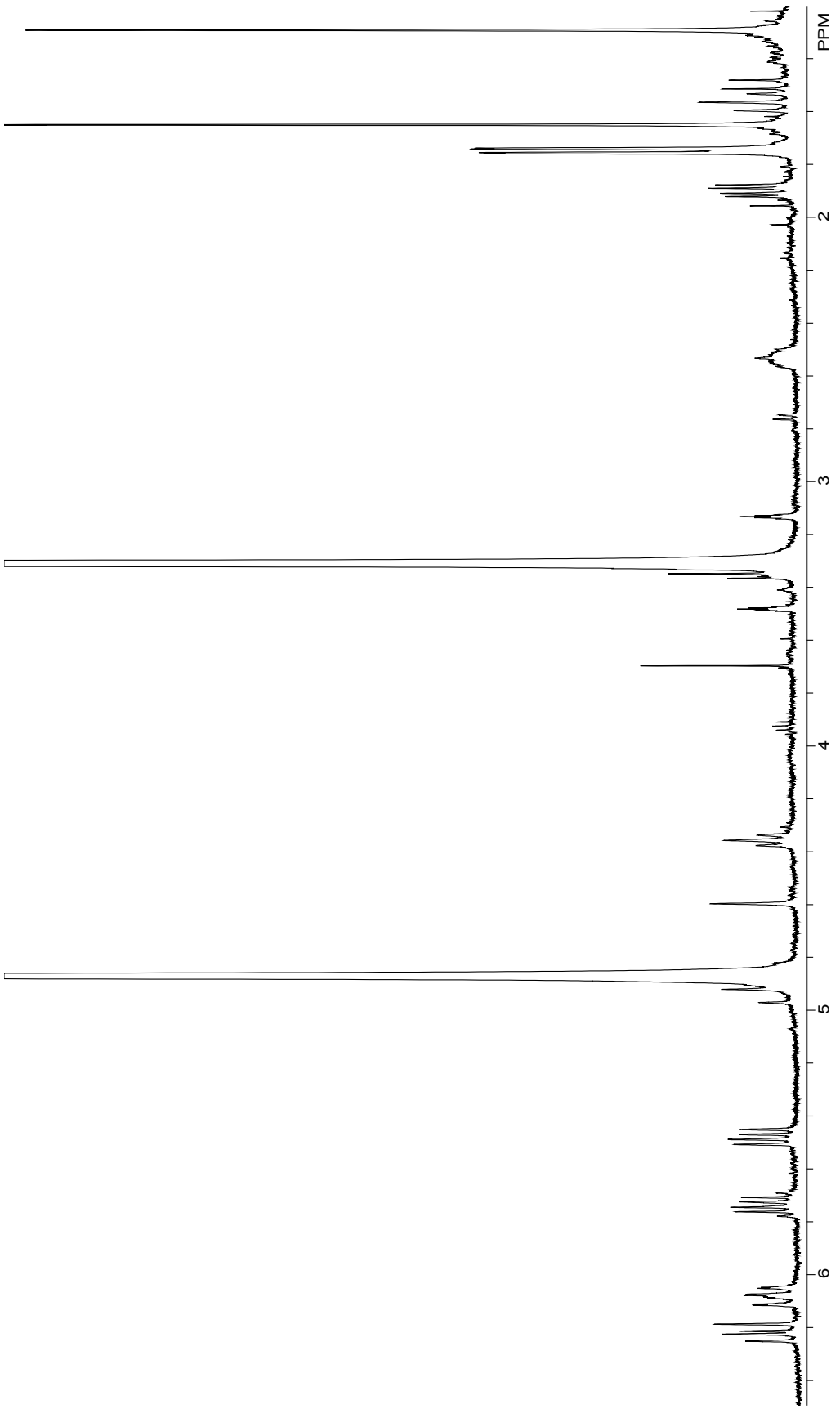

Figure A29. ^{1}H NMR Spectrum of Tetrahydrosorbicillinol (**71**; 400 MHz, CD_3OD)

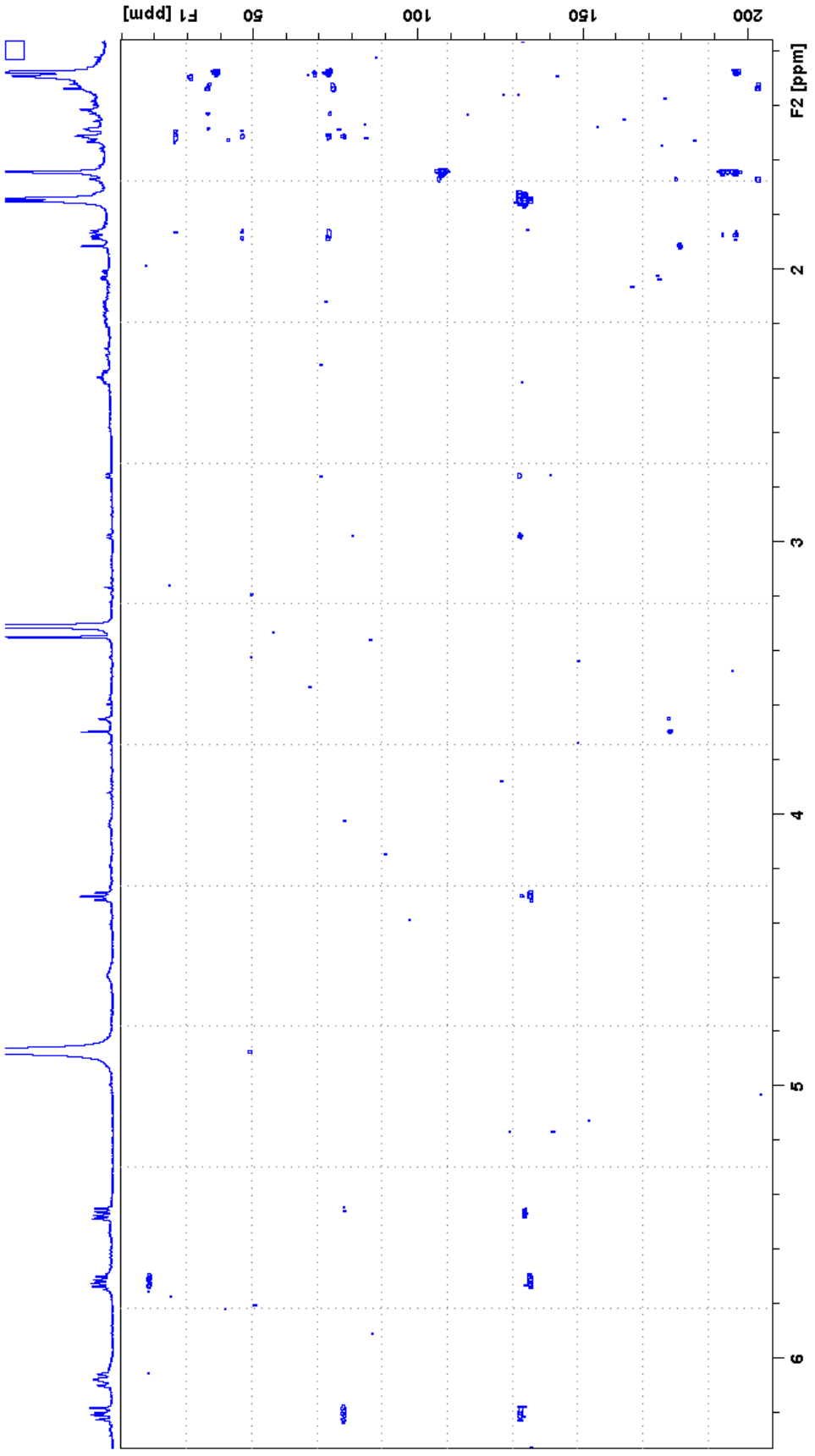

Figure A30. HMBC Spectrum of Tetrahydrosorbicillinol (**71**; 600 MHz, CD_3OD)

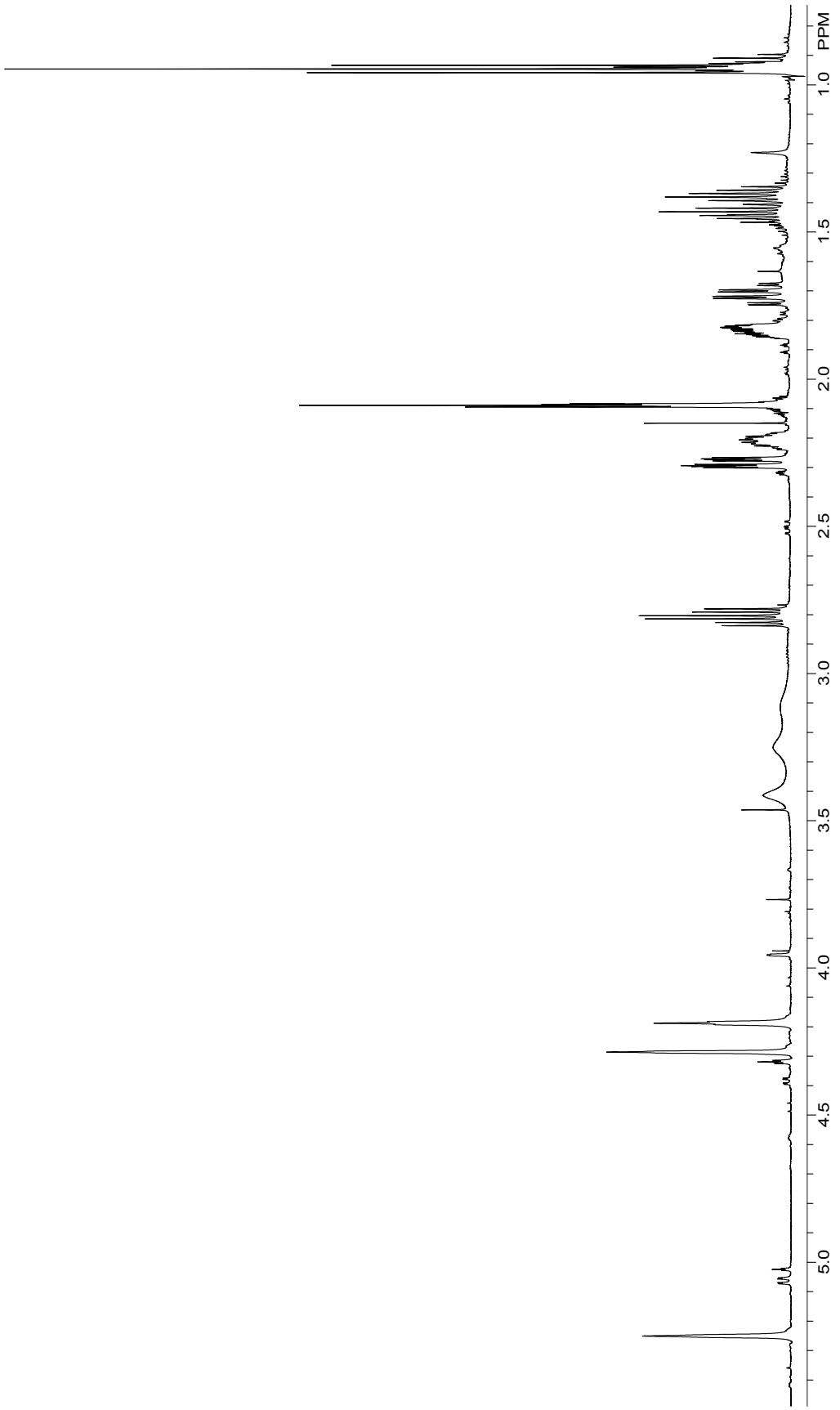

Figure A31. ^{1}H NMR Spectrum of Agistatine F (**77**; 600 MHz, $CDCl_3$)

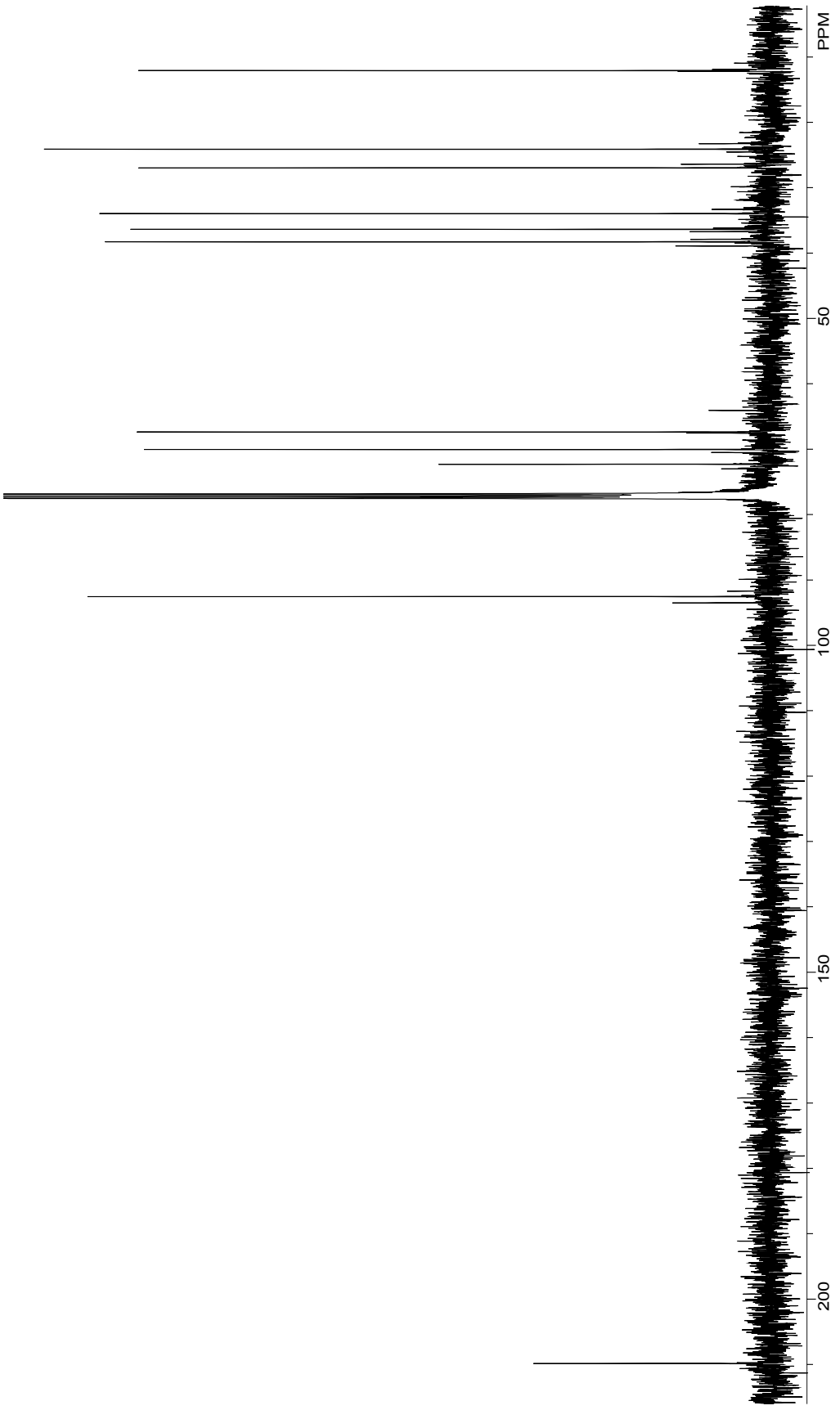

Figure A32. ^{13}C NMR Spectrum of Agistatine F (**77**; 100 MHz, $CDCl_3$)

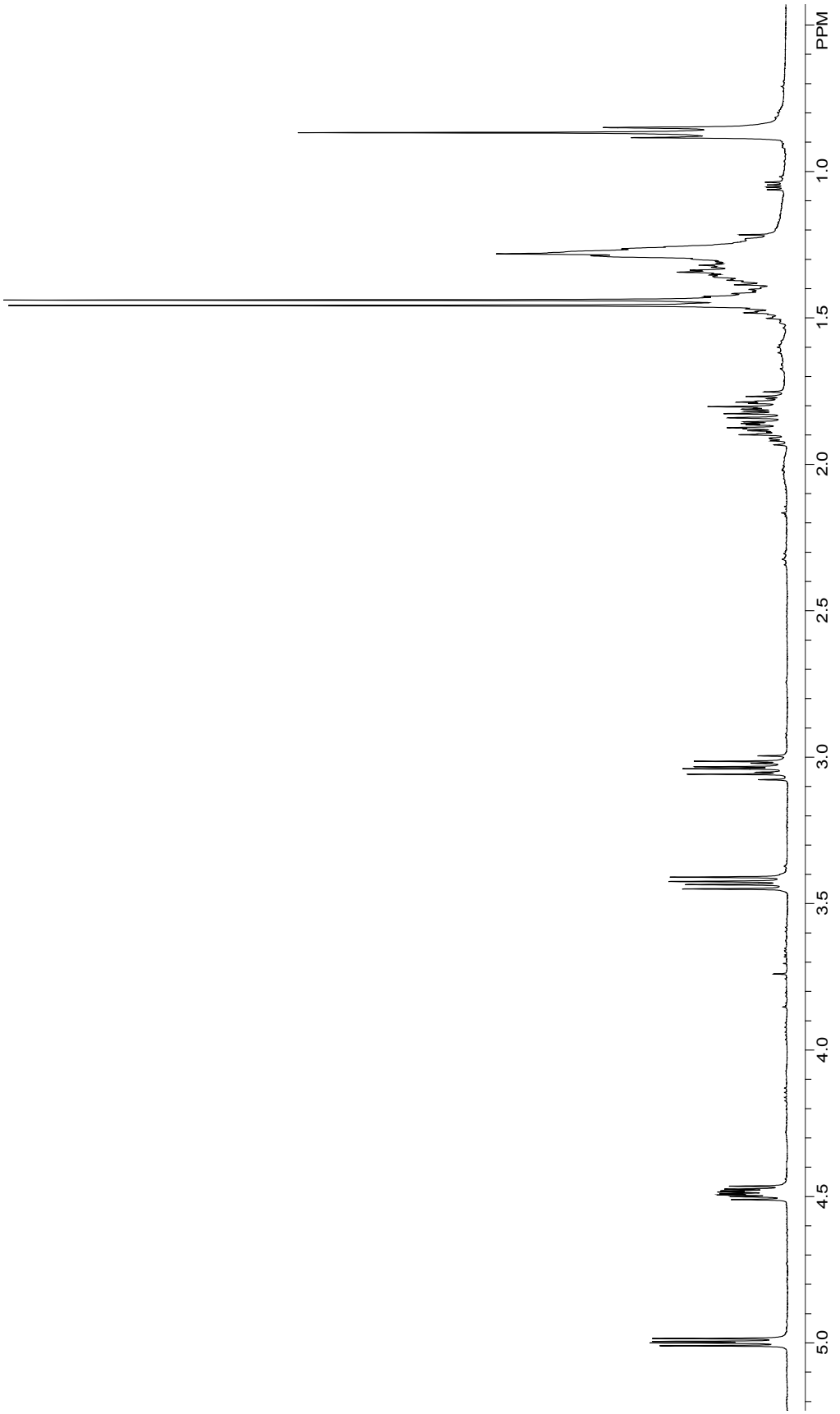

Figure A33. ^{1}H NMR Spectrum of Dihydrosporothriolide (**82**; 400 MHz, $CDCl_3$)

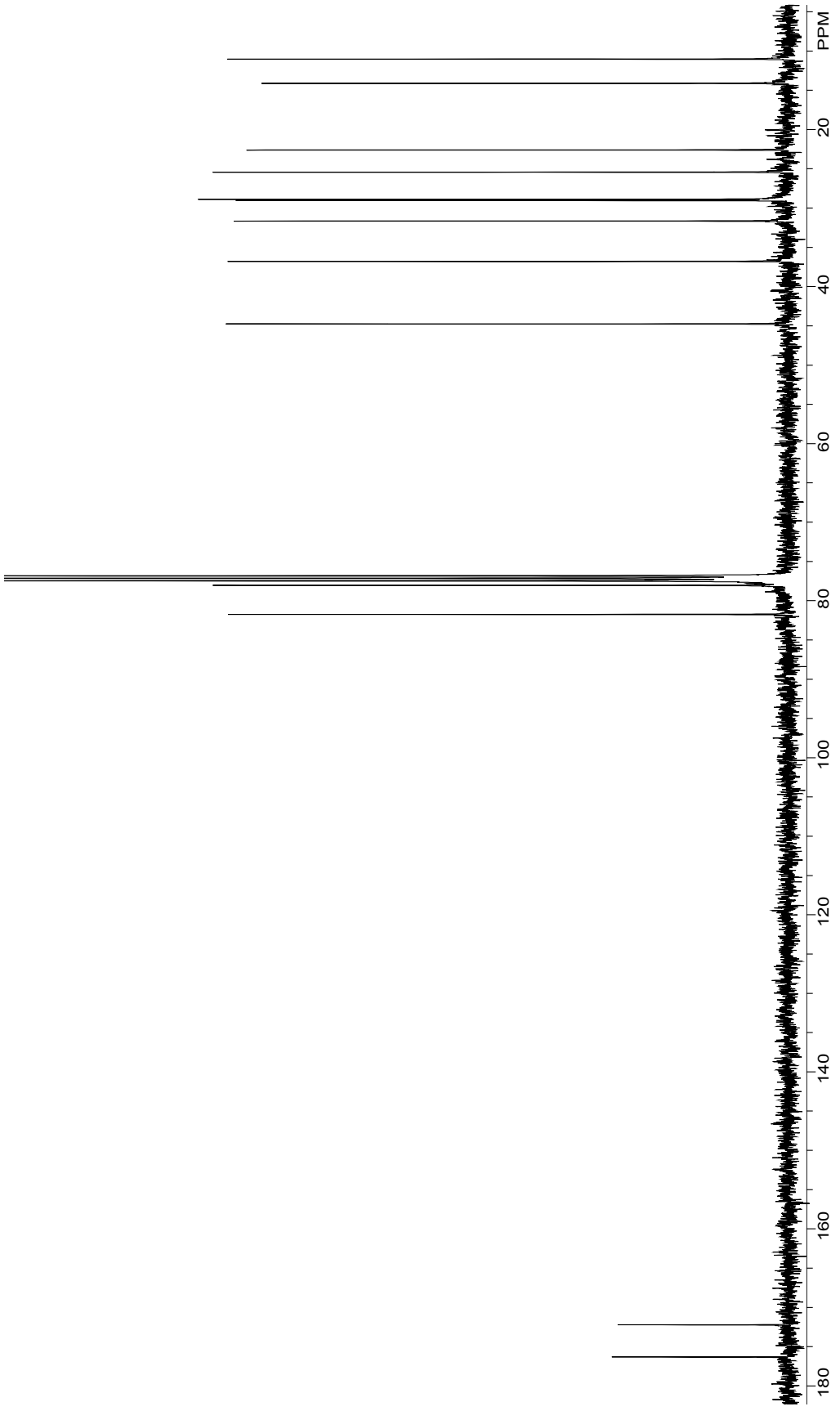

Figure A34. ^{13}C NMR Spectrum of Dihydrosporothriolide (**82**; 400 MHz, $CDCl_3$)

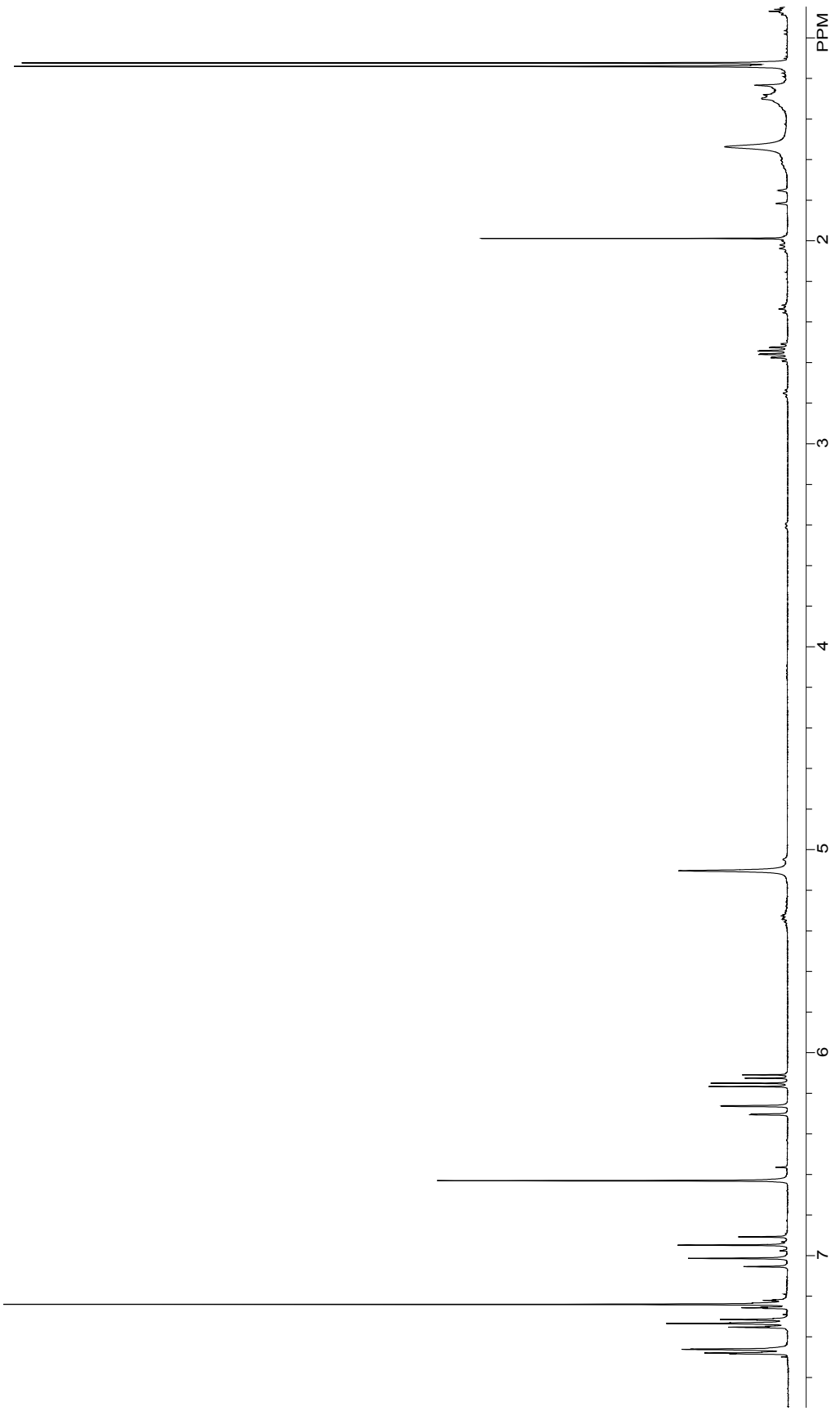

Figure A35. ^{1}H NMR Spectrum of Arahypin-1 (**86**; 400 MHz, $CDCl_3$)

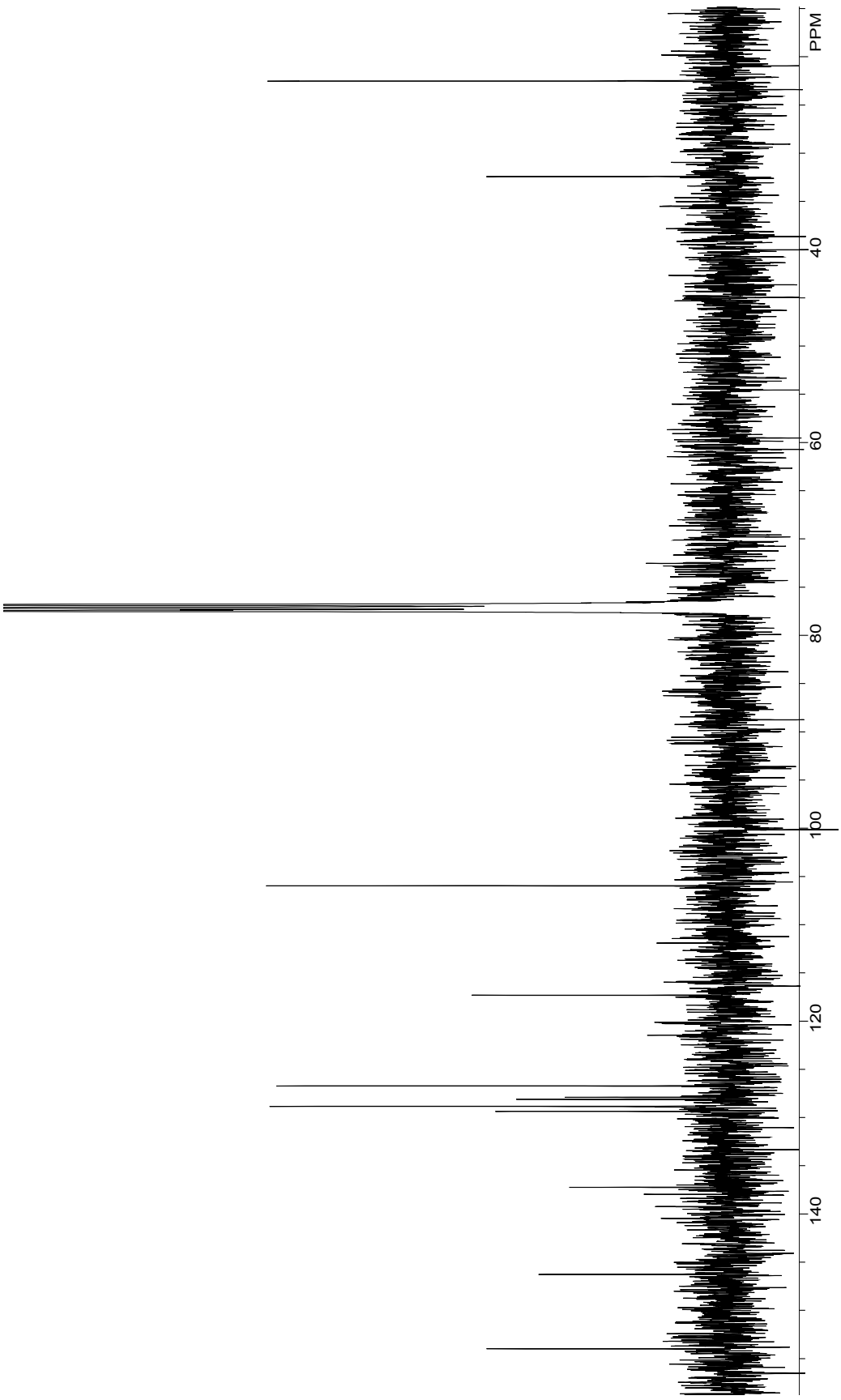

Figure A36. ^{13}C NMR Spectrum of Arahypin-1 (**86**; 100 MHz, $CDCl_3$)

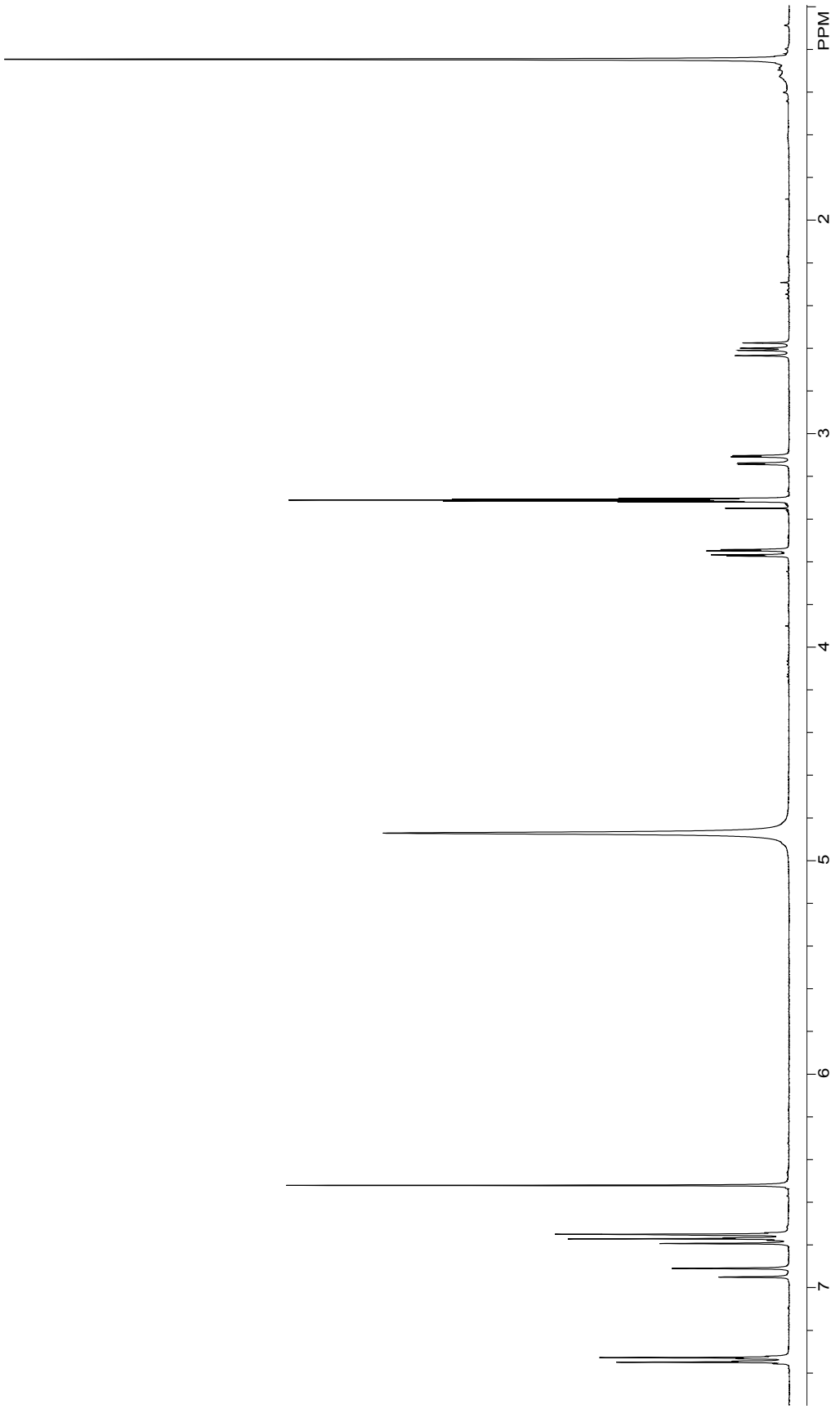

Figure A37. ^{1}H NMR Spectrum of Arahypin-3 (**87**; 400 MHz, CD_3OD)

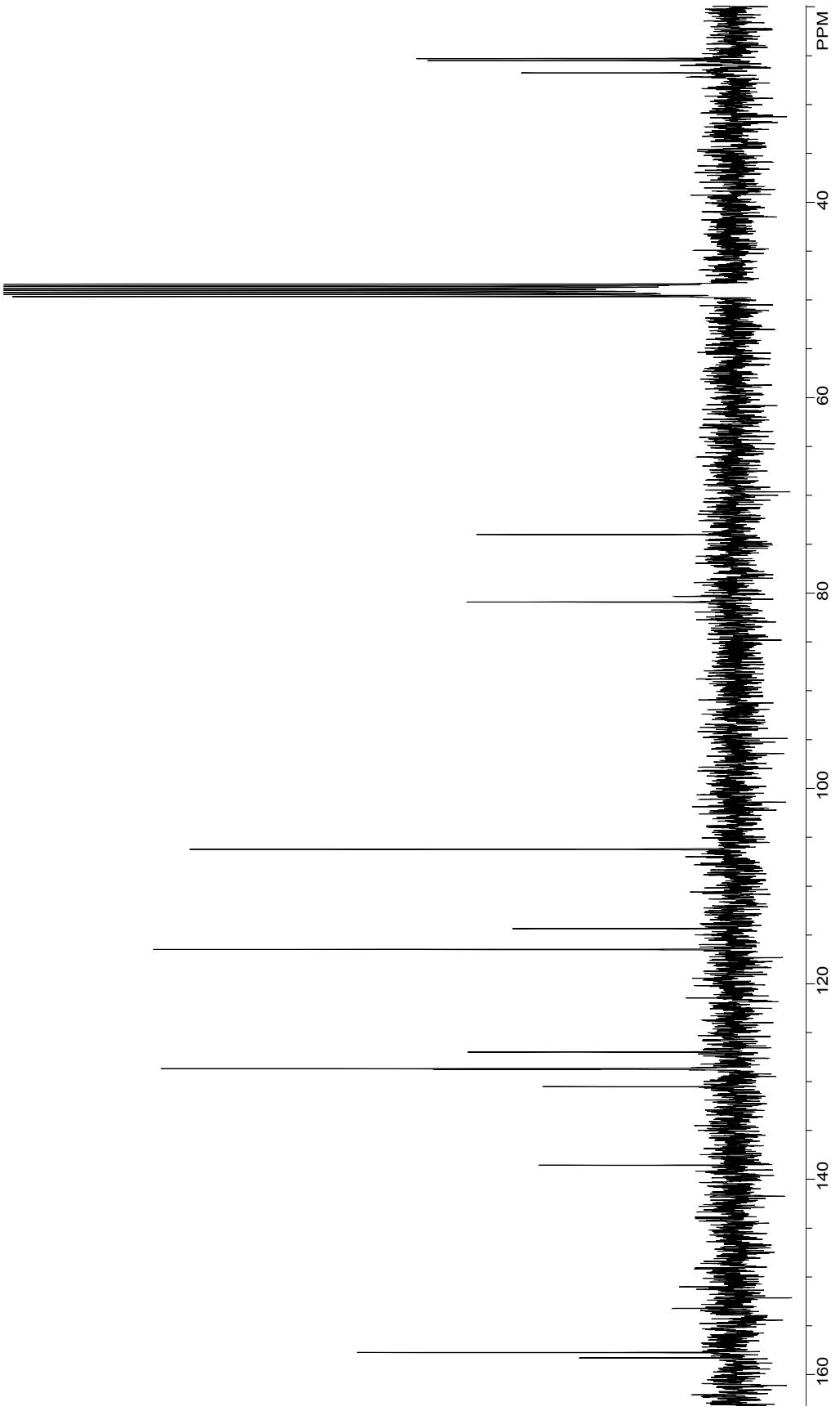

Figure A38. ^{13}C NMR Spectrum of Arahypin-3 (**87**; 100 MHz, CD_3OD)

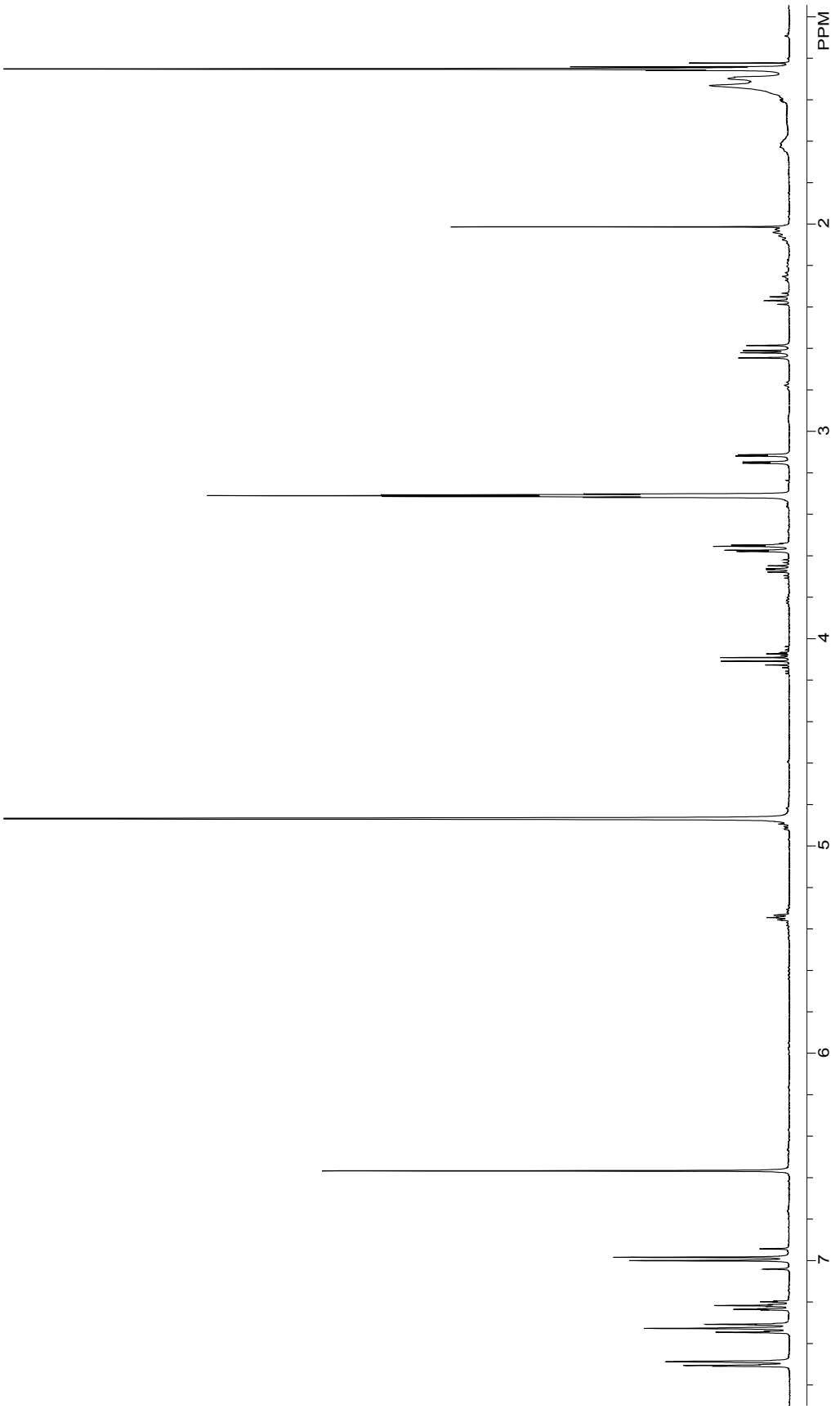

Figure A39. ^{1}H NMR Spectrum of Arahypin-4 (**88**; 400 MHz, CD_3OD)

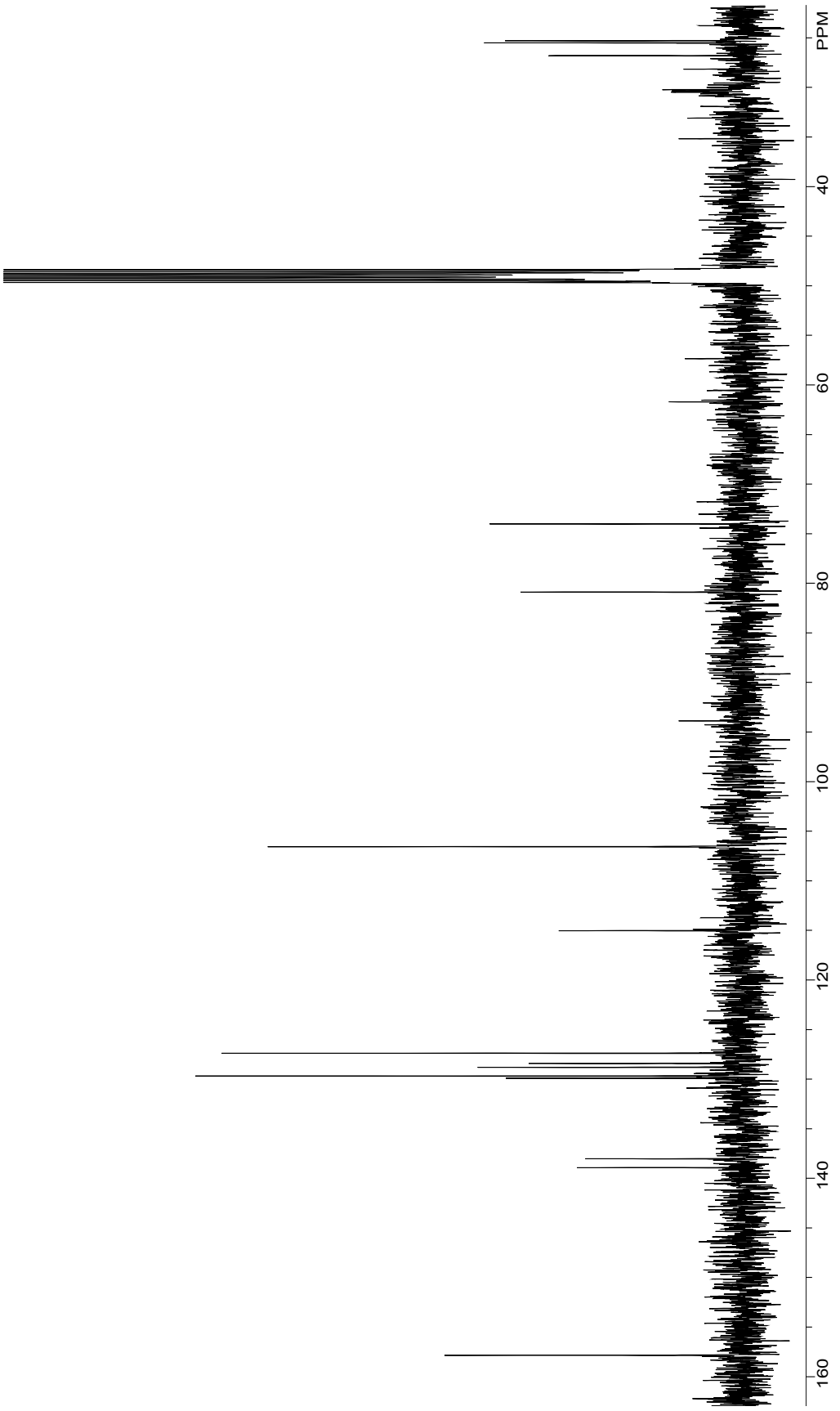

Figure A40. ^{13}C NMR Spectrum of Arahypin-4 (**88**; 100 MHz, CD_3OD)

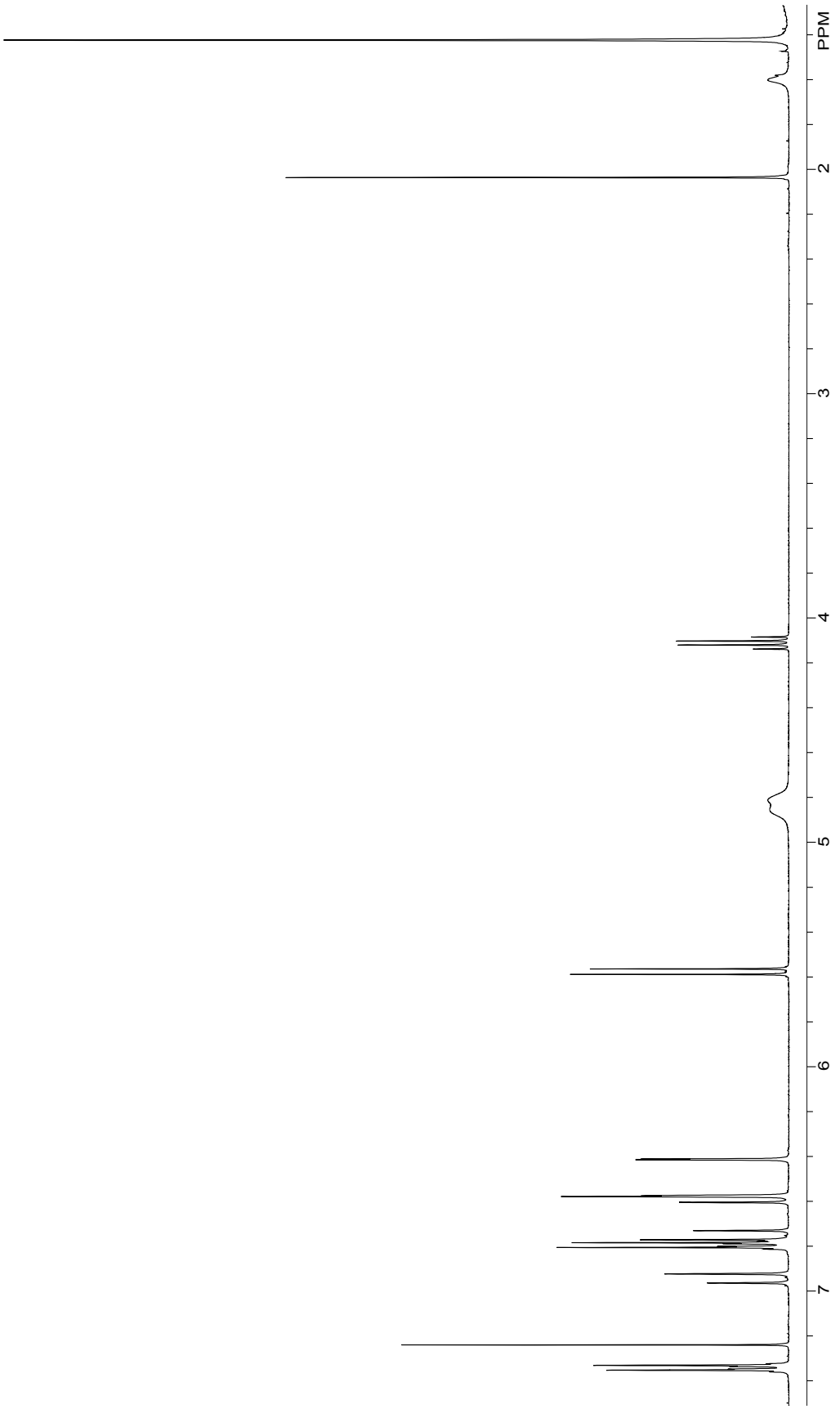

Figure A41. ^{1}H NMR Spectrumof Arahypin-5 (**89**; 400 MHz, $CDCl_3$)

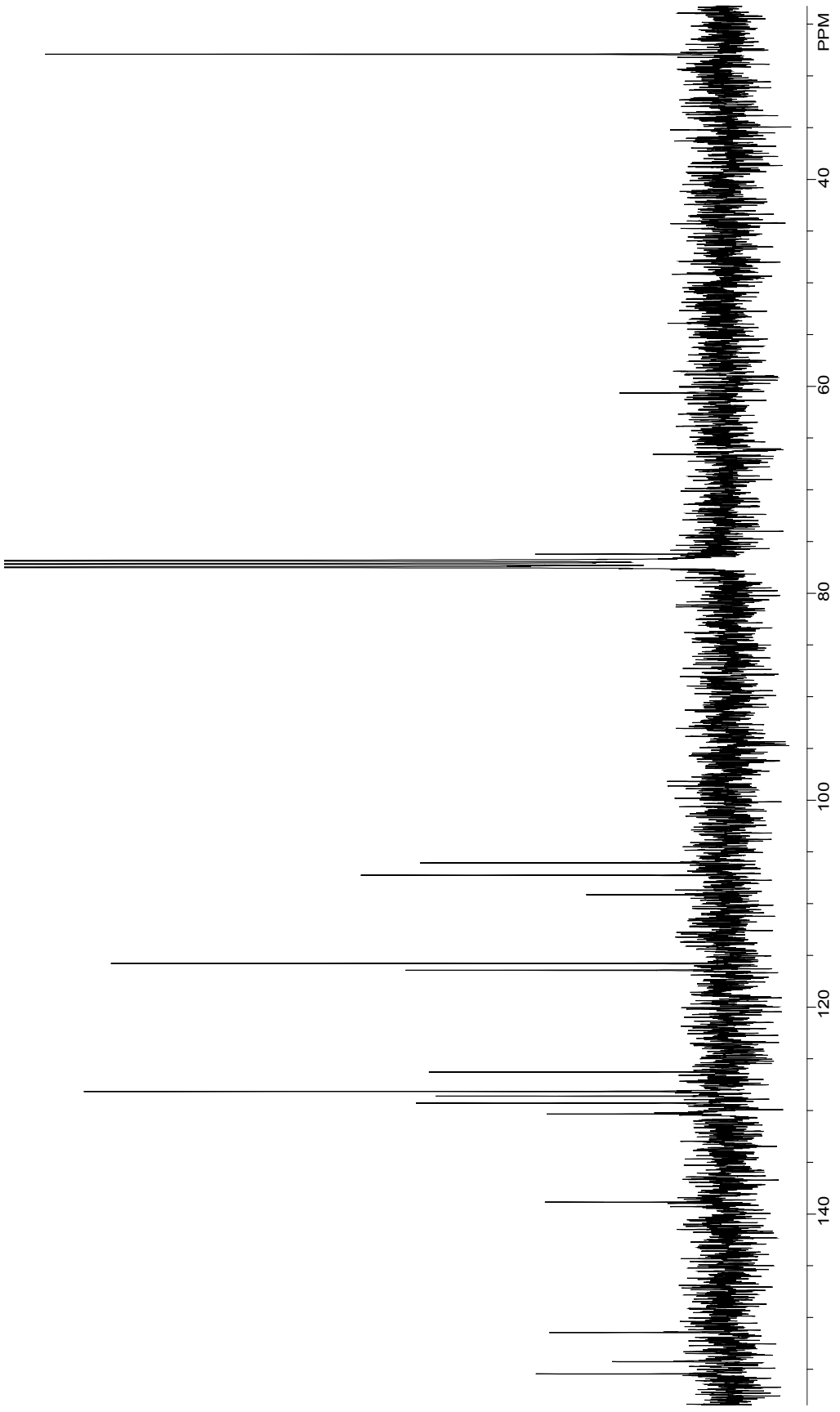

Figure A42. ^{13}C NMR Spectrum of Arahypin-5 (**89**; 100 MHz, $CDCl_3$)

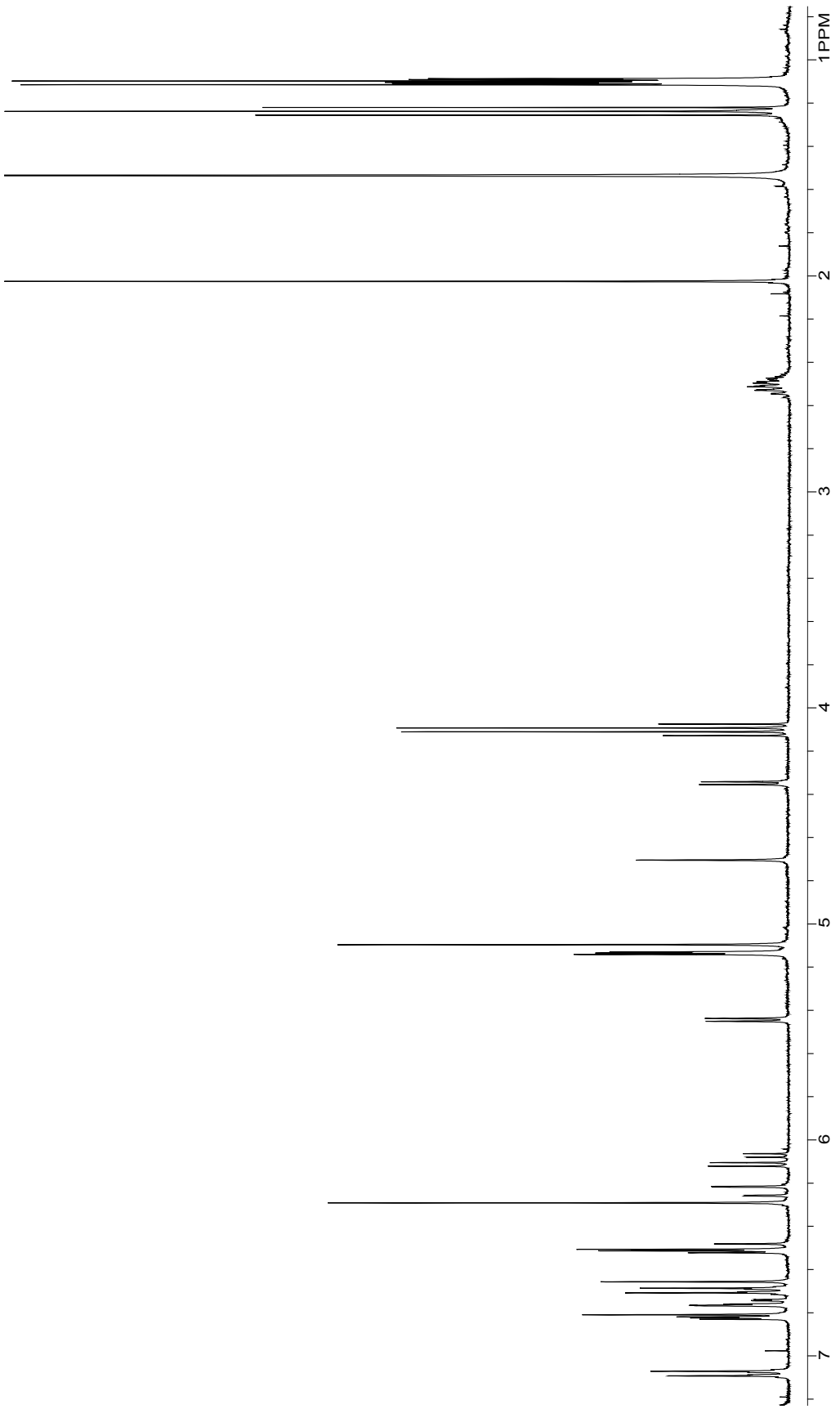

Figure A43. ^{1}H NMR Spectrum of Arahypin-6 (**90**; 400 MHz, $CDCl_3$)

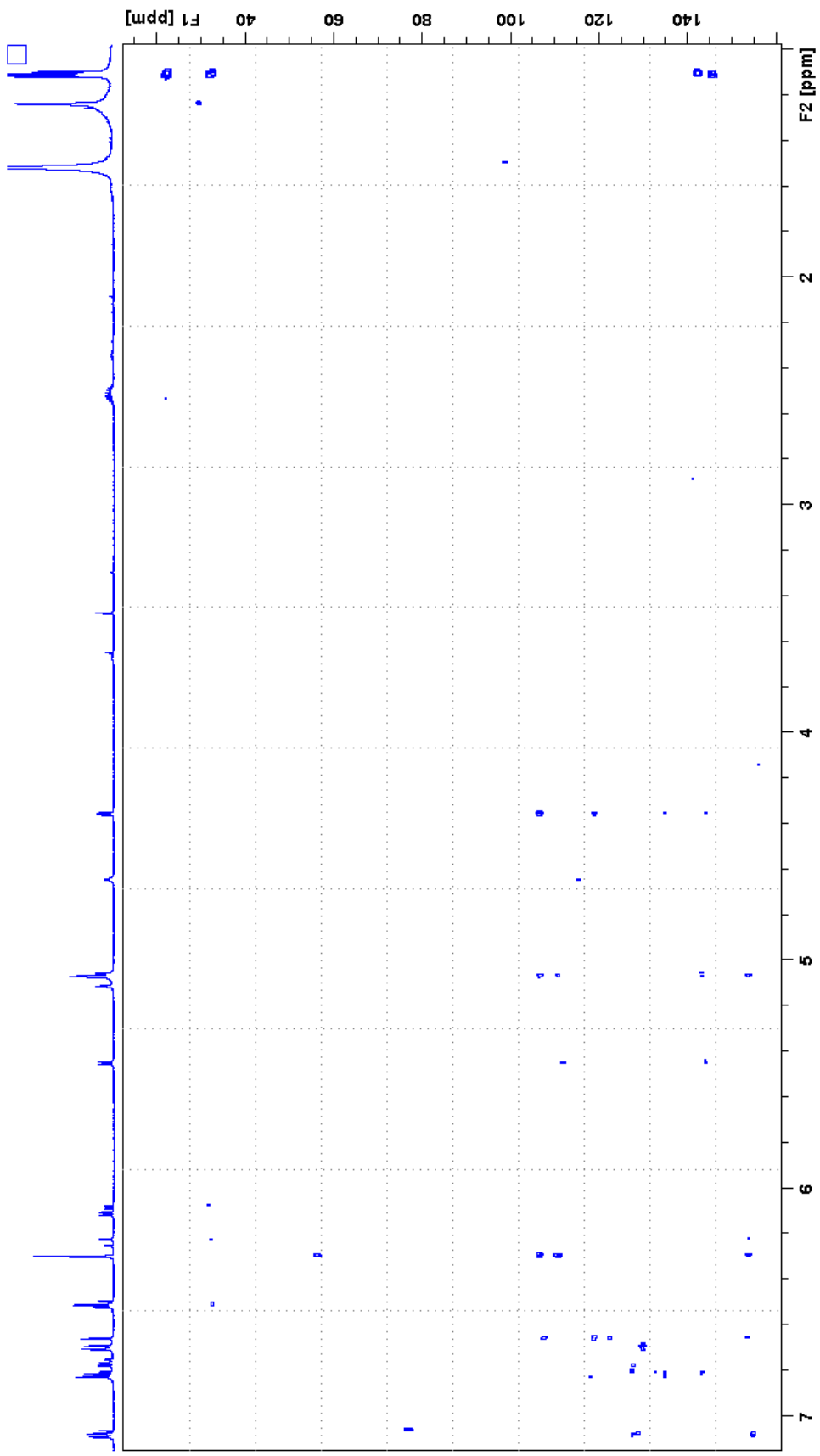

Figure A44. HMBC Spectrum of Arahypin-6 (**90**; 600 MHz, $CDCl_3$)

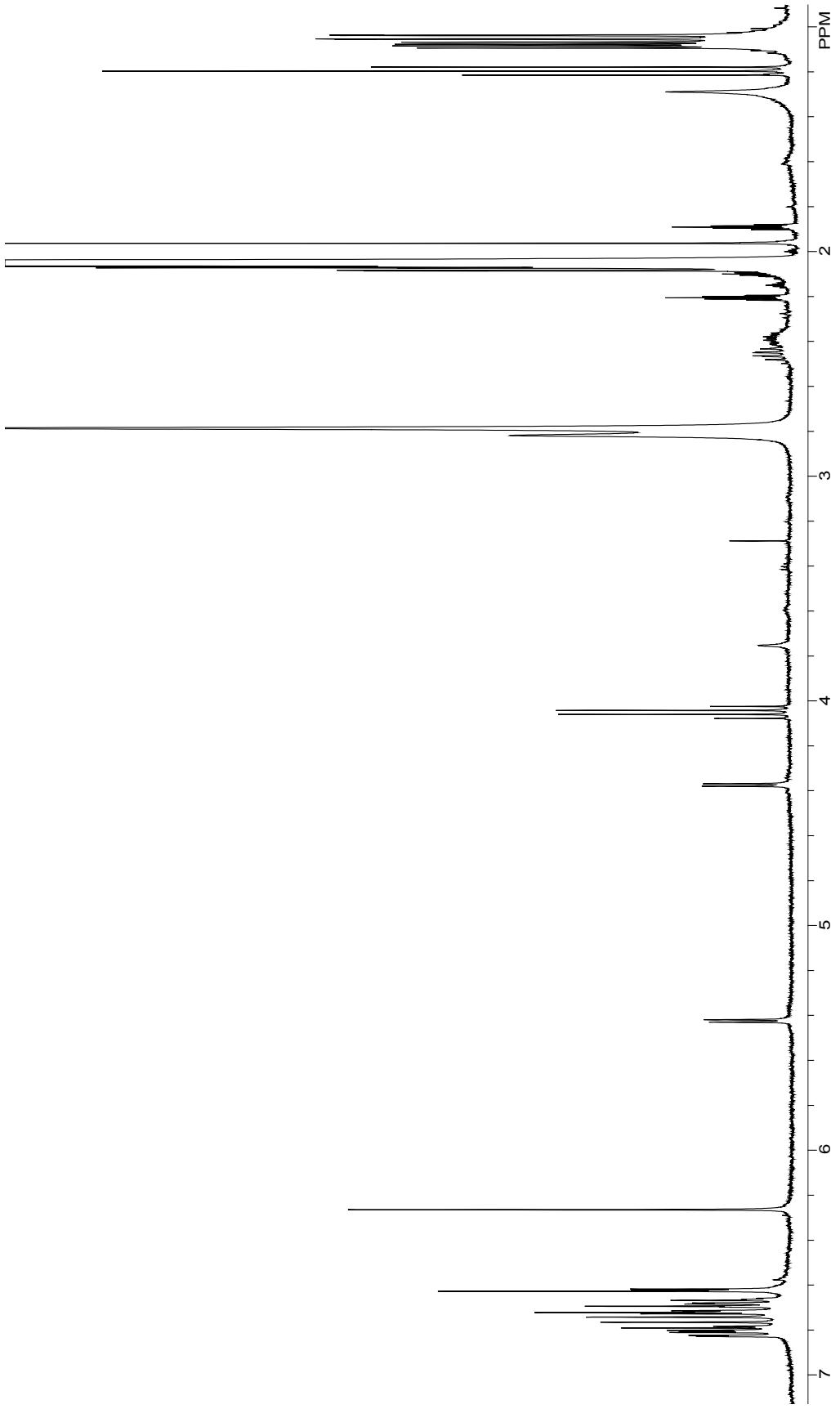

Figure A45. ^{1}H NMR Spectrum of Arahypin-7 (**91**; 400 MHz, Acetone-d_6)

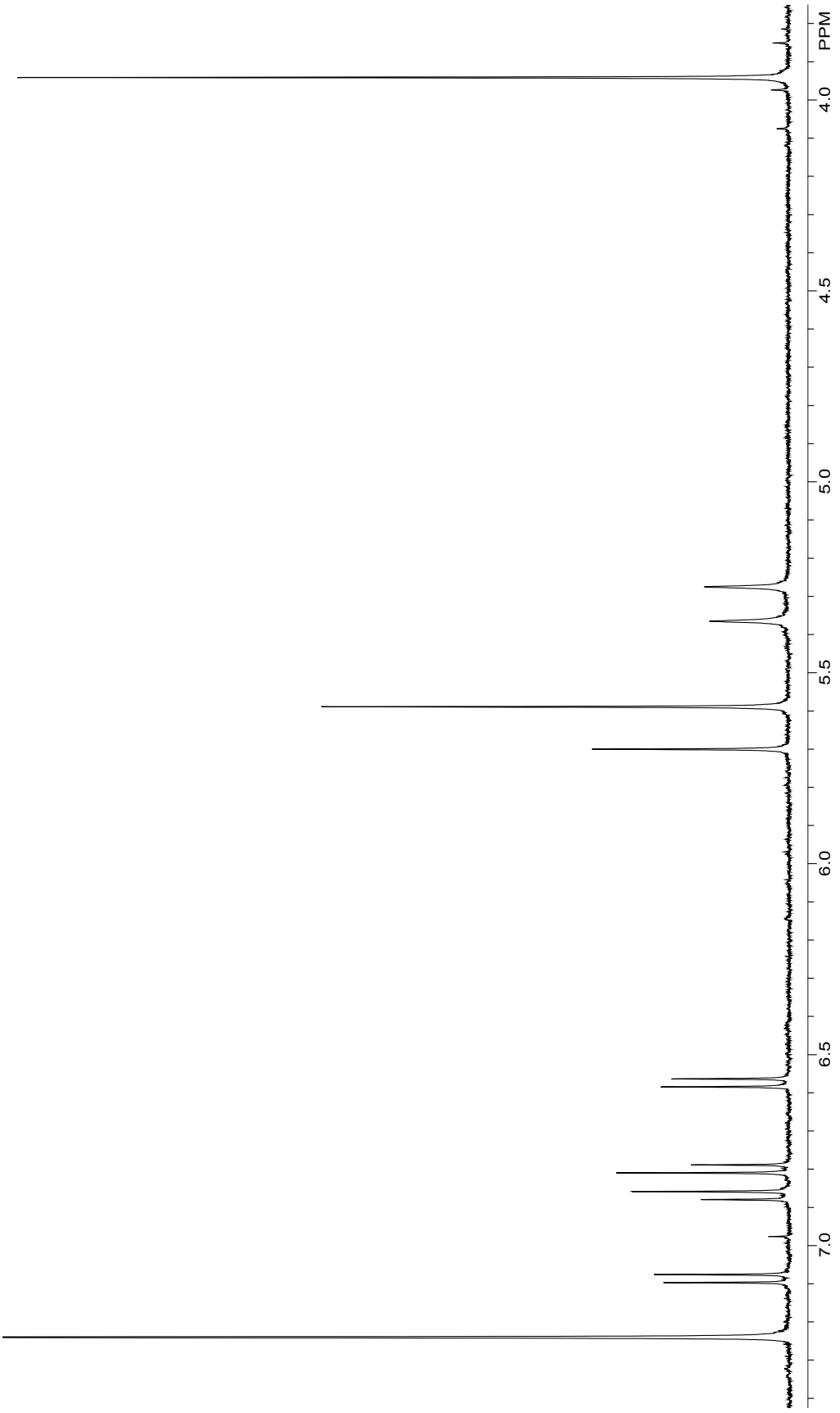

Figure A46. ^{1}H NMR Spectrum of Aracarpene-1 (**92**; 400 MHz, $CDCl_3$)

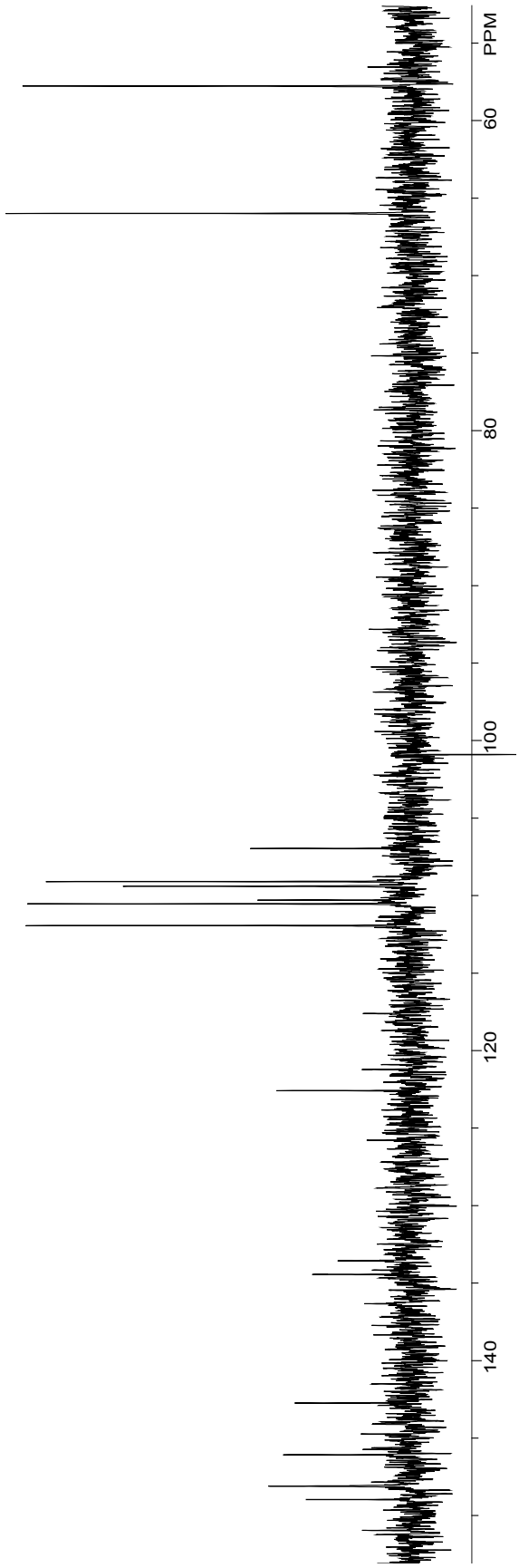

Figure A47. ^{13}C NMR Spectrum of Aracarpene-1 (**92**; 100 MHz, Acetone-d_6)

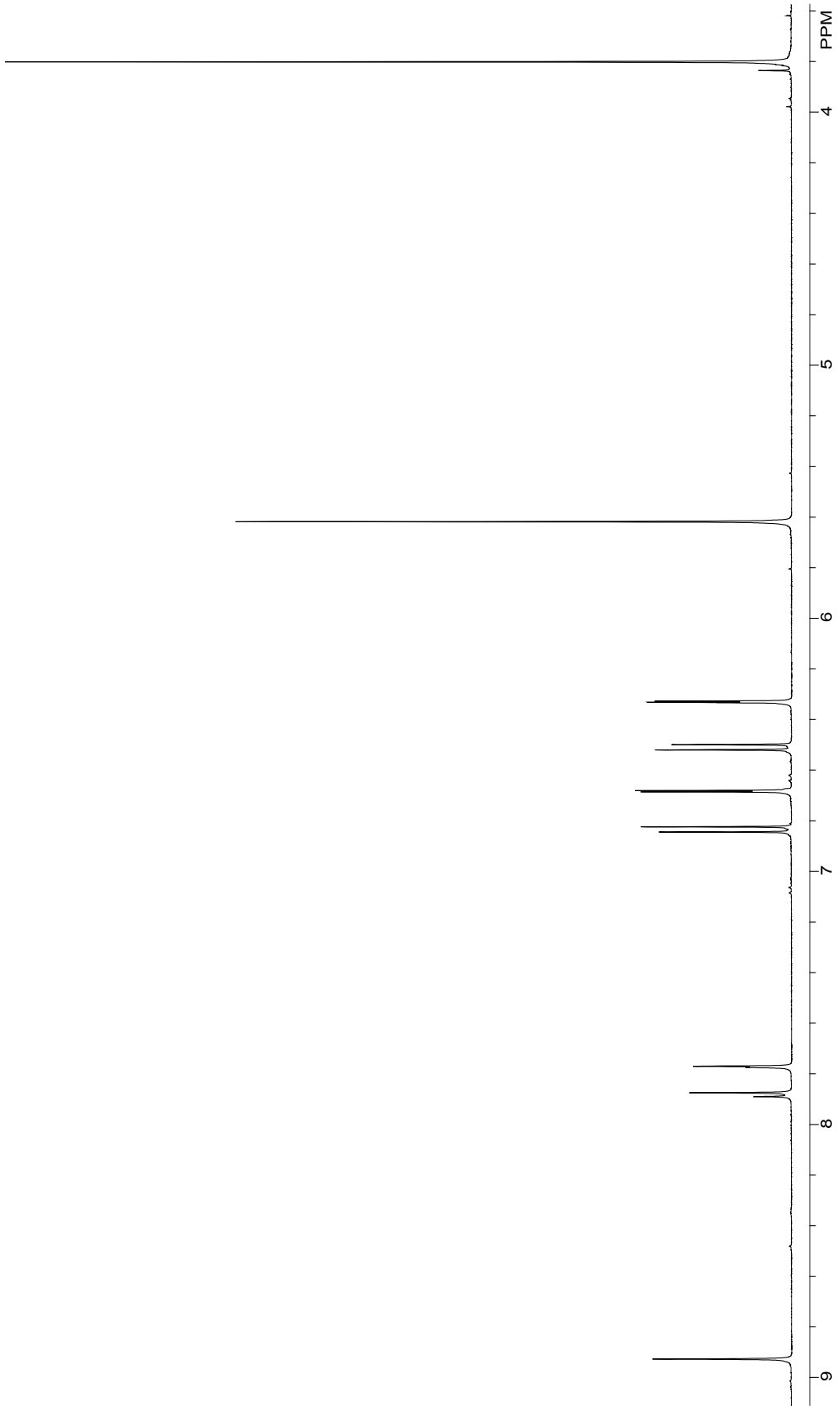

Figure A48. ^{1}H NMR Spectrum of Aracarpene-2 (**93**; 400 MHz, Acetone-d_6)

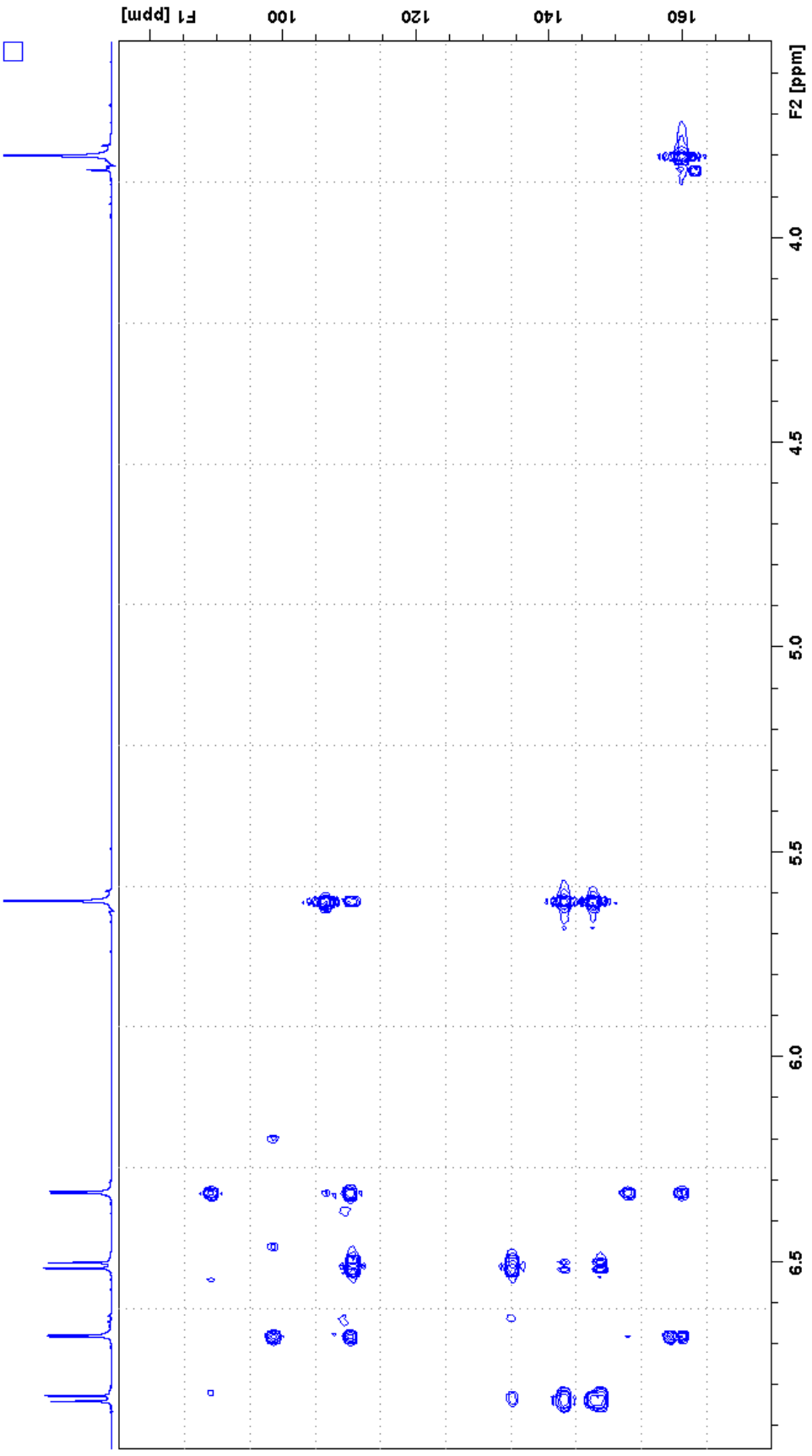

Figure A49. HMBC Spectrum of Aracarpene-2 (**93**; 600 MHz, Acetone-d_6)

REFERENCES

1. Hawksworth, D. L. *Mycol. Res.* **1991**, *95*, 641-655.
2. Hawksworth, D. L. *Mycol. Res.* **2001**, *105*, 1422-1432.
3. Trappe, J. M.; Luoma, D. L. In *The Fungal Community: Its Organization and Role in the Ecosystem*; 2nd ed.; Carroll, G. C.; Wicklow, D. T., Eds.; Marcel Dekker, Inc.: New York, 1992; Vol. 9, pp 17-27.
4. Dalldorf, D. *Fungi and Fungal Diseases*, Charles C. Thomas Publishers, Springfield, Illinois, 1962, pp 1-34.
5. *The Fungi III: The Fungal Population*, Ainsworth, G. C.; Sussman, A. S., Eds.; Academic Press: New York & London, 1968.
6. Gloer, J. B. In *The Mycota IV: Environmental and Microbial Relationships IV*; 2nd ed.; Kubicek, C. P.; Druzhinia, I. S. Eds.; Springer-Verlag: Berlin, 2007; Vol. IV, pp 257-283.
7. Daemmrigh, A.; Bowden, M. E. *Chem. Eng. News* **2005**, *83*, 3.
8. Orru, B.; Riva, A.; Fruciano, E. *Giuseppe Brotzu and the Discovery of Cephalosporins* veprints.unica.it/148/1/orru-poster.pdf (Accessed August 2011)
9. Itokazu, G. *Cephalosporins* www.uic.edu/pharmacy/courses/pmpr342/itokazu/cephalosporins (Accessed August 2011).
10. Chin, Y. W.; Balunas, M. J.; Chai, H. B.; Kinghorn, A. D. *The AAPS Journal* **2006**, *8*, E239-E253.
11. Newman, D. J.; Cragg, G. M. *J. Nat. Prod.* **2007**, *70*, 461-477.
12. Siddiqui, I. N.; Zahoor, A.; Hussain, H.; Ahmed, I.; Ahmad, V. U.; Padula, D.; Draeger, S.; Schulz, B.; Meier, K.; Steinert, M.; Kurtan, T.; Florke, U.; Pescitelli, G.; Krohn, K. *J. Nat. Prod.* **2011**, *74*, 365-373.
13. Parish, C. A.; Smith, S. K.; Calati, K.; Zink, D.; Wilson, K.; Roemer, T.; Jiang, B.; Xu, D.; Bills, G.; Platas, G.; Pelaes, F.; Diez, M. T.; Tsou, N.; McKeown, A. E.; Ball, R. G.; Powles, M. A.; Yeung, L.; Liberator, P.; Harris, G. *J. Am. Chem. Soc.* **2008**, *130*, 7060-7066.
14. Corrado, M.; Rodrigues, K. F. *J. Basic Microbiol.* **2004**, *44*, 157-160.
15. Pesctielli, G.; Kurtan, T.; Florke, U.; Krohn, K. *Chirality* **2009**, *21*, E181-E201.
16. Chen, C. S.; Shieh, W. R.; Lu, P. H.; Harriman, S.; Chen, C. Y. *Biochim Biophysi Acta* **1991**, *1078*, 411-417.

17. Odds, F. C. *Mycologist* **2003**, *17*, 51-55.

18. MacMillan, J. *J. Chem. Soc.* **1959**, 1823.

19. Brown, W. A. C.; Sim, G. A. *J. Chem. Soc.* **1963**, 1050.

20. Eichelbaum, M. *Stereochemical Aspects of Drug Action and Disposition*; Testa, B., Somogyi, A., Eds.; Springer: Berlin, 2003.

21. EMEA. *Investigation of Chiral Active Substances* Report 3CC29a, EMEA; London, 1993, pp 381-391.

22. Sahajwalla, C. Regulatory Considerations in Drug Development of Stereoisomers, In *Chirality in Drug Design and Development*; Reddy, K.; Mehvar, R., Eds.; Marcel Dekker: New York, 2004, pp 419-432.

23. Miller, C. P.; Ulrich, J. W. *Chirality* **2008**, *20*, 762-770.

24. Contreras, R. H.; Peralta, J. E. *Prog. Nucl. Magn. Reson. Spectrosc.* **2000**, *37*, 321-425.

25. Hoye, T. R.; Jeffery, C. S.; Shao, F. *Nat. Protocols* **2007**, *2*, 2451-2457.

26. Autschbach, J. *Chirality* **2009**, *21*, E116-E152.

27. Barron, L. D.; *Molecular Light Scattering and Optical Activity,* 2nd Ed.; Cambridge University Press: Cambridge, UK., 2004.

28. Paly, G.; Zucchi, C.; Caglioti, L., Eds.; *Progress in Biological Chirality* Elsevier Science: Oxford, UK., 2004.

29. Buckingham, A. D.; Stiles, P. *J. Acc. Chem. Res.* **1974**, *7*, 258.

30. Schellman, J. A. *Chem. Rev.* **1975**, *75*, 323.

31. Wagniere, G. *J. Am. Chem. Soc.* **1966**, *88*, 3937.

32. Greenfield, N. J. Analysis of Circular Dichroism Data, In *Methods in Enzymology*, Vol. 383; Elsevier, 2004, pp 282-317.

33. Nave, C. R. *Classification of Polarization*, In *HyperPhysics*; Georgia State University, 2011 hyperphysics.phy-astr.gsu.edu/hbase/phyopt/polclas.html#c3 (Accessed August 2011).

34. Woody, R. W. Theory of Circular Dichroism of Proteins, In *Circular Dichroism and the Conformational Analysis of Biomolecules*; Fasman, G. D., Editor; Plenum Press: New York, 1996, pp 25-67, (and references therein).

35. Prelog, V.; Helmchen, G. *Helv. Chim. Acta* **1972**, *55*, 2581-2598.

36. Djerassi, C. *Optical Rotatory Dispersion* McGraw-Hill Book Co. Inc.: New York, 1960.

37. Gillard, R. D. *Analyst* **1963**, *88*, 825-828.

38. Snatzke, G. *Pure & Appl. Chem.* **1979**, *51*, 769-785.

39. Eliel, E. L.; Wilen, S. H. *Stereochemistry of Organic Compounds*, Wiley-VCH: New York, 1994.

40. Snatzke, G. *Angew. Chem., Int. Ed. Engl.* **1979**, *18*, 363-377.

41. Ciardelli, F.; Slavadori, P. *Fundamental Aspects and Recent Developments in Optical Rotatory Dispersion and Circular Dichroism*; Heyden: London, 1973.

42. Lightner, D. A. The Octant Rule, In *Circular Dichroism: Principles and Applications*, 2nd ed.; Berova, B.; Nakanishi, K.; Woody, R. W., Eds.; Wiley-VCH: New York, 2000, pp 261-303.

43. Berova, N.; Nakanishi, K. Exciton Chirality Method: Principles and Applications, In *Circular Dichroism: Principles and Applications*, 2nd ed.; Berova, B.; Nakanishi, K.; Woody, R. W., Eds.; Wiley-VCH: New York, 2000, pp 337-395.

44. Berova, N.; Di Bari, L.; Pescitelli, G. *Chem. Soc. Rev.* **2007**, *36*, 914-931.

45. Harada, N.; Nakanishi, K. *Circular Dichroic Spectroscopy – Exciton Coupling in Organic Stereochemistry*; University Science Books: Mill Valey, California, 1983.

46. Crawford, T. D. *Theor. Chem. Acc.* **2006**, *115*, 227-245.

47. Pecul, M.; Ruud, K. *Adv. Quantum Chem.* **2005**, *50*, 185-212.

48. Gross, E. K. U.; Burke, K. *Basics in Time-Dependent Density Functional Theory*; Springer: Berlin, 2006, pp 1-13.

49. Rappoport, D.; Furche, F. *Excited States and Photochemistry*; Springer: Berlin, 2006, pp 337-354.

50. Crawford, T. D.; Tam, M. C.; Abrams, M. L. *J. Phys. Chem. A* **2007**, *111*, 12057-12068, (and references therein).

51. Furche, F.; Ahirich, R.; Wachmann, C.; Weber, E.; Sobanski, A.; Vogtle, F.; Grimme, S. *J. Am. Chem. Soc.* **2000**, *122*, 1717-1724.

52. Autschbach, J.; Ziegler, T. *J. Chem. Phys.* **2002**, *116*, 891-896.

53. Ruud, K.; Helgaker, T. *Chem. Phys. Lett.* **2002**, *352*, 533-539.

54. Mazzini, F.; Pescitelli, G.; di Bari, L.; Netscher, T.; Salvadori, P. *Chirality* **2009**, *21*, 35-43.

55. Stephens, P. J.; McCann, D. M.; Cheeseman, J. R.; Frisch, M. J. *Chirality* **2005**, *17*, S52-S64.

56. Adano, C.; Barone, V. *J. Chem. Phys.* **1999**, *110*, 6158-6170.

57. Becke, A. D. *J. Chem. Phys.* **1993**, *98*, 1372-1377.

58. Becke, A. D. *Phys. Rev. A* **1988**, 3098-3100.

59. Perdew, J. P. *Phys. Rev. B* **1986**, *33*, 8822-8824.

60. Schafer, A.; Huber, C.; Ahirichs, R. *J. Chem. Phys.* **1994**, *100*, 5829-5835.

61. Kurtan, T.; Pescitelli, G.; Salvadori, P.; Kenez, A.; Antus, S.; Szilagyi, L.; Illyes, T. Z.; Szabo, I. *Chirality* **2008**, 379-385.

62. Canal-Neto, A.; Jorge, F. E. *Chirality* **2007**, *19*, 67-73.

63. Kendall, R. A.; Dunning, T. H.; Harrison, R. J. *J. Chem. Phys.* **1992**, *96*, 6796-6806.

64. *Continuum Solvation Models in Chemical Physics: From Theory to Applications*; Tomasi, J.; Mennucci, B.; Cammi, R., Eds.; Wiley: Chichester, 2007.

65. Diedrich, C.; Gimme, S. *J. Phys. Chem. A* **2003**, *107*, 2524-2539.

66. Cachet, N.; Genta-Jouve, G.; Regalado, E. L.; Mokrini, R.; Amade, P.; Culioli, G.; Thomas, O. P. *J. Nat. Prod.* **2009**, *72*, 1612-1615.

67. Ding, Y.; Li, X. C.; Ferreira, D. *J. Nat. Prod.* **2009**, *72*, 327-335.

68. Pescitelli, G.; Di Bari, L.; Caporusso, A. M.; Salvadori, P. *Chirality* **2008**, *20*, 393-399.

69. Bringmann, G.; Bruhn, T.; Maksimenka, K.; Hemberger, Y. *Eur. J. Org. Chem.* **2009**, *20*, 664-672.

70. Bringmann, G.; Gulder, T. A. M.; Reichert, M.; Gulder, T. *Chirality* **2008**, *20*, 628-642.

71. Krohn, K.; Farooq, U.; Florke, U.; Schulz, B.; Draeger, S.; Pescitelli, G.; Salvadori, P.; Antus, S.; Kurtan, T. *Eur. J. Org. Chem.* **2007**, 3206-3211.

72. Jones, P. G. *Acta. Crystallogr.* **1984**, *40*, 663-668.

73. Jones, P. G. Absolute Structure and How Not to Determine It, In *Crystallographic Computing 3: Data Collection, Structure Determination, Proteins, and Databases*; Sheldrick G. M.; Kruger, C.; Goddard, D., Eds.; Oxford University Press: New York, 1985, pp 260-273.

74. Kuroda, R. Solid-state CD: Application to Inorganic and Organic Chemistry, In *Circular Dichroism: Principles and Applications*, 2nd ed.; Berova, N.; Nakanishi, K.; Wood, R. W., Eds.; Wiley-VCH: New York, 2000, pp 159-184.

75. Kuroda, R.; Honma, T. *Chirality* **2000**, *12*, 269-277.

76. Polavarapu, P. L. *Mol. Phys.* **1997**, *91*, 551-554.

77. Polavarapu, P. L. Chakraborty, D. K. *Chem. Phys.* **1999**, *240*, 1-8.

78. Polavarapu, P. L. *Angew. Chem., Int. Ed.* **2002**, *41*, 4544-4546.

79. Polavarapu, P. L. *J. Phys. Chem. A* **2005**, *109*, 7013-7023.

80. Cheeseman, J. R.; Frisch, M. J.; Devlin, F. J.; Stephens, P. J. *J. Phys. Chem. A* **2000**, *104*, 1039-1046.

81. Vereshchangia, A. A.; Sapteeva, T. I.; Slivkin, L. G.; Garmashov, V. I.; Rudakov, G. A. *J. Appl. Chem USSR* **1982**, *55*, 409.

82. Anderson, N. H.; Falcone, M. S.; *Chemistry and Industry* **1971**, 62-63.

83. Kondru, R. K.; Wipf, P.; Beratan, D. N. *J. Am. Chem. Soc.* **1998**, *120*, 2204-2205.

84. Kondru, R. K.; Wipf, P.; Beratan, D. N. *Science* **1998**, *282*, 2247-2250.

85. Perry, T. L.; Dickerson, A.; Kahn, A. A.; Kondru, R. K.; Beratan, D. N.; Wipf, P.; Kelly, M.; Hamann, M. T. *Tetrahedron* **2001**, *57*, 1483-1487.

86. Ribe, S.; Kondru, R. K.; Beratan, D. N.; Wipf, P. *J. Am. Chem. Soc.* **2000**, *122*, 4608-4617.

87. Nagle, D. G.; Park, P. U.; Paul, V. J. *Tetrahedron Let*t. **1997**, *38*, 6969-6972.

88. Amos, R. D. *Chem. Phys. Lett.* **1982**, *87*, 23-26.

89. Rotzinger, F. P. *J. Am. Chem. Soc.* **1996**, *118*, 6760-6766.

90. Sobolev, V. S.; Neff, S. A.; Gloer, J. B. *J. Agric. Food Chem.* **2009**, *57*, 62-68.

91. Sobolev, V. S.; Neff, S. A.; Gloer, J. B. *J. Agric. Food Chem.* **2010**, *58*, 878-881.

92. Sobolev, V. S.; Neff, S. A.; Gloer, J. B.; Khan, S. I.; Tabanca, N.; De Lucca, A. J.; Wedge, D. E. *Phytochemistry* **2010**, *71*, 2099-2107.

93. Sobolev, V. S.; Khan, S. I.; Tabanca, N.; Wedge, D. E.; Manly, S. P.; Cutler, S. J.; Coy, M. R.; Becnel, J. J.; Neff, S. A.; Gloer, J. B. *J. Agric. Food Chem.* **2011**, *59*, 1673-1682.

94. quickstats.nass.usda.gov/data/printable/6E96A4FB-05C3-3E6E-8E10-68A29DA9B45A; United States Department of Agriculture, National Agricultural Statistics Service (Accessed September 2011).

95. Jaganath, I. B.; Crozier, A. Dietary Flavonoids and Phenolic Compounds. In *Plant Phenolics and Human Health: Biochemistry, Nutrition, and Pharmacology*; Fraga, C. G., Ed.; Wiley & Sons, Inc.: New York, 2010; pp 1-49.

96. Sobolev, V. R.; Sy, A. A.; Gloer, J. B. *J. Agric. Food Chem.* **2008**, *56*, 2960-2969.

97. Kim, J. S.; Lee, S. Y.; Park, S. U. *Afr. J. Biotechnol.* **2008**, *7*, 3788-3709.

98. Edwards, C.; Strange, R. N.; Cole, D. L. *Plant Pathol.* **1995**, *44*, 573-579.

99. Sobolev, V. R.; Horn, B. W.; Potter, T. L.; Deyrup, S. T.; Gloer, J. B. *J. Agric. Food Chem.* **2006**, *54*, 3505-3511.

100. Ingham, J. L. *Phytochemistry* **1976**, *15*, 1791-1793.

101. Cooksey, C. J.; Garratt, P. J.; Richards, S. E.; Strange, R. N. *Phytochemistry* **1988**, *27*, 115-116.

102. Wotton, H. R.; Strange, R. N. *J. Gen. Microbiol.* **1985**, *131*, 487-494.

103. Keen, N. T. *Phytopathology* **1975**, *65*, 91-92.

104. Jeandet, P.; Delaunois, B.; Conreux, A.; Donnez, D.; Nuzzo, V.; Cordelier, S.; Clement, C.; Courot, E. *BioFactors* **2010**, *36*, 331-334.

105. Ku, K. L.; Chang, P. S.; Cheng, Y. C.; Lien, C. Y. *J. Agric. Food Chem.* **2005**, *53*, 3877-3881.

106. Takaoka, M. *Nippon Kagaku Kaishi* **1939**, *60*, 1261-1264.

107. Sobolev, V. S. *Beneficial Uses of Peanut By-products*. www.ars.usda.gov/Research/docs.htm?docid=16814 (Accessed August 2011).

108. Gloer, J. B. *Acc. Chem. Res.* **1995**, *28*, 343-350, (and references therein).

109. Lumsden, R. D. *The Fungal Community: Its Organization and Role in the Ecosystem*; 2nd ed.; Carroll, G. C.; Wicklow, D. T., Eds.; Marcel Dekker, Inc.: New York, 1992; Vol. 9, pp 275-293.

110. Shim, S. H.; Baltrusaitis, J.; Gloer, J. B.; Wicklow, D. T. *J. Nat. Prod.* **2011**, *74*, 398-401.

111. Schmidt, L. E.; Deyrup, S. T.; Baltrusaitis, J.; Swenson, D. C.; Wicklow, D. T.; Gloer, J. B. *J. Nat. Prod.* **2010**, *73*, 404-408.

112. Sy, A. A.; Swenson, D. C.; Gloer, J. B.; Wicklow, D. T. *J. Nat. Prod.* **2008**, *71*, 415-419.

113. Deyrup, S. T.; Gloer, J. B.; O'Donnell, K.; Wicklow, D. T. *J. Nat. Prod.* **2007**, *70*, 378-382.

114. Jiao, P.; Mudur, S. V.; Gloer, J. B.; Wicklow, D. T. *J. Nat. Prod.* **2007**, *70*, 1308-1311.

115. Shim, S. H.; Swenson, D. C.; Gloer, J. B.; Dowd, P. F.; Wicklow, D. T. *Org. Lett.* **2006**, *8*, 1225-1228.

116. Bodey, G. P.; Vartivarian, S. *Eur. J. Clin. Microbiol.* **1994**, *60*, 847-852.

117. Smith, J. E.; Moss, M. O. *Mycotoxins: Formation, Analysis, and Significance*; Wiley: New York, 1985, pp1-148.

118. Chu, Y.; Gloer, J. B.; Koster, B.; Malloch, D. *J. Nat. Prod.* **2002**, *65*, 916-919.

119. Poling, S. M.; Wicklow, D. T.; Rogers, K. D.; Gloer, J. B. *J. Agric. Food Chem.* **2008**, *56*, 3006-3009.

120. Wicklow, D. T.; Jordan, A. M.; Gloer, J. B. *Mycol. Res.* **2009**, *113*, 1433-1442.

121. quickstats.nass.usda.gov/data/printable/7F05D28C-CB8C-3757-BD39-2F2DCAB12B6D; United States Department of Agriculture, National Agricultural Statistics Service (Accessed August 2011).

122. Dictionary of Natural Products, Web Edition, 20.1; Taylor & Francis Group/CRC Press, 2011.

123. SciFinder Scholar, Web Edition; American Chemical Society, 2011.

124. Che, Y. Chemical Investigations of Mycoparasitic and Coprophilous Fungi., Ph. D. Thesis, University of Iowa, Iowa City, IA, May 2000.

125. Kobayashi, R.; Samejima, S.; Nakajima, S.; Kawai, K.; Udagawa, S. *Chem. Pharm. Bull.* **1987**, *35*, 1347-1352.

126. Dalsgaard, P. W.; Larsen, T. O.; Christophersen, C. *J. Antibiot.* **2005**, *58*, 141-144.

127. Munro, H. D.; Musgrave, O. C.; Templeton, R. *J. Chem. Soc. C* **1967**, 947-948.

128. Keller-Schierlein, W.; Kupfer, E. *Helv. Chim. Acta.* **1979**, *21*, 1501-1524.

129. Naruse, N.; Yamamoto, H.; Murata, S.; Swanda, Y.; Fukagawa, Y.; Oki, T. *J. Antibiot.* **1993**, *46*, 679-681.

130. Zhou, G. X.; Wijeratne, E. M. K.; Bigelow, D.; Pierson, L. S.; VanEtten, H. D.; Gunatilaka, A. A. L. *J. Nat. Prod.* **2004**, *67*, 328-332.

131. Kohno, J.; Nonaka, N.; Nishio, M.; Ohnuki, T.; Kawano, K.; Okuda, T.; Komatsubara, S. *J. Antibiot.* **1999**, *52*, 575-577.

132. Gutierrez, M.; Theoduloz, C.; Rodriguez, J.; Lolas, M.; Schmeda-Hirschmann, G. *J. Agric. Food Chem.* **2005**, *53*, 7701-7708.

133. Xie, L. W.; Ouyang, Y. G.; Zou, K.; Wang, G. H.; Chen, M. J.; Sun, H. M.; Dai, S.; Li. *Appl. Biochem. Biotechnol.* **2009**, *159*, 284-293.

134. Fang, F.; Ui, H.; Shiomi, K.; Masuma, R.; Yamaguchi, Y.; Zhang, C. G.; Zhang, X. W.; Tanaka, Y.; Omura, S. *J. Antibiot.* **1997**, *50*, 919-925.

135. Krough, P.; Hasselager, E.; Friis, P. *Acta. Pathol. Microbiol. Scand., Sect. B: Microbiol. Immunol.* **1970**, *78*, 401-413.

136. Barber, J.; Cornford, J. L.; Howard, T. D.; Sharpless, D. *J. Chem. Soc., Perkin Trans. 1* **1987**, 2743-2744.

137. Macias, M.; Ulloa, M.; Gamboa, A.; Mata, R. *J. Nat. Prod.* **2000**, *63*, 757-761.

138. Schmidt, L. E. Chemical Investigations of Fungicolous/Mycoparasitic Fungi from Hawaii., Ph. D. Thesis, University of Iowa, Iowa City, IA, December 2007.

139. Ruegger, A.; Kuhn, M.; Lichti, H.; Loosli, H. R.; Huguenin, R.; Quiquerez, C.; von Wartburg, A. *Helv. Chim. Acta.* **1976**, *59*, 1075-1092

140. Traber, R.; Loosli, H.; Hofmann, H.; Kuhn, M.; Von Wartburg, A. *Helv. Chim. Acta.* **1982**, *65*, 1655-1677.

141. Turner, W. B.; Aldridge, D. C. Secondary Metabolites Derived from Amino-acids, In *Fungal Metabolites II*; Academic Press: London, 1983, p 433 (cyclsosporin A) and p 462 (chetoglobosins A & F), (and references therein).

142. Sawai, K.; Okuno, T.; Terada, Y.; Harada, Y.; Sawamura, K.; Sasaki, H.; Takao, S. *Agric. Biol. Chem.* **1981**, *45*, 1223-1228.

143. Cutler, H. G.; Springer, J. P.; Arrendale, R. F.; Arison, B. H.; Cole, P. D.; Roberts, R. G. *Agric. Biol. Chem.* **1988**, *52*, 1725-1733.

144. Cutler, H. G.; Crumley, F. G.; Springer, J. P.; Cox, R. H. *J. Agric. Food Chem.* **1981**, *29*, 981-983.

145. Cutler, H. G.; Ammermann, E.; Springer, J. P. *ACS Symposium Series* **1988**, *380*, 79-90.

146. Wicklow, D. T.; Rogers, K. D.; Dowd, P. F.; Gloer, J. B. *Fungal Biology* **2011**, *115*, 133-142.

147. Qin, J. C.; Zhang, Y. M.; Gao, J. M.; Bai, M. S.; Yang, S. X.; Laatsch, H.; Zhang, A. L. *Bioorg. Med. Chem. Lett.* **2009**, *19*, 1572-1574.

148. Momesso, L. S.; Kawano, C. Y.; Ribeiro, P. H.; Nomizo, A.; Goldman, G. H.; Pupo, M. T. *Quim. Nova.* **2008**, *31*, 1680-1685.

149. Oh, H. Chemical Investigations of *Chaetomium* sp. and Aquatic and Sclerotium-Producing Fungi, Ph. D. Thesis, University of Iowa, Iowa City, IA, May 1998.

150. Vesonder, R. F.; Tjarks, L. W.; Rohwedder, W. K.; Burmeister, H. R.; Laugal, J. A. *J. Antibiot.* **1979**, *32*, 759-761.

151. Singh, S. B.; Zink, D. L.; Goetz, M. A.; Dombrowski, A. W.; Polishook, J. D.; Hazuda, D. J. *Tetrahedron Lett.* **1998**, *39*, 2243-2246.

152. Kim, J. C.; Park, J. H.; Choi, G. J.; Kim, H. T.; Choi, Y. H.; Cho, K. Y. *Han'guk Misaengmul-Saengmyongkong Hakhoechi* **2002**, *30*, 339-345 (accessed through SciFinder September 2011).

153. Isaka, M.; Berkaew, P.; Intereya, K.; Komijit, S.; Sathitkunanon, T. *Tetrahedron* **2007**, *63*, 6855-6860.

154. Joshi, B. K.; Gloer, J. B.; Wicklow, D. T. *J. Nat. Prod.* **1999**, *62*, 730-733.

155. Matsumoto, M.; Minato, H.; Kondo, E.; Mitsugi, T.; Katagiri, K. *J. Antibiot.* **1975**, *28*, 602-604.

156. Polavarapu, P. L.; Jeirath, N.; Kurtan, T.; Pescitelli, G.; Krohn, K. Chirality 2009, 21, E202-E207.

157. Scherlach, K.; Hertweck, C. *Org. Biomol. Chem.* **2006**, *4*, 3517-3520.

158. Kimura, Y.; Kusano, M.; Koshino, H.; Uzawa, J.; Fujioka, S.; Tani, K. *Tetrahedron Lett.* **1996**, *37*, 4961-4964.

159. Kusano, M.; Koshino, H.; Uzawa, J.; Fujioka, S.; Kawano, T.; Kimura, Y. *Biosci. Biotechnol. Biochem.* **2000**, *64*, 2559-2568.

160. Larsen, T. O.; Frydenvang, K.; Frisvad, J. C.; Christophersen, C. *J. Nat. Prod.* **1998**, *61*, 1154-1157.

161. Arai, K.; Shimizu, S.; Yamamoto, Y. *Chem. Pharm. Bull.* **1981**, *29*, 1005-1012.

162. Lee, S. U.; Asami, Y.; Lee, D.; Jang, J.-H.; Ahn, J.-S.; Oh, H. *J. Nat. Prod*. **2011**, *74*, 1284-1287

163. He, J.; Lion, U.; Sattler, I.; Gollmick, F. A.; Grabley, S.; Cai, J.; Meiners, M.; Schünke, H.; Schamann, K.; Dechert, U.; Krohn, M. *J. Nat. Prod.* **2005**, *68*, 1397-1399.

164. Peterson, S. W. *Mycologia* **2008**, *100*, 205–226.

165. Li, K.; Horanyi, P. S.; Collins, R.; Phillips, R. S.; Eriksson, K. L. *Enzyme Microb. Technol.* **2001**, *28*, 301-307.

166. Nobiaki, K.; Tukashi, Y.; Naoko, M. Jpn. Kokai Tokkyo Koho **2003**, JP 2003096080 (A).

167. Birch, A. J.; Musgrave, O. C.; Rickards, R. W.; Smith, H. *J. Chem. Soc.* **1959**, 3146-3152.

168. Lai, S.; Shizuri, Y.; Yamamura, S.; Kawai, K.; Terada, Y.; Furukawa, H. *Tetrahedron Lett.* **1989**, *30*, 2241-2244.

169. Watanabe, T.; Arisawa, M.; Narusuye, K.; Alam, M. S.; Yamamoto, K.; Mitomi, M.; Ozoe, Y.; Nishida, A. *Bioorg. Med. Chem.* **2009**, *17*, 94-110.

170. quickstats.nass.usda.gov/data/printable/523AF159-E34C-3DFB-84A1-1CD8A3EC3151; United States Department of Agriculture, National Agricultural Statistics Service (Accessed September 2011).

171. Kralj, A.; Kehraus, S.; Krick, A.; Eguereva, E.; Kelter, G.; Maurer, M.; Wortmann, Fiebig, H. H.; Konig, G. M. *J. Nat. Prod.* **2006**, *69*, 995-1000.

172. *Fungal Metabolites II*; Turner, W. B.; Aldridge, D. C. Eds.; Academic Press: London, 1983, pp. 182-192.

173. Nozawa, K.; Udagawa, S.; Nakajima, S.; Kawai, K. J. *Chem. Soc., Chem. Commun.* **1987**, 1157-1159.

174. Seya, H.; Nozawa, K.; Nakajima, S.; Kawai, K.; Udagawa, S. *J. Chem. Soc. Perkin Trans. 1* **1986**, 109-116.

175. Fujimoto, H.; Satoh, Y.; Yamaguchi, K.; Yamazaki, M. Chem. Pharm. Bull. 1998, 46, 1506-1510.

176. Hamasaki, T.; Nakajima, H; Yokota, T.; Kimura, Y. *Agric. Biol. Chem.* **1983**, *47*, 891-892.

177. Fujita, M.; Yamada, M.; Nakajima, S.; Kawai, K.; Nagai, M. *Chem. Pharm. Bull.* **1984**, *32*, 2622-2627.

178. Suemitsu, R.; Ohnishi, K.; Horiuchi, M.; Morikawa, Y.; Sakaki, Y.; Matsumoto, Y. *Biosci. Biotech. Biochem.* **1993**, *57*, 334-335.

179. Rank, C.; Nielsen, K. F.; Larsen, T. O.; Varga, J.; Samson, R. A.; Frisvad, J. C. *Fungal Biology* **2011**, *115*, 406-420.

180. Lee, Y. M,; Li, H.; Hong, J.; Cho, H. Y.; Bae, K. S.; Kim, M. A.; Kim, D.; Jung, J. H. *Arch. Pharm. Res.* **2010**, *33*, 231-235.

181. Jiao, P. Chemical Investigations of Freshwater and Fungicolous Fungi, Ph. D. Thesis, University of Iowa, Iowa City, IA, December 2006.

182. Terao, K.; Emiko, I.; Kawai, K.; Nozawa, K.; Udagawa, S. *Mycopathologia* **1990**, *112*, 71-79.

183. Ueno, Y.; Umemori, K.; Niimi, E.; Tanuma, S.; Nagata, S.; Sugamata, M.; Ihara, T.; Sekijima, M.; Kawai, K.; Ueno, I.; Tashiro, F. *Natural Toxins* **1995**, *3*, 129-137.

184. Herath, K. B.; Jayasuriya, H.; Ondeyka, J. G.; Polishook, J. D.; Bills, G. F.; Dombrowski, A. W.; Cabello, A.; Vicario, P. P.; Zweerink, H.; Guan, Z. Singh, S. B. *J. Antibiot.* **2005**, *58*, 686-694.

185. Seya, H.; Nozawa, K.; Udagawa, S.; Nakajima, S.; Kawai, K. *Chem. Pharm. Bull.* **1986**, *34*, 2411-2416.

186. Jayasuriya, H.; Guan, Z.; Dombrowski, A. W.; Bills, G. F.; Polishook J. D.; Jenkins, R. G.; Koch, L.; Crumley, T.; Tamas, T.; Dunois, M.; Misura, A.; Darkin-Rattray, S. J.; Gregory, L.; Singh, S. B. *J. Nat. Prod.* **2007**, *70*, 1364-1367.

187. Akashi, K.; Palermo, R. E. *J. Org. Chem.* **1978**, *43*, 2063-2066.

188. Sharpless, K. B.; Akashi, K. *J. Am. Chem. Soc.* **1976**, 1986-1987.

189. Kokke, W. C. M. C.; Varkevisser, F. A. *J. Org. Chem.* **1974**, *39*, 1535-1539.

190. Bonini, C.; Chiummiento, L.; Funicello, M.; Lupattelli, P.; Pullez, M. *Eur. J. Org. Chem.* **2006**, 80-83.

191. Shaabani, A.; Tavasoli-Rad, F.; Lee, D. G. *Synthetic Communications* **2005**, *35*, 571-580

192. Bailey, P. S. *Ozonization in Organic Chemistry*, Vol. 1, Academic Press, New York, 1978.

193. Rueppel, M. L.; Rapoport, H. *J. Am. Chem. Soc.* **1972**, *94*, 3877-3883

194. Paukstelis, J. V.; Macharia, B. W. *J. Org. Chem.* **1973**, *38*, 646-648

195. Amagata, T.; Usami, Y.; Minoura, K.; Ito, T.; Numata, A. *J. Antibiot.* **1998**, *51*, 33-40.

196. Abe, N.; Murata, T.; Hirota, A. *Biosci. Biotechnol. Biochem.* **1998**, *62*, 2120-2126.

197. Abe, N.; Sugimoto, O.; Tanji, K.; Hirota, A. *J. Am. Chem. Soc.* **2000**, *122*, 12606-12607.

198. Abe, N.; Yamamoto, K.; Hirota, A. *Biosci. Biotechnol. Biochem.* **2000**, *64*, 620-622.

199. Nozawa, Y.; Yamamoto, K.; Ito, M.; Sakai, N.; Mizoue, K.; Mizobe, F.; Hanada, K. *J. Antibiot.* **1997**, *50*, 635-640.

200. Gregory, L.; Pestka, J. J.; Dearborn, D. G.; Rand, T. G. *Toxicol. Pathol.* **2004**, *32*, 26-34.

201. Mudur, S. V. Bioactive Secondary Metabolites from Mycoparasitic, Fungicolous, and Freshwater Fungi, Ph. D. Thesis; University of Iowa, Iowa City, IA, December 2006.

202. Gohrt, A.; Grabley, S.; Thiericke, R.; Zeeck, A. *Liebigs. Ann.* **1996**, 627-633.

203. Krohn, K.; Ludewig, K.; Aust, H.; Draeger, S.; Schulz, B. *J. Antibiot.* **1994**, *47*, 113-118.

204. Paxton, J. D. Biosynthesis and Accumulation of Legume Phytoalexins, In *Mycotoxins and Phytoalexins*; Sharma, R. P.; Salunkhe, D. K., Eds.; CRC Press: Boca Raton, FL, 1991; pp 485-499.

205. Subba Rao, P. V.; Strange, R. N. Chemistry, Biology, and Role of Groundnut Phytoalexins in Resistance to Fungal Attack, In *Handbook of Phytoalexin Metabolism and Action*; Daniel, M., Purkayastha, R. P., Eds.; Marcel Dekker, Inc.: New York, 1995; pp 199-227.

206. Cole, R. J.; Cox, R. H. *Handbook of Toxic Fungal Metabolites*; Academic Press: New York, 1981; pp 937.

207. Cole, R. J.; Dorner, J. W. *Peanut Phytoalexins*. In *Mycotoxins and Phytoalexins*; Sharma, R. P.; Salunkhe, D. K., Eds.; CRC Press: Boca Raton, FL, 1991; pp 501-509.

208. Dorner, J. W.; Cole, R. J.; Sanders, T. H.; Blankenship, P. D. *Mycopathologia* **1989**, *105*, 117-128.

209. Sobolev, V. S.; Guo, B. Z.; Holbrook, C. C.; Lynch, R. E. *J. Agric. Food. Chem.* **2007**, *55*, 2195-2200.

210. Keen, N. T.; Ingham, J. L. *Phytochemistry* **1976**, *15*, 1794-1795.

211. Aguamah, G. A.; Langcake, P.; Leworthy, D. P.; Page, J. A.; Pryce, R. J.; Strange, R. N. *Phytochemistry* **1981**, *20*, 1381-1383.

212. Cooksey, C. J.; Garratt, P. J.; Richards, S. E.; Strange, R. N. *Phytochemistry* **1988**, *27*, 1015-1016.

213. Sobolev, V. S.; Potter, T. L.; Horn, B. W. *Phytochem. Anal.* **2006**, *17*, 312-322.

214. Sobolev, V. S.; Deyrup, S. T.; Gloer, J. B. *J. Agric. Food Chem.* **2006**, *54*, 2111-2115.

215. Hahlbrook, K.; Scheel, D. *Annu. Rev. Plant Physiol. Plant Mol. Biol.* **1989**, *40*, 347-369.

216. Morita, H.; Noguchi, H.; Schroder, J.; Abe, I. *Eur. J. Biochem.* **2001**, *268*, 3759-3766.

217. Dixon, R. A.; Pavia, N. L. *Plant Cell* **1995**, *7*, 1085-1097.

218. Hart, J. H. *Annu. Rev. Phytopathol.* **1981**, *19*, 437-458.

219. Ioset, J. R.; Marston, A.; Gupta, M. P.; Hostettman, K. *J. Nat. Prod.* **2001**, *64*, 710-715.

220. Su, B. N.; Cuendet, M.; Hawthorne, M. E.; Kardano, L. B. S.; Riswan, S.; Fong, H. H. S.; Mehta, R. G.; Pezzuto, J. M.; Kinghorn, A. D. *J. Nat. Prod.* **2002**, *65*, 163-169.

221. Langcake, P.; Pryce, R. *J. Experientia* **1977**, *33*, 151-152.

222. Yoder, B. J.; Cao, S.; Norris, A.; Miller, J. S.; Ratovoson, F.; Razafitsalama, J.; Andriantsiferana, R.; Rasamison, V. E.; Kingston, D. G. I. *J. Nat. Prod.* **2007**, *70*, 342-346.

223. Huang, K. S.; Wang, Y. H.; Li, R. L.; Lin, M. *Phytochemistry* **2000**, *54*, 875-881.

224. Pezet, R.; Perret, C.; Jean-Denis, J. B.; Tabacchi, R.; Gindro, K.; Viret, O. *J. Agric. Food Chem.* **2003**, *51*, 5488-5492.

225. Syah, Y. M.; Achmad, S. A.; Ghisalberti, E. L.; Hakim, E. H.; Iman, M. Z. N.; Makmur, L.; Mujahiddin, D. *Fitoterapia* **2000**, *71*, 630-635.

226. Iliya, I.; Ali, Z.; Tanaka, T.; Iinuma, M.; Furasawa, M.; Nakaya, K.; Shirataki, Y.; Murata, J.; Darnaedi, D.; Matsuura, N.; Ubukata, M. *Chem. Pharm. Bull.* **2003**, *51*, 85-88.

227. Jeandet, P.; Douillet-Breuil, A. C.; Bessis, R.; Debord, S.; Sbaghi, M.; Adrian, M. *J. Agric. Food Chem.* **2002**, *50*, 2731-2741.

228. He, S.; Wu, B.; Pan, Y.; Jiang, L. *J. Org. Chem.* **2008**, *73*, 5233–5241.

229. Lam, S. H.; Chen, J. M.; Kang, C. J.; Chen, C. H.; Lee, S. S. *Phytochemistry* **2008**, *69*, 1173-1178.

230. Likhitwitayawuid, K.; Sritularak, B. *J. Nat. Prod.* **2001**, *64*, 1457-1459.

231. Ohyama, M.; Tanaka, T.; Ito, T; Iinuma, M.; Bastow, K. F.; Lee, K. H. *Bioorg. Med.Chem. Lett.* **1999**, *9*, 3057-3060.

232. Huang, K. S.; Lin, M.; Cheng, G. F. *Phytochemistry* **2001**, *58*, 357-362.

233. He, S.; Lu, Y.; Wu, B.; Pan, Y. *J. Chromatogr. A* **2007**, *1151*, 175–179.

234. Guo, X. Y.; Wang, J.; Wang, N. L.; Kitanaka, S.; Liu, H. W.; Yao, X. S. *Chem. Pharm. Bull.* **2006**, *54*, 21-25.

235. Marino, S. D.; Gala, F.; Borbone, N.; Zollo, F.; Vitalini, S.; Visioli, F.; Iorizzi, M. *Phytochemistry* **2007**, *68*, 1805-1812.

236. Fang, N.; Casida, J. E. *J. Nat. Prod.* **1999**, *62*, 205-210.

237. Minezawa, N.; Gordon, M. S. *J. Phys. Chem. A* **2011**, *115*, 7901-7911.

238. Kurihara, H.; Kawabata, J.; Ichikawa, S.; Mishima, M.; Mizutani, J. *Phytochemistry* **1991**, *30*, 649-653.

239. Kurihara, H.; Kawabata, J.; Ichikawa, S.; Mizutani, J. *Agric. Biol. Chem.* **1990**, *54*, 1097-1099.

240. Schultz, T. P.; Nicholas, D. D.; Fisher, T. H. *Agric. Food Chem* **1997**, *1*, 289-299.

241. Schultz, T. P.; Boldin, W. D.; Fisher, T. H.; Nicholas, D. D.; McMurtrey, K. D.; Pobanz, K. *Phytochemistry* **1992**, *31*, 3801-3806.

242. Bokel, M.; Diyasena, M. N. C.; Gunatilaka, A. A. L.; Kraus, W.; Sotheeswaran, S. *Phytochemistry* **1988**, *27*, 377-380.

243. Al-Hazimi, H. M. G.; Alkhathlan, H. Z.; *Naturally Occurring Pterocarpanoids and Related Compounds.* J. King Saud Univ., Riyadh **2000**, *12*, 93-122.

244. Jiménez-González, L.; Álvarez-Corral, M.; Muñoz-Dorado, M.; Rodríguez-García, I. *Phytochem. Rev.* **2008**, *7*, 125-154.

245. He, J.; Chen, L.; Heber, D.; Shi, W.; Lu, Q. Y. *J. Nat. Prod.* **2006**, *69*, 121-124.

246. Tanaka, H.; Hirata, M.; Etoh, H.; Watanabe, N.; Shimizu, H.; Ahmad, M.; Khan, Z.; Anwar, M. *Heterocycles* **2001**, *55*, 2341-2347.

247. Rukachaisirikul, T.; Innok, P.; Aroonrerk, N.; Boonamnuaylap, W.; Limrangsun, S.; Boonyon, C.; Woonjina, U.; Suksamrarn, A. *J. Ethnopharmacol.* **2007**, *110*, 171-175.

248. Mitscher, L. A.; Ward, J. A.; Drake, S.; Rao, G. S. *Heterocycles* **1984**, *22*, 1673-1675.

249. Njamen, D.; Talla, E.; Mbafor, J. T.; Fomum, Z. T.; Kamanyi, A.; Mbanya, J. C.; Cerda-Nicolas, M.; Giner, R. M.; Recio, M. C.; Rios, J. L. *Eur. J. Pharmacol.* **2003**, *468*, 67-74.

250. Selvam, C.; Jachak, S. M.; Oli, R. G.; Thilagavathi, R.; Chakraborti, A. K.; Bhutani, K. K. *Tetrahedron Lett.* **2004**, *45*, 4311-4314.

251. Chaudhuri, S. K.; Huang, L.; Fullas, F.; Brown, D. M.; Wani, M. C.; Wall, M. E.; Tucker, J. C.; Beecher, C. W. W.; Kinghorn, A. D. *J. Nat. Prod.* **1995**, *58*, 966-1969.

252. Maurich, T.; Lorio, M.; Chimenti, D.; Turchi, G. *Chem. Biol. Interact.* **2006**, *159*, 104-116.

253. Miyase, T.; Sano, M.; Nakai, H.; Muraoka, M.; Nakazawa, M.; Suzuki, M.; Yoshino, K.; Nishihara, Y.; Tanai, J. *Phytochemistry* **1999**, *52*, 303-310.

254. Chanphen, R.; Thebtaranonth, Y.; Wanauppathamkul, S.; Yuthavong, Y. *J. Nat. Prod.* **1998**, *61*, 1146-1147.

255. Salem, M. M.; Werbovetz, K. A. *J. Nat. Prod.* **2006**, *69*, 43-49.

256. Joseph, C. C.; Ndoile, M. M.; Malima, R. C.; Nkunya, M. H. H. *Trans. R. Soc. Trop. Med. Hyg.* **2004**, *98*, 451-455.

257. Morimoto, M.; Fukumto, H.; Hiratani, M.; Chavasiri, W.; Komai, K. *Biosci. Biotech.* **2006**, *70*, 1864-1868.

258. Boland, G. M.; Donnelly, D. M. X. *Nat. Prod. Rep.* **1998**, *15*, 241-260.

259. Chansakaow, S.; Ishikawa, T.; Sekine, K.; Okada, M.; Higuchi, Y.; Kudo, M.; Chaichantipyuth, C. *Planta Med.* **2000**, *66*, 572-575.

260. Ferreira, M. A.; Moir, M.; Thomson, R. H. *J. C. S Perkin 1* **1974**, 2429-2435.

261. Ingham, J.; Dewick, P. M. *Phytochemistry* **1978**, *17*, 535-538.

262. De Lucca, A. J.; Bland, J. M.; Vigo, C. B.; Cushion, M.; Selitrennikoff, C. P.; Walsh, T. *J. Med. Mycol.* **2002**, *40*, 131-137.

263. O'Donnell, K. *Sydowia* **1996**, *48*, 57-70.

264. White, T. J.; Bruns, T.; Lee, S.; Taylor, J. W. In *PCR Protocols: A Guide to Methods and Applications*; Innis, M. A.; Gelfand, D. H.; Sninsky, J. J.; White, T. J., Eds.; Academic Press: New York, **1990**; pp 315-322.

265. Schaefer, A.; Horn, H.; Ahlrichs, R. *J. Chem. Phys*. **1992**, *97*, 2571-2577.

266. Eichkorn, K.; Weigend, F.; Treutler, O.; Ahlrichs, R. *Theoret. Chim. Acta* **1997**, *97*, 119-124.

267. Eichkorn, K.; Treutler, O.; Öhm, H.; Häser, M.; Ahlrichs, R. *Chem. Phys. Lett*. **1995**, *240*, 283-289.

268. Becke, A. D. *J. Chem. Phys*. **1993**, *98*, 5648-5652.

269. Lee, C.; Yang, W.; Parr, R. G. *Phys. Rev. B*, **1988**, *37*, 785-789.

270. Neese, F.; Wennmohs, F.; Hansen, A.; Becker, U. *Chem. Phys*. **2009**, *356*, 98-109.

271. Sinnecker, S.; Rajendran, A.; Klamt, A.; Diedenhofen, M.; Neese, F. *J. Phys. Chem. A* **2006**, *110*, 2235-2245.

272. Neese, F. ORCA, Version 2.8, Universität Bonn, Bonn, Germany, 2010.

273. Bruhn, T.; Hemberger, Y.; Schaumlöffel, A.; Bringmann, G. SpecDis, Version 1.50, Universität Würzburg, Würzburg Germany, 2010.

274. Raper, K. B.; Fennell, D. I. *The Genus Aspergillus*, Williams & Wilkins: Baltimore, MD, 1965.

275. Samuels, G.J., Petrini, O., Kuhls, K., Lieckfeldt, E., and Kubicek, C.P. 1998. The *Hypocrea schweinitzii* complex and *Trichoderma* sect. *Longibrachiatum*. Studies in Mycology 41:1-54.

276. Ellis, M. B. *Dematiaceous Hyphomycetes* Commonwealth Mycological Institute, Kew, Surrey, England; **1971**, p. 608.